ABSTRACT

CHEN, HAO. Protein-DNA Interactions and Protein-Protein Interactions Affect Transcriptional Regulation of Wood Cell Wall Biosynthesis in *Populus trichocarpa*. (Under the direction of Dr. Vincent Chiang.)

Wood formation and secondary cell wall component biosynthesis has been intensively studied due to the importance of these processes to plant biology and to the biofuel industry. Wood formation and secondary cell wall component biosynthesis are closely interacting biological processes. The transcriptional regulation of wood formation and secondary cell wall biosynthesis are usually dissected by genetic analyses of individual genes. In my dissertation, we show how some of TF-DNA and TF-TF interactions affect the transcriptional regulation of these processes. The works was performed using the woody species, *Populus trichocarpa* as a model system.

The first part of my dissertation (Chapter 1) introduces the background knowledges and current progress for the related researches about the molecular dissection of wood formation and cell wall biosynthesis. The second part of my dissertation (Chapter 2) focuses on how transcription factor (TF)-DNA interactions regulate wood cell wall biosynthesis. We identified 56 direct TF-promoter interactions using chromatin immunoprecipitation coupled with TF-overexpression assays in stem-differentiating xylem protoplasts. These regulatory interactions are physically detected between 18 transcription factor genes and 27 genes encoding the biosynthetic enzymes of cellulose, hemicelluloses, and lignins. Using these genes as nodes and the interactions as edges, we generated a SND1-B1 directed four-layered hierarchical transcriptional regulatory network. This network not only elucidates the mechanism of how these TFs regulate the wood cell wall biosynthesis, but also provides us with information describing the cooperative and combinatorial behaviors of these TFs in the regulation. Furthermore, the regulatory effects of the interactions within the networks have been validated using stable transgenesis in *Populus trichocarpa*. The third part of my dissertation (Chapter 3) addresses how TF-TF interactions affect the

transcriptional regulation of vascular related NAC domain proteins (VNDs) and secondary wall-associated NAC domain proteins (SNDs), which are regulators for xylem differentiation and secondary wall formation. A splice variant, PtrVND6C1^{IR}, is expressed from the intron retention of PtrVND6C1 mRNA. PtrVND6C1^{IR} is a protein with the incomplete NAC domain. Overexpression of PtrVND6-C1^{IR} protein attenuated the expression of *PtrMYB21* that is a master regulator of the secondary cell wall biosynthesis. PtrVND6-C1^{IR} also inhibits the expression of other members of the PtrSND1 and PtrVND6 gene family. PtrVND6-C1^{IR} lacks DNA binding and transactivation activity but retains dimerization ability. Protein translocation and bimolecular fluorescence complementation assays demonstrate the formation of heterodimers between PtrVND6C1^{IR} and PtrSND1s, PtrVND6s. The promoter-GUS and transactivation assays then indicated that the heterodimers don't have transactivation activity. These heterodimers may function as dominant negative repressors that inhibit the self-activation and cross-regulation of PtrVND6s and PtrSND1s. This study partly elucidates, at least in part, how TF interactions affect the transcriptional functions of PtrVND6s and PtrSND1s.

Protein-DNA Interactions and Protein-Protein Interactions Affect Transcriptional Regulation of Wood Cell Wall Biosynthesis in *Populus trichocarpa*

by
Hao Chen

A dissertation submitted to the Graduate Faculty of
North Carolina State University
in partial fulfillment of the
requirements for the degree of
Doctor of Philosophy

Forestry and Environmental Resources

Raleigh, North Carolina

2017

APPROVED BY:

_____	_____
Marcela Pierce	Jose Alonso
_____	_____
Ron Sederoff	Vincent Chiang Chair of Advisory Committee

DEDICATION

Do one thing at a time, and do it well.

BIOGRAPHY

Hao Chen was born July 14, 1990 in Yuncheng, Shandong province, China. In his small hometown, he has a happy childhood with his family. He graduated from Yuncheng No.1 Middle School in 2007. In July 2011, Hao was graduated from Shandong Agricultural University with Bachelor of Science Degree in Biotechnology and Bachelor of Art Degree. During his study in university, he worked as lab assistant in State Key Laboratory of Crop Biology, China. To continue studying in plant biology, Hao moved to North Carolina State University to pursue a Master of Science Degree in Forestry under the direct of Dr. Chiang and Dr. Sederoff. After he obtain this degree, Hao continue to study with the experienced and smart researchers for get Ph.D. degree in Forest biotechnology group. During this process, Hao learned much knowledge and appreciate many excellent qualities, and manage to get his Ph.D. degree. Hao will continue to study in biology.

ACKNOWLEDGMENTS

Thank you to my family and friends for their love and support.

Thank you to Prof. Chiang for providing an opportunity to study with you at NCSU. Researches have been carried out that has improved my design and operation of experiments, but the works have also modified my character and enhanced my personal strength.

Thank you to Prof. Sederoff for improving my ability how to read, write and present research work. With your hard-work in revising my dissertation, my dissertation became much better.

Thank you to Prof. Rojas-Pierce and Prof. Alonso for their advice and help for my graduation.

Thank you to all the members of the Forest biotechnology group at NCSU. Without your help, my research work could not have been not finished.

Thank you to the Department of Energy and the National Science Foundation for your generous support.

TABLE OF CONTENTS

LISTS OF TABLES

CHAPTER 1

CHAPTER 2

CHAPTER 3

LISTS OF FIGURES

CHAPTER 2

CHAPTER 3

CHAPTER 1
BACKGROUND REVIEW

Wood, a specific tissue of plant vascular systems, not only provides mechanical support and water transport ability for the plant, but also plays a crucial role in terrestrial ecosystem carbon-cycling. Wood usually refers to secondary xylem. The formation of secondary xylem needs multiple steps, usually described as cambial cell division, cell expansion, cell wall deposition and programmed cell death (Plomion et al., 2001, Demura and Fukuda, 2007). Through these processes, xylem cells generate secondary cell walls that form the largest part of plant lignocellulosic biomass. For the last decade, rapid progress has been made in researches on the molecular regulation of wood formation and secondary cell wall biosynthesis. The purpose of this introduction is to provide the reader with an overview of the topic, and to highlight the questions that still need to be solved for this topic.

1.1 Wood formation and secondary cell wall biosynthesis

1.1.1 Wood formation: the products from vascular development

Secondary xylem (wood) functions to transport water and is derived from the vascular cambium, which also gives rise to the other conductive tissue, phloem, required for transport of sucrose and other nutrients. Both phloem and xylem are derived from the division and differentiation of the vascular cambium, and the activity of the vascular cambium largely determines the rate of wood formation (Evert, 2006). After the cambial cells proliferate, xylem mother cells enter into a radial expansion zone, and divide into two daughter cells. Then these cells (xylem mother cells and daughter cells) differentiate into vessel, fiber, and parenchymal cells in woody angiosperms (Siedlecka et al., 2008). The vessel cells are specialized for water and nutrient conduction and the fiber cells are specialized for mechanical support (Esau et al.,

1965). Vessels and fibers then undergo the formation of secondary walls, based on the deposition of cellulose, lignin, and hemicelluloses.

1.1.2 Secondary cell wall biosynthesis: physiological, architectural and chemical views

Plants form two types of cell walls: primary and secondary walls, which are distinct in function and structure. Primary cell walls provide some mechanical strength and allow the cell to grow and divide via expanding the structure. Secondary cell walls that are much thicker and stronger are deposited between the plasma membrane and the primary cell wall when the cells stop expansion (Raven, 1999). In tree species, secondary cell walls are most abundantly distributed in fibers and tracheary elements. Fiber cells are differentiated cells that support the woody tissue and tracheary elements are specialized cells that transport water and solutes up the plant. In fiber cells, secondary cell walls are distributed evenly on the inside of the primary cell wall. In tracheary elements of protoxylem, the secondary cell walls are typically organized in a helical or annular pattern that can allow the elongating organs to continue to grow. In tracheary elements of metaxylem, secondary walls are usually deposited as a reticulated or pitted pattern on non-elongating organs. The regulation of these distinct wall deposition patterns is involved with the vesicle transport and microtubule activities (Paradez et al., 2006, Zhou et al., 2007). Many cortical microtubules aggregate in the areas where the secondary cell wall thickens. Disruption of cortical microtubules altered the secondary cell wall distribution (Baskin, 2001, Zhong et al., 2002, Oda and Hasezawa, 2006).

In secondary cell walls of the woody angiosperms, cellulose usually accounts for 50% of the mass, while lignin and hemicelluloses account for about 25% and 20%, respectively. Cellulose, lignin, and hemicelluloses are essential for maintaining the normal strength of secondary walls because a reduction in any one of three

components leads to defects in secondary cell walls (Turner and Somerville, 1997; Jones et al., 2001). Owing to the importance of cellulose, hemicelluloses, and lignin in wood properties and biomass production, research into the biosynthesis of these components has been pursued for over half a century. Additionally, the proportion of individual components in secondary cell walls varies with species and cell types. For example, cotton fibers are composed of up to 95% cellulose and little of other components. Understanding the regulation of cell wall components biosynthesis not only provides clues for explaining why secondary walls vary between species and cell types, but also gives us a chance to modify the secondary walls that serve as major resources of textiles, timber, and biofuels.

1.1.3 The biosynthesis of cellulose, lignin, and hemicellulose

Cellulose is produced by cellulose synthases, which form complexes located in the plasma membrane (Delmer, 1999). Visualized by transmission electron microscopy, these complexes are composed of six particles as a rosette structure (Delmer, 1999). Each particle in the rosette is formed by six cellulose synthase catalytic subunits. Each subunit produces one chain of β-1,4-glucan, and the whole rosette together generates 36 β-1,4-glucan chains to bundle as a microfibril (Somerville, 2006). Biochemical and genetic studies indicated that three cellulose synthase genes with non-redundant functions are required for cellulose synthesis in Arabidopsis and rice (Tanaka et al., 2003; Taylor et al., 2004). Homologs of these three cellulose synthase genes are also present in tree species (Joshi and Mansfield, 2007). In *Populus trichocarpa*, 18 cellulose synthase gene loci have been identified in genome sequences. Co-immunoprecipitation and proteomic analysis show these cellulose synthases formed two cellulose synthase rosette complexes in poplar xylem (Song et al., 2010).

Lignin is typically polymerized from three precursors (monolignols) as ρ-coumaryl alcohol, coniferyl alcohol and syringyl alcohol. These monolignols are produced from

the phenylpropanoid pathway, and then are converted and activated through a trifurcate synthesis pathway. Deposition of lignin occurs mainly in the terminally differentiating secondary cell walls of xylem tissues. Lignin provides xylem tissues with the ability to withstand the force of gravity, mechanical stress, and the negative pressure generated by transpiration. Although lignin is required for stress defense and cell wall strength, it can hinder the human utilization of biomass from plants, such as in the processes of paper-making, cellulose extraction, and biofuel production (Vanholme et al., 2008). Therefore, it is desirable to generate transgenics with engineered secondary cell walls with less lignin or the lignin that can be easily degraded. Genes encoding the monolignol pathway enzymes have been characterized in many species (Shi et al., 2010; Bonawitz & Chapple., 2010; Vanholme et al., 2013; Wang et al., 2014). These enzymes perform a series of hydroxylation and O-methylation reactions to modify the aromatic ring of cinnamic acid, and to activate the side chains from acids to coenzyme-A esters, and subsequently to reduce the end groups to aldehydes and alcohols, resulting in the production of the monolignols (Bonawitz & Chapple., 2010).

Hemicelluloses are composed of xylan, glucuronoxylan, arabinoxylan, glucomannan, and xyloglucan. In xylem of woody angiosperms, hemicelluloses are mainly composed of glucomannan and xylan, with approximate proportions of 15% and 85%, respectively (Timell, 1967). Hemicelluloses are synthesized using sugar nucleotides in the cell's Golgi apparatus (Dhugga et al., 2004; Suzuki et al., 2006; Liepman et al., 2007). Detailed knowledge of the biosynthesis of hemicelluloses is limited. After biosynthesis, hemicelluloses are transported to the plasma membrane via Golgi vesicles. These hemicelluloses are then constructed into cell wall, however, the mechanism of how the construction happen is still unclear.

1.2 Transcriptional regulation of wood cell wall biosynthesis

1.2.1 Transcriptional regulation of cell differentiation from vascular cambium to secondary xylem

Vascular cambium is one specific type of plant lateral meristem in which cell fates and activities are usually regulated by receptor-like kinases (RLKs) and their signaling partners small peptide ligands (Matsubayashi et al., 2003; Sablowski et al., 2011; Endo et al., 2014; Wang et al., 2016). A receptor kinase PXY (PHLOEM INTERCALATED WITH XYLEM) can interact with peptide ligand CLE41/44 (Hirakawa et al., 2007) to initiate a transcriptional cascade. At least 18 TFs are involved in the differentiation from vascular cambium to secondary xylem (Table 1). WOX4 and WOX14 act downstream of the PXY-CLE41/44 complex to regulate vascular cambial maintenance and proliferation (Hirawaka et al., 2010; Etchells et al., 2013). Following the initial vascular cambial differentiation, the development of vascular xylem is regulated by *HD-ZIP* transcription factors, which are expressed in the procambium, cambium and developing xylem (Ilegems et al. 2010). In Arabidopsis, five HD-ZIP TF genes have been identified as *HB14/ PHB* (*PHABULOSA*), *HB9/PHV* (*PHAVOLUTA*), *REV/IFL1* (*REVOLUTA/INTERFASCICULAR FIBERLESS1*), *HB15/ CNA/ /ICU4* (*CORONA/INCURVATA4*) and *HB8* (Table 1). These TFs determine the asymmetric distribution of xylem cell types (Kerstetter et al. 2001, Prigge et al. 2005), suggesting that the proteins play important roles in vascular patterning, the differentiation of secondary xylem, and interfascicular fibers. In poplar, overexpression and downregulation of the HD-ZIP III homologs also revealed their roles in controlling secondary xylem differentiation (Robischon et al., 2011; Du et al., 2011; Zhu et al., 2013). The overexpression of the poplar homolog of Arabidopsis *IFL1/REV*, *PopREVOLUTA*, results in ectopic vascular cambium formation and secondary xylem development in transgenic poplar (Robischon et al., 2011). The overexpression and downregulation of the poplar homolog of the Arabidopsis gene AtHB8, PtrHB7, affects

the differentiation of cambium cells into secondary xylem (Zhu et al., 2013). Similar phenotypes were observed in transgenic poplar overexpressing PopCORONA, which is a homolog of Arabidopsis Corona/ATHB-15 (Du et al., 2011). In Arabidopsis, the TFs SHORTROOT (SHR) and SCARECROW (SCR) (Carlsbecker et al. 2010) induce the expression of miRNA165/166, which can degrade the transcripts of these HD-ZIP TFs. Through this regulation, protoxylem formation was changed (Ohashi-Ito and Fukuda, 2010). Furthermore, other vascular related TFs, such as *AtMD* (Hamann et al., 2002; Scarpella et al., 2006; Donner et al., 2009), *AtBDL* (Hamann et al., 2002), *AtMYC2* (Thines et al., 2007; Sehr et al., 2010), *PtaLBD1* (Yordanov et al, 2010), *AtARK1/PtoARK1* (Andrew et al., 2006; Gerttula et al., 2015), *PtoARK2* (Du et al., 2009), and *AtKAN* (Emery et al., 2003; Llegems et al., 2010), have been observed to regulate secondary xylem and vascular tissue formation in knock-out mutants or in *gain-of-function* transgenics (Table 1). It is important to ask what genes these vascular related TFs regulate, and whether and how these TFs cooperatively and combinatorially regulate secondary xylem differentiation in wood formation.

1.2.2 Coordinated transcriptional regulation of vascular cell differentiation and cell wall component biosynthesis

Vascular cell differentiation and cell wall component gene biosynthesis are closely related biological processes because both processes can be regulated by the same signaling pathway (Ito et al., 2006; Etchells and Turner, 2010). Many TFs regulate both vascular cell differentiation and cell-wall component biosynthesis. APETALA2-domain TF PLETHORAs (PLTs) control the stem cell development and *plt1plt2* double mutants display stem cell loss and reduced cell enlargement in Arabidopsis (Kareem et al., 2015). PLT1 also directly regulates a pectin synthesis gene FLY1 for controlling the biosynthesis of pectin in primary cell walls (Voiniciuc et al., 2013; Voiniciuc et al., 2015). Class I KNOX TFs, such as STM, KNAT1, BP, promote vascular cell differentiation (Long et al., 1996; Vollbrecht et al., 2000; Douglas et al., 2002; Mele et

al., 2005) upregulate primary and secondary cell-wall cellulose synthase genes (Liebsch et al., 2014), or downregulate some monolignol pathway genes (Mele et al., 2005). Some GRAS family TFs LOMs (LOSS MERISTEMS) promote vascular cell differentiation in Arabidopsis shoot meristem (Schulze et al., 2010). LOM1 and LOM2 directly regulate the expression of genes encoding the ß-glucosidases, BGLU45 and BGLU46, which may hydrolyze coniferin for lignin polymerization (Schulze et al., 2010; Chapelle et al., 2012).

Several NAC domain TFs have been found to not only specify xylem tissue identity by regulating vessel and fiber cell differentiation, but also directly and indirectly regulate secondary cell wall component genes. These TFs include *NST1* (*NAC SECONDARY WALL THICKENING PROMOTING FACTOR1*), *NST3/SND1* (*SECONDARY WALL-ASSOCIATED NAC DOMAIN PROTEIN 1*), VASCULAR-RELATED NAC-DOMAIN6 (VND6) and VND7. A double knockout of NST1 and NST3/SND1 or dominant repression of SND1 results in the striking phenotype of no secondary cell wall development in inter-fascicular and vascular fibers. In the anther endothecium of Arabidopsis, secondary wall thickening is controlled non-redundantly by NST1 and NST2 (Mitsuda et al., 2005), and overexpression of these NAC transcription factors leads to ectopic deposition of the lignin in leaves. In Arabidopsis, the NAC domain TFs VND6 and VND7 not only control secondary wall development, but also direct programmed cell death (PCD) of the vessels in both root and shoot tissues (Kubo et al., 2005; Yamaguchi et al., 2008). The above NAC transcription factors are phylogenetically clustered in the same subgroup (Shen et al., 2009). The function of these NAC transcription factors is redundant because the overexpression of VND6 and VND7 using a 35S promoter can complement the *nst1nst3* double mutant phenotype as the loss of secondary cell wall in Arabidopsis. The function of these NAC family members is also being investigated in some woody species.

A subfamily of wood-associated NAC domain transcription factors are homologs of the group of closely related Arabidopsis NAC domain transcription factors, including SNDs, NSTs, and VNDs (Zhong et al., 2010a; Zhong et al., 2010b; Ohtani et al., 2011; Li et al., 2012b). Zhong et al., 2010 PtrWNDs; Ohtani et al., 2011 PtrVNSs; Li et al., 2012b PtrSND-1s/SND-2/3s/VNDs; Table 2). Overexpression of these wood-associated NAC domain transcription factors can effectively rescue the secondary cell wall defect of the *snd1nst1* double mutant (Zhong et al., 2010 PtrWND2B PtrWND6B; Ohtani et al., 2011 PtrVNS1-12) and lead to ectopic secondary cell wall thickening in poplar leaves. These *Populus* TFs function similarly to SND1 and NST1 and control the program of secondary cell wall formation. But unlike specific expression of SNDs in fiber cells and specific expression of VNDs in vessel cells in Arabidopsis, all these wood-associated NAC domain transcription factors are highly expressed in the all cell types of developing secondary xylem, including vessels, fibers and ray parenchyma. To explain why these wood NAC domain TFs are expressed together in the same cell-type, it is necessary to investigate the target genes of these TFs and describe the specific function of each TF. Such an investigation may provide a basis to establish the transcriptional regulatory networks.

1.2.3 Transcriptional regulation of secondary wall component biosynthesis encompassing NAC and MYB transcription factors

Until now, at least 202 TFs have been identified to regulate secondary wall component biosynthesis (Table 2). The whole-genome transcriptional analyses using Arabidopsis transgenic lines and transformed Arabidopsis suspension cells, combining with electrophoretic mobility shift assay (EMSA) and transactivation analysis, have identified the target genes of *VND6/7, SND1*, and *NST1/NST2* in Arabidopsis (Zhong et al., 2008; Ohashi-Ito et al., 2010; Zhong et al., 2010 a; Yamaguchi et al., 2011; Wang et al.,2012; Table 2).These detailed analyses provide important insights into the complex regulatory network of secondary cell wall formation. In the regulatory

hierarchical network, *SND1, NST1/NST2, and VND6/7* are first-level regulators. *SND1, NST1/NST2,* and *VND6/7* have conserved function and regulate some of same downstream targets as second layer (Zhong et al., 2008). The second layer of transcription factors controlled by *SND1, NST1/NST2,* and *VND6/7* are mostly MYB transcription factors (*MYB20, MYB42, MYB43, MYB46, MYB52, MYB54, MYB58, MYB69, MYB61, MYB63, MYB83, MYB85, and MYB103*). Of these MYB transcription factors, the downstream transcription factors of *MYB46* and *MYB83* are identified in Arabidopsis (Zhong et al. 2007a, McCarthy et al. 2009; Zhong et al. 2012; Table 2), some of which are specifically involved in the regulation of lignin biosynthesis (*MYB58, MYB63 and MYB85*) while others are important for regulating secondary wall thickening (*MYB52* and *MYB54*). Furthermore, MYB46 directly regulates three secondary wall-associated cellulose synthases (*CESA4*, *CESA7*, and *CESA8*) and some lignin related enzymes (phenylalanine ammonia lyases (*PALs*), caffeoyl CoA 3-O-methyltransferases (*CCoAOMTs*)) (Ko et al., 2009; Ko et al., 2012; Kim et al., 2013). *MYB103* is expressed primarily in inter-fascicular fibers and xylem tissues (Nakano et al., 2010; Yamaguchi et al., 2010, 2011; Öhman et al., 2013). Even though RNAi-based down-regulation of MYB103 did not result in any visible phenotype, overexpression of *MYB103* in Arabidopsis resulted in thicker secondary cell walls, while dominant repression of *MYB103* resulted in thinner walls. MYB103 activated the CESA8 promoter in a protoplast transactivation system and modulated the S lignin biosynthesis via regulation of F5H (Zhong et al., 2008, Öhman et al., 2013). Another pair of MYB TFs *MYB58/ MYB63* are also the downstream genes of *MYB46/MYB83*, but are not direct target genes of secondary cell wall related NACs (Zhong et al., 2010). Dominant repression of *MYB58/MYB63* led to a reduction in secondary wall thickening and lignin content. Direct target analysis using a steroid receptor–inducible system showed that *MYB58* and *MYB63* are master regulators for lignin biosynthesis because they can specifically activate all monolignol biosynthetic genes (*PAL1*, *4CL1*, hydroxycinnamoyl CoA:shikimate/ quinate hydroxycinnamoyltransferase (*HCT*), p-coumarate 3- hydroxylase 1 (*C3H1*),C4H, *CCoAOMT1*, cinnamoyl CoA reductase

(*CCR1*), and cinnamyl alcohol dehydrogenase 6 (*CAD6*) except *F5H*, concomitant with that misexpression of *MYB58/ MYB63* generated ectopic deposition of lignin in cells that are normally unlignified. Additionally, *MYB58* can directly activate the expression of the lignin polymerization related gene laccase 4 (*LAC4*). Overexpression of another secondary wall–associated MYB protein, MYB85, results in ectopic deposition of lignin (Zhong et al., 2008). MYB85 activates lignin biosynthetic genes, but no direct targets of MYB85 have been identified. Furthermore, *MYB20, MYB26,* and *MYB69* were also up-regulated by indirect regulation of SND1/VND6/VND7, and had been shown to activate genes in secondary cell wall formation (Yang et al., 2006; Demura et al., 2010).

In addition to these MYBs, the transcription factors SND2, SND3, KNAT7 and AtC3H14 zinc finger proteins also serve as regulators in the second layer of the network, and among them, the downstream genes regulated by SND2 and KNAT7 were identified via transcriptome analyses of transgenic lines and mutant lines, respectively (Ko et al., 2009; Hussey et al.,2011; Li et al., 2012). A transcription factor complex KNAT7-MYB75-OFP has also been identified a repressor of secondary cell wall formation in Arabidopsis. KNAT7 forms a heterodimer with MYB75 to repress secondary cell wall biosynthesis both in stem and seed coat in Arabidopsis (Bhargava et al., 2010; Bhargava et al., 2013). Otherwise, KNAT7 has been shown to interact with OFP1 and OFP4, and genetic analyses suggested that the KNAT7-OFP complex also acts as a repressor regulating secondary cell wall biosynthesis (Li et al., 2011). Further research showed that KNAT7-MYB75-OFP was formed in the stem and regulates the secondary cell wall biosynthesis (Unpublished data from Douglas group). *KNAT7* is activated by SND1 and VND6/7, showed negative regulation of secondary cell wall biosynthesis. In this transcriptional repression complex, *MYB75* responds to auxin, ethylene, and jasmonic acid (Peng et al., 2011; Lewis et al., 2011; Das et al., 2012). It will be interesting to determine whether hormonal signals modulate secondary cell wall biosynthesis by controlling the expression of *MYB75*.

Studies in transcriptional regulation of cell wall biosynthesis genes in wood formation mostly focused on the function of individual transcription factors (TFs) and TF pairs, including PtrMYB2/3/20/21, PttMYB21a, PtrWND/VNSs, PtoMYB92; PtrMYB152, PtoMYB216, PtrSND1-A2^{IR}, PtrWRKY19 from poplar (Karpinska et al., 2004; Zhong et al.,2011; Ohtani et al., 2011; Li et al., 2012; Tian et al., 2013; Wang et al., 2014; Li et al., 2015; Yang et al., 2016), PtMYB1, PtMYB4, and PtMYB8 from pine (Patzlaff et al., 2003a, b), EgMYB1 and EgMYB2 from *Eucalyptus* (Goicoechea et al., 2005; Legay et al., 2010). PgMYB1/8 and PgMYB14/15 in spruce (Bomal et al., 2013). Given that *P. trichocarpa* is model species for woody plants, constructing the transcriptional regulation network of secondary cell wall biosynthesis in *P. trichocarpa* is an urgent question for the researchers in forest biotechnology and bioenergy.

1.3 Construction of transcriptional regulatory networks

1.3.1 Why need transcriptional regulatory networks for wood cell wall biosynthesis?

Gene networks are usually illustrated as nodes connected by edges. Nodes represent proteins or genes, and edges often represent relationship or interactions between nodes. For transcriptional networks, the nodes are TFs and their target genes, and edges usually represent the TF-DNA interactions. Several reasons attract us to focus on the transcriptional regulatory network (TRN)s for wood cell wall biosynthesis. Firstly, a TF–DNA interaction-based TRN was established for describing secondary cell wall biosynthesis in Arabidopsis (Taylor-Teeples et al., 2015). Some of the regulation identified from their network were not discovered by genetic analyses, including several feed-back and feed-forward loops. Therefore, network construction will provide more knowledge needed for understanding wood cell wall biosynthesis. Secondly, a transcriptional regulatory network can provide a landscape for the regulation of specific process. This would help us understand how the coordination and interactions of TFs determine the quantity and quality of the biomass and what

drives the expression of pathway enzymes spatially and temporally. Such understanding can help us generate the desired changes in chemical and physical properties of the resulting biomass for woody plants. For example, transgenic Arabidopsis plants with improved biomass production have been generated based on the knowledge from transcriptional network of secondary cell wall biosynthesis (Petersen et al., 2012). They developed a xylem-engineering approach to reintroduce xylan biosynthesis specifically into xylem vessels in the Arabidopsis *Irx7, Irx8, and Irx9* mutant backgrounds by driving the expression of the respective glycosyltransferases with vessel-specific promoters of VND6 and VND7. The Arabidopsis plants with 23% xylose reduction and 18% reduction in lignin when compared to wild type, had a 42% increase in saccharification yield. Thirdly, cell wall architecture can be affected by developmental signals and the biotic and abiotic stress (Gall et al., 2015). Illustration of the interactions and components in transcriptional regulatory networks can help us understand how the dynamics of wood cell wall biosynthesis respond to its environmental and developmental signals.

1.3.2 Approaches to construct transcriptional regulatory networks

Based on the genes initially used to generating transcriptional regulatory networks, there are two approaches: a TF-centered approach and a target gene-centered approach. The strategy of TF-centered approach is to identify the downstream target genes of the TF of interest. This approach usually is applied to the identified regulators, which have been characterized by genetic analyses. Commonly, genetic analysis could show the TFs that affect specific pathways and processes, but the underlying mechanisms are still elusive. Therefore, identifying what genes are directly regulated by the specific TFs can elucidate why the TFs function and link some unknown target enzyme genes to the biological processes. For the TF-centered approach, ChIP is the technique that usually applied to determine TF-DNA interactions. Using this technique, TFs were cross-linked with their targeted DNA sequences, and the TF-DNA

complexes were then precipitated by specific antibody. The precipitated DNA fragments were analyzed by PCR, microarray, or RNA-seq. For the transcriptional regulation of secondary cell walls, ChIP assays only identified AtVND6 and PtrSND1-B1 downstream targets (Ohashi-Ito et al., 2010; Lin et al., 2013). Other approaches, such as inducible gene expression systems, also can identify the direct targets of specific TFs. The systems rely on animal nuclear receptors, including the glucocorticoid (GR) receptor, the β-estradiol receptor, or the androgen receptor. The GR receptor and estradiol receptor coupling with posttranslational activation are widely applied for the TFs regulating secondary cell wall biosynthesis (Zhong et al., 2008; Ohashi-Ito et al., 2010; Zhong et al., 2010a; Yamaguchi et al., 2011; Wang et al.,2012; Kim et al., 2013). The receptor fused TFs stay out of the nucleus in absence of hormone such as dexamethasone. Once the animal hormone is added, the TFs can enter the nucleus and regulate their downstream targets. The protein synthesis inhibitor cycloheximide, if added along with the hormone, impairs *de novo* synthesis of new TFs and allows monitoring the transcripts of direct targets (Yamaguchi et al., 2015). This technique is usually performed in isolated protoplasts, suspension cells or in seedling that are easily treated with hormone and protein synthesis inhibitors.

In the target genes centered approach, the target genes are previously identified to participate in the specific process. The approach focuses on identifying the upstream regulators that can bind the promoters of target genes. Yeast one hybrid (Y1H) is the common technique that determine which TFs bind to the specific promoters. The technique needs a collection of cloned TFs. A large-scale TF collection enables a genome-wide identification of TF regulators for the selected genes. Y1H has been used to characterize the root expressed TFs that can regulate the enzymes of cellulose, lignin, and hemicellulose through TF-promoter interactions. Another technique used to identify interactions is the electrophoretic mobility shift assays (EMSAs). EMSA is based on the simple rationale that proteins with different size, molecular weight, and charge have different electrophoretic mobilities in a non-

denaturing gel matrix with bound to a promoter like fragment of DNA. The technique not only detects the TF-DNA interactions but also may identify the DNA motif that TFs bind to. For the cell wall component genes, the secondary wall MYB-responsive elements (SMRE motif) are bound by AtMYB46/83 and their homologs, and tracheary element-regulating cis-elements (TERE motif) are bound by AtVNDs (Zhong et al., 2012; Zhong et al., 2013; Endo et al., 2015).

1.3.3 Validation of the derived TRN through the biological effects of TFs *in planta*

Specific TFs may have many different targets. For example, Y1H assays determined that *REVOLUTA* (REV) binds to the promoters and represses the expression of genes involving monolignol biosynthesis (Taylor-Teeples et al., 2015). By contrast, a glucocorticoid receptor-based inducible assay did not identify these monolignol biosynthetic genes as targets (Reinhart et al., 2013). Thus, a transcriptional network is needed to validate their existence and their biological significance *in vivo*.

TRNs consist of TFs, target genes, and their regulatory interactions. Genetic analysis can be used to validate the occurrence of the regulatory interactions. If the regulatory interactions exist, the perturbation or overexpression of the TF will result in the change of the transcript of target genes. The test can be achieved by the misexpression of the TFs *in planta*, the transient overexpression of the TFs in protoplasts, or co-expression of the TF and promoter-GUS fusions. The validated transcriptional network would then be more convincing and robust.

1.4 Alternative splicing and transcription factor function in xylem differentiation and secondary cell wall biosynthesis

1.4.1 Competitive inhibition of transcription factor function by its own splicing variant

Alternative splicing is a frequent phenomenon in higher eukaryotes that involves the production of multiple distinct transcript isoforms from a single gene. Genome-wide studies have shown that the pre-mRNAs of around 40% of plant genes are alternatively spliced (Filichkin et al., 2010). The first role identified for alternative splicing products is a mechanism for controlling gene expression at the post transcriptional level (Lewis et al., 2003). The second role is a mechanism for increasing protein diversity (Nilsen et al., 2010). In animals, the alternatively spliced isoforms of transcription factors usually play a negative role in regulating gene expression. The E3 transcriptional activator mTFE3 regulates the expression of a immunoglobulin heavy chain gene by binding its promoter (Roman et al., 1991). The truncated proteins were generated from spliced E3 mRNA, which lacks 105 nucleotides encoding the transcriptional activation domain (Roman et al., 1991). The spliced isoform can efficiently lower the transcriptional activation activity by forming a heterodimer with the full length *mTFE3* (Roman et al., 1991). The alternative splicing isoform of transcription factors serve as dominate negative regulators not only for the transcriptional activator, but also for transcriptional repressors. The transcriptional repressor TEL/ETV6 acts as a suppressor for tumor formation (Sasaki et al., 2004). The splicing variant lacking the DNA-binding domain can form a heterodimer with the TEL proteins and inhibit the activities of these TEL proteins (Sasaki et al., 2004).

Alternative splicing is involved in most plant processes (Reddy et al., 2013; Staiger et al., 2013). The small interfering peptides generated from alternative splicing often play a primary role inhibiting the dimerization of transcription factors in plants. The complete structure of transcription factors commonly consists of three protein domains

responsible for DNA binding, dimerization, and activation or repression. Alternative splicing of one single transcription factor gene can produce multiple proteins with different domain compositions and activities. Truncated proteins generated from alternative splicing of transcription factors have incomplete domain composition and can negatively regulate the target transcription factors by interfering with the dimerization process (Seo et al., 2011b; Seo et al., 2013). Transcription factors that generate a truncated splicing variant serve as the dominant repressors in many biological processes such as starch metabolism, cold tolerance, flowering time control and secondary cell wall formation. Alternative splicing of the Arabidopsis *INDETERMINATE DOMAIN 14 (IDD14*) gene regulates starch metabolism (Seo et al., 2011a). In response to cold stress, IDD14 not only generates a functional full size IDD14α, but also produces non-functional truncated IDD14β. The IDD14β that lacks the DNA-binding domain can interact with IDD14α to interfere with the formation of functional IDD14α homodimers. Meanwhile, overexpression of IDD14α can reduce the starch content, whereas overexpression of IDD14β increases the starch content in Arabidopsis. Accordingly, the IDD14α negatively regulates starch metabolism. Furthermore, the alternative splicing of transcription factors not only interfere with the formation of the functional homodimers, but also affects the formation of the functional heterodimers. For example, the heterodimers formed by *CCA1* and *LHY* transcriptionally regulate the *DEHYDRATION REPSONSIVE ELEMENTS BINDING FACTORS* for regulating the cold tolerance (Dong et al., 2012). The *CCA1* gene undergoes alternative splicing and produces two splice variants, CCA1α and CCA1β (Park et al., 2012; Seo et al., 2012). The truncated CCA1β form lacks a MYB DNA-binding domain, but has domains for dimerization and transcriptional regulation. It inhibits the formation of the DNA binding CCA1α-LHY heterodimer to generate the dimers CCA1α- CCA1β, whereas CCA1α-LHY can bind to the *CBF* gene promoters for induction of freezing tolerance (Dong et al., 2010; Seo et al., 2012). Genetic evidence also showed that the *35S:CCA1β* transgenic plants exhibit a phenotype which is similar to the the *cca1α-lhy* double mutant. These observations confirmed the

inhibitory role of the truncated CCA1β in cold freezing via interfering with the function of CCA1α and LHY. Not only does the transcription factor mRNA intron retention result in non-functional small peptides, but the exon skipping of transcription factor mRNA may also generate interfering splicing variants. A *Poncirus trifoliata* MADS-box gene homologous with an Arabidopsis flowering time vital player *Flowering LOCUS C,* can generate five splice variants. The smaller splice variants possibly act as dominant negative repressors by forming complexes with the functional transcription factors (Chen and Coleman, 2006; Zhang et al., 2009). Recently, *FLOWERING LOCUS M* (*FLM*) has been found to generate two protein splice variants, FLM-β and FLM-δ that compete for the interaction with the floral repressor SHORT VEGETATIVE PHASE (SVP) (Posé et al., 2013). SVP-FLM-β serves as the repressor for the flowering at low temperature, whereas SVP- FLM-δ acts as activator of flowering at higher temperature.

1.4.2 Splicing variants of wood associated NAC transcription factors negatively regulate secondary cell wall formation in *P. trichocarpa*

Genome-wide detection of alternative splicing in non-woody plants such as Arabidopsis and rice have been conducted in various tissues, cell types and under different treatments (Campbell et al., 2007; Filichkin et al., 2010). Recently, comprehensive analyses of alternative splicing revealed the high level of alternative splicing in *P. trichocarpa* (Bao et al., 2013). In this study, 149 cell wall biosynthesis related genes have evidence for alternative splicing, accounting for 38.9% of total cell wall biosynthesis related genes in *P. trichocarpa* genome. Upstream regulators transcription factors also have a high proportion (38.7%) that undergo the alternative splicing. Among these alternative splicing events that happen in the secondary cell wall related NAC family and MYB family, most of them are unique to one individual of all 18 trees, such *as SND1-A1, SND1-A2, SND1-B1*, and *SND1-B2*, suggesting that alternative splicing event may be induced by environmental conditions and genomic differences. The splice variant of *PtrSND1-A2* has been analyzed in detail (Li et al.,

2012b). PtrSND1-A2 is a master regulator in secondary cell wall biosynthesis and can activate *PtrMYB021* and ectopic expression of *PtrSND1-A2* results in xylogenesis (Mitusha et al., 2012). Splicing of *PtrSND1-A2* mRNA produces a truncated isoform through intron retention. The truncated isoform can suppress the expression of *PtrSND1* family members and *PtrMYB021*, suggesting an inhibitory role of the truncated isoform in secondary cell wall formation. Yeast two-hybrid, subcellular localization, and Biomolecular Fluorescence Complementation (BIFC) demonstrated that the truncated PtrSND1-A2 protein forms non-functional heterodimers with members of the *PtrSND1* family (Li et al., 2012b). Although the detailed functional analyses of PtrSND1-A2 splice variant have been conducted in *Populus*, many questions about other splicing variants of secondary cell wall related NACs needed to be investigated. Until now, no studies showed under what conditions the alternative splicing of secondary cell wall related NACs mRNAs are dramatically altered in expression. Identification of such conditions will be helpful for analyzing how the expression of these NACs are regulated at the post-transcriptional level.

1.5 Protein-protein interactions affect the function of NAC domain transcription factors

Several transcription factors have been shown to be involved in the regulation of NAC expression (Soyano et al., 2008; Yamaguchi et al., 2010). As a negative regulator for VNDs, VNI2, a naturally expressed NAC, was identified to interact with VND7 using a yeast two hybrid system (Yamaguchi et al., 2010). Both *35S::VNI2-SRDX* and *35S::VNI2* exhibited discontinuous vessel formation, suggesting that VNI2 is a repressor for vessel formation. This phenotype was also found in the plant overexpressing VND7-SRDX (Kubo et al., 2005) or C-terminally truncated VND7 (Yamaguchi et al., 2008), suggesting a functional interaction of VND7 and VNI. Expression profiles of VNI2 overexpressing plants showed that the downstream genes of VND7 are also down-regulated by VNI2 overexpression. These results suggested that VNI2 may form a non-functional heterodimer or repression heterodimer with

VND7 to regulate xylem development (Yamaguchi et al., 2010a). Conversely, LBD18/30 have been identified as the activators of VNDs. Overexpression of LBD18/LBD30 induced the formation of tracheary element-like cells, and ectopic expression of VND7 was detected in LBD18 overexpressing plants (Soyano et al., 2008). By investigating the VND6/7s and their activators and inhibitors, mounting evidences that VND6/7s may themselves be under positive and negative regulation (Figure 3). VNI2 negatively regulates the expression of VND7 and the expression of VNI2 has been shown to be up-regulated by VND7 in Arabidopsis and poplar (Yamaguchi et al., 2010b; Ohtani et al., 2011), suggesting that VNDs can be regulated under a negative feedback loop. Likewise, the VND6/7 activators LBD18/LBD30 are also directly activated by VND6/7, showing a positive feedback loop for VND7 expression (Soyano et al., 2008).

In Arabidopsis, the auxin, cytokinin, and brassinosteroids that play roles in xylem vessel formation can increase the expression of VND6 and VND7 using promoter-GUS fusions (Kubo et al., 2005). But no direct evidences showed how these hormones regulated the expression of VND6 and VND7. By investigating the existence of both positive and negative feedback regulation of VNDs, the regulatory effects of hormone towards VNDs have begun to be elucidated. The VND activators LBD18/LBD30 respond to auxin (Chapman et al., 2009), and the dominant negative suppression of LBD18/LBD30 poplar homologs caused the decrease in diameter growth and highly irregular phloem development in *Populus tremula x Populus alba* (Yordan et al., 2010). LBD18/LBD30 may transfer auxin signals to VND6/VND7, and they function together to regulate the xylem development and secondary cell formation. Additionally, an inhibitor of VNDs, VNI, can be regulated by ABA (Yang et al., 2011), suggesting that ABA may repress the activity of VNDs through regulating VNI. ABA plays a critical role in response to various stress signals, including biotic stress. VND7 has been shown to relate to biotic stress (Reusche et al., 2012). In *Brassica napus* and *Arabidopsis thaliana*, verticillium infection can induce *de novo* xylem formation via

controlling VND7 (Reusche et al., 2012). Taken together, VNDs can be affected by various upstream signals to induce xylem vessel development and secondary cell wall formation. To further understand the molecular mechanisms of how VND6 and VND7 receive upstream signals from the environment stimuli and hormones and regulate the secondary cell wall formation and xylem development, the downstream genes of VNDs need to be analyzed in overexpression plants or cells (Kyoko et al., 2010; Yamaguchi et al., 2011, Ohtani et al., 2011).

Table 1. The TFs regulating vascular meristem maintenance, proliferation, and differentiation.

Type of meristems	*Developmental activities*	*Transcription factor*	*Gene family*	*References*
Vascular meristem	*Stem cell initiation, maintance and proliferation*	*AtMP*	*ARF*	*Hamann et al., 2002; Scarpella et al., 2006; Donner et al., 2009*
		AtBDL	*IAA*	*Hamann et al., 2002*
		AtMYC2	*MYC*	*Thines et al., 2007; Sehr et al., 2010*
		AtWOX4	*WOX*	*Hirawaka et al., 2010; Suer et al., 2011*
		PtaLBD1	*LBD*	*Yordanov et al, 2010*
		AtARK1/PtoARK1	*KNOX*	*Andrew et al., 2006; Gerttula et al., 2015*
		PtoARK2	*KNOX*	*Du et al., 2009*
		AtKAN	*GARP*	*Emery et al., 2003; Llegems et al., 2010*
	Stem cell differentiation	*AtHB8*	*HB*	*Hardtke & Berleth, 1998; Donner et al., 2009*
		AtPHB	*HD-ZIP*	*Carlsbecker et al., 2010*
		AtPHV	*HD-ZIP*	*Carlsbecker et al., 2010*
		AtREV	*HD-ZIP*	*Carlsbecker et al., 2010*
		AtHB15	*HD-ZIP*	*Carlsbecker et al., 2010*
		AtVND6	*NAC*	*Kubo et al., 2005*
		AtVND7	*NAC*	*Kubo et al., 2005*
		AtAPL	*MYB*	*Bonke et al., 2003*
		AtHCA2	*DOF*	*Guo et al., 2009*

Table 2. 202 TFs in Arabidopsis have been found to regulate cell wall biosynthetic genes.

Species	Transcription factors (TFs)	Gene ID	Downstream regulatory targets			References
			Monolignol biosyntheic enzymes	Secondary wall cellulose synthases	Hemicellulose enzymes	
Arabidopsis thaliana	AtMYB4	AT4G38620	AtC4H At4CL1 At4CL3			Jin et al., 2000
	AtMYB20	AT1G66230	AtPAL1 AtC4H At4CL1 AtC3H1 AtHCT AtCCoAOMT1 AtCCR1 AtC4H			Öhman et al., 2013; Taylor-Teeples., 2015
	AtMYB32	AT4G34990	AtCOMT			Preston et al., 2004
	AtMYB46	AT5G12870	At4CL1 At4CL2 At4CL4 AtCCoAOMT1 AtPAL1 AtPAL4 AtC4H AtC3H1 AtCAD2 AtCAD6	AtCESA4, 7, 8	AtIRX8, 9, 10, 14, 15, FRA8	Kim et al., 2013; Ko et al., 2009; Zhong et al., 2007; Zhong et al., 2012
	AtMYB52	AT1G17950	AtCCoAOMT1 AtPAL4	AtCESA8	AtIRX9	Ko et al., 2009
	AtMYB54	AT1G73410	At4CL1	AtCESA8	AtIRX9	Zhong et al., 2008
	AtMYB58	AT1G16490	AtPAL1 AtC4H At4CL1 AtC3H1 AtHCT AtCCoAOMT1 AtCCR1 AtCOMT AtCAD6			Zhou et al., 2009; Mitsuda et al., 2010; Taylor-Teeples., 2015
	AtMYB61	AT1G09540	AtCCoAOMT7			Romano et al., 2012
	AtMYB63	AT1G79180	AtPAL1 AtC4H At4CL1 AtC3H1 AtHCT1 AtCCoAOMT1 AtCCR1			Zhou et al., 2009, Taylor-Teeples., 2015
	AtMYB75	AT1G56650	AtPAL1 AtC4H At4CL1 AtC3H1 AtHCT AtCCoAOMT1 AtF5H1	AtCESA4, 7, 8	AtIRX8, 9	Bhargava et al., 2010
	AtMYB83	AT3G08500	At4CL1 AtCCoAOMT1 AtPAL1 At4CL1 AtHCT	AtCESA4, 7, 8	AtFRA8	McCathy et al., 2009; Zhong et al., 2012; Taylor-Teeples., 2015
	AtMYB85	AT4G22680	At4CL1AtC4H At4CL1 AtHCT AtCCoAOMT1			Zhong et al., 2009; Taylor-Teeples., 2015
	AtMYB103	AT1G63910	AtF5H1 AtCCoAOMT1 At4CL1 AtHCT	AtCESA8		Zhong et al., 2008; Ohman et al., 2013; Taylor-Teeples., 2015
	AtSND1/AtNST3	AT1G32770	At4CL1 AtCCoAOMT1 AtPAL1 At4CL3 AtCCoAOMT1	AtCESA4, 7, 8	AtIRX6, 8,9,10,13, 14, AtGXM1, 2, 3,,	Zhong et al., 2006; Kim et al., 2007; Ohashi-Ito et al., 2010, Lee et al., 2012
	AtSND2	AT4G28500	AtCCoAOMT1	AtCESA4, 7, 8	AtCSLA9, AtIRX10,	Hussey et al., 2011
	AtSND3	AT1G28470		AtCESA8		Zhong et al., 2008
	AtNST1	AT2G46770	AtCCR1 AtCOMT1	AtCESA4, 7, 8	AtIRX8,13,	Mitsuda et al., 2005; Kim et al., 2007;
	AtNST2	AT3G61910	AtCCR1			Mitsuda et al., 2005; Mitsuda et al.,
	AtVND1	AT2G18060	AtPAL1 AtHCT AtCCoAOMT1	AtCESA4, 7, 8	ATGATL1, AtFRA8, AtIRX9	Zhou et al., 2014
	AtVND2	AT4G36160	AtPAL1 AtHCT AtCCoAOMT1	AtCESA4, 7, 8	ATGATL1, AtFRA8,	Zhou et al., 2014
	AtVND3	AT5G66300	AtPAL1 AtHCT AtCCoAOMT1	AtCESA4, 7, 8	ATGATL1, AtFRA8,	Zhou et al., 2014
	AtVND4	AT1G12260	AtPAL1 AtHCT AtCCoAOMT1	AtCESA4, 7, 8	ATGATL1, AtFRA8,	Zhou et al., 2014
	AtVND5	AT1G62700	AtPAL1 AtHCT AtCCoAOMT1	AtCESA4, 7, 8	ATGATL1, AtFRA8,	Zhou et al., 2014
	AtVND6	AT5G62380	AtCCoAOMT7	AtCESA4		Yamaguchi et al., 2010
	AtVND7	AT1G71930	AtCCoAOMT7	AtCESA4, 8	AtIRX10, 13, 14	Yamaguchi et al., 2010
	AtKNAT1	AT4G08150	AtCOM AtCCoAOMT			Meele et al., 2003
	AtKNAT7	AT1G62990	AtPAL1 AtC4H At4CL1 AtC3H1 AtHCT1 AtCCoAOMT1 AtCOMT	AtCESA7, 8	AtFRA8,AtIRX8,9	Li et al., 2012
	AtC3H14	AT1G66810	AtCCoAOMT1 AtPAL4 AtCAD6 AtCCoAOMT1 AtPAL4	AtCESA4	AtFRA8, AtIRX15, AtGXM3	Ko et al., 2009; Chai et al., 2015
	AtC3H15	AT1G68200	AtCCoAOMT1 AtCAD6	AtCESA4	AtFRA8, AtIRX15,	Chai et al., 2015
	AtWRKY13	AT4G39410	AtPAL4, At4CL1, AtCAD6,	AtCESA7, 8		Taylor-Teeples., 2015
	AtANAC032	AT1G77450	At4CL1 AtHCT1 AtC3H1			Taylor-Teeples., 2015
	AtANAC087	AT5G18270	AtHCT1 At4CL1 AtC4H			Taylor-Teeples., 2015
	AtANAC102	AT5G63790	At4CL1 AtC3H AtHCT AtCCoAOMT1 AtCAD4			Taylor-Teeples., 2015
	AtTED5	AT5G11260	AtPAL1 AtC4H AtHCT1			Taylor-Teeples., 2015
	AtAP-LIKE	AT1G12630	AtC4H AtHCT1			Taylor-Teeples., 2015
	AtTLP6	AT1G47270	AtC4H			Taylor-Teeples., 2015
	AtCBF2	AT4G25470	AtC3H			Taylor-Teeples., 2015
	AtCBF4	AT5G51990	AtC3H AtC4H AtCAD4			Taylor-Teeples., 2015
	AtASIL1	AT1G54060	AtC4H AtHCT AtCCoAOMT1 AtCAD4			Taylor-Teeples., 2015
	AtASIL2	AT3G14180	AtC4H			Taylor-Teeples., 2015
	AtHB9	AT1G30490	At4CL1 AtC4H			Taylor-Teeples., 2015
	AtERF2	AT5G47220	AtCCR1			Taylor-Teeples., 2015
	AtERF4	AT3G15210	AtC4H			Taylor-Teeples., 2015
	AtERF9	AT5G44210	AtC4H			Taylor-Teeples., 2015
	AtERF109	AT4G34410	AtCCoAOMT1			Taylor-Teeples., 2015
	AtRAP2.12	AT1G53910	AtHCT			Taylor-Teeples., 2015
	AtE2F2	AT1G47870	AtC4H AtCAD4			Taylor-Teeples., 2015
	AtBLH3	AT1G75410	AtC4H			Taylor-Teeples., 2015

Table 2. Continued

Species	Transcription factors (TFs)	Gene ID	Downstream regulatory targets			References
			Monolignol biosyntheic enzymes	Secondary wall cellulose synthases	Hemicellulose enzymes	
Arabidopsis thaliana	AtOBF5	AT5G06960	AtC3H			Taylor-Teeples., 2015
	AtbZIP12	AT2G47460	At4CL1			Taylor-Teeples., 2015
	AtbZIP17	AT2G40950	AtC4H			Taylor-Teeples., 2015
	AtbZIP19	AT4G35040	AtC3H			Taylor-Teeples., 2015
	AtILR3	AT5G54680	AtHCT1 AtC3H AtC4H AtCAD4			Taylor-Teeples., 2015
	AtCIB3	AT3G07340	AtC3H			Taylor-Teeples., 2015
	AtNF-YB10	AT3G53340	AtC4H			Taylor-Teeples., 2015
	AtDREB-LIKE	AT4G28140	AtCCoAOMT1			Taylor-Teeples., 2015
	ATWIND1	AT1G78080	AtCCoAOMT1			Taylor-Teeples., 2015
	AtRAP2.4	AT1G22190	AtCCoAOMT1			Taylor-Teeples., 2015
	AtDREB26	AT1G21910	At4CL1 AtC4H			Taylor-Teeples., 2015
	AtStorekeeper 1	AT1G61730	AtC3H AtC4H AtCCR1 At4CL1			Taylor-Teeples., 2015
	AtEIL1	AT2G27050	AtC4H			Taylor-Teeples., 2015
	AtARID	AT1G20910	AtHCT1 AtC3H AtC4H AtCAD4			Taylor-Teeples., 2015
	ATHB6	AT2G22430	AtC3H			Taylor-Teeples., 2015
	AtHB30	AT5G15210	At4CL1 AtC3H			Taylor-Teeples., 2015
	AtHB34	AT3G28920	AtC3H			Taylor-Teeples., 2015
	AtHB-LIKE 1	AT5G01380	AtC3H			Taylor-Teeples., 2015
	AtHB-LIKE 2	AT1G19000	AtC3H			Taylor-Teeples., 2015
	AtAGL16	AT3G57230	At4CL1			Taylor-Teeples., 2015
	AtHAP5c	AT1G08970	At4CL1			Taylor-Teeples., 2015
	AtOBP4	AT5G60850	AtHCT1 At4CL1 AtC3H			Taylor-Teeples., 2015
	AtPAT1	AT5G48150	At4CL1 AtHCT			Taylor-Teeples., 2015
	AtTMO6	AT5G60200	At4CL1 AtC3H			Taylor-Teeples., 2015
	AtDDF1	AT1G12610	At4CL1 AtC3H AtHCT AtCCoAOMT1			Taylor-Teeples., 2015
	AtWRKY15	AT2G23320	AtCCoAOMT1			Taylor-Teeples., 2015
	AtTCP14	AT3G47620	AtCCoAOMT1			Taylor-Teeples., 2015
	AtAIF2	AT3G06590	AtCCR1			Taylor-Teeples., 2015
	AtC2H2-LIKE	AT2G29660	AtCCR1			Taylor-Teeples., 2015
	AtMNM1	AT5G54930	AtC3H			Taylor-Teeples., 2015
	AtGRF1	AT2G22840	AtC3H			Taylor-Teeples., 2015
	AtBBX22	AT1G78600	AtC3H			Taylor-Teeples., 2015
	AtBBX31	AT3G21890	AtC3H			Taylor-Teeples., 2015
	AtGIS1	AT3G58070	AtC3H			Taylor-Teeples., 2015
	AtHSFB2A	AT5G62020	AtC3H			Taylor-Teeples., 2015
	AtGT-1	AT1G13450	AtC3H			Taylor-Teeples., 2015
	AtVHB-1	AT3G11280	AtC3H			Taylor-Teeples., 2015
	AtZML2	AT1G51600	AtHCT1			Taylor-Teeples., 2015
	Alcohol dehydrogenase Myb/SANT-like TF	AT2G44730	AtC3H AtCCR2 AtC4H AtCAD4 AtCCoAOMT7	AtCESA4, 7 AtIRX6	AtGUX2 AtIRX9	Taylor-Teeples., 2015
	AtGRF3	AT2G36400			AtIRX9	Taylor-Teeples., 2015
	AtTG	AT1G36060			AtIRX9	Taylor-Teeples., 2015
	AtEIL3	AT1G73730			AtIRX9	Taylor-Teeples., 2015
	AtHAT1	AT4G17460			AtIRX9	Taylor-Teeples., 2015
	ATHB33	AT1G75240			AtIRX9	Taylor-Teeples., 2015
	ABF4	AT3G19290			AtIRX9	Taylor-Teeples., 2015
	ATBZIP54	AT4G01120		AtCESA4, 7	AtIRX9 AtGUX2	Taylor-Teeples., 2015
	AtBZIP30	AT2G21230		AtCESA4, 7	AtIRX9 AtGUX2	Taylor-Teeples., 2015

Table 2. Continued

Species	Transcription factors (TFs)	Gene ID	Downstream regulatory targets			References
			Monolignol biosyntheic enzymes	Secondary wall cellulose synthases	Hemicellulose enzymes	
Arabidopsis thaliana	AtDEAR3	AT2G23340			AtIRX9	Taylor-Teeples., 2015
	ATMYB73	AT4G37260	At4CL1, AtCAD4, AtHCT	AtCESA7, 8	AtIRX9, 10 AtFRA8 AtGUX1, 2	Taylor-Teeples., 2015
	AtERF105	AT5G51190	AtPAL4	AtIRX6	AtIRX9	Taylor-Teeples., 2015
	AtCRF7	AT1G22985			AtIRX9	Taylor-Teeples., 2015
	AtZFP7	AT1G24625			AtIRX9, AtGUX1	Taylor-Teeples., 2015
	AtDF1	AT1G76880	AtC4H	AtIRX6	AtIRX9 FRA8 GUX2	Taylor-Teeples., 2015
	AtERF3	AT1G50640		AtIRX6	AtGXM3 AtIRX 9	Taylor-Teeples., 2015
	AtAIL6	AT5G10510		AtCESA4, 7 AtIRX6		Taylor-Teeples., 2015
	AtARF9	AT4G23980	AtPAL4	AtCESA4, 7, 8 AtIRX6	AtGUX2	Taylor-Teeples., 2015
	AtRVE4	AT5G02840	AtPAL4	AtCESA4		Taylor-Teeples., 2015
	AtAP2	AT4G36920		AtCESA7		Taylor-Teeples., 2015
	AtDREB2A	AT5G05410		AtCESA7	AtGUX2	Taylor-Teeples., 2015
	AtHB21	AT2G02540		AtCESA8	AtFRA8	Taylor-Teeples., 2015
	AtHB23	AT5G39760		AtCESA8	AtFRA8	Taylor-Teeples., 2015
	Duplicated	AT5G08520		AtCESA8		Taylor-Teeples., 2015
	AtERF107	AT5G61590			AtGXM3	Taylor-Teeples., 2015
	AtTCP20	AT3G27010		AtIRX6	AtGXM3	Taylor-Teeples., 2015
	AtERF70	AT1G71130		AtIRX6	AtGXM3	Taylor-Teeples., 2015
	AtLEP	AT5G13910		AtIRX6	AtGXM3	Taylor-Teeples., 2015
	C2H2 zinc finger TF	AT4G27240			AtIRX10	Taylor-Teeples., 2015
	AtGATA8	AT3G54810	AtPAL4		AtIRX10	Taylor-Teeples., 2015
	AtWRKY20	AT4G26640			AtIRX10	Taylor-Teeples., 2015
	AtGATA26	AT4G17570			AtIRX10	Taylor-Teeples., 2015
	AtMYB13	AT1G06180	At4CL1 AtHCT			Taylor-Teeples., 2015
	ATBZIP12	AT2G41070	At4CL1	AtIRX6		Taylor-Teeples., 2015
	ATMYB86	AT5G26660	At4CL1 AtC4H AtCCoAOMT1 AtHCT			Taylor-Teeples., 2015
	AtMYB3	AT1G22640	At4CL1 AtC4H AtHCT			Taylor-Teeples., 2015
	AtMYB56	AT5G17800	AtC4H			Taylor-Teeples., 2015
	AtGATA19	AT4G36620	AtPAL4			Taylor-Teeples., 2015
	AtMYB3R-4	AT5G11510	AtPAL4			Taylor-Teeples., 2015
	AtERF6	AT4G17490	AtPAL4			Taylor-Teeples., 2015
	AtCAMTA2	AT5G64220	AtPAL4			Taylor-Teeples., 2015
	AtREVOLUTA	AT5G60690	AtPAL4			Taylor-Teeples., 2015
	AtGATA12	AT5G25830			AtGUX1	Taylor-Teeples., 2015
	AtGATA4	AT3G60530			AtGUX1	Taylor-Teeples., 2015
	AtBHLH13	AT1G01260			AtGUX1	Taylor-Teeples., 2015
	AtDREB19	AT2G38340			AtGUX1	Taylor-Teeples., 2015
	AtGATA9	AT4G32890			AtGUX1	Taylor-Teeples., 2015
	RING/U-box TF	AT3G62240	AtCCoAOMT7			Taylor-Teeples., 2015
	storekeeper TF	AT4G25210			AtGUX2	Taylor-Teeples., 2015
	AtAIF3	AT3G17100			AtGUX2	Taylor-Teeples., 2015
	AtARF12	AT1G34310			AtGUX2	Taylor-Teeples., 2015
	AtGBF3	AT2G46270			AtGUX2	Taylor-Teeples., 2015
	AtERF104	AT5G61600		AtIRX6		Taylor-Teeples., 2015
	AtERF5	AT5G47230		AtIRX6		Taylor-Teeples., 2015
	AtERF7	AT3G20310		AtIRX6		Taylor-Teeples., 2015
	ANAC053	AT3G10500		AtIRX6		Taylor-Teeples., 2015

Table 2. Continued

Species	Transcription factors (TFs)	Gene ID	Downstream regulatory targets			References
			Monolignol biosyntheic enzymes	Secondary wall cellulose synthases	Hemicellulose enzymes	
Arabidopsis thaliana	ARID/BRIGHT DNA-binding TF	AT1G76510		AtIRX6		Taylor-Teeples., 2015
	AtBHLH121	AT3G19860		AtIRX6		Taylor-Teeples., 2015
	AtERF11	AT1G28370		AtIRX6		Taylor-Teeples., 2015
	AtERF-LIKE	AT5G61890		AtIRX6		Taylor-Teeples., 2015
Antirrhinum	AmMYB308	P81393	Am4CL			Tamagnone et al., 1998
Brachypodium	BdSWN5			BdCesA4		Valdivia et al., 2013
Chrysanthemum morifolium		JF795917	At4CL1, AtHCT, AtCCR1, AtF5H	AtCesA4, 7, 8	AtIRX8, 9	Zhu et al., 2013
Eucalyptus gunnii	EgMYB1	CAE09058	EgCCR, EgCAD2; PtrPAL2, Ptr4CL3, PtrCOMT2, PtrHCT1, PtrCCR2, PtrCAD1, PtrC3H3, PtrC4H1, PtrC4H2	PtrCesA1, 2, 3	PtrFRA8, PtrIRX8	Legay et al., 2007, Legay et al., 2010
	EgMYB2	CAE09059	NtPAL, NtC4H, Nt4CL, NtC3H, NtHCT, NtCOMT, NtF5H,			Goicoechea et al., 2005
Eriobotrya japonica	EjMYB1	KF767453	Ej4CL1; Nt4CL1; AtPAL1, AtPAL2, AtC4H, At4CL1, At4CL2, AtHCT,			Xu et al., 2014
	EjNAC1	KJ919962	EjPAL1, Ej4CL1; AtPAL1, AtPAL2, AtC4H, At4CL1, AtHCT,			Xu et al., 2015
Gossypium hirsutum	GhMYB7	AAS92346	AtPAL1, At4CL1, AtCCoAOMT1	AtCesA4, 7, 8		Huang et al., 2016
	GhMYBL1	KF430216	AtPAL1, At4CL1, AtCCoAOMT1, AtF5H1	AtCesA4, 7, 8	AtFRA8, AtIRX12	Sun et al., 2015
	GhKNL1	KC200250		GhCesA1, 2, 4		Gong et al., 2014
Leucaena	LlMYB1	GU901209	NtPAL, NtC4H, Nt4CL, NtC3H, ,			Omer et al., 2013
Medicago	MtNST1		MtF5H1	MtCesA4, 7, 8	MtIRX8, 14, AtIRX1	Zhao et al., 2010a; Zhao et al., 2010b
Nicotiana tabacum	NtMYBBJS1	BP137305	NtPAL, NtC4H, Nt4CL, Nt4CL			Gális et al., 2006
	NtLIM	AFY06680	NtPAL, NtCAD, Nt4CL,			Kawaoka et al., 2000
Oryza sativa	OsMYB46	Os12g33070	Os4CL1	OsCesA7	OsFRA8	Zhong et al., 2011
	OsMYB55/61	Os01g0285300	OsCAD2			Hirano et al., 2013
	OsMYB58/63	Os04g0594100	OsCAD2			Hirano et al., 2013
	OsMYB103L	Os08g05520		OsCesA4, 7, 9		Yang et al., 2014
	OsSWN1	Os05g37080		OsCesA4, 7		Chai et al., 2015
	OsSHN2	Os06g40150	Os4CL, OsCAD	OsCesA1, 4, 7, 9		Ambavaram et al., 2011
	OsNAC029			OsCesA4, 7, 9		Huang et al., 2014
	OsNAC031			OsCesA4, 7, 9		Huang et al., 2014
	OsMYB061			OsCesA4, 7, 9		Huang et al., 2014
	OsSH5	Os05g38120	OsPAL1, OsCCR2, OsCCR19, OsCOMT2			Yoon et al., 2014
	OsBLH6	Os03g0165300	OsCAD2			Hirano et al., 2013
	OsRSS3	Os11g0446000	OsPAL, OsCAD, OsCOMT			Toda et al., 2013
Panicum virgatum	PvMYB4	JF299185	PvPAL, PvC4H, Pv4CL, PvC3H, PvHCT, PvCOMT, PvF5H, PvCCoAOMT, PvCCR, PvCAD			Shen et al., 2012
Picea glauca	PgMYB1/8	ABQ51217/ABQ51224	PgCOMT, Pg4CL	PgCesA		Bomal et al., 2013
	PgMYB14/15		PgCOMT, Pg4CL			Bomal et al., 2013
Pinus taeda	PtMYB1	AY356372	PtPAL, Pt4CL, PtCOMT, PtHCT, PtCOMT, , PtCCoAOMT, PtCCR, PtCAD, PtC3H, PtC4HPtPAL2PtPAL			Patzlaff et al., 2003a; Bomal et al., 2008; Blanca et al., 2013
	PtMYB4	AY356371	PtCOMT, PtCCoAOMT, PtCCR, PtC3H, PtPAL			Patzlaff et al., 2003b; Blanca et al., 2013
	PtMYB8	DQ399057	PtPAL, Pt4CL, PtCOMT, PtHCT, PtCCR, PtCAD, PtC3H, PtC4H,			Bomal et al., 2008; Blanca et al., 2013
Populus trichocarpa	PtrMYB2	Potri.001G258700	At4CL1, AtCCoAOMT1; PtCOMT1, PtCCoAOMT1	PtrCesA4, 8, 17	PtrGT43B, PtrGT47c, PtrIRX10	McCarthy et al., 2010; Zhong et al., 2013
	PtrMYB3	Potri.001G267300	PtCOMT1, PtCCoAOMT1	PtrCesA4, 8, 17	PtrGT43B, PtrGT47c, PtrIRX10	McCarthy et al., 2010; Zhong et al., 2013
	PtrMYB20	Potri.009G061500	PtCOMT1, PtCCoAOMT1	PtrCesA4, 8, 17	PtrGT43B, PtrGT47c, PtrIRX10	McCarthy et al., 2010; Zhong et al., 2013
	PtrMYB21	Potri.009G053900	PtCOMT1, PtCCoAOMT1	PtrCesA4, 8, 17	PtrGT43B, PtrGT47c, PtrIRX10	McCarthy et al., 2010; Zhong et al., 2013
	PtrMYB152	Potri.017G130300	At4CL1, AtHCT, AtC3H1, AtCCoAOMT1, AtCAD6;PtrPAL4, Pt4CL3, Ptr4CL5, PtrC4H2, PtrCCoAOMT1, PtrCCR2, PtrHCT1	PtrCesA2B, 3A	PtrGT43B, D	Li et al., 2014; Wang et al., 2014
	PtrWND2B	Potri.002G178700	PtrCOMT2, PtrCCoAOMT1	PtrCesA4, 7, 8, 17, 18	PtrGT43A, PtrGT47C	Zhong et al., 2011
	PtrWND6B	Potri.019G083600	PtrCOMT2, PtrCCoAOMT1	PtrCesA4, 8, 17	PtrGT43A, PtrGT47C	Zhong et al., 2011
	PtrWRKY19	Potri.014G050000	PtoCAD1, PtoCCR2, PtoC4H2	AtCesA8		Yang et al., 2015

Table 2. Continued

Species	Transcription factors (TFs)	Gene ID	Downstream regulatory targets			References
			Monolignol biosyntheic enzymes	Secondary wall cellulose synthases	Hemicellulose enzymes	
Populus tomentosa Carr. Populus tremula × tremuloides	PtoMYB216	AFI80906	PtoPAL4, , Pto4CL5, PtoC4H2, PtoC3H3	PtoCesA3A	PtrGT43B, D	Tian et al., 2013
	PttMYB21a	AF062888	PttCCoAOMT2			Karpinska et al., 2004
Populus alba × Solanum lycopersicum	PttARK2	Potri.002G113300	PttF5H, PttCOMT, PttC3H, Ptt4CL,	PttCesA1,PttCesA2, Ptt		Du et al., 2009
	LeT6	AF000141	LeCAD; Nt4CL, NtCAD, NtCCR			Townsley et al., 2013
Sorghum bicolor	SbbHLH1	Sb03g046090	At4CL1, AtHCT, AtCOMT, AtPAL1,			Yan et al., 2013
Triticum aestivum	TaMYB4	JF746995	NtCAD, NtCCR; OsCAD			Ma et al., 2011
Vitis vinifera	VvMYB5a	AY555190	NtCCoAOMT1, NtCCoAOMT6			Deluc et al., 2006
	VvWRKY2	AY596466	NtCOMT1, NtPAL2, NtC4HNtC4H			Guillaumie et al., 2010
Zea mays	ZmMYB31	NP_001105949	AtCOMT, At4CL, AtC3H, AtF5H; ZmCOMT, ZmF5H			Fornalé et al, 2010
	ZmMYB42	NP_001106009	AtCOMT,			Fornalé et al, 2006
	ZmKN1	NP_001105436	Nt4CL, NtCAD, NtCCR			Townsley et al., 2013

REFERENCES

1. Anders N, Dupree P. Glycosyltransferases of the GT43 family. *Annual Plant Reviews: Plant Polysaccharides, Biosynthesis and Bioengineering, Volume 41*. 2010:251-263.

2. Aspeborg H, Schrader J, Coutinho PM, et al. Carbohydrate-active enzymes involved in the secondary cell wall biogenesis in hybrid aspen. *Plant Physiol*. 2005;137(3):983-997.

3. Bennett T, van den Toorn A, Sanchez-Perez GF, et al. SOMBRERO, BEARSKIN1, and BEARSKIN2 regulate root cap maturation in Arabidopsis. *Plant Cell*. 2010;22(3):640-654.

4. Bhargava A. Functional analysis of the MYB75 transcription factor as a regulator of secondary cell wall formation in Arabidopsis. 2010.

5. Bhargava A, Mansfield SD, Hall HC, Douglas CJ, Ellis BE. MYB75 functions in regulation of secondary cell wall formation in the Arabidopsis inflorescence stem. *Plant Physiol*. 2010;154(3):1428-1438.

6. Bomal C, Bedon F, Caron S, et al. Involvement of *pinus taeda* MYB1 and MYB8 in phenylpropanoid metabolism and secondary cell wall biogenesis: A comparative in planta analysis. *J Exp Bot*. 2008;59(14):3925-3939.

7. Bonke M, Thitamadee S, Mähönen AP, Hauser M, Helariutta Y. APL regulates vascular tissue identity in Arabidopsis. *Nature*. 2003;426(6963):181-186.

8. Brown DM, Goubet F, Wong VW, et al. Comparison of five xylan synthesis mutants reveals new insight into the mechanisms of xylan synthesis. *The Plant Journal*. 2007;52(6):1154-1168.

9. Brown DM, Zeef LA, Ellis J, Goodacre R, Turner SR. Identification of novel genes in Arabidopsis involved in secondary cell wall formation using expression profiling and reverse genetics. *The Plant Cell*. 2005;17(8):2281-2295.

10. Brunecky R, Alahuhta M, Xu Q, et al. Revealing nature's cellulase diversity: The digestion mechanism of caldicellulosiruptor bescii CelA. *Science*. 2013;342(6165):1513-1516.

11. Byrne ME, Barley R, Curtis M, et al. *Asymmetric leaves 1* mediates leaf patterning and stem cell function in Arabidopsis. *Nature*. 2000;408(6815):967-971.

12. Cassan-Wang H, Goué N, Saidi MN, et al. Identification of novel transcription factors regulating secondary cell wall formation in Arabidopsis. *Frontiers in plant science*. 2013;4.

13. Chalfun-Junior A, Franken J, Mes JJ, Marsch-Martinez N, Pereira A, Angenent GC. *ASYMMETRIC LEAVES2-LIKE1* gene, a member of the AS2/LOB family, controls proximal–distal patterning in Arabidopsis petals. *Plant Mol Biol*. 2005;57(4):559-575.

14. Chapelle A, Morreel K, Vanholme R, et al. Impact of the absence of stem-specific beta-glucosidases on lignin and monolignols. *Plant Physiol*. 2012;160(3):1204-1217.

15. Chapman EJ, Estelle M. Mechanism of auxin-regulated gene expression in plants. *Annu Rev Genet*. 2009; 43:265-285.

16. Chini A, Fonseca S, Fernandez G, et al. The JAZ family of repressors is the missing link in jasmonate signalling. *Nature*. 2007;448(7154):666-671.

17. Chuang CF, Meyerowitz EM. Specific and heritable genetic interference by double-stranded RNA in Arabidopsis thaliana. *Proc Natl Acad Sci U S A*. 2000;97(9):4985-4990.

18. Clark SE, Jacobsen SE, Levin JZ, Meyerowitz EM. The CLAVATA and SHOOT MERISTEMLESS loci competitively regulate meristem activity in Arabidopsis. *Development*. 1996;122(5):1567-1575.

19. Crawford BC, Sewell J, Golembeski G, Roshan C, Long JA, Yanofsky MF. Plant development. genetic control of distal stem cell fate within root and embryonic meristems. *Science*. 2015;347(6222):655-659.

20. Cui H, Levesque MP, Vernoux T, et al. An evolutionarily conserved mechanism delimiting SHR movement defines a single layer of endodermis in plants. *Science*. 2007;316(5823):421-425.

21. Das PK, Shin DH, Choi S, Yoo S, Choi G, Park Y. Cytokinins enhance sugar-induced anthocyanin biosynthesis in Arabidopsis. *Mol Cells*. 2012;34(1):93-101.

22. Das P, Ito T, Wellmer F, et al. Floral stem cell termination involves the direct regulation of AGAMOUS by PERIANTHIA. *Development*. 2009;136(10):1605-1611.

23. De Rybel B, Möller B, Yoshida S, et al. A bHLH complex controls embryonic vascular tissue establishment and indeterminate growth in Arabidopsis. *Developmental Cell*. 2013;24(4):426-437.

24. Delmer DP. Cellulose biosynthesis: Exciting times for a difficult field of study. *Annual review of plant biology*. 1999;50(1):245-276.

25. Demura T, Fukuda H. Transcriptional regulation in wood formation. *Trends Plant Sci*. 2007;12(2):64-70.

26. Demura T, Tashiro G, Horiguchi G, et al. Visualization by comprehensive microarray analysis of gene expression programs during transdifferentiation of mesophyll cells into xylem cells. *Proceedings of the National Academy of Sciences*. 2002;99(24):15794-15799.

27. Demura T, Ye Z. Regulation of plant biomass production. *Curr Opin Plant Biol*. 2010;13(3):298-303.

28. Dhugga KS, Barreiro R, Whitten B, et al. Guar seed ß-mannan synthase is a member of the cellulose synthase super gene family. *Science*. 2004;303(5656):363-366.

29. Douglas SJ, Chuck G, Dengler RE, Pelecanda L, Riggs CD. KNAT1 and ERECTA regulate inflorescence architecture in Arabidopsis. *Plant Cell*. 2002;14(3):547-558.

30. Du J, Miura E, Robischon M, Martinez C, Groover A. The populus class III HD ZIP transcription factor *POPCORONA* affects cell differentiation during secondary growth of woody stems. *PLoS One*. 2011;6(2): e17458.

31. Endo S, Betsuyaku S, Fukuda H. Endogenous peptide ligand–receptor systems for diverse signaling networks in plants. *Curr Opin Plant Biol*. 2014;21: 140-146.

32. Endo H, Yamaguchi M, Tamura T, et al. Multiple classes of transcription factors regulate the expression of VASCULAR-RELATED NAC-DOMAIN7, a master switch of xylem vessel differentiation. *Plant Cell Physiol*. 2015;56(2):242-254.

33. Esau K. Vascular differentiation in plants. 1965.

34. Etchells JP, Provost CM, Mishra L, Turner SR. WOX4 and WOX14 act downstream of the PXY receptor kinase to regulate plant vascular proliferation independently of any role in vascular organisation. *Development*. 2013;140(10):2224-2234.

35. Etchells JP, Turner SR. The PXY-CLE41 receptor ligand pair defines a multifunctional pathway that controls the rate and orientation of vascular cell division. *Development*. 2010;137(5):767-774.

36. Evert RF. *Esau's plant anatomy: Meristems, cells, and tissues of the plant body: Their structure, function, and development.* John Wiley & Sons; 2006.

37. Furuta KM, Yadav SR, Lehesranta S, et al. Plant development. Arabidopsis NAC45/86 direct sieve element morphogenesis culminating in enucleation. *Science*. 2014;345(6199):933-937.

38. Gallagher KL, Paquette AJ, Nakajima K, Benfey PN. Mechanisms regulating SHORT-ROOT intercellular movement. *Current biology*. 2004;14(20):1847-1851.

39. Gerttula S, Zinkgraf M, Muday GK, et al. Transcriptional and hormonal regulation of gravitropism of woody stems in *Populus*. *Plant Cell*. 2015;27(10):2800-2813.

40. Goicoechea M, Lacombe E, Legay S, et al. EgMYB2, a new transcriptional activator from eucalyptus xylem, regulates secondary cell wall formation and lignin biosynthesis. *The Plant Journal*. 2005;43(4):553-567.

41. Greb T, Clarenz O, Schafer E, et al. Molecular analysis of the *LATERAL SUPPRESSOR* gene in Arabidopsis reveals a conserved control mechanism for axillary meristem formation. *Genes Dev*. 2003;17(9):1175-1187.

42. Green KA, Prigge MJ, Katzman RB, Clark SE. *CORONA*, a member of the class III homeodomain leucine zipper gene family in Arabidopsis, regulates stem cell specification and organogenesis. *Plant Cell*. 2005;17(3):691-704.

43. Grigg SP, Galinha C, Kornet N, Canales C, Scheres B, Tsiantis M. Repression of apical homeobox genes is required for embryonic root development in Arabidopsis. *Current Biology*. 2009;19(17):1485-1490.

44. Groover AT, Mansfield SD, DiFazio SP, et al. The populus homeobox gene ARBORKNOX1 reveals overlapping mechanisms regulating the shoot apical meristem and the vascular cambium. *Plant Mol Biol*. 2006;61(6):917-932.

45. Guo Y, Qin G, Gu H, Qu LJ. Dof5.6/HCA2, a dof transcription factor gene, regulates interfascicular cambium formation and vascular tissue development in Arabidopsis. *Plant Cell*. 2009;21(11):3518-3534.

46. Helariutta Y, Fukaki H, Wysocka-Diller J, et al. The *SHORT-ROOT* gene controls radial patterning of the Arabidopsis root through radial signaling. *Cell*. 2000;101(5):555-567.

47. Hirakawa Y, Shinohara H, Kondo Y, et al. Non-cell-autonomous control of vascular stem cell fate by a CLE peptide/receptor system. *Proc Natl Acad Sci U S A*. 2008;105(39):15208-15213.

48. Hu R, Qi G, Kong Y, Kong D, Gao Q, Zhou G. Comprehensive analysis of NAC domain transcription factor gene family in populus trichocarpa. *BMC plant biology*. 2010;10(1):145.

49. Hussey SG, Mizrachi E, Spokevicius AV, Bossinger G, Berger DK, Myburg AA. SND2, a NAC transcription factor gene, regulates genes involved in secondary cell wall development in Arabidopsis fibres and increases fibre cell area in eucalyptus. *BMC plant biology*. 2011;11(1):173.

50. Ito Y, Nakanomyo I, Motose H, et al. Dodeca-CLE peptides as suppressors of plant stem cell differentiation. *Science*. 2006;313(5788):842-845.

51. Jansson S, Douglas CJ. *Populus*: A model system for plant biology. *Annu.Rev.Plant Biol.* 2007;58:435-458.

52. Ji H, Wang S, Li K, Szakonyi D, Koncz C, Li X. PRL1 modulates root stem cell niche activity and meristem size through WOX5 and PLTs in Arabidopsis. *The Plant Journal*. 2015;81(3):399-412.

53. Jones L, Ennos AR, Turner SR. Cloning and characterization of irregular xylem4 (irx4): A severely lignin-deficient mutant of Arabidopsis. *The Plant Journal*. 2001;26(2):205-216.

54. Joshi CP, Mansfield SD. The cellulose paradox—simple molecule, complex biosynthesis. *Curr Opin Plant Biol*. 2007;10(3):220-226.

55. Kalluri UC, Joshi CP. Differential expression patterns of two cellulose synthase genes are associated with primary and secondary cell wall development in aspen trees. *Planta*. 2004;220(1):47-55.

56. Karpinska B, Karlsson M, Srivastava M, et al. MYB transcription factors are differentially expressed and regulated during secondary vascular tissue development in hybrid aspen. *Plant Mol Biol*. 2004;56(2):255-270.

57. Kerstetter RA, Bollman K, Taylor RA, Bomblies K, Poethig RS. *KANADI* regulates organ polarity in Arabidopsis. *Nature*. 2001;411(6838):706-709.

58. Khanday I, Yadav SR, Vijayraghavan U. Rice *LHS1/OsMADS1* controls floret meristem specification by coordinated regulation of transcription factors and hormone signaling pathways. *Plant Physiol*. 2013;161(4):1970-1983.

59. Kim W, Kim J, Ko J, Kim J, Han K. Transcription factor MYB46 is an obligate component of the transcriptional regulatory complex for functional expression of secondary wall-associated cellulose synthases in *Arabidopsis thaliana*. *J Plant Physiol*. 2013.

60. Kim W, Ko J, Kim J, Kim J, Bae H, Han K. MYB46 directly regulates the gene expression of secondary wall-associated cellulose synthases in Arabidopsis. *The Plant Journal*. 2013;73(1):26-36.

61. Ko J, Kim W, Han K. Ectopic expression of MYB46 identifies transcriptional regulatory genes involved in secondary wall biosynthesis in Arabidopsis. *The Plant Journal*. 2009;60(4):649-665.

62. Kubo M, Udagawa M, Nishikubo N, et al. Transcription switches for protoxylem and metaxylem vessel formation. *Genes Dev*. 2005;19(16):1855-1860.

63. Laux T, Mayer KF, Berger J, Jurgens G. The WUSCHEL gene is required for shoot and floral meristem integrity in Arabidopsis. *Development*. 1996;122(1):87-96.

64. Lee C, Teng Q, Zhong R, Ye Z. Molecular dissection of xylan biosynthesis during wood formation in poplar. *Molecular plant*. 2011;4(4):730-747.

65. Lee HW, Kim NY, Lee DJ, Kim J. LBD18/ASL20 regulates lateral root formation in combination with LBD16/ASL18 downstream of ARF7 and ARF19 in Arabidopsis. *Plant Physiol*. 2009;151(3):1377-1389.

66. Legay S, Lacombe E, Goicoechea M, et al. Molecular characterization of *EgMYB1*, a putative transcriptional repressor of the lignin biosynthetic pathway. *Plant Science*. 2007;173(5):542-549.

67. Lenhard M, Jurgens G, Laux T. The WUSCHEL and SHOOTMERISTEMLESS genes fulfil complementary roles in Arabidopsis shoot meristem regulation. *Development*. 2002;129(13):3195-3206.

68. Levesque MP, Vernoux T, Busch W, et al. Whole-genome analysis of the SHORT-ROOT developmental pathway in Arabidopsis. *PLoS Biol*. 2006;4(5): e143.

69. Lewis DR, Ramirez MV, Miller ND, et al. Auxin and ethylene induce flavonol accumulation through distinct transcriptional networks. *Plant Physiol*. 2011;156(1):144-164.

70. Li E, Bhargava A, Qiang W, et al. The class II KNOX gene KNAT7 negatively regulates secondary wall formation in Arabidopsis and is functionally conserved in *Populus*. *New Phytol*. 2012;194(1):102-115.

71. Li E, Wang S, Liu Y, Chen J, Douglas CJ. OVATE FAMILY PROTEIN4 (OFP4) interaction with KNAT7 regulates secondary cell wall formation in Arabidopsis thaliana. *The Plant Journal*. 2011;67(2):328-341.

72. Liebsch D, Sunaryo W, Holmlund M, et al. Class I KNOX transcription factors promote differentiation of cambial derivatives into xylem fibers in the Arabidopsis hypocotyl. *Development*. 2014;141(22):4311-4319.

73. Liepman AH, Nairn CJ, Willats WG, Sørensen I, Roberts AW, Keegstra K. Functional genomic analysis supports conservation of function among cellulose synthase-like A gene family members and suggests diverse roles of mannans in plants. *Plant Physiol*. 2007;143(4):1881-1893.

74. Lodha M, Marco CF, Timmermans MC. The ASYMMETRIC LEAVES complex maintains repression of KNOX homeobox genes via direct recruitment of polycomb-repressive complex2. *Genes Dev*. 2013;27(6):596-601.

75. Long JA, Moan EI, Medford JI, Barton MK. A member of the KNOTTED class of homeodomain proteins encoded by the STM gene of Arabidopsis. *Nature*. 1996;379(6560):66.

76. Long Y, Smet W, Cruz-Ramirez A, et al. Arabidopsis BIRD zinc finger proteins jointly stabilize tissue boundaries by confining the cell fate regulator SHORT-ROOT and contributing to fate specification. *Plant Cell*. 2015;27(4):1185-1199.

77. Mangeon A, Lin W, Springer PS. Functional divergence in the Arabidopsis LOB-domain gene family. *Plant signaling & behavior*. 2012;7(12):1544-1547.

78. Matsubayashi Y. Ligand-receptor pairs in plant peptide signaling. *J Cell Sci*. 2003;116(Pt 19):3863-3870.

79. Mayer KF, Schoof H, Haecker A, Lenhard M, Jürgens G, Laux T. Role of WUSCHEL in regulating stem cell fate in the Arabidopsis shoot meristem. *Cell*. 1998;95(6):805-815.

80. McCarthy RL, Zhong R, Fowler S, et al. The poplar MYB transcription factors, PtrMYB3 and PtrMYB20, are involved in the regulation of secondary wall biosynthesis. *Plant and cell physiology*. 2010;51(6):1084-1090.

81. Mele G, Ori N, Sato Y, Hake S. The knotted1-like homeobox gene BREVIPEDICELLUS regulates cell differentiation by modulating metabolic pathways. *Genes Dev*. 2003;17(17):2088-2093.

82. Mizukami Y, Fischer RL. Plant organ size control: *AINTEGUMENTA* regulates growth and cell numbers during organogenesis. *Proc Natl Acad Sci U S A*. 2000;97(2):942-947.

83. Moubayidin L, Di Mambro R, Sozzani R, et al. Spatial coordination between stem cell activity and cell differentiation in the root meristem. *Developmental cell*. 2013;26(4):405-415.

84. Mudunkothge JS, Krizek BA. Three Arabidopsis AIL/PLT genes act in combination to regulate shoot apical meristem function. *The Plant Journal*. 2012;71(1):108-121.

85. Muller CJ, Valdes AE, Wang G, et al. PHABULOSA mediates an auxin signaling loop to regulate vascular patterning in Arabidopsis. *Plant Physiol*. 2016;170(2):956-970.

86. Nakajima K, Sena G, Nawy T, Benfey PN. Intercellular movement of the putative transcription factor SHR in root patterning. *Nature*. 2001;413(6853):307-311.

87. Nakano Y, Nishikubo N, Goué N, et al. MYB transcription factors orchestrating the developmental program of xylem vessels in Arabidopsis roots. *Plant biotechnology*. 2010;27(3):267-272.

88. Oda Y, Hasezawa S. Cytoskeletal organization during xylem cell differentiation. *J Plant Res*. 2006;119(3):167-177.

89. Ogasawara H, Kaimi R, Colasanti J, Kozaki A. Activity of transcription factor JACKDAW is essential for SHR/SCR-dependent activation of SCARECROW and MAGPIE and is modulated by reciprocal interactions with MAGPIE, SCARECROW and SHORT ROOT. *Plant Mol Biol*. 2011;77(4-5):489-499.

90. Ohashi-Ito K, Bergmann DC. Regulation of the Arabidopsis root vascular initial population by LONESOME HIGHWAY. *Development*. 2007;134(16):2959-2968. doi: dev.006296 [pii].

91. Ohashi-Ito K, Oguchi M, Kojima M, Sakakibara H, Fukuda H. Auxin-associated initiation of vascular cell differentiation by LONESOME HIGHWAY. *Development*. 2013;140(4):765-769.

92. Öhman D, Demedts B, Kumar M, et al. MYB103 is required for FERULATE-5-HYDROXYLASE expression and syringyl lignin biosynthesis in Arabidopsis stems. *The Plant Journal*. 2013;73(1):63-76.

93. Paredez AR, Somerville CR, Ehrhardt DW. Visualization of cellulose synthase demonstrates functional association with microtubules. *Science*. 2006;312(5779):1491-1495.

94. Patzlaff A, McInnis S, Courtenay A, et al. Characterisation of a pine MYB that regulates lignification. *The Plant Journal*. 2003;36(6):743-754.

95. Patzlaff A, Newman LJ, Dubos C, et al. Characterisation of PtMYB1, an R2R3-MYB from pine xylem. *Plant Mol Biol*. 2003;53(4):597-608.

96. Pautler M, Eveland AL, LaRue T, et al. FASCIATED EAR4 encodes a bZIP transcription factor that regulates shoot meristem size in maize. *Plant Cell*. 2015;27(1):104-120.

97. Peña MJ, Zhong R, Zhou G, et al. Arabidopsis irregular xylem8 and irregular xylem9: Implications for the complexity of glucuronoxylan biosynthesis. *The Plant Cell Online*. 2007;19(2):549-563.

98. Peng Z, Han C, Yuan L, Zhang K, Huang H, Ren C. Brassinosteroid enhances Jasmonate-Induced anthocyanin accumulation in Arabidopsis seedlings. *Journal of Integrative Plant Biology*. 2011;53(8):632-640.

99. Pi L, Aichinger E, van der Graaff E, et al. Organizer-derived WOX5 signal maintains root columella stem cells through chromatin-mediated repression of CDF4 expression. *Developmental cell*. 2015;33(5):576-588.

100. Prigge MJ, Otsuga D, Alonso JM, Ecker JR, Drews GN, Clark SE. Class III homeodomain-leucine zipper gene family members have overlapping, antagonistic, and distinct roles in Arabidopsis development. *Plant Cell*. 2005;17(1):61-76.

101. Reinhart BJ, Liu T, Newell NR, et al. Establishing a framework for the Ad/abaxial regulatory network of Arabidopsis: Ascertaining targets of class III homeodomain leucine zipper and KANADI regulation. *Plant Cell*. 2013;25(9):3228-3249.

102. Robischon M, Du J, Miura E, Groover A. The populus class III HD ZIP, *popREVOLUTA*, influences cambium initiation and patterning of woody stems. *Plant Physiol*. 2011;155(3):1214-1225.

103. Robischon M, Du J, Miura E, Groover A. The populus class III HD ZIP, popREVOLUTA, influences cambium initiation and patterning of woody stems. *Plant Physiol*. 2011;155(3):1214-1225.

104. Rodriguez RE, Ercoli MF, Debernardi JM, et al. MicroRNA miR396 regulates the switch between stem cells and transit-amplifying cells in Arabidopsis roots. *Plant Cell*. 2015;27(12):3354-3366.

105. Running MP, Meyerowitz EM. Mutations in the *PERIANTHIA* gene of Arabidopsis specifically alter floral organ number and initiation pattern. *Development*. 1996;122(4):1261-1269.

106. Rutjens B, Bao D, Eck-Stouten V, Brand M, Smeekens S, Proveniers M. Shoot apical meristem function in Arabidopsis requires the combined activities of three BEL1-like homeodomain proteins. *The Plant Journal*. 2009;58(4):641-654.

107. Sablowski R. Plant stem cell niches: From signalling to execution. *Curr Opin Plant Biol*. 2011;14(1):4-9.

108. Sarkar AK, Luijten M, Miyashima S, et al. Conserved factors regulate signalling in *Arabidopsis thaliana* shoot and root stem cell organizers. *Nature*. 2007;446(7137):811-814.

109. Scarpella E, Marcos D, Friml J, Berleth T. Control of leaf vascular patterning by polar auxin transport. *Genes Dev*. 2006;20(8):1015-1027.

110. Schlereth A, Möller B, Liu W, et al. MONOPTEROS controls embryonic root initiation by regulating a mobile transcription factor. *Nature*. 2010;464(7290):913-916.

111. Schulze S, Schäfer BN, Parizotto EA, Voinnet O, Theres K. LOST *MERISTEMS* genes regulate cell differentiation of central zone descendants in Arabidopsis shoot meristems. *The Plant Journal*. 2010;64(4):668-678.

112. Scofield S, Dewitte W, Murray JA. STM sustains stem cell function in the Arabidopsis shoot apical meristem and controls *KNOX* gene expression independently of the transcriptional repressor AS1. *Plant signaling & behavior*. 2014;9(6): e28934.

113. Sebastian J, Ryu KH, Zhou J, et al. *PHABULOSA* controls the quiescent center-independent root meristem activities in Arabidopsis thaliana. *PLoS Genet*. 2015;11(3): e1004973.

114. Sehr EM, Agusti J, Lehner R, Farmer EE, Schwarz M, Greb T. Analysis of secondary growth in the Arabidopsis shoot reveals a positive role of jasmonate signalling in cambium formation. *The Plant Journal*. 2010;63(5):811-822.

115. Seo PJ, Hong S, Kim S, Park C. Competitive inhibition of transcription factors by small interfering peptides. *Trends Plant Sci*. 2011;16(10):541-549.

116. Siedlecka A, Wiklund S, Peronne MA, et al. Pectin methyl esterase inhibits intrusive and symplastic cell growth in developing wood cells of *Populus*. *Plant Physiol*. 2008;146(2):554-565.

117. Somerville C. Cellulose synthesis in higher plants. *Annu Rev Cell Dev Biol*. 2006;22:53-78.

118. Song D, Shen J, Li L. Characterization of cellulose synthase complexes in *Populus* xylem differentiation. *New Phytol*. 2010;187(3):777-790.

119. Soyano T, Thitamadee S, Machida Y, Chua N. *Asymmetric leaves2-like19/lateral organ boundaries domain 30* and *Asl20/Lbd18* regulate tracheary element differentiation in Arabidopsis. *The Plant Cell* 2008;20(12):3359-3373.

120. Suer S, Agusti J, Sanchez P, Schwarz M, Greb T. WOX4 imparts auxin responsiveness to cambium cells in Arabidopsis. *Plant Cell*. 2011;23(9):3247-3259.

121. Sunkar R, Zhu J. Novel and stress-regulated microRNAs and other small RNAs from Arabidopsis. *The Plant Cell Online*. 2004;16(8):2001-2019.

122. Tanaka K, Murata K, Yamazaki M, Onosato K, Miyao A, Hirochika H. Three distinct rice cellulose synthase catalytic subunit genes required for cellulose synthesis in the secondary wall. *Plant Physiol*. 2003;133(1):73-83.

123. Taylor NG, Gardiner JC, Whiteman R, Turner SR. Cellulose synthesis in the Arabidopsis secondary cell wall. *Cellulose*. 2004;11(3-4):329-338.

124. Taylor-Teeples M, Lin L, de Lucas M, et al. An Arabidopsis gene regulatory network for secondary cell wall synthesis. *Nature*. 2015;517(7536):571-575.

125. Thines B, Katsir L, Melotto M, et al. JAZ repressor proteins are targets of the SCFCOI1 complex during jasmonate signalling. *Nature*. 2007;448(7154):661-665.

126. Thompson D, Regev A, Roy S. Comparative analysis of gene regulatory networks: From network reconstruction to evolution. *Annu Rev Cell Dev Biol*. 2015; 31:399-428.

127. Timell TE. Recent progress in the chemistry of wood hemicelluloses. *Wood Sci Technol*. 1967;1(1):45-70.

128. Turner SR, Somerville CR. Collapsed xylem phenotype of Arabidopsis identifies mutants deficient in cellulose deposition in the secondary cell wall. *The Plant Cell Online*. 1997;9(5):689-701.

129. Vanholme R, Cesarino I, Rataj K, et al. Caffeoyl shikimate esterase (CSE) is an enzyme in the lignin biosynthetic pathway in Arabidopsis. *Science*. 2013;341(6150):1103-1106.

130. Venglat SP, Dumonceaux T, Rozwadowski K, et al. The homeobox gene *BREVIPEDICELLUS* is a key regulator of inflorescence architecture in Arabidopsis. *Proc Natl Acad Sci U S A*. 2002;99(7):4730-4735.

131. Voiniciuc C, Yang B, Schmidt MH, Günl M, Usadel B. Starting to gel: How Arabidopsis seed coat epidermal cells produce specialized secondary cell walls. *International journal of molecular sciences*. 2015;16(2):3452-3473.

132. Voiniciuc C, Dean GH, Griffiths JS, et al. Flying saucer1 is a transmembrane RING E3 ubiquitin ligase that regulates the degree of pectin methyl-esterification in Arabidopsis seed mucilage. *Plant Cell*. 2013;25(3):944-959.

133. Vollbrecht E, Reiser L, Hake S. Shoot meristem size is dependent on inbred background and presence of the maize homeobox gene, knotted1. *DEVELOPMENT-CAMBRIDGE-*. 2000;127(14):3161-3172.

134. Wang H, Avci U, Nakashima J, Hahn MG, Chen F, Dixon RA. Mutation of WRKY transcription factors initiates pith secondary wall formation and increases stem biomass in dicotyledonous plants. *Proceedings of the National Academy of Sciences*. 2010;107(51):22338-22343.

135. Wang H, Dixon RA. On–off switches for secondary cell wall biosynthesis. *Molecular plant*. 2012;5(2):297-303.

136. Wang Q, Hasson A, Rossmann S, Theres K. Divide et impera: Boundaries shape the plant body and initiate new meristems. *New Phytol*. 2016;209(2):485-498.

137. Wang JP, Naik PP, Chen HC, et al. Complete proteomic-based enzyme reaction and inhibition kinetics reveal how monolignol biosynthetic enzyme families affect metabolic flux and lignin in *Populus trichocarpa*. *Plant Cell*. 2014;26(3):894-914.

138. Willemsen V, Bauch M, Bennett T, et al. The NAC domain transcription factors FEZ and SOMBRERO control the orientation of cell division plane in Arabidopsis root stem cells. *Developmental cell*. 2008;15(6):913-922.

139. Wurschum T, Gross-Hardt R, Laux T. APETALA2 regulates the stem cell niche in the Arabidopsis shoot meristem. *Plant Cell*. 2006;18(2):295-307.

140. Yamaguchi M, Goué N, Igarashi H, et al. VASCULAR-RELATED NAC-DOMAIN6 and VASCULAR-RELATED NAC-DOMAIN7 effectively induce transdifferentiation into xylem vessel elements under control of an induction system. *Plant Physiol*. 2010;153(3):906-914.

141. Yamaguchi M, Kubo M, Fukuda H, Demura T. VASCULAR-RELATED NAC-DOMAIN7 is involved in the differentiation of all types of xylem vessels in Arabidopsis roots and shoots. *The Plant Journal*. 2008;55(4):652-664.

142. Yamaguchi M, Ohtani M, Mitsuda N, et al. VND-INTERACTING2, a NAC domain transcription factor, negatively regulates xylem vessel formation in Arabidopsis. *The Plant Cell Online*. 2010;22(4):1249-1263.

143. Yamaguchi M, Goue N, Igarashi H, et al. VASCULAR-RELATED NAC-DOMAIN6 and VASCULAR-RELATED NAC-DOMAIN7 effectively induce transdifferentiation into xylem vessel elements under control of an induction system. *Plant Physiol*. 2010;153(3):906-914. doi: 10.1104/pp.110.154013 [doi].

144. Yan L, Xu C, Kang Y, et al. The heterologous expression in Arabidopsis thaliana of sorghum transcription factor SbbHLH1 downregulates lignin synthesis. *J Exp Bot*. 2013.

145. Yang C, Xu Z, Song J, Conner K, Barrena GV, Wilson ZA. Arabidopsis MYB26/MALE STERILE35 regulates secondary thickening in the endothecium and is essential for anther dehiscence. *The Plant Cell Online*. 2007;19(2):534-548.

146. Yang S, Seo PJ, Yoon H, Park C. The Arabidopsis NAC transcription factor VNI2 integrates abscisic acid signals into leaf senescence via the COR/RD genes. *The Plant Cell Online*. 2011;23(6):2155-2168.

147. Yordanov YS, Regan S, Busov V. Members of the LATERAL ORGAN BOUNDARIES DOMAIN transcription factor family are involved in the regulation of secondary growth in populus. *Plant Cell*. 2010;22(11):3662-3677.

148. Zhang Y, Jiao Y, Liu Z, Zhu Y. ROW1 maintains quiescent centre identity by confining WOX5 expression to specific cells. *Nature communications*. 2015;6.

149. Zhao C, Craig JC, Petzold HE, Dickerman AW, Beers EP. The xylem and phloem transcriptomes from secondary tissues of the Arabidopsis root-hypocotyl. *Plant Physiol*. 2005;138(2):803-818.

150. Zhao Y, Medrano L, Ohashi K, et al. HANABA TARANU is a GATA transcription factor that regulates shoot apical meristem and flower development in Arabidopsis. *Plant Cell*. 2004;16(10):2586-2600

151. Zhong R, Burk DH, Morrison WH, Ye Z. A kinesin-like protein is essential for oriented deposition of cellulose microfibrils and cell wall strength. *The Plant Cell Online*. 2002;14(12):3101-3117.

152. Zhong R, Lee C, Ye Z. Evolutionary conservation of the transcriptional network regulating secondary cell wall biosynthesis. *Trends Plant Sci*. 2010;15(11):625-632.

153. Zhong R, Lee C, Zhou J, McCarthy RL, Ye Z. A battery of transcription factors involved in the regulation of secondary cell wall biosynthesis in Arabidopsis. *The Plant Cell Online*. 2008;20(10):2763-2782.

154. Zhong R, McCarthy RL, Haghighat M, Ye Z. The poplar MYB master switches bind to the SMRE site and activate the secondary wall biosynthetic program during wood formation. *PLOS ONE*. 2013;8(7): e69219.

155. Zhong R, McCarthy RL, Lee C, Ye Z. Dissection of the transcriptional program regulating secondary wall biosynthesis during wood formation in poplar. *Plant Physiol*. 2011;157(3):1452-1468.

156. Zhong R, Ye Z. MYB46 and MYB83 bind to the SMRE sites and directly activate a suite of transcription factors and secondary wall biosynthetic genes. *Plant and Cell Physiology*. 2012;53(2):368-380.

157. Zhong R, Ye Z. Regulation of cell wall biosynthesis. *Curr Opin Plant Biol*. 2007;10(6):564-572.

158. Zhou J, Qiu J, Ye Z. Alteration in secondary wall deposition by overexpression of the fragile Fiber1 Kinesin-Like protein in Arabidopsis. *Journal of Integrative Plant Biology*. 2007;49(8):1235-1243.

159. Zhou Y, Liu X, Engstrom EM, et al. Control of plant stem cell function by conserved interacting transcriptional regulators. *Nature*. 2015;517(7534):377-380.

CHAPTER 2
PTRSND1-B1 DIRECTED QUANTITATIVE HIERARCHICAL TRANSCRIPTION FACTOR AND CHROMATIN BINDING NETWORK IN *POPULUS TRICHOCARPA* FOR WOOD FORMATION

2.1 Abstract

Wood is an important feedstock to the global bio-renewable economy. We established a four-layer quantitative hierarchical transcriptional regulatory network (TRN) associated with wood formation. Our TRN includes 18 transcription factors and 27 cell-wall biosynthetic genes involved in the formation of cellulose (5), hemicelluloses (5) and lignin (17). To build this TRN, we identified 56 direct TF-DNA regulatory interactions using chromatin immunoprecipitation coupling with TF-overexpression assays in stem-differentiating xylem protoplasts. These 56 direct TF-DNA interactions constitute 55 transactivations and one repression, as shown by the transcripts change of target genes in protoplasts overexpressing specific TFs. These direct TF-DNA interactions reveal how the 18 TFs cooperatively and combinatorially regulate the cell wall biosynthetic genes during wood formation. We individually downregulated three key TFs in the TRN (*MYB21*, *MYB74*, *MYB90*) by *P. trichocarpa* transgenesis to validate the evidence for transactivation and repression. 91% of the tested regulatory interactions in the TRN were consistent with the regulatory effects in the transgenics. ChIP assays coupled with TF overexpression in stem-differentiating xylem protoplasts may sufficiently capture TF-DNA regulatory interactions in wood-forming cells, without requiring stable transgenics. Further comparative studies between our network in wood cell wall biosynthesis and the herbaceous plant cell wall biosynthesis may elucidate the conserved and divergent regulatory mechanisms in plant evolution.

2.2 Introduction

A current goal in systems and molecular biology is to define the transcriptional regulatory network (TRNs) coordinating and regulating the expression of enzyme

encoding genes for the specific biological process (Gerstein et al., 2012; Thompson et al., 2015; Sorrells et al., 2015). Biosynthesis of plant cell walls is a multistep and enzyme-catalyzed process where the carbohydrates are converted and organized into polymers—cellulose, hemicelluloses, and lignin (Sarkanen et al., 1971; Northcote et al., 1972). The composition of plant cell walls varies depending on cell types in various tissues (Freshour et al., 1996; Pauly and Keegstra, 2008). What is needed is to elucidate the TRNs for cell wall biosynthesis in the specialized tissues with economic and environmental value. Cell walls produced from xylem tissue are the wood, which provides mechanical strength and water transport for trees and form the basis for biofuel, timber, and pulp and paper industrial products (Sarkanen et al., 1976; Chiang et al., 2002; Evert, 2006). Dissection of the TRN regulating cell wall biosynthesis in wood formation is imperative for basic plant biology and will have impacts on biotechnological based industrials.

The TRNs control the function of TFs for their corresponding target genes through regulatory hierarchies. A key mechanism in the transcriptional regulation is through sequence dependent binding of TFs to the promoters of their target genes. Studies in transcriptional regulation of cell wall biosynthesis genes in wood formation have mostly focused on the function of individual transcription factors (TF) and TF pairs, including PtrMYB2/3/20/21, PttMYB21a, PtrWND/VNSs, PtoMYB92; PtrMYB152, PtoMYB216, PtrSND1-A2^{IR}, PtrWRKY19 from poplars (Karpinska et al., 2004; Zhong et al.,2011; Ohtani et al., 2011; Li et al., 2012; Tian et al., 2013; Wang et al., 2014; Li et al., 2015; Yang et al., 2016), PtMYB1, PtMYB4, and PtMYB8 from pine (Patzlaff et al., 2003a, b), EgMYB1 and EgMYB2 from *Eucalyptus* (Goicoechea et al., 2005; Legay et al., 2010). PgMYB1/8 and PgMYB14/15 in spruce (Bomal et al., 2013). The knowledge of direct physical interactions between TF and cell wall biosynthesis genes is limited in these studies, and not enough to generate a comprehensive TRN for cell wall biosynthesis in woody species. Currently, network-based approaches manage to illustrate the wood cell wall biosynthesis TRN using computational and experimental

methods (Yang et al., 2012; Lin et al., 2013; Cai et al., 2014; Duval et al., 2014). A Two-layered PtrSND1-B1-directed network (Lin et al., 2013) was constructed using physical interactions (as direct protein-DNA interactions) and regulatory relationships (as induction of target gene expression by TF overexpression). No PtrSND1-B1 targeted genes encode enzymes for cellulose, lignin, and hemicellulose biosynthesis, however, PtrSND1-B1 overexpression can induce cellulose synthase genes and ectopic secondary walls in poplar leaves and seedlings (Ohtani et al., 2011). These results suggest that these enzyme-encoding genes, are indirect targets of PtrSND1-B1, which are directly targeted by PtrSND1-B1 downstream TFs. Therefore, identifying these downstream TFs and mapping the protein-DNA interactions between TFs and their targeted genes, allow us to construct a more comprehensive TRN for wood cell wall biosynthesis.

To achieve this goal, it is necessary to use a reliable and effective experimental approach. Many experimental approaches have been used in mapping TRNs in plants, including genetic approaches such as analyses of mutants and transgenics, and molecular approaches such as steroid receptor based inducible assays (inducible assays), electrophoretic mobility shift assays (EMSA), yeast one-hybrid (Y1H) assays, chromosome immunoprecipitation (ChIP) assays, or DNA affinity binding assays (Blais et al., 2005; Krouk et al., 2013; O'Malley et al., 2016; Yang et al., 2016). Using genetic approaches, a hierarchical multi-layer transcriptional network was identified to be comprised of top layer NACs (VND and NST/SND)-second layer core MYBs (MYB46/83)-third layer MYBs (MYB4/7/32, MYB20/63, MYB52/54, MYB58/63/85, MYB103) and -fourth layer cell wall biosynthesis genes in Arabidopsis (Zhong et al., 2010a; Wang et al., 2012; Nakano et al., 2015). These genetic approaches require mutants or transgenics with detectable phenotypes as the starting points. However, for tree species, the high costs of genetic analysis are a challenge for generating transgenics or mutants using transformation, and genetic redundancy is another challenge for obtaining detectable phenotypes in the transgenics or mutants (Merkle

and Dean, 2000; Tuskan et al., 2005; Nystedt et al., 2013). To overcome these disadvantages, construction of TRNs in woody species can be carried out using molecular approaches as core techniques (Sun et al., 2010; Gaudinier et al., 2011; Brady et al., 2011; Franco-Zorrilla et al., 2014; Lindemose et al., 2014; Taylor-Teeples et al., 2015; O'Malley et al., 2016). Among these approaches, ChIP assays, which can detect *in vivo* protein-DNA interactions without using transgenics or mutants (Lin et al., 2013; Liu et al., 2015a, Liu et al., 2015b), are more reliable and preferred.

In traditional ChIP assays, specific antibodies against native TF proteins is essential, but the quality of antibodies for IP are difficult to generate for many TFs in network-scale experiments (Mourik et al., 2015). To overcome the problems, each TF protein of interest can be transgenically overexpressed with a tag, and then be pulled down with the chromatins using commercial antibodies in ChIP assays. Due to the difficulty of generating transgenic trees, overexpression of these epitope-tagged TF proteins can be performed in cultured cells that retain the identity of wood forming tissues. Fresh isolated *Populus* stem differentiating xylem (SDX) protoplasts represent the transcriptome of the intact wood forming tissue (Lin et al.,2013), and have been successfully used to study gene transactivation using TF overexpression (Lin et al., 2013; Lin et al., 2014). Transient overexpression of tagged TF in SDX protoplasts and the following ChIP assays can identify physical TF-DNA interactions on a large-scale (Lin et al., 2013). Furthermore, the TF-induced differential expression can then be analyzed to reveal the regulatory effects of the identified TF-DNA interactions. Thus, the integration of SDX protoplasts with ChIP and transactivation assays as an approach allows for the establishment of a wood cell wall TRN where the direct TF-DNA interactions can be identified and quantified for their effects.

Using this approach, we describe a four-layered PtrSND1-B1-regulated TRN, and provide evidence that this TRN is part of the transcriptional program of wood cell wall biosynthesis. The network is comprised of 18 TF genes, and 27 cell wall biosynthetic

genes, and 56 direct TF-DNA interactions identified using ChIP assays in SDX protoplasts. Transcriptional profiling using RNA-seq and qRT-PCR was used to quantitatively measure the regulatory effects of the TF-DNA interactions characterized in SDX protoplasts. We finally used transgenics to experimentally validate the occurrence of the transcriptional network for wood cell wall biosynthesis. Through these analyses, we expand the knowledge of transcriptional regulation of wood cell wall biosynthesis, and thus establish a framework for generating a comprehensive TRN in woody species.

2.3 Results

2.3.1 PtrMYB21 and PtrMYB74 are transcriptional activators in stem differentiating xylem fibers and vessels of *Populus trichocarpa*

We previously established a two-layer PtrSND1-B1 TRN associated with wood formation in *P. trichocarpa* (Lin et al., 2013). This TRN includes 10 TFs in the second layer. From these 10 TFs, we employed PtrMYB21 and PtrMYB74 (named as MYB50 in Lin et al., 2013), to expand the network. We selected these two MYBs because their expression is the most xylem-abundant and -specific among the 10 second-layer TFs (Lin et al., 2013). To test whether these two MYBs and their upstream regulator, PtrSND1-B1, are associated with wood formation, we examined the expression of these three TFs in wood-forming cells. We used laser capture microdissection (LCM) to isolate differentiating fiber and vessel cells from stem cross-sections of *P. trichocarpa* (Figure 2A-D). The cell-type specific transcript abundances of these three TFs were quantified using qRT-PCR (Figure 2E-G). qRT-PCR showed that these three TFs are co-expressed in both fiber and vessel cells, the two major wood-forming cells, suggesting their functions are closely associated with wood formation.

We next analyzed the subcellular locations of PtrMYB21 and PtrMYB74 proteins in wood forming cells. The PtrSND1-B1 has been demonstrated as a nuclear protein (Lin et al., 2013). We transfected SDX protoplasts with PtrMYB21-GFP and PtrMYB74-

GFP fusions, as well as H2A-mcherry as a nuclear marker. Each of these PtrMYBs co-localized with H2A-mcherry in the nucleus (Figure 1H-M), demonstrating that these PtrMYBs are nuclear proteins, as is their direct upstream regulator, PtrSND1-B1. To verify whether these two nuclear proteins have transcriptional activities, we performed yeast-based transregulation assays and found that these two PtrMYBs function as transcriptional activators (Figure 2N). We then investigated the roles of these transcriptional activators and the identity of their downstream targets to continue to elaborate the SND1-B1 mediated TRN in wood formation.

2.3.2 PtrMYB21 and PtrMYB74 regulate genes associated with xylem cell wall formation

We overexpressed PtrMYB21 and PtrMYB74 in our SDX protoplast-based transregulation system to identify the downstream genes regulated by these PtrMYBs. We transfected the SDX protoplasts with plasmid DNA, *pUC19-35S::PtrMYB21-35S::sGFP* or *pUC19-35S::Ptr-MYB74-35S::sGFP*. Protoplasts transfected with *pUC19-35S::sGFP* plasmids were used as a control. The transfected protoplasts were incubated for 7h and collected for RNA-seq analyses (three biological replicates). The resulting transcriptomes of the PtrMYB21- or PtrMYB74-transfected protoplasts were compared with those of sGFP transfected. Overexpression of PtrMYB21 and PtrMYB74 affected the expression of 164 (False Discovery Rate (FDR) < 0.05, > 2-fold changes) and 135 (FDR <0.05, > 2-fold changes) genes, respectively (Figure 3; Table 1 and 2). The expression of these affected genes was all up-regulated, confirming the trans-activator function of PtrMYB21 and PtrMYB74 *in vivo*. To continue the discovery of the transcriptional regulatory network (TRN) in wood formation, we then focused on the TFs and the cell-wall biosynthetic genes in the 164 genes regulated by PtrMYB21 and in the 135 genes regulated by PtrMYB74.

Based on the annotation of the *P. trichocarpa* genome (Phytozome 11, https://phytozome.jgi.doe.gov/pz/portal.html) and the plant transcription factor database (PlantTFDB) (Goodstein et al., 2012; Jin et al., 2014), we identified 17 *TFs* from the 164 genes regulated by PtrMYB21, and 13 *TFs* from the 135 genes regulated by PtrMYB74. We next carried out GO analysis (G:profiler, http://biit.cs.ut.ee/gprofiler/; Reimand et al., 2016) on the remaining genes regulated by PtrMYB21 and PtrMYB74 to screen for cell-wall biosynthetic genes . Most of the significant GO biological process terms for these PtrMYB21 and PtrMYB74 regulated genes are associated with cell wall biosynthesis: including the “plant-type secondary cell wall biogenesis”, “lignin metabolic process”, and “lignin catabolic process” (Table 3 and 4). We found 19 PtrMYB21-regulated genes (Table 5) and 18 PtrMYB74-regulated genes (Table 6) that are associated with these cell wall biosynthesis processes. These genes include those encoding laccases and peroxidases for lignin polymerization, PtrCPR2, PtrPAL2, and PtrADT1 for monolignol biosynthesis, PtrFRA1 and PtrIRX6 for cellulose biosynthesis, and PtrIRX9 and PtrIRX14 for hemicellulose biosynthesis (Table 5 and 6).

Our *P. trichocarpa* tissue specific RNA-seq data (GSE81077, Shi et al. 2017) revealed that, of the 19 cell-wall biosynthesis process genes regulated by PtrMYB21, 14 are expressed specifically and abundantly in SDX, compared to leaves, juvenile shoots, and stem differentiating phloem (Table 7). Therefore, these 14 genes are likely associated with wood formation. Of the 18 cell-wall biosynthetic process genes regulated by PtrMYB74, 13 are SDX abundant and specific and therefore are more closely associated with wood formation. We also investigated the tissue specific expression of the TFs regulated by PtrMYB21 and PtrMYB74. All the TFs are expressed in xylem (Table 8). Although some of these TFs are expressed at low levels in xylem, we still included them in further studies because only a small amount of a TF may be necessary to activate a cascade of other genes (Kaufmann et al., 2011; Jones et al., 2015).

In summary, PtrMYB21 overexpression activated the expression of 17 TFs and 14 wood cell-wall biosynthetic genes. PtrMYB74 overexpression upregulated 13 TFs and 13 wood cell-wall biosynthetic genes (Table 1, 2, 3, and 4). Next, we used ChIP to analyze whether PtrMYB21 and PtrMYB74 directly regulate these TFs and cell-wall biosynthetic genes *in vivo* to validate the hierarchical layers of the transcriptional regulatory network.

2.3.3 Construction of regulatory hierarchies of the SND1-B1 network regulated by PtrMYB21 or PtrMYB74

To identify the direct targets of PtrMYB21 and PtrMYB74, we overexpressed PtrMYB21-GFP and PtrMYB74-GFP individually in SDX protoplasts, and performed ChIP analysis on the resulting protoplasts using anti-GFP antibody. We first tested whether the GFP-tagged MYB retains its transactivation ability as the native proteins do. To test this, PtrMYB21-GFP and the untagged PtrMYB21 were overexpressed in SDX protoplasts independently, and the transcript abundance of a gene (Potri. 005G129500) randomly selected from the 164 genes upregulated by PtrMYB21 was quantified by qRT-PCR. Both PtrMYB21-GFP and PtrMYB21 proteins can upregulate the expression of this randomly selected target gene (Figure 4A). PtrMYB74-GFP and PtrMYB74 could similarly upregulate a PtrMYB74 target gene (Figure 4B). Therefore, a GFP fusion of PtrMYB21 or PtrMYB74 does not affect their transactivation ability, and is suitable for identifying the direct targets of these PtrMYBs in ChIP assays.

We performed PCR amplification of the chromatin DNA products focusing on the approximately 2-kb promoter sequence (2000 to 1 bp) upstream of each cell-wall biosynthetic gene regulated by PtrMYB21 or PtrMYB74 (Figure 5A). We found that PtrMYB21 directly binds to the promoters of genes involving in monolignol biosynthesis (*PtrPAL2*), lignin polymerization (*PtrLAC21* and *PtrLAC26*), hemicellulose biosynthesis (*PtrIRX9* and Ptr*IRX14-L*), and cellulose biosynthesis

(PtrFRA1) (Figure 5B and D), while PtrMYB74 directly targets the promoters of lignin polymerization genes (*PtrLAC19*, *PtrLAC21*, and *PtrLAC26*), and cell-wall modification genes (*PtrPec9-1*, *PtrFLA17*, *PtrFLA18*, and *PtrQRT3*) (Figure 5C and D). These results revealed the divergent functions of PtrMYB21 and PtrMYB74 in regulating cell wall biosynthesis.

We then focused on other potential promoter sequences of targeted TF genes in the chromatin DNA products (Figure 6A). We found that PtrMYB21 can directly bind to the promoters of 10 TFs (Figure 6B). The 10 TFs included four MYB TFs, three Bel-like TFs, two NAC TFs, and one GRAS TF (Figure 6B; Table 1). Likewise, PtrMYB74 directly targets the promoters of 10 TFs, of which are six MYB TFs, three NAC TFs, and one Bel-like TF (Figure 6C, Table 1). Together, PtrMYB21 and PtrMYB74 directly regulate 15 TFs, with five being common targets (Figure 6D), suggesting redundant and combinatorial regulatory roles for the two PtrMYBs. Three of the identified 15 TFs, PtrMYB90, PtrMYB161, and PtrNAC123, have Arabidopsis homologs which have been discovered based on their roles in secondary cell wall formation (Hussey et al., 2011; Cassan-Wang et al., 2013). This suggests that PtrMYB21 and PtrMYB74 have roles in regulating cell wall biosynthesis through controlling their direct targeted TFs. The functions of the remaining 12 TFs in the formation of vascular xylem cell walls have not previously been determined. We then investigated the regulatory roles of the 15 TFs on the biosynthetic enzymes of cell-wall components.

2.3.4 Expanding PtrSND1-B1 network into the bottom HRN layer from TFs directed by PtrMYB21 or PtrMYB74

Cellulose, lignin, and hemicellulose are the major components of wood cell wall (Hagglund et al., 1951). Because the identification of the biosynthetic genes of hemicelluloses in tree species remains incomplete, we focused on the biosynthetic genes of cellulose and monolignols that are expressed in wood forming tissue (SDX). We identified 36 cell-wall component genes (Table 9), including nine primary cellulose

synthase genes (*PtrPRC1-1, 2, PtrIXR1-1, 2, 3, 4, PtrRSW1-1, 2,* and *PtrCesA9-3*, Suzuki et al, 2006; Kumar et al., 2009), five secondary cellulose synthase genes (*PtrCesA4, 7, 8, 17*, and *18*; Kumar et al., 2009; Song et al., 2010), and 22 monolignol biosynthetic genes from 11 families (*PAL*, *C4H*, *4CL*, *C3H*, *HCT*, *CCoAOMT*, *AldOMT*, *CAld5H*, *CCR*, *CAD*, *CSE*; Rui et al., 2009; Wang et al., 2014). The expression of these 36 genes was examined using qRT-PCR in the transfected SDX protoplasts overexpressing each of 15 TFs that are directly regulated by PtrMYB21 or PtrMYB74. The examined genes, whose expression increased 2-fold or decreased to 0.8-fold in a specific TF-transfected SDX protoplasts compared to control, are identified to be regulated by the TF.

9 of these 15 TFs (PtrMYB90, 161, 174, 175, PtrWBLH1, 2, and PtrNAC123) could regulate the expression of 25 of the 36 cell-wall component biosynthetic genes in transfected SDX protoplasts (Figure 7). These 25 genes include all primary and secondary cellulose synthase genes, and members from all monolignol gene families except CCR. We then tested which of these 9 TFs directly bind to the promoters of their regulated cell-wall component genes. Each of the 9 TFs was fused to GFP and overexpressed in SDX protoplasts. The DNAs coupled with each recombinant TF protein were precipitated using anti-GFP antibodies. We amplified the promoter sequences from the precipitated DNAs using the appropriate primers. The primers were designed in a similar way as the promoters of PtrMYB21 and PtrMYB74 targets (Figure 8A).

We found that 6 (PtrMYB90, 161, 174, PtrWBLH1, 2, and PtrNAC123) of the 9 TFs directly bind to the promoters that are upstream of 15 of the 25 cell-wall component genes (Figure 8). PtrWBLH1, 2, PtrMYB174, and PtrNAC123 directly regulate monolignol biosynthetic genes (*PtrCCoAOMT1, 2, PtrHCT1, 6, PtrCAld5H1* and *PtrCSE2*), whereas PtrMYB90 and PtrMYB161 directly regulate both cellulose synthase genes (*PtrCes4, 17, 18, PtrRSW1-1, 2*) and monolignol biosynthetic genes

(*PtrCCoAOMT1, 2, PtrCAld5H1,2,* and *PtrCOMT2*) (Figure 8B and C). We also observed that PtrMYB90, 161, and PtrWBLH1 bind to the same fragment (500 to 1bp) of *PtrCCoAOMT2* promoter, PtrMYB90, 161, and PtrWBLH2 bind to the fragment of the *PtrCAld5H1* promoter which range from 1000bp to 500 bp, and PtrMYB90 and PtrNAC123 bind to the promoter sequence of *PtrCCoAOMT1* (500 to 1bp) (Figure 8), suggesting that these TFs may form protein complexes in regulating the three monolignol genes. These identified 15 cell-wall component genes, together with the cell-wall biosynthetic genes directly regulated by PtrMYB21 and PtrMYB74, were placed at the bottom layer of the TRN.

2.3.5 An SDX protoplast based four-layered network mediated by PtrSND1-B1 in wood-forming cells

The constructed four-layered hierarchical TRN integrated 57 TF-DNA regulatory interactions between 18 TFs and 27 cell-wall biosynthetic genes (Figure 9). In this TRN, PtrSND1-B1 is at the top layer, PtrMYB21 and PtrMYB74 are at the second layer, 15 TFs directed by PtrMYB21 and PtrMYB74 are at the third layer, 27 cell-wall biosynthetic genes are at the bottom layer (Figure 9). We found most of the direct regulatory interactions (56/57) (Table 10) result in the activation of the target gene expression, suggesting that this PtrSND1-B1 directed four-layered TRN is mainly involved with the activation of xylem cell wall biosynthesis in wood formation. For each regulatory interaction, its regulatory effect is quantitatively determined (Figure 9) based on the qRT-PCR and RNA-seq analyses in SDX protoplasts (Table 1 and 2; Figure 7).

We next asked whether the TFs and their targets are co-expressed within a SDX-cell type. For the top and second layer TFs (PtrSND1-B1, PtrMYB21, and PtrMYB74), their transcripts have been demonstrated to co-exist in SDX fiber and vessel cells (Table 9). We next investigated the expression of the third-layer TFs using xylem cell specific RNA-seq data (GSE81077). 11 of the 15 third-layer TFs are co-expressed in

xylem fiber and vessel cells, whereas the transcripts of the other four TFs (*PtrMYB59, 88, 175*, and *PtrNAC125*) could not be detected in either fiber or vessel cells (Table 11). The absence of the transcripts of these four TFs in the specific SDX cells may be attributed to other regulation, such as microRNA cleavage of transcripts. Further expression analyses showed that these 27 bottom-layer genes are expressed in both fiber and vessel cells with their upstream TFs (Table 12). In summary, the results demonstrated that 91% (41/45) of the TRN-containing genes have transcripts in both fiber and vessel cells, suggesting a functional association of this TRN with wood formation *in planta*.

Finally, we used transgenic *P. trichocarpa* plants to verify the adequacy of this TRN to represent gene regulation that occurs in wood formation. We tested whether the regulatory effects of these ChIP verified TF–DNA interactions take place in SDX of transgenic *P. trichocarpa* plants by knocking down some TFs from the TRN.

2.3.6 Transgenic *P. trichocarpa* with decreased *PtrMYB21*, *74*, and *90* expression demonstrates that most direct target genes of PtrMYBs are downregulated in the SDX tissues

We showed that ~90% of the protoplast-inferred TF–DNA interactions tested were validated for their regulatory effects in PtrSND1-B1 transgenic trees. (Lin et al., 2013). The verified interactions included the direct regulation of PtrSND1-B1 for PtrMYB21 and PtrMYB74 (Lin et al., 2013). Therefore, we then selected PtrMYB21 and PtrMYB74 as targets to be knocked down in *P. trichocarpa* SDX. The SDX-specific promoter 4CLXP, which was cloned from the *Ptr4CL3* promoter (Wang et al., 2014), was used to drive the RNAi inverted repeat sequences that target *PtrMYB21* and *PtrMYB74* transcripts. The generated constructs *4CLXP::siRNA-PtrMYB21* and *4CLXP::siRNA-PtrMYB74* were then transformed into *P. trichocarpa*, (Materials and Methods). 12 independent *PtrMYB21* RNAi lines were generated, and the three lines with lowest transgene levels were selected for analyzing the expression of the

protoplast-inferred target genes (Figure 10A). Similarly, from nine independent PtrMYB74 RNAi lines, we selected three PtrMYB74 transgenic lines with the lowest transgene level for further characterization (Figure 10B).

Using the SDX protoplast system, 10 TFs and 8 cell wall biosynthetic genes were identified to be directly activated by PtrMYB21 (Figure 5 and 6). qRT-PCR analyses of these 18 genes in the SDX tissue of PtrMYB21 RNAi lines showed that the expression of ~90% (16/18) of the protoplasts-inferred PtrMYB21 targets (Figure 11A) were down-regulated compared to the wild-type trees, suggesting that our TF overexpression coupled with ChIP approaches using SDX protoplasts can reveal the regulation of TFs in wood-forming tissue. This finding was also verified by gene expression analyses in the *PtrMYB74* transgenics. For 10 TFs and 7 cell wall biosynthetic genes directly activated by PtrMYB74 in protoplasts, the analyses showed that ~90% (15/17) (Figure 11B) have down-regulated expression in *PtrMYB74* RNAi lines compared to wild-type trees.

We have validated that our PtrSND1-B1 directed network can predict the effects of the regulatory interactions directed by PtrMYB21 or PtrMYB74, which we placed at the second-layer of the TRN. We then tested whether the direct regulation of the third-layered TFs for their target genes takes place in intact SDX tissue of *P. trichocarpa*. PtrMYB90, a common target of PtrMYB21 and PtrMYB74, was selected to be knocked down in *P. trichocarpa* SDX. We designed an artificial microRNA that targets PtrMYB90 transcripts, and created *4CLXP::miRNA-PtrMYB90* for the transformation in *P. trichocarpa* (Shi et al., 2010). Nine independent transgenic *P. trichocarpa* lines were generated, and three with the lowest transcript level of the PtrMYB90 were selected for further study (Figure 10). We identified seven cell-wall component genes targeted by PtrMYB90 using SDX protoplasts (Figure 8). We quantified the transcript abundance of these seven genes in the selected transgenic lines, and found that 100% (7/7) of genes have reduced expression compared to controls (Figure 11C). Overall,

our results showed that the regulatory effects of PtrMYB21, PtrMYB74, and PtrMYB90 can be (~90.4%) inferred by our TRN for their direct targets in SDX tissue, suggesting that our TF overexpression following with ChIP assays in SDX protoplast system is sufficient to reveal wood-forming cell-specific TF-DNA regulatory networks, without using stable transgenics.

2.4 Discussion

A PtrSND1-B1 mediated four-layered TRN was constructed using transient overexpression of TFs and by investigating gene expression and ChIP in SDX protoplasts. This TRN elucidates how PtrSND1-B1 and its downstream TFs regulate cell wall biosynthetic genes through the direct TF-DNA interactions. From the network, we can quantitatively describe and predict the regulatory effects of the TF-DNA interactions. Most of these TF-DNA interactions result in the activation of the target genes, demonstrating that most TFs in our network function as transcriptional activators. The expression of these transcriptional regulators, and their targets were observed in stem differentiating fiber and vessel cells, which undergo wood forming processes. Using expression profiling to test the selected TFs (PtrMYB21, PtrMYB74, and PtrMYB90) in transgenics, 90.4% of the identified TF-DNA interactions can be validated for their regulatory effects. Therefore, the TF-overexpression coupled with ChIP assays in SDX protoplasts enable the identification of the TFs that influence cell wall biosynthetic genes in wood formation with a high success rate.

2.4.1 A transient overexpression system for TF target discovery

We previously established a SDX protoplasts system for transient gene expression and transactivation assays. Here, we coupled this system with the epitope-based ChIP assays to identify the direct targets of the TFs. This modification provides information on the direct TF-DNA interactions. One advantage of the modified system lies in the quantitative measurement of the direct TF-DNA interactions. We quantified the

transcript abundance change of the target genes in response to the TF overexpression in SDX protoplasts. Then the direct protein-DNA interactions between TFs and the promoters of targets were characterized in the SDX protoplasts overexpressing the tagged TFs. Through these two steps, each TF-DNA interaction was quantified for its effects in SDX protoplasts. This advantage makes our system a powerful tool for *in planta* verification and quantification of specific TF-target interactions that are otherwise characterized by Y1H or EMSA. Another advantage is that the experiments using our system take less time to identify the direct targets compared to the traditional ChIP experiments. A traditional ChIP experiment is performed using transgenic plant lines expressing tagged TF-of-interest for transcriptomic and DNA-binding analyses (Monke et al., 2012; Mourik et al., 2015). Using SDX protoplasts, the direct targets of a candidate TF can now be determined in experiments within several hours rather than the months required to generate of stable transgenic plants. This protoplast-based system could be widely used for many woody species that are either difficult or time-consuming to be stably transformed. Our modified system combined with transient gene expression and ChIP assays enable the rapid and quantitative assessment of TF-DNA interactions and provide a basis for transcriptional regulatory network construction.

2.4.2 Limitations: false positives and false negatives

Although our system is effective at identifying the targets regulated by TFs in wood forming tissue, we may still miss many target genes. First, if the regulation of a subset of targets need some cofactors that interact with the specific TF, we might not detect these targets because we only overexpressed the specific TF, not the cofactors, in SDX protoplasts. Second, we used a cutoff (False Discovery Rate (FDR) < 0.05, > 2-fold changes) to identify the differential expressed genes (DEGs) in response to the overexpression of PtrMYB21 and PtrMYB74, and we eliminated the rest of the DEGs. Some of the direct targets of these two PtrMYBs may exist in the eliminated DEGs

with high FDR or low fold change. Thirdly, our ChIP assays may also not detect some direct regulation because some TFs bind to promoter regions, which are not included in 2kb promoter upstream of the start codon we selected.

It is also possible that some of the identified genes are not true targets of the TFs. The TF proteins are expressed at high levels in the transgenic protoplasts and may bind to sites not targeted by these TFs at normal concentrations in intact wood-forming tissue. Additionally, the protoplasts are sensitive to environmental factors, such as light, temperature, and osmotic stress. These environmental factors may affect the binding of TFs to the promoter sequences. Therefore, additional genetic and gene expression studies are required to validate the TF-DNA interactions, but the identified targets provide good starting points for such further studies.

2.4.3 Validation of our PtrSND1-B1 directed four layer TRN in developing SDX

Large scale screening of TF-DNA interactions inherently includes false positive results, and thus interactions to be analyzed for biological significance need to validated *in planta*. The biological significance of these interactions can be revealed by the ability of a TF to regulate these targets. Genetic analysis is a common approach for validating the occurrence of the regulation. We tested the expression of target genes in the transgenics (RNAi or amiRNA transgenics) of a TF (PtrMYB21, 74, or 90) relative to the wild type. 90.4% of the TF-DNA interactions were detected with the altered levels of target gene expression (Figure 8). The results suggest that our SDX system with the transient TF overexpression followed by target expression and DNA-binding assays can eliminate false positives efficiently and effectively. Additionally, we observed that the expression of the target genes is downregulated slightly (decreasing to 50% to 80%) in the selected transgenic lines whose expression is significantly decreased (decreasing to 20% to 30%) (Figure 10 and 11). This phenomenon can be explained by the extensive genetic redundancy in *Populus* (Tuskan et al., 2006), which

suggests that other unknown TFs also regulate these targeted cell wall biosynthetic genes in wood formation.

Another approach to test the existence of the TF-DNA regulatory interactions is to analyze the transcript abundance changes of the TFs and targets in a dynamic biological process. Wood formation is a dynamic developmental process from cambium to mature xylem. Ko et al.,2012 profiled the transcriptome changes in wood formation by time-series microarray analyses of cambium, developing xylem, and mature xylem tissues. Due to the limitation of microarray detection for the whole transcriptome, only 30 of 45 the network-included genes can be detected by these microarray analyses. As shown in Figure 12, the expression of these 30 genes are slightly increased from cambium to developing xylem. From developing xylem to mature xylem, the expression of all 15 third-layer genes except PtrMYB174, 175, and NAC105, are upregulated, consistent with the increased expression of activators PtrSND1-B1, and PtrMYB21, 74 (Figure 12. Correspondingly, the expression of cell wall biosynthetic genes in the fourth-layer, except RSW1-2, are upregulated in concert with that of their upstream regulator (Figure 12). Strong correlation coefficients can be observed between the expression of TFs and their target genes during wood formation, confirming the effects of the TF-DNA interactions identified by ChIP assays.

2.4.4 PtrMYB74, a woody plant specific TF, has potential roles in regulating wood formation

As illustrated in our TRN (Figure 9), PtrMYB74 directly regulates 7 cell wall biosynthetic genes and 10 TF genes. These cell wall biosynthetic genes are mainly involved with lignin polymerization and cell wall modification (Table 2). Four of the 10 TF genes (*PtrMYB90*, *161*, *174*, and *PtrWBLH1*) directly regulate cell-wall component genes through TF-DNA interactions (Figure 9). Our protoplast system coupled with ChIP also identified some indirect targets of PtrMYB74 (Figure 5). These indirect targets also have been shown to regulate some wood formation processes. For

example, *PtrFLA17* encodes a fasciclin-like arabinogalactan protein (Potri.013G151300), whose transgenic poplars have altered stem mechanical properties and cell wall composition (Wang et al., 2014). Some of these indirect targets have Arabidopsis homologs involving cell-wall component biosynthesis, including *PtrIRX6* and *PtrFRA1* homologs for cellulose synthesis (Sato et al., 2010; Zhu et al., 2015), a *PtrBBE13-like* homolog for the monolignol synthesis (Daniels et al., 2015), and a *PtrIRX15-like* homolog for hemicellulose synthesis (Jensen et al., 2010). RNA-seq analyses showed that PtrMYB74 regulates metabolic genes of the brassinosteroid, gibberellic acid, and phosphoglycerolipid pathways (Table 2 and 14). These metabolites regulate xylem cell development during wood formation (Eriksson et al., 2000; Kondo et al., 2014; Noh et al., 2015; Gujas and Rodriguez-Villalon, 2016). Further investigation of the mechanism regarding how PtrMYB74 regulates these indirect targets will expand our TRN, thus providing new knowledge for the transcriptional regulation of wood formation.

In woody species, early studies found several TFs, such as SNDs, VNDs, and HBs, that function in regulating wood formation (Zhong and Ye, 2015). These TFs were initially characterized using genetic studies of their Arabidopsis homologs (Table 1 in Zhong and Ye, 2015). These characterized TFs usually share similar molecular functions with their Arabidopsis homologs (Nakano et al., 2015; Ohtani et al., 2017). Thus, identification of TFs directly in woody species is required. This approach need to identify TFs that have regulatory functions for specific processes in wood formation, which can be specific TFs for woody plants. We proposed that PtrMYB74 is such a TF. The function of PtrMYB74 is different from its Arabidopsis homologs *AtMYB17* and *AtMYB35*, which were characterized as regulators of meristem and flower development (Zhu et al., 2008; Pastore et al., 2011). The protein sequence alignment of the homologs of PtrMYB74 from 69 diverse plant species (Phytozome 12; https://phytozome.jgi.doe.gov/) shows that these homologs that have high protein sequence similarity with PtrMYB74 are from woody species. The phylogenetic tree of

the selected homologs (filtered using >60% protein similarity with PtrMYB74; Figure 13) clearly indicates that the homologs from woody dicots are clustered in clade 1 and the homologs from herbaceous dicots are clustered in clades 2 and 3. The proteins in clade 1 have high protein similarity with PtrMYB74, and the proteins in clade 2 and 3 share low protein similarity with PtrMYB74. Therefore, the functional association of PtrMYB74 in woody species will be important for later investigation.

2.4.5 The regulators of cell wall biosynthetic genes

Our transient overexpression of the PtrSND1-B1 downstream TFs found several TFs that function in regulating cell wall component genes. Except PtrMYB21 (Zhong et al., 2013) and PtrMYB74 discussed earlier, 9 other cell wall regulators were identified. These 9 TFs can be classified into three different types based on their overexpression effects on the cell wall component genes (Figure 7). Type I TFs, including PtrMYB90, 161, 175, PtrWBLH1, 2, PtrNAC123 positively regulate cell wall component genes. Type II TFs, including PtrMYB174 and PtrNAC125, negatively regulate cell wall component genes. PtrWBLH3 is classified as Type III because the overexpression effects of PtrWBLH3 up-regulate some cell wall component genes and down-regulate some others.

PtrMYB90, PtrMYB161 and PtrMYB175 are phylogenetically paired MYB homologs in the *P. trichocarpa* genome. The most similar Arabidopsis homologous protein with these three TFs is AtMYB52. The protein similarities between AtMYB52 and PtrMYB161, PtrMYB175 are 66.5%, 63.6%, and 61.7%, respectively. The only cell wall biosynthetic gene targeted by AtMYB52 in previous studies is AtPAL1 in Arabidopsis leaves (Ko et al., 2009). PtrMYB90, PtrMYB161, and PtrMYB175 can up-regulate 12, 13, and 5 of the 36 cell wall component genes, respectively (Figure 5). Our results expand the knowledge of the function of AtMYB52 and its homologs in regulating cell wall biosynthesis. Another TF family in Type I TFs is the Bel-like family, including PtrWBLH1 and 2. PtrWBLH1 effectively regulates the expression of *PtrPAL2*,

PtrC4H1, *Ptr4CL3*, *Ptr4CL5*, and *PtrCAD1* (Figure 7), indicating that it can affect much of the whole monolignol pathway, especially for H-lignin synthesis. PtrWBLH2 strongly activates the expression of *PtrCAld5H1*, *PtrCAld5H2*, and *PtrHCT1* (Figure 5), indicating an important role in regulating S-lignin biosynthesis. The Arabidopsis homologs of PtrWBLH1 and 2 are *AtBLH1* and *AtBLH7*, which have not been shown any association with cell wall biosynthesis.

Another finding is the identification of a transcriptional activator and repressor of the caffeoyl shikimate esterase (CSE). CSE converts caffeoyl shikimate to caffeate, and its mutants have reduced lignin content and collapsed vessel elements (Vanholme et al., 2013). PtrWBLH1 positively regulates the expression of PtrCSE2, while PtrMYB174 negatively regulates its expression. ChIP assays found that PtrWBLH1 interacts directly with the promoter of PtrCSE2. The results provide evidence for the transcriptional regulation of CSE in a woody plant. The functional differences between these regulators and the corresponding Arabidopsis homologs motivated us to compare *Populus* and Arabidopsis cell wall biosynthesis.

2.4.6 Comparison of gene regulatory networks in cell wall biosynthesis between *Populus* and Arabidopsis

Our PtrSND1-B1 mediated four-layered network, as a representative of transcriptional regulation of xylem cell wall biosynthesis in *Populus*, can be compared with the transcriptional regulation in Arabidopsis. Many studies in transcriptional regulation of cell wall biosynthesis were performed in Arabidopsis, a herbaceous genetic model species. (Kubo et al., 2005; Zhong et al., 2006; Mitsuda et al., 2007; McCarthy et al., 2009; Ko et al., 2012, 2014). The comparative analyses of cell wall biosynthesis related TRNs between *Populus* and Arabidopsis elucidated underlying differences in the transcriptional regulation for cell wall biosynthesis. The results from these analyses could help understanding of why the cell wall compositions of woody plants

are fundamentally different from that of herbaceous plants (Pauly and Keegstra, 2008) by exploring differences at the transcriptional level.

Recently, 467 Arabidopsis root TFs were screened for interactions by Y1H analysis with promoters of 45 genes implicated in root cell-wall formation (Taylor-Teeple et al., 2015). This study yielded a 5-layer TRN that included 209 (~42% of 467) root TFs, mediating 617 TF-DNA interactions (Taylor-Teeples et al., 2015). Comparing this TRN with our results, 4 of 209 Arabidopsis TFs have homologs in the PtrSND1-B1 mediated four-layered TRN. These 4 TFs directly mediate 9 TF-DNA interactions. Only the interaction between AtSND2 and AtCCoAOMT1 have the parallel regulation in our network (PtrNAC123 and PtrCCoAOMT1). Such a small amount of overlap may result from the differences in the tissues studied (root vs stem differentiating xylem). Another possible reason for differences is the methods used for generating the network. For example, Y1H assays determined that REVOLUTA (REV) binds to the promoters and represses the expression of genes involving monolignol biosynthesis (Taylor-Teeples et al., 2015). However, glucocorticoid receptor-based inducible assays can't identify monolignol biosynthetic genes as the targets of REV (Brenda et al., 2013). To reduce the bias, the TRNs used for comparison should be generated from similar tissues using similar methods.

Our PtrSND1-B1 mediated TRN was established using two core approaches: 1. Quantification of the regulatory effects of TF perturbation or overexpression of the targets. 2. Determination of whether the regulation acts through direct or indirect TF-DNA interactions. We queried the PubMed database for experimental evidence of the involvement of the 202 Arabidopsis TFs associated with cell wall biosynthesis (Chapter 1, Table 2), and checked the researches on the TFs using techniques similar to ours. Seven TFs (AtMYB46, AtMYB58, AtMYB63, AtMYB83, AtMYB103, AtSND1, and AtVND6) were identified (Table 15), two (AtSND1 and AtMYB46) of which have homologs with *Populus* genes in our network. Based on studies using inducible

assays, EMSA, Y1H, or ChIP assays (Zhong et al., 2007; Zhong et al., 2010; Zhong et al., 2012; Kim et al., 2013; Taylor-Teeple et al., 2015), 14 TF and 9 cell wall biosynthetic genes were identified as the direct targets of AtSND1, and 17 TF and 12 cell wall biosynthetic genes are direct targets of AtMYB46. Using these TF-DNA interactions, a three-layered hierarchical TRN directed by AtSND1 and MYB46 was constructed as illustrated in Figure 14 for Arabidopsis stem cell wall biosynthesis.

We focused on the conserved interactions between TFs and cell wall biosynthetic genes between Arabidopsis and *Populus* in the network. AtSND1 and PtrSND1-B1 are top regulators that initiate each of the networks respectively. PtrSND1-B1 directly regulates 10 TF and 2 cell wall biosynthetic genes (Lin et al., 2013), and AtSND1 directly regulates 14 TFs and 9 cell (Figure 14; Table 15). Compared to the targets of PtrSND1-B1, AtSND1 specifically regulates TFs involving vascular meristem and secondary tissue differentiation, such as *AtLBD15*, *AtWOX13*, *AtSAC51*, *AtXND1*, and *AtIBH1* (Grant et al., 2010; Ikeda et al., 2012; Yoshimoto et al., 2012; Sun et al., 2013; Dolzblasz et al., 2016), suggesting that PtrSND1-B1 and AtSND1 have different regulatory functions. This hypothesis is also validated because none of the cell wall biosynthetic genes or their homologs are common targets for PtrSND1-B1 and AtSND1. The only identified common targets are MYB homologs (PtrMYB2, 21 and AtMYB46). Comparison of the targets of AtMYB46 and PtrMYB21 revealed the differences and commonalities of the regulatory functions of these MYB homologs. Some common targets regulated by these MYBs were identified, which encode 6 TFs (PtrMYB90, 161, 175, and WBLH1, 2, 3), one hemicellulose biosynthesis enzyme (PtrIRX14-L), and one lignin polymerization enzyme (PtrLAC19). The regulatory cascades AtSND1(PtrSND1-B1)-AtMYB46(PtrMYB21)-AtMYB52(PtrMYB90, 161, and 175), and AtSND1(PtrSND1-B1)-AtMYB46(PtrMYB21)-AtBLH2, 3, and 6 (PtrWBLH1, 2, and 3) are conserved between Arabidopsis and *Populus*. However, TF homologs regulate different cell wall biosynthetic genes in Arabidopsis and *Populus*. While PtrMYB21 directly regulated *PtrPAL2* (Figure 7), its Arabidopsis homolog

AtMYB46 directly regulates *AtCAD4, AtCCoAOMT1, AtCCR-like1, 2, At4CL3, AtPAL1,2, 4*, demonstrating that differences between AtMYB46 and PtrMYB21 regulation. The findings are consistent with the divergent function between PtrSND1-B1 and AtSND1 because they regulate the different cell wall biosynthetic targets. Therefore, the mechanism how cell wall biosynthetic related TFs function is required to analyze in woody plants, even if these TFs or their homologs have been functionally characterized in Arabidopsis. It must now be considered that the differences in the activity and specificity of the genes in the regulatory network may contribute to the differences in the composition and organization of the differentiating xylem in these two different plant species.

2.4.7 Possible TF complexes regulating cell wall biosynthesis are implicated by DNA-binding assays

Several TF complexes have been shown to regulate cell wall biosynthesis, including AtVND-INTERACTING2 (VNI2)/VND6 heterodimers (Yamaguchi et al., 2015), PtrSND1/SND1-A2^{IR} heterodimers (Li et al., 2012), and AtBLH6-KNAT7 heterodimers (Liu et al., 2014). The regulatory mechanisms of these TF complexes are either negative regulators (VNI2, or SND1-A2^{IR}) that interact with a TF activator (VND, or SNDs) to inactivate the activation abilities of the TFs, or by forming complexes with the repressors, such as BLH6 and KNAT7. Previous studies have not identified a TF complex formed by the activators that regulates cell wall biosynthesis genes. 7 activators from our network were shown to directly regulate cell wall biosynthesis genes (Figure 9). Four groups of TFs have been identified to bind to the same promoter sequences, including group of PtrMYB21 and PtrMYB74, a group of PtrMYB90, 161, and PtrWBLH1, a group of PtrMYB90, 161, and PtrWBLH2, and a group of PtrMYB90 and PtrNAC123. These identified TFs are also co-expressed in the wood-forming cells (Table 11 and 12). These results provide several candidate activators that can form TF complexes regulating cell wall biosynthetic genes. The

coordination and cooperation of these TFs in complexes may generate some novel functions that each individual TF does not have.

2.4.8 Do vascular development TFs regulate the PtrSND1-B1 directed network?

Vascular development and xylem cell wall biosynthesis are closely related biological processes that are affected by the same signaling pathway (Ito et al., 2006; Etchells and Turner, 2010). PtrSND1-B1 have been shown to regulate genes involved in vascular development (Lin et al., 2013). Thus, identifying other developmentally related TFs regulating our TRN is now required. In *Populus*, several TFs have been functionally characterized to regulate vascular differentiation and development, including ARBORKNOX1 (PtrARK1) and PtrARK2 (Groover et al., 2006; Du et al., 2009), Class III HD ZIPs popREVOLUTA (PtrPRE), popCORONA (PtrPCN), and PtrHB7 (Du et al., 2011; Robischon et al., 2011; Zhu et al., 2013). Subsequent ChIP analyses identified the targets of these TFs (Liu et al., 2015 a, b). Their targets only include PtrWBLH2, which locate in the third layer of our TRN. Whether the vascular development related TFs affecting our PtrSND1-B1 TRN has not been answered by previous studies, and needs further investigation.

2.4.9 Alteration of the PtrSND1-B1 mediated TRN in tension wood development and differentiation

Tension wood forms on the upper side of a bent stem in response to mechanical stress, and has increased cellulose and decreased lignin (Timell 1969; Joseleau et al. 2004). Comparative transcriptome analyses of tension wood-forming tissue and normal wood-forming tissue provides us a chance to investigate the expression change of genes in our TRN in response to mechanical stress. In tension wood, we found that 94% (17/18) of TF genes in our TRN are downregulated, and 96% (26/27) of their targets are correspondingly downregulated (Table 16), consistent with the activation activities of most identified TFs. The activities of our TRN are silenced during tension

wood formation. Given our TRN represents transcriptional regulation in normal wood formation, these findings suggest that tension wood formation experiences a transcriptome remodeling and has a distinct regulatory network regulating cell wall biosynthesis. Therefore, identifying a TRN which specifically regulates cell wall biosynthesis in tension wood formation is essential to understand the mechanism of the formation of cell walls with high cellulose and low lignin contents.

2.5 Conclusion and perspective

The modified SDX protoplast system coupled with ChIP assays not only can effectively study the complex regulatory functions of the TFs in wood formation, but it can also provide information on TF-DNA interactions in a complex regulatory hierarchy. We discovered that some of direct regulatory targets of PtrMYB21 and PtrMYB74 are activated within 7 h after two of these MYBs are used for transfection and overexpression (Figure 5 and 6). These direct targets of PtrMYB21 and PtrMYB74 included unique genes encoding 15 TFs and 12 cell wall biosynthetic enzymes. This approach using transient TF overexpression with ChIP assays then allows the sequential description of a regulatory network of a specific TF. In this study on 15 TFs in a third hierarchical layer, this approach led to the fourth hierarchical layer, encompassing ultimately 15 cell wall component genes. We used the same approach to analyze whether each of the third-layer TFs could regulate PtrMYB21, 74, or PtrSND1-B1, thereby forming feedback or feed forward regulatory loops. Subsequently, a more comprehensive regulatory network can be identified to describe wood cell wall biosynthetic genes. Overall, all identified hierarchical TRNs are part of functional networks depicting not only connectivity but quantitative information of transregulation effects of the direct TF-DNA interactions. These analyses expand our knowledge of the transcriptional program regulating wood cell wall biosynthesis in *P. trichocarpa*.

2.6 Materials and Methods

2.6.1 Plant Materials

P. trichocarpa plants (genotype *Nisqually-1*) were maintained and cultured in a greenhouse. Plant branches (~10 cm) from *Nisqually-1* plants were cut and then rooted in water. The rooted branches were planted into a mixture of 1/4 Miracle-Gro® soil (Scotts Miracle-Gro Products, Marysville, OH, USA) and 3/4 Metro-Mix 200 (Sun Gro, Bellevue, WA, USA) in 16 cm pots, watered thoroughly, and maintained in a greenhouse (17–26°C, 16 h light/8 h dark cycle with supplemental lighting of ~300 μE m^{-2} s^{-1}). When plants reached about half meter, they were transplanted into 28 cm pots. Plants were fertilized with 500 ml per pot with 2 g Miracle-Gro N-P-K (15-30-15) (Scotts Miracle-Gro Products) every 10 d (Song et al., 2006). Stem internodes of healthy 3- to 9-month-old plants were used to collect xylem tissue used for RNA isolation and SDX protoplast isolation.

2.6.2 Plant transformation

We prepared the medium (CIM1, CIM2, SIM1, SIM2, SIM3, and RIM1) as described in Song et al., 2006 for culturing the transfected stems. The stem fragments of the fifth to the ninth internodes were harvested from healthy, 5- to 6-month-old greenhouse-grown Nisqually-1. The fragments were sterilized in 10% Clorox (Clorox, Oakland, CA, USA) for 20 min and rinsed three times for 3 min each time using 1 L sterilized distilled water. Stem segments were cut from each fragment and inoculated for 5 min in an *Agrobacterium* culture by swirling. The cut segments were placed horizontally and co-cultivated with the unrinsed *Agrobacterium* culture on CIM1 in the dark for 2 d at 25°C. The co-cultivated segments were washed four times using sterilized distilled water for 2 min each. Each washed segment was briefly blotted dry on sterile filter paper, and then cultured on CIM2 at 25°C in the dark for 5 days. The new CIM2 was refreshed for culturing these segments after 5 days. These explants were transferred to fresh CIM2

every 14 d until calli formed. The white, hard calli were cultivated at 25°C under a 16 h light /8 h dark cycle in the following series: 20d on SIM1, 40 d on SIM2 for the green calli formation. These calli-containing segments were then transferred onto SIM3 media 20 days for generating transgenic shoots. Transgenic shoots were excised and rooted on RM for 30 days. Transgenic plants with root systems were obtained usually after 30 days on RM, and could be transplanted into soil and maintained in a greenhouse.

2.6.3 Primer design

Primer-Blast (https://www.ncbi.nlm.nih.gov/tools/primer-blast/) was used to design primers for the cloning of gene coding sequence, transcriptional activity assays, subcellular location assays, RNA silencing, and microRNA cleavage. The sequences were based on phytozome database. These primers were listed in Table 13. Likewise, Genescript (https://www.genscript.com/tools/real-time-pcr-tagman-primer-design-tool) was used to design the qRT-PCR primers, which are listed in Table 13. ChIP-PCR primers were designed based on the protocol (http://fg.cns.utexas.edu/fg/protocol__ChIP-DNA_primer_design.html). Four primers were designed for covering the 2kb sequence upstream of the start site of each gene.

2.6.4 Amplification of gene encoding sequences

Total RNA from developing xylem, developing phloem, mature leaves, juvenile shoots, and mature roots of *P. trichocarpa* was isolated with the RNeasy Plant RNA Isolation Kit (Qiagen, Valencia, CA, USA). Two micrograms of total RNA from each tissue was reverse transcribed to cDNA (Omniscript RT Kit; Qiagen) in 20μl and then diluted to 200 μl after transcription. The amplification and cloning of the *PtrWBLH1*, *2*, *3*, *PtrNAC125*, *127*, *PtrMYB21*, *74*, *88*, *90*, *161*, *174* and *175* coding sequences was obtained from developing xylem cDNA. The amplification of *PtrNAC123* came from cDNA of juvenile shoots, the cDNAs of *PtrMYB59*, *PtrHAM3*, and *PtrNAC105* were

amplified from cDNA of developing phloem, and cDNAs for *PtrMYB93* were obtained from the cDNA of mature leaves. Each amplification was conducted in 50 µl reactions containing 1× polymerase chain reaction (PCR) buffer, 0.4 mM forward and reverse primers, 4 µl of cDNA template, 2 mM dNTP and 2.5 U of PfuUltra high fidelity DNA polymerase (Stratagene, Santa Clara, CA, USA). The PCR products were purified using the QIAquick Gel Extraction Kit (Qiagen), and transferred into *pENTR-D-TOPO* vectors.

2.6.5 Plasmid Construction

For constructing plasmids used for RNAi suppression, the vector system that is amenable to *Agrobacterium*-mediated transformation was applied following Miki et al. (2005). A 680 bp GUS linker was amplified with a pair of primers, 5′-TGACCTCGAGGTCGAC GATATCGTCGTCATGAAGATGCGGAC-3′ and 5′-CTAGACTAGTCC CGGGGGTACC ATCCACGCCGTATTCGGTG-3′, and cloned into the pCR2.1 Vector at XhoI/SacI, resulting in *pCR2.1-GUS* Linker (pCR2.1-GL). The inverted repeat sequence consists of chimeric sequences from PtrMYB21. A 250bp fragment from *PtrMYB21* coding sequence using PtrMYB21RNAiSF and PtrMYB21RNAiSR as sense strand, and an antisense strand was cloned by PtrMYB21RNAiASF and PtrMYB21RNAiASR. These primers are listed in Table 13. The sense and antisense fragments were inserted in pCR2.1-GL at XbaI/XhoI and SpeI/SacI, respectively, to produce pCR2.1-sense-GL-antisense-MYB21(RNAi-MYB21). Likewise, we use PtrMYB74RNAiSF, R primers and PtrMYB21RNAiASF, R primers to clone the sense and antisense fragments of PtrMYB74 (266bp length). These fragments were inserted into pCR2.1-GL to generate *RNAi-PtrMYB74*.

For constructing the amiRNA vector for PtrMYB90, amiRNAs (21 nucleotides) (TATCGTAGAACTCAATCGGGC) were manually designed based on the target gene sequences following Schwab et al. (2006). At least one nucleotide mismatch was

introduced at the 3′end of the amiRNA, and the uridine at 5′position 1 and adenine at position 10. We use pri-miR408 as a backbone to set the amiRNA sequences on. The amiRNA (*amiRNA-PtrMYB90*), was designed to specifically cleave transcripts of *PtrMYB90*.

For constructing the transient overexpression vectors of a specific TF without a GFP tag, the *pENTR-D-TOPO* vectors containing each of 17 TF coding sequences (*PtrWBLH1, 2, 3, PtrNAC105, 123, 125,127, PtrHAM3, PtrMYB21, 74, 59, 88, 90, 93,161,174* and *175*) were amplified in *E. coli* and purified using the Qiagen mini prep kit. Then these vectors were used for LR recombination to replace the *RfA* in *pUC19-35S-RfA-35S-sGFP* (Li et al., 2012). With these reactions, the *pUC19-35S-TF-35S-sGFP* vectors are generated for all the 17 TFs. For generating the transient overexpression vectors of a specific TF with a GFP tag, the primers (Table 13) were used to amplify each coding sequence of 11 TFs (*PtrMYB21*, *74*, *90*, *161*, *174*, *175*, *PtrWBLH1*, *2*, and *PtrNAC123*). The amplified sequences were digested by corresponding enzymes, and then ligated into pUC19-GFP for generating vectors expressing TF-GFP fused proteins. The plasmid constructs of *PtrMYB21* and *PtrMYB74* are also used for subcellular location.

For constructing vectors using for transcriptional activity assays in yeast, we use GBPtrMYB21F/R, and GBPtrMYB74F/R to amplify the coding sequences of *PtrMYB21* and *PtrMYB74*. The NdeI and SmaI enzymes were used to digest the amplified *PtrMYB21*, and NdeI and BamHI were used to digest the amplified *PtrMYB74* sequences. These full-length *PtrMYB21* and *PtrMYB7*4 cDNA was individually fused in frame with the GAL4 DNA-binding domain in *pGBKT7* (Clontech), resulting in yeast expression vectors.

2.6.6 Transcriptional activity assays in yeasts

For transcriptional activation analysis, the recombinant vectors and the *pGBKT7* empty vector (control) were transferred into *Saccharomyces cerevisiae* AH109 using the lithium acetate method (Clontech). The transformed strains were cultured on minimal medium (Clontech) without -*His* or -*Trp* and the transactivation activity of each protein was evaluated according to the growth status for several days.

2.6.7 Subcellular location

Constructs for full length *PtrMYB21*, *PtrMYB74* and GFP fusion proteins were prepared to determine the subcellular localization of each of these PtrMYB members. Each of the vectors *PUC19-MYB21:sGFP* and *PUC19-MYB74:sGFP* was expressed in SDX protoplasts driven by a 35S promoter. We also co-transformed *pUC19-35S-PtrH2A-cherry* plasmids with each PtrMYB to mark the subcellular location of the expressed PtrMYB proteins. After 7 to 12h, the fluorescence in SDX protoplasts was observed under a Zeiss LSM 710 laser-scanning microscope. The excitation wavelength and the emission wavelengths were 488 nm and 492–543 nm, respectively, for GFP, and 561 nm and 582–662 nm, respectively, for mCherry.

2.6.8 Stem differentiating xylem protoplast preparation and transformation

Our protocols are modified from Yoon et al. (2007). Cellulolytic enzyme solutions and buffers from the TEAMP system were modified to isolate SDX protoplasts. In the modified protocol, the mannitol concentration was adjusted to 0.4 M in the enzyme digestion solution and in the MMG solution (4 mM MES, pH 5.7, 0.5 M mannitol, and 15 mM MgCl2), whereas 0.1 M glucose was added in the W5 solution (2 mM MES, pH 5.7, 125 mM CaCl2, 154 mM NaCl, 0.1 M glucose, and 5 mM KCl). SDX cell walls were digested (20 mM MES (pH5.7),0.4 M mannitol, 20 mM KCl, 1.5% (wt/vol) cellulase R-10 (Yakult), 0.4% Macerozyme R-10 (Yakult), 10 mM CaCl2, and 0.1%

(vol/vol) BSA) in the debarked stem segments (9~11 cm) when these segments were submerged into the freshly prepared enzyme solution for 1~2 h in a 50mL Falcon tube. The SDX protoplasts were then released with gentle shaking for 1~3 min in W5 solution. The released protoplasts were collected by centrifugation at 200xg for 2 min after filtering through a 75 μm nylon mesh. The SDX protoplast pellet was resuspended by gentle swirling in 15mL W5 solution and then chilled on ice for 30min. The protoplasts were centrifuged again to form a pellet and then were resuspended with 2mL MMG solution. By counting the cell number using a hemocytometer under the microscope, the concentration of SDX protoplasts was adjusted to 2×10^5 cells per mL for transformation. Plasmid DNA constructed for transient overexpression of TFs was prepared using CsCl density gradient ultracentrifugation (Sambrook et al., 1989). One hundred microliter plasmid DNA (100 μg), 1 mL protoplasts (2×10^5 cells), and 1.1 mL freshly prepared PEG solution (20% PEG4000, 0.2M mannitol, and 100mM CaCl2) were mixed in a 15mL centrifuge tube and held at room temperature for 10 min, followed by the addition of 5 mL of W5 solution to stop the transfection. Transfected protoplasts were collected by centrifugation at 200 ×g for 3 min. The protoplast pellet was resuspended in 10 mL freshly prepared WI solution (4 mM Mes, pH 5.7, 0.5 M mannitol, 20 mM KCl), and the protoplast solution was transferred into a Petri dish (100 mm2 × 15m) which had been coated using 5% FBS (Fetal Bovine Serum), and held at room temperature in the dark. 7hs after introduction of the gene expression construct, the transfected protoplasts were lysed for RNA extraction, ChIP assays or visualized for subcellular location.

2.6.9 ChIP assays

10^7 to 10^8 TF-GFP transfected SDX protoplasts were collected, and resuspended using WI buffer. Formaldehyde was diluted into the final concentration of 1% in WI buffer, and then incubated with suspended cells for 10 min for cross-linking. The crosslinked SDX protoplasts were washed using cold WI buffer, and the rest of the

formaldehyde was rinsed out by glycine. The washed protoplasts were resuspended in lysis buffer, and sonicated in a Branson sonifier 250 to generate DNA fragments ranging from 0.2kb to 2kb, that was bounding to proteins. The solution with DNA-protein complexes was diluted ten-folds into ChIP dilution buffer. The DNA-protein complexes in the diluted solution were incubated with anti-GFP antibodies (About 10 to 15 µg) for 24h at 4 °C. To isolate the antibody-DNA-TF complex, Dynabeads with protein G were added to the solution and then incubated for 4h at 4 °C. The dynabead protein complexes were washed using low salt buffer, a high salt wash, LiCl washing buffer, and TF buffer sequentially to rinse out the nonspecific binding complexes. After washing, the immunoprecipitated protein-DNA complexes were eluted using pre-warmed elution buffer. The eluted complexes were reverse-crosslinked using 5M NaCl at 65°C overnight. The separated DNA was isolated using a Qiagen miniprep to generate the IP sample. The input and mock samples were collected as instructed by Li et al., (2014). All reagents and buffers were prepared based on Li et al., (2014).

2.6.10 Laser capture microdissection

The stem differentiating fiber cells, vessel cells, or a mixture of these three different cell types (fiber, vessel, and ray) were collected from 6-month-old greenhouse-grown *P. trichocarpa* using a Laser Microdissection 7000 (Leica) instrument as described in Chen et al., 2011. Total RNA from the three samples was isolated, amplified, and analyzed by qRT-PCR following procedures of Chen et al., (2014).

2.6.11 qRT-PCR

The transformed SDX protoplasts were collected at 7h by centrifugation at 500xg for 3 mins. Total RNAs were isolated from the SDX protoplast pellet using a RNeasy plant RNA isolation kit (Qiagen) and treated with RNase-free DNase I (Qiagen) to remove the genomic DNA and the residue plasmid by using the RNase-free DNase Set

(Qiagen). The quality of the extracted RNA was examined by gel electrophoresis and UV spectrogram scanning. Total RNA (80 ng) was reverse transcribed, using TaqMan reverse transcription reagents (Applied Biosystems, Roche). qRT-PCR was conducted with an Applied Biosystems 7900HT Sequence Detection System. For each reaction, a 25-μL mixture contained the first strand cDNA (equivalent to 1- 5 ng of total RNA), 5 pmol each of the forward and reverse primers of PtrMYB021, SND1s, and VNDs (Table 3), and 12.5 μL 2 × SYBR green PCR master mix. The amplification program was as follows: 95 °C for 10 min, then 45 cycles of 95°C for 15 sec and 60°C for 1 min, after which a thermal denaturing cycle was added, to determine the dissociation curve of the PCR products for checking the amplification specificity. A formula for absolute quantification of the transcript copy numbers per unit mass of total RNA was derived, according to a previous publication from our lab (Shi et al., 2010). For relative quantification, each reaction was repeated at least three times and the transcript level was normalized to that of 18S rRNA. Such normalized values allowed the comparison of the expression levels of different genes and are calculated as described by Schmittgen et al., (2008).

2.6.12 Transcriptome analyses of the transfected SDX protoplasts and identification of DEGs

RNA-seq was performed with three biological replicates each for SDX protoplasts transfected with PtrMYB21, PtrMYB74, and sGFP at 7h. Total RNA from each sample (750 ng) was extracted and then used for library construction using Illumina TruSeq RNA sample preparation kit. Each library was constructed using different index sequences as adaptors. The quality and concentration of these libraries was examined by the Agilent 2100 Bioanalyzer using Agilent high-sensitivity DNA assay chips. These libraries were pooled by mixing equal quantities of DNA. The mixed sample was sequenced in one lane. The resulting 72-bp average read lengths were generated. After removing the 4-bp library sequence index sequences from each read, the remaining 68 bp were mapped to the reference *P. trichocarpa* genome release

v2.2 and v3.0 (Phytozome V7.0; http://www.phytozome.com) using the program TOPHAT (Trapnell et al., 2009). The normalized raw counts were determined as described by Lin et al., (2013). The PtrMYB21-regulated genes and PtrMYB74-regulated genes were identified using edgeR (Robinson et al., 2010) by comparing the relative transcript abundance for each gene between each of the PtrMYB21 and PtrMYB74 transfection and the *sGFP* (control) transfection. The false discovery rate was set at 0.05, and fold changes were > 2, for the TF-regulated genes.

2.6.13 Gene ontology functional enrichment analysis

This analysis was performed for the genes activated by PtrMYB21 and PtrMYB74. These activated genes were annotated using the g: Profiler Web server (http://biit.cs.ut.ee/gprofiler/; Reimand et al., 2016). The *P. trichocarpa* GO functional enrichment analysis in the g:Profiler Web server is based on the Ensemble Genome (http://www.ensembl.org) annotation for *P. trichocarpa*. The background controls are all *P. trichocarpa* genes identified in the genome. The statistical significances of functional enrichment are calculated (g: Profiler) for the PtrMYB21 and PtrMYB74 activated genes, respectively.

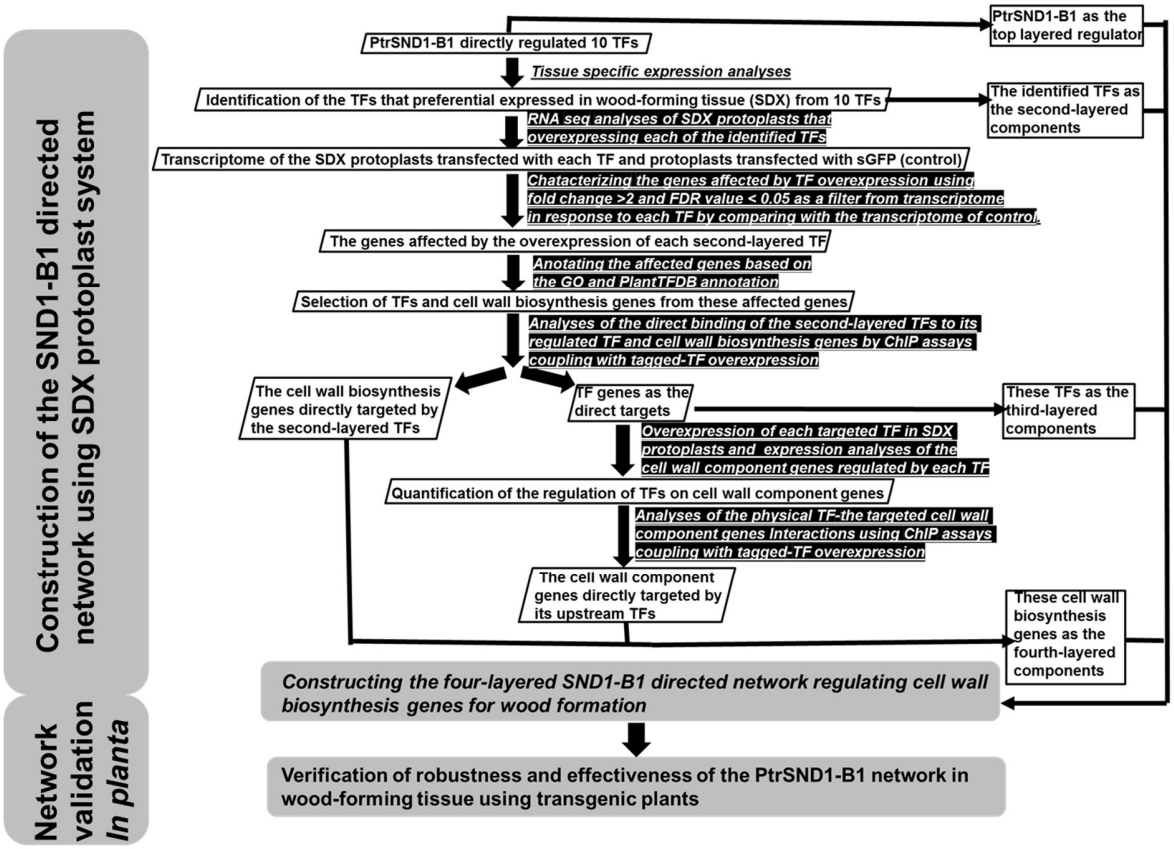

Figure 1. Flow chart for methodology of research. A graph depicting a pipeline how to construct and verify the PtrSND1-B1 four-layered network using experimental approaches.

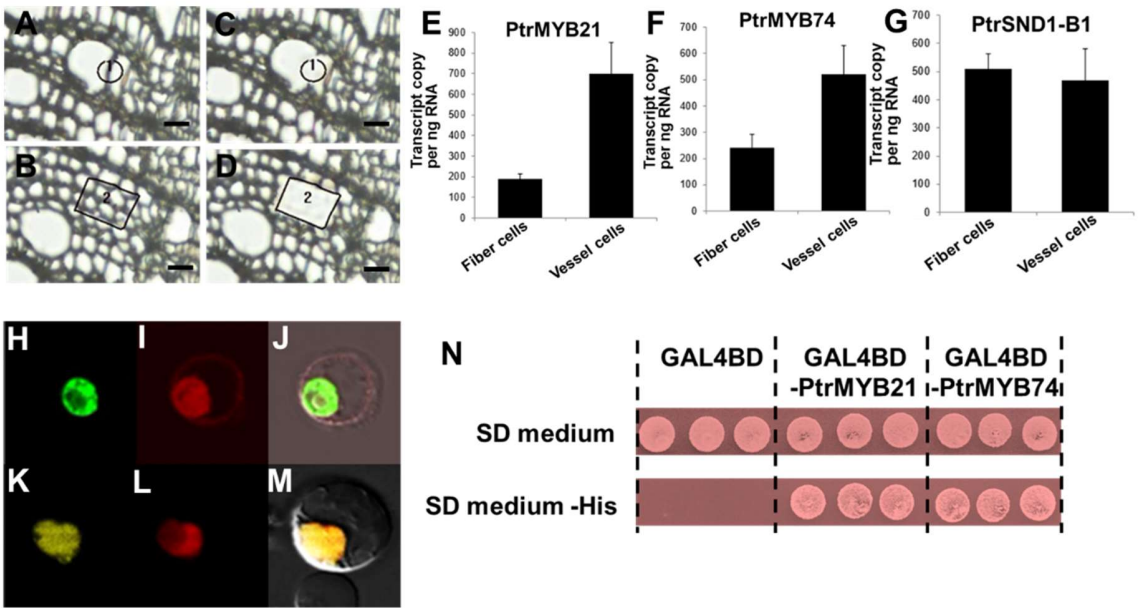

Figure 2. Wood-forming cell specific expression, and subcellular location, transcriptional activity of PtrMYB21 and PtrMYB74. (A-D). (**A**). Xylem cross-section before the LCM treatment of vessel cells. (**C**). Xylem cross-section after the LCM treatment of vessel cells. **(B).** Xylem cross-section before the LCM treatment of fiber cells. (**D).** Xylem cross-section after the LCM treatment of vessel cells. Scale bar in (A-D) is 20μm **(A)** and **(C)** indicates the dissected vessel cells, and 2 in **(B)** and **(D)** indicates the dissected fiber cells. **(E-G).** Quantitative analysis of the transcript abundance of PtrSND1-B1, PtrMYB21 and PtrMYB74 in SDX cells isolated by laser-dissection. The absolute values are shown from three biological replicates. **(G-L)** The subcellular location of **(H-J)** PtrMYB21 and **(K-M)** PtrMYB74 fused proteins. The MYB21-GFP signal **(H)**, the MYB74-GFP signal **(K)**, and the H2A-mcherry signals **(I)** and **(L)**, and merged images **(J)** using **(H)** and **(I),** and **(M)** of **(K)** and **(L)** are shown. **(N)**. Transcriptional activation analysis of PtrMYB21 and PtrMYB74 fused with the GAL4 DNA binding domain (GAL4DB) in yeast. Yeast transformed with GAL4BD-PtrMYB21 or GAL4BD-PtrMYB74 are able to survive on SD medium without histidine, and the controls are not.

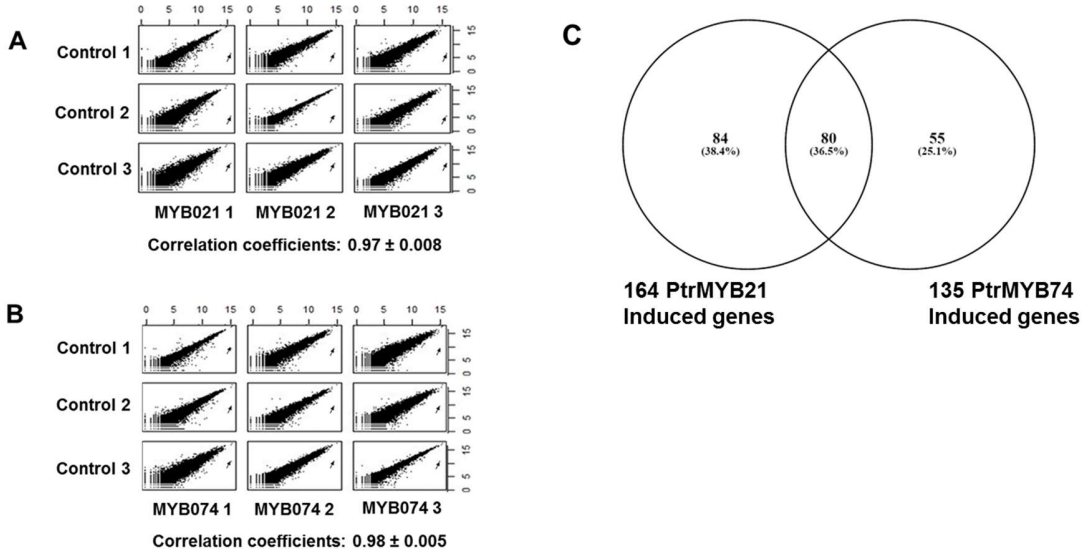

Figure 3. Genes regulated by PtrMYB21 and PtrMYB74 in SDX protoplasts at 7h after transfection. Scatterplots of the RNA-seq read counts (Log2) from three biological replicates of PtrMYB21, PtrMYB74, and sGFP (control) transfected SDX protoplasts show high Pearson correlation coefficients of the gene expression between PtrMYB21 and sGFP (A), and between PtrMYB74 and sGFP (B) after 7h incubation. Dots indicated by arrows represent the transcript abundance of PtrMYB21 in (A), and of PtrMYB74 in (B). (C) Venn diagram of the genes upregulated by PtrMYB21 and PtrMYB74 at 7h incubation of SDX protoplasts.

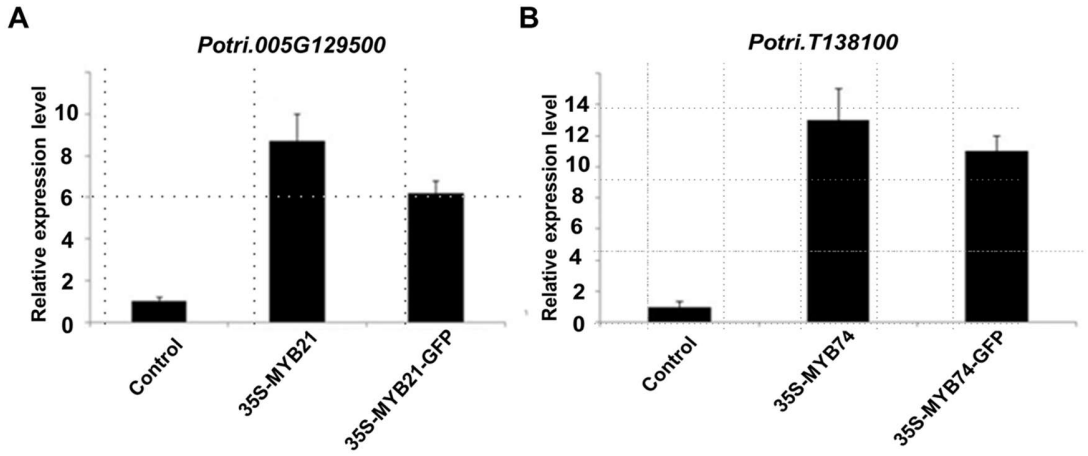

Figure 4. The transcriptional activation abilities of the GFP-tagged PtrMYB21 and PtrMYB74 in SDX protoplasts. qRT-PCR showed that PtrMYB21-GFP and PtrMYB21 can similarly activate the *Potri.005G129500* **(A)**, and PtrMYB74-GFP and PtrMYB74 can similarly activate *Potri.T138100* **(B)**. *Potri.005G129500* and *Potr.T138100* were respectively selected from PtrMYB21 and PtrMYB74-regulated genes.

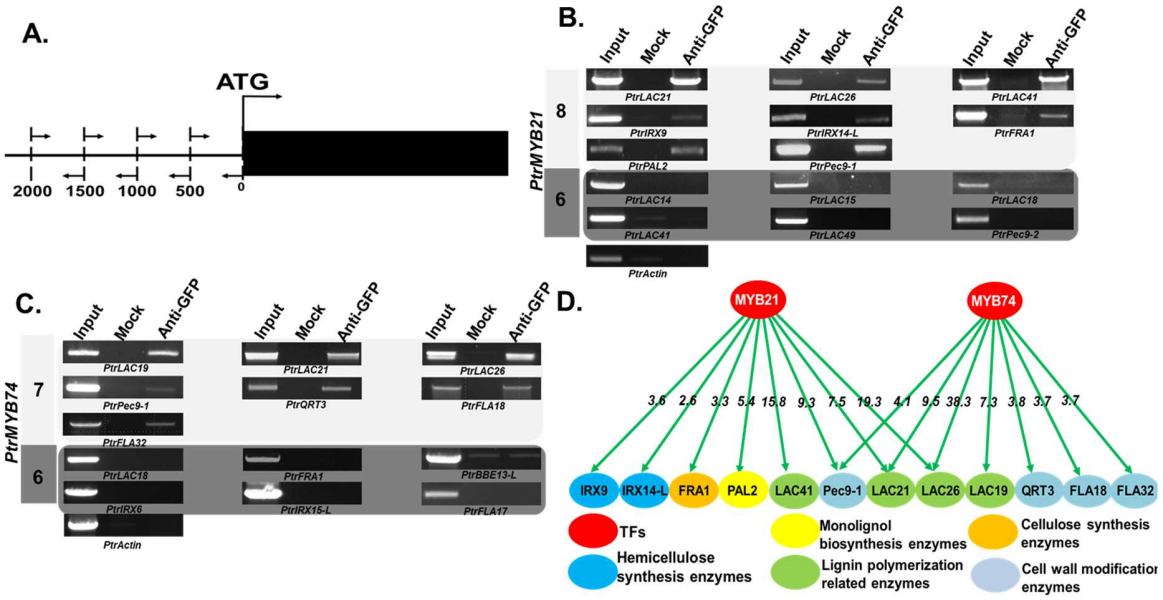

Figure 5. ChIP identification of cell wall biosynthetic genes directly targeted by PtrMYB21 and PtrMYB74. (A) A diagram depicting the approximate locations of the promoter sequences amplified by PCR following the ChIP assays. The rectangles show the genes, and the lines represent a gene promoter that drives its gene. The arrowheads show the approximate location of promoter region that were assigned to design primers for PCR amplification. (B) to (C). ChIP-PCR assays of cell wall biosynthetic genes regulated by PtrMYB21(B) and by PtrMYB74 (C). The direct targets of PtrMYB21 and PtrMYB74 are shown in the white box. The indirect targets of PtrMYB21 and PtrMYB74 are shown in the shaded box. Input, mock and anti-GFP are PCR reactions using the chromatin preparations before immunoprecipitation, immunoprecipitated with pre-immune serum and immunoprecipitated with anti-GFP antibody, respectively. Four independent biological replicates of ChIP assays were performed, and the results of one biological replicate are presented. (D). The diagram showing that PtrMYB21 and PtrMYB74 regulate the cell wall biosynthetic genes. The arrow lines indicate the protein-DNA regulatory interaction with activation ability Number on brown lines indicated the quantitative measurement of the effects of these regulatory interactions in SDX protoplasts.

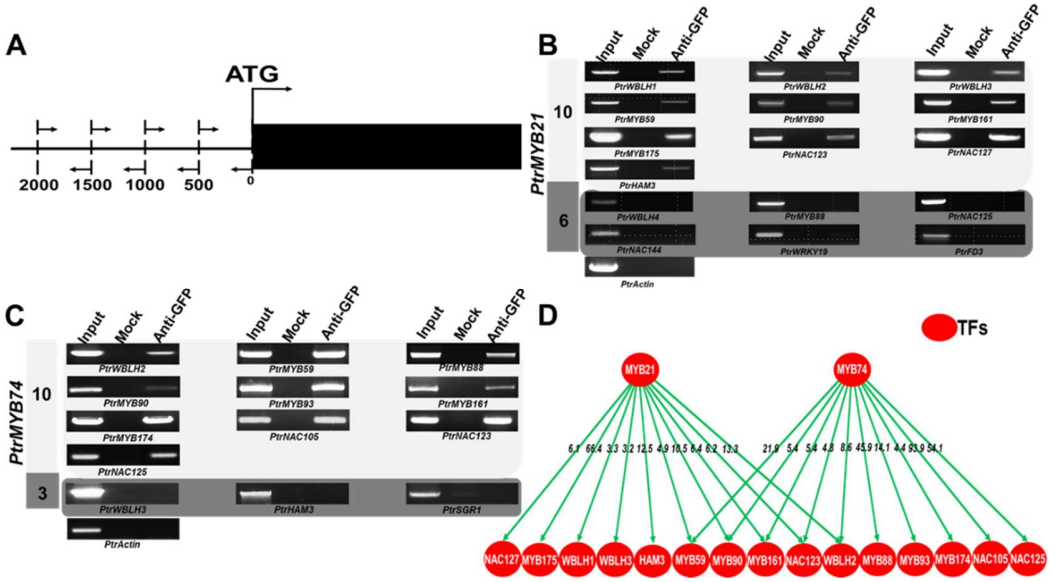

Figure 6. ChIP identification of TF genes directly targeted by PtrMYB21 and PtrMYB74. (A) A diagram depicting the approximate locations of the promoter sequences amplified by PCR following the ChIP assays, which are described in Figure 3.**(B) to (C)**. ChIP-PCR assays of TF genes from PtrMYB21-regulated genes **(B)** and PtrMYB74-regulated genes **(C).** In white area, the number of PtrMYB21 and PtrMYB74 direct targets is 10 and 10, respectively. The 6 and 3 in the shaded area is the indirect targets of PtrMYB21 and PtrMYB74. Input, mock and anti-GFP are PCR reactions using the chromatin preparations before immunoprecipitation, immunoprecipitated with pre-immune serum and immunoprecipitated with anti-GFP antibody, respectively. For these experiments, PtrACTIN was used as a negative control. Four independent biological replicates of ChIP assays were performed, and the positive results of one biological replicate are shown. **(D)**. A network describing TF genes targeted by PtrMYB21 and PtrMYB74. The TF genes are shown in red. The brown lines indicate the protein-DNA regulatory interactions. The number on brown lines indicates the quantitative measurements of the effects for these regulatory interactions in SDX cells. Arrows indicate an activation edge.

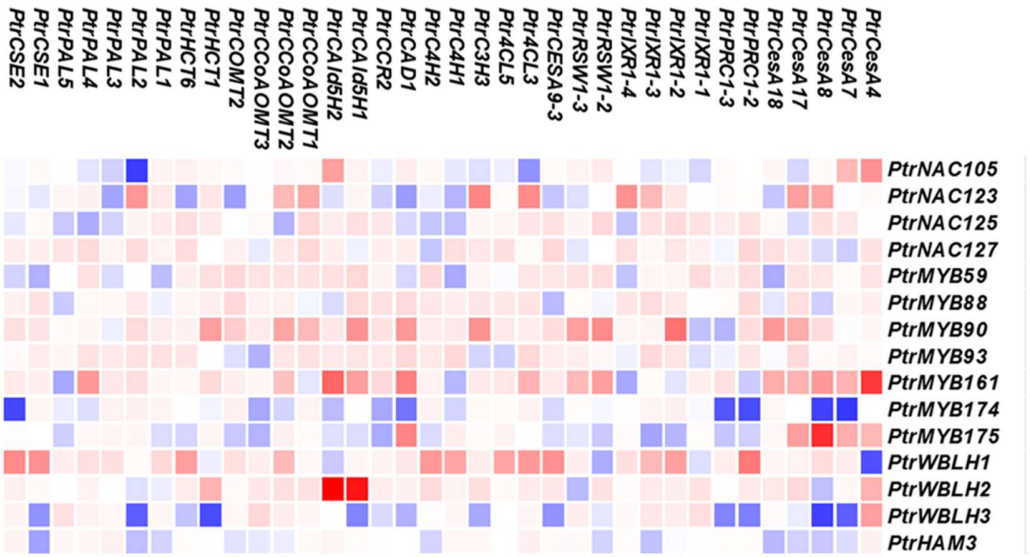

Figure 7. Heat map showing the differential expression of 36 cell-wall component genes in response to the overexpression of each 15 TFs directly regulated by PtrMYB21 and PtrMYB74. For each cell-wall component gene, the expression in sGFP transfected protoplasts (control) is set to 1. Heat map represents the relative expression values of the genes in SDX protoplasts overexpressing each TF compared to the control. The genes with a relative expression value >2 or < 0.8 are identified as TF-regulated genes. The cell-wall component genes are shown on the left, and the TFs are shown in the upper part. The bar at the bottom indicates the relative expression ratio, where blue, white and red colors represent downregulation, no change and upregulation, respectively.

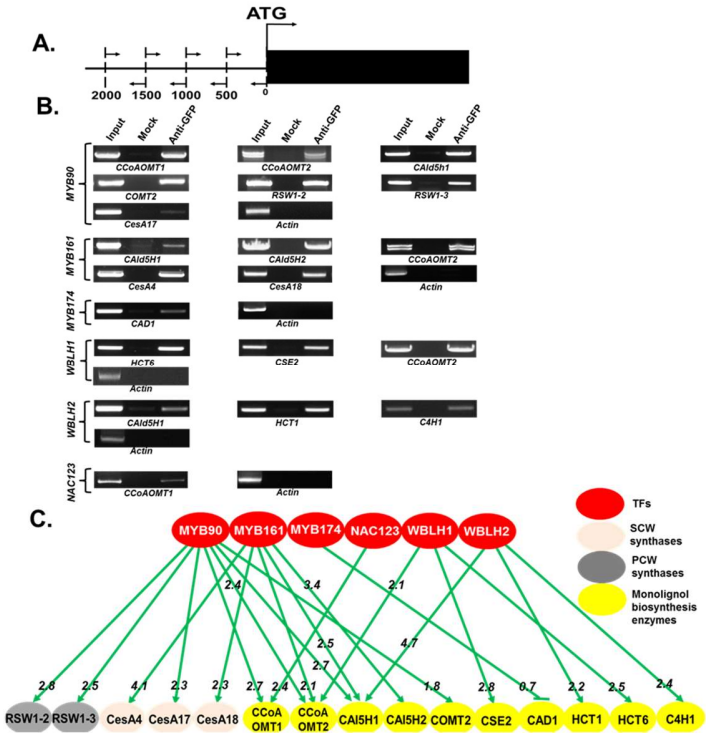

Figure 8. Characterization of the TF-DNA regulatory interactions between the third-layered TFs and their regulated cell-wall component genes. (A). A diagram depicting the locations of the promoter sequences amplified by PCR following the ChIP assays, which are described in Figure 3. (B). ChIP assays identifying 6 of the third-layer TFs that directly regulate 15 cell-wall component genes achieved through TF-promoter interactions. Four independent biological replicates of ChIP assays were performed, and the positive results of one biological replicate are shown. For the 76 regulatory hierarchies in Figure 5, 19 are achieved by direct TF-DNA interactions as shown in Figure 6B. (C). The network depicts how 6 TFs directly regulate 15 cell wall biosynthesis genes. The genes are categorized into 4 functional groups shown in different colors. The lines indicate the protein-DNA regulatory interactions. Numbers on brown lines indicate the quantitative measurement of the effects for these regulatory interactions in SDX cells. Arrows indicate the positive regulation, and blunt arrows indicate negative regulation.

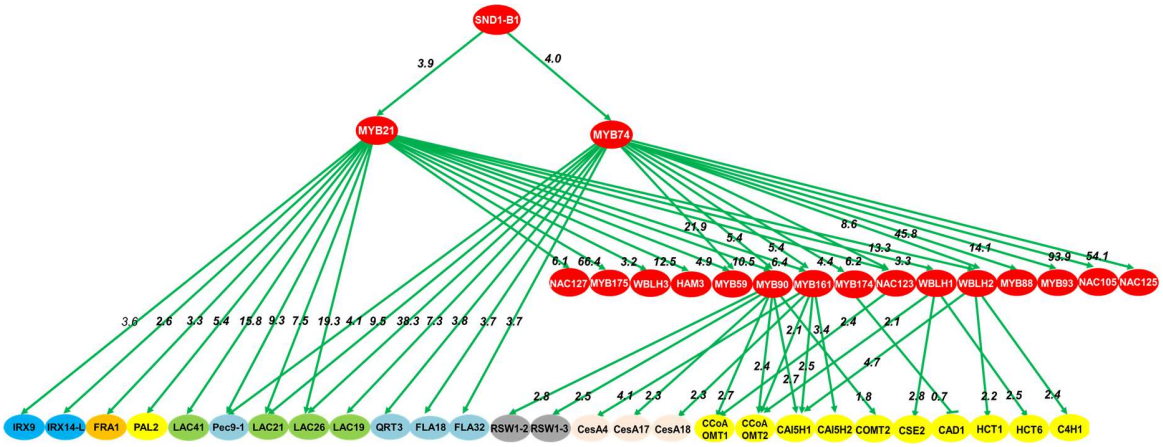

Figure 9. The four-layered PtrSND1-B1 mediated network for analyzing transcriptional regulation of cell wall biosynthetic genes. The 18 TFs and 27 cell wall biosynthetic genes are shown in a hierarchical network. The brown lines show the protein-DNA interactions. Number on brown lines indicated the quantitative measurement of the effects for these regulatory interactions in SDX cells. Arrows indicate positive regulation, and blunt arrows indicate negative regulation.

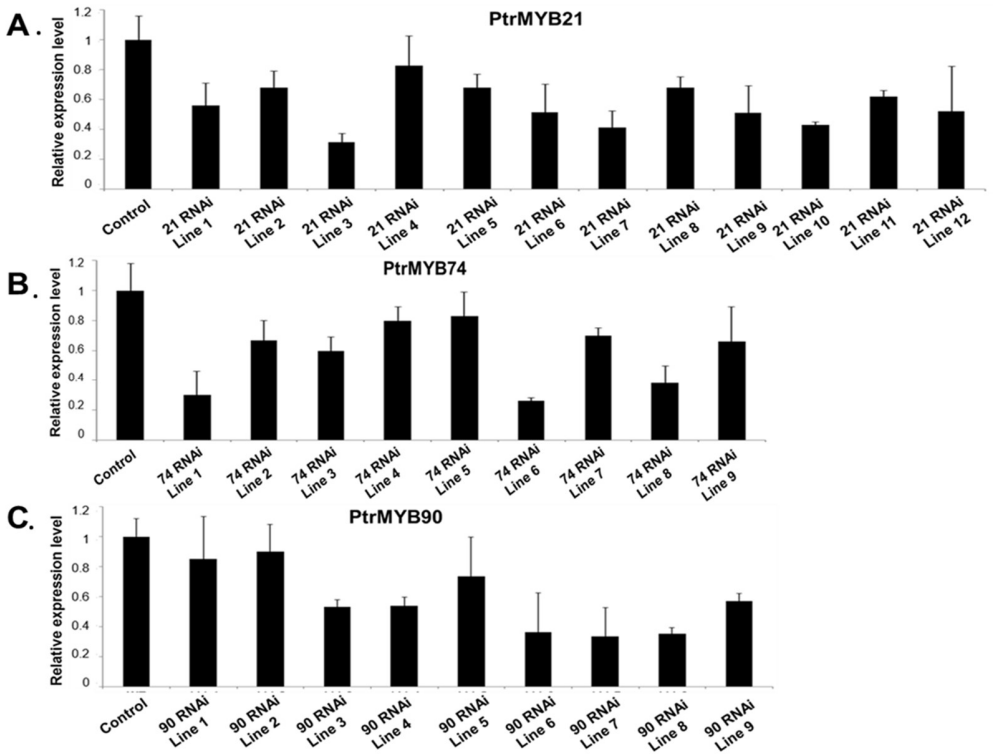

Figure 10. The expression of PtrMYB21, PtrMYB74, and PtrMYB90 in the knocking-down transgenic *P. trichocarpa* plants. Each of the MYB TF was knocked down in *P. trichocarpa* SDX. The transcript abundance of each MYB gene in three wild-type (WT) plants and its transgenic lines was estimated by qRT-PCR. The average of three biological replicates of wild-type plants was set as 1. Error bars in three transgenic lines represent the SE of three qRT-PCR technical replicates.

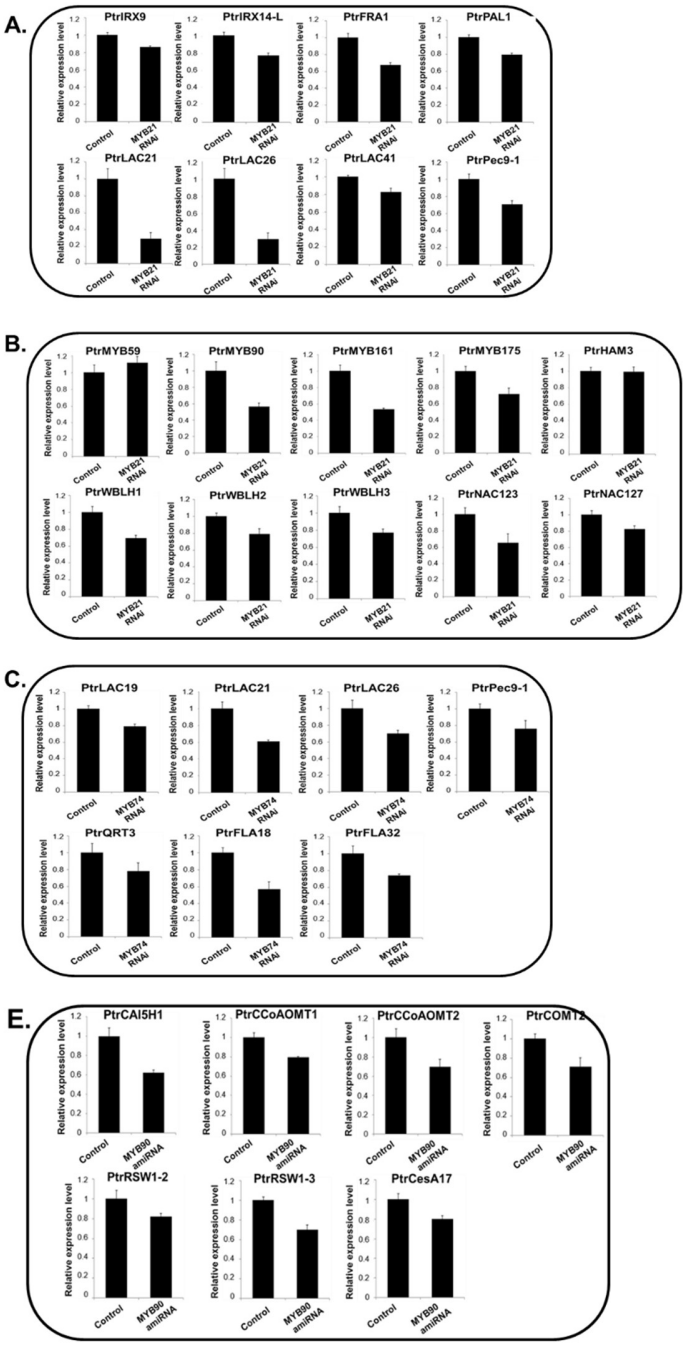

Figure 11. Validation of the direct regulation of PtrMYB21, PtrMYB74, and PtrMYB90 in stable transgenic *P. trichocarpa*. The direct target genes of PtrMYB21, PtrMYB74, and PtrMYB90 derived from the SDX protoplast system were

verified by qRT-PCR for their down-regulated expression in differentiating xylem of stable transgenic *P. trichocarpa* plants by knocking-down *PtrMYB21*, *PtrMYB74*, or *PtrMYB90*. (A) and (B) The transcript abundance of ChIP-PCR verified cell-wall component genes (A), and TF genes (B) in PtrMYB21 transgenic plants (21-2, 21-7, and 21-10) and three wild-type (WT) lines. The average of three biological replicates of wild-type plants was set as 1. Error bars in three transgenic lines represent the SE of three qRT-PCR technical replicates. PtrMYB59 was the only gene not affected by the knocking-down of PtrMYB21 in stable transgenic *P. trichocarpa*. (C) to (D). The transcript abundance ChIP-PCR verified targets in PtrMYB74 transgenics. ChIP-PCR verified cell wall biosynthesis genes (C), and ChIP-PCR verified TF genes (D) were quantified by qRT-PCR in three wild-type (WT) and three PtrMYB74 transgenic lines (74-2, 74-6, and 74-8). *PtrMYB59* and *PtrMYB88* were two genes not affected by PtrMYB74 knock-down in stable transgenic *P. trichocarpa*. (E). The transcript abundance of ChIP-PCR verified cell wall component genes in PtrMYB90 transgenics. The average of three biological replicates of wild-type plants was set as 1. Error bars in three transgenic lines represent the SE of three qRT-PCR technical replicates.

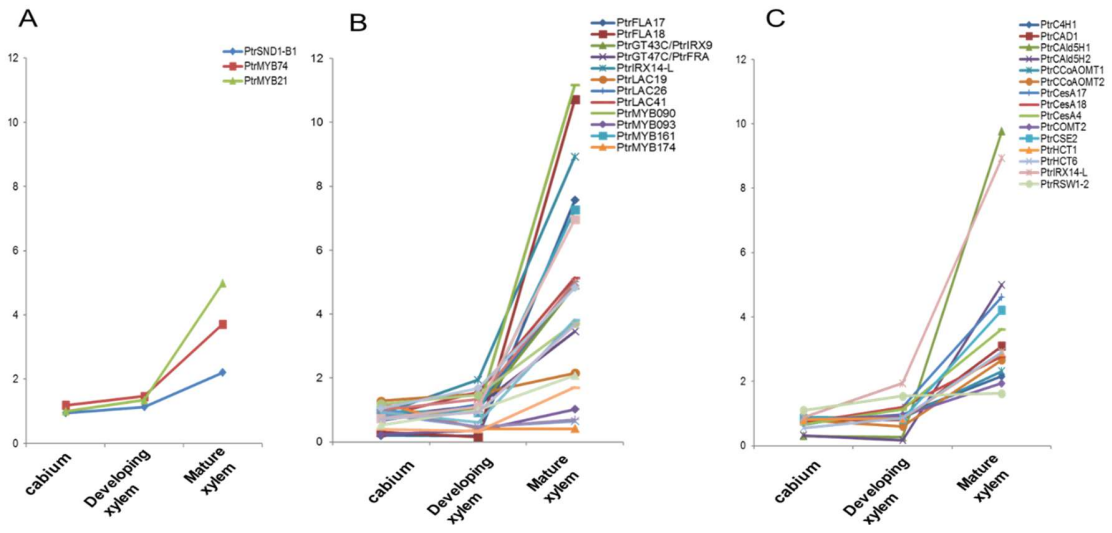

Figure 12. **Gene expression change of network-included genes in cambium, developing xylem, and mature xylem tissues.** (A). Expression profiling of *PtrSND1-B1*, *PtrMYB21*, and *PtrMYB74*. (B). Expression profiling of PtrMYB21 and PtrMYB74-regulated genes that can be detected by the *Populus* Nimblegen microarray. (C). Expression profiling of genes regulated by the third-layer TFs.

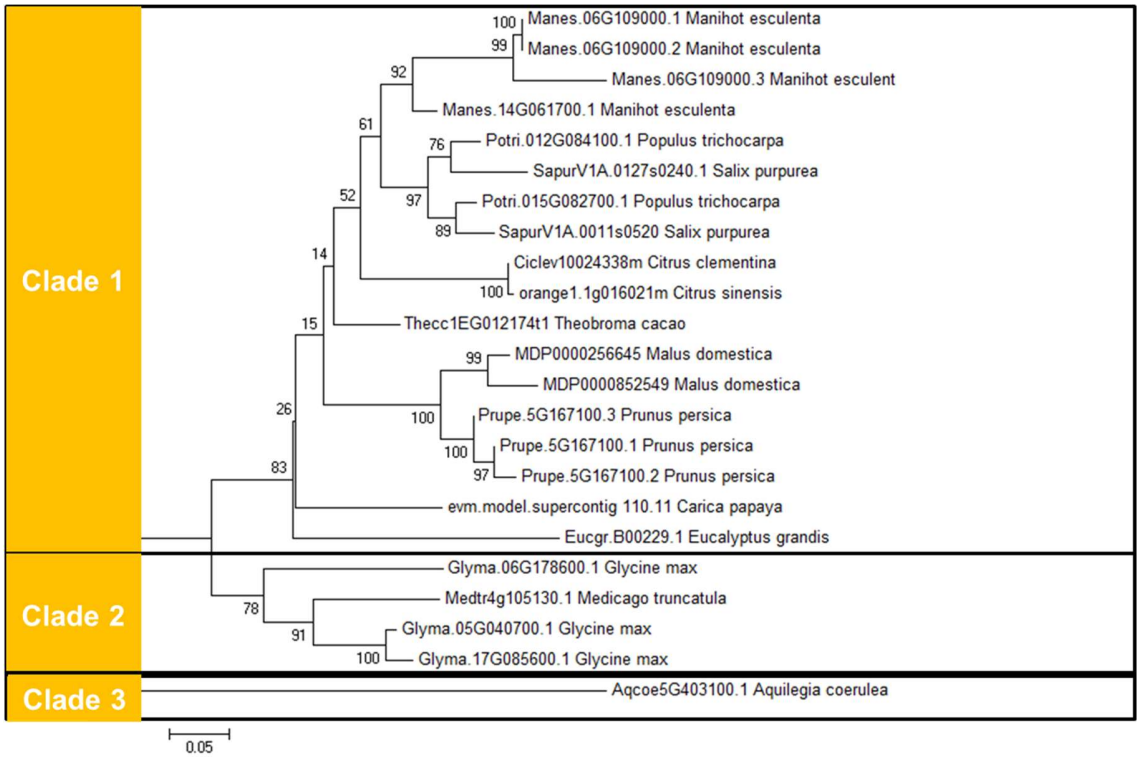

Figure 13. Phylogenetic tree of PtrMYB74 homologs (>60% protein sequence similarity with PtrMYB74) in plants. The proteins in clade 1 are from *Manihot esculenta, Populus trichocarpa, Salix purpurea, Citrus clementina, Theobroma cacao, Prunus persica, Carica papaya, Eucalyptus grandis,* which are woody species (http://woodyplants.cals.cornell.edu/plant/search). The proteins in clade 2 are from *Glycine max*, and *Medicago truncatula*. The protein in clade 3 is from *Aquilegia coerulea*, an herbaceous plant.

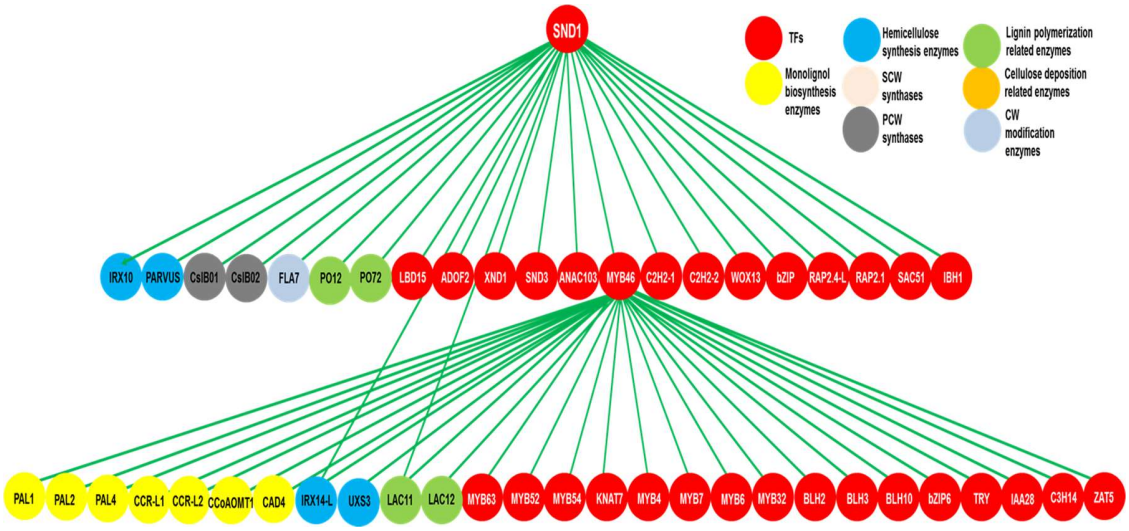

Figure 14. The three-layered network encompassed by AtSND1 and AtMYB46 regulating cell wall biosynthetic genes. The 31 TFs and 18 cell wall biosynthetic genes are shown in the hierarchical network. The lines show the protein-DNA interactions. Number on lines indicate the quantitative measurement of the effects for these regulatory interactions in SDX protoplasts. All these lines stand for the activation function.

Table 1. Functional classification of the 164 genes regulated by PtrMYB21.

DEG Number	*Populus trichocarpa* V3.0 gene model name	Fold change, as gene expression in treatment/control	FDR value	Closest Arabidopsis homolog	Annotated function of the Arabidopsis homolog	Populus name
MYB21D1	Potri.017G031600	71.64663289	0.005149	AT5G13180	ANAC083	PtrNAC125
MYB21D2	Potri.011G058400	6.433549871	0	AT4G28500	ANAC73/SND2	PtrNAC123/SND2/3A1
MYB21D3	Potri.006G152700	6.077874983	0.000667	AT4G29230	ANAC075	PtrNAC127/SND2/3-L1
MYB21D4	Potri.019G031600	2.0865059	0.014407	AT5G18270	ANAC087	PtrNAC144
MYB21D5	Potri.005G109500	8.135528109	0.00034	AT4G35900	ATBZIP14	PtrFD2
MYB21D6	Potri.019G081500	2.150988657	0.037988	AT1G22640	ATMYB3	PtrMYB168
MYB21D7	Potri.018G095900	15.05568037	0.020835	AT5G57620	ATMYB36	PtrMYB088
MYB21D8	Potri.007G134500	10.47032268	0.000389	AT1G17950	ATMYB52	PtrMYB161
MYB21D9	Potri.015G033600	4.904381953	0.031385	AT1G17950	ATMYB52	PtrMYB090
MYB21D10	Potri.017G017600	66.44570303	0.029663	AT1G17950	ATMYB52	PtrMYB175
MYB21D11	Potri.019G050900	12.52641781	0.004421	AT3G02940	ATMYB107	PtrMYB059
MYB21D12	Potri.014G050000	2.33133124	0.02539	AT2G44745	ATWRKY12	PtrWRKY19
MYB21D13	Potri.005G129500	13.28880067	0	AT4G36870	BEL1-LIKE HOMEODOMAIN 2, BLH2	PtrWBLH2
MYB21D14	Potri.007G032700	10.24682463	0	AT4G36870	BEL1-LIKE HOMEODOMAIN 2, BLH2	PtrWBLH4
MYB21D15	Potri.004G159300	3.249412726	0.000043	AT4G34610	BEL1-LIKE HOMEODOMAIN 6, BLH6	PtrWBLH3
MYB21D16	Potri.002G031000	3.352262211	0.000076	AT1G75410	BEL1-LIKE HOMEODOMAIN 3, BLH3	PtrWBLH1
MYB21D17	Potri.003G110800	6.203446637	0.018242	AT4G00150	HAIRY MERISTEM 3, HAM3	PtrHAM3/PtrGRAS22
MYB21D18	Potri.002G081800	19.91916132	0	AT1G44170	ALDEHYDE DEHYDROGENASE 4	
MYB21D19	Potri.018G136400	34.39640782	0.02221	AT4G15093	catalytic LigB subunitof aromatic dioxygenase	
MYB21D20	Potri.011G150300	25.25876156	0	AT4G10500	DMR6-LIKE OXYGENASE 1	
MYB21D21	Potri.006G112900	115.8213173	0.000033	AT5G05320	FAD/NAD(P)-binding oxidoreductase family protein	
MYB21D22	Potri.014G073700	10.75332564	0.009199	AT4G25420	GIBBERELLIN 20-OXIDASE 1	
MYB21D23	Potri.014G117300	8.459691186	0.000036	AT1G02400	GIBBERELLIN 2-OXIDASE 6	
MYB21D24	Potri.008G073800	7.556609127	0.000001	AT5G05390	LACCASE 12	PtrLAC19
MYB21D25	Potri.001G248700	104.590427	0	AT2G38080	LACCASE 4	PtrLAC04
MYB21D26	Potri.006G096900	4.267274744	0.00037	AT2G38080	LACCASE 4	PtrLAC14
MYB21D27	Potri.006G097000	4.277444097	0.00034	AT2G38080	LACCASE 4	PtrLAC15
MYB21D28	Potri.009G042500	7.54128305	0	AT2G38080	LACCASE 4	PtrLAC21
MYB21D29	Potri.016G112100	15.76650517	0	AT2G38080	LACCASE 4	PtrLAC41
MYB21D30	Potri.006G097100	4.759325082	0.000191	AT2G38080	LACCASE 4	PtrLAC49
MYB21D31	Potri.008G073700	9.661023246	0	AT2G40370	LACCASE 5	PtrLAC18
MYB21D32	Potri.010G183600	19.38003136	0	AT2G40370	LACCASE 5	PtrLAC26
MYB21D33	Potri.010G134500	5.70199194	0.008459	AT1G68850	Peroxidase superfamily protein	
MYB21D34	Potri.006G196200	2.331088859	0.002417	AT3G58490	SPHINGOID PHOSPHATE PHOSPHATASE 1	
MYB21D35	Potri.014G049600	4.307972379	0.001519	AT3G60280	UCLACYANIN 3	
MYB21D36	Potri.010G177300	5.698688758	0	AT1G65610	GLYCOSYL HYDROLASE 9A2 (KOR2)	PtrKOR1
MYB21D37	Potri.009G109900	6.870242391	0.029257	AT1G49430	LONG-CHAIN ACYL-COA SYNTHETASE 2 (LACS2)	
MYB21D38	Potri.001G088700	3.509861251	0.002526	AT5G46290	3-KETOACYL-ACYL CARRIER PROTEIN SYNTHASE I	
MYB21D39	Potri.008G160000	13.93776181	0.000001	AT2G26640	3-KETOACYL-COA SYNTHASE 11	
MYB21D40	Potri.010G079300	14.2691748	0	AT2G26640	3-KETOACYL-COA SYNTHASE 11	
MYB21D41	Potri.010G079400	14.81746762	0	AT5G43760	3-KETOACYL-COA SYNTHASE 20	
MYB21D42	Potri.015G100800	5.900834517	0.013005	AT5G41040	ALIPHATIC SUBERIN FERULOYL-TRANSFERASE (HHT)	
MYB21D43	Potri.011G004700	5.049466611	0.000162	AT1G11790	AROGENATE DEHYDRATASE 1 (ADT)	PtrADT
MYB21D44	Potri.007G047500	2.632374381	0.0479	AT5G67230	IRX (irregular xylem)14-L	PtrIRX14-L
MYB21D45	Potri.010G145800	1.000097739	0.000141	AT5G49460	ATP CITRATE LYASE SUBUNIT B 2	
MYB21D46	Potri.007G098600	17.2997346	0.000462	AT5G64440	FATTY ACID AMIDE HYDROLASE	
MYB21D47	Potri.012G068700	29.30624048	0.000002	AT1G74460	GDSL-motif esterase/acyltransferase/lipase	
MYB21D48	Potri.016G086400	3.602523896	0.000046	AT2G37090	IRREGULAR XYLEM 9 (GT43 family glycosyltransferases)	PtrGT43C/PtrIRX9
MYB21D49	Potri.008G201600	2.340417645	0.005149	AT3G23590	MED33A	
MYB21D50	Potri.003G074700	2.421911252	0.027701	AT2G35020	N-ACETYLGLUCOSAMINE-1-PHOSPHATE URIDYLYLTRANSFERASE 2	
MYB21D51	Potri.012G142300	9.346537461	0	AT5G23870	PECTIN ACETYLESTERASE 9	
MYB21D52	Potri.015G145400	2.477681939	0.033016	AT5G23870	PECTIN ACETYLESTERASE 9	
MYB21D53	Potri.008G038200	5.383770829	0.000413	AT2G37040	PHE AMMONIA LYASE 1(PAL1)	PtrPAL2
MYB21D54	Potri.011G101400	5.508310937	0.027617	AT1G78510	SOLANESYL DIPHOSPHATE SYNTHASE 1	
MYB21D55	Potri.003G022700	6.14490199	0.000759	AT3G26410	TRNA MODIFICATION 11	
MYB21D56	Potri.013G118700	11.78855513	0.000004	AT5G17050	UDP-GLUCOSYL TRANSFERASE 78D2	
MYB21D57	Potri.016G124800	11.36011867	0	AT1G22400	UDP-GLUCOSYL TRANSFERASE 85A1	
MYB21D58	Potri.011G143700	4.516712232	0.001547	AT1G56050	ENGD-2 (GTP-binding protein-related)	
MYB21D59	Potri.006G025300	6.284805076	0.000002	AT1G67440	EMBRYO DEFECTIVE 1688 (GTP-binding protein-related)	
MYB21D60	Potri.016G023500	2.730952081	0.020606	AT1G67440	EMBRYO DEFECTIVE 1688 (GTP-binding protein-related)	
MYB21D61	Potri.002G247100	3.141117694	0.000705	AT3G07270	GTP cyclohydrolase I	
MYB21D62	Potri.001G329700	2.412643911	0.010846	AT3G27060	TSO2 (the 3 ribonucleotide reductase)	
MYB21D63	Potri.014G024700	3.283150762	0.00005	AT5G47820	FRAGILE FIBER 1 (KINESIN)	PtrGT47C/PtrFRA
MYB21D64	Potri.018G028100	2.384445817	0.00142	AT3G49500	RNA-DEPENDENT RNA POLYMERASE 6	
MYB21D65	Potri.001G032600	3.007973798	0.00015	AT4G26760	microtubule-associated protein 65-2 (MAP65-2)	
MYB21D66	Potri.002G094800	5.416474016	0.046897	AT5G65160	TETRATRICOPEPTIDE REPEAT 14,	
MYB21D67	Potri.012G007600	5.142004954	0.000171	AT5G54130	Calcium-binding endonuclease/exonuclease/phosphatase family	
MYB21D68	Potri.016G108700	12.20420996	0.001261	AT3G48750	CELL DIVISION CONTROL 2 (cyclin-dependent kinase)	
MYB21D69	Potri.001G274200	10.20525976	0.004676	AT5G12235	CLAVATA3/ESR-RELATED 22	
MYB21D70	Potri.010G121100	14.13494143	0.000005	AT1G25390	LEAF RUST 10 DISEASE-RESISTANCE LOCUS RECEPTOR-LIKE PROTEIN KINASE-LIKE 4	
MYB21D71	Potri.010G121100	15.73037327	0.001519	AT1G25390	LEAF RUST 10 DISEASE-RESISTANCE LOCUS RECEPTOR-LIKE PROTEIN KINASE-LIKE 4	
MYB21D72	Potri.010G121100	41.63615673	0	AT1G25390	LEAF RUST 10 DISEASE-RESISTANCE LOCUS RECEPTOR-LIKE PROTEIN KINASE-LIKE 4	

Table 1. Continued

DEG Number	*Populus trichocarpa* V3.0 gene model name	Fold change, as gene expression in treatment/control	FDR value	Closest Arabidopsis homolog	Annotated function of the Arabidopsis homolog
MYB21D73	Potri.003G211700	24.57999982	0.000001	AT1G34300	lectin protein kinase family protein
MYB21D74	Potri.013G098900	7.729178046	0.000278	AT1G33610	Leucine-rich repeat (LRR) family protein
MYB21D75	Potri.001G302500	13.98354265	0.040315	AT4G06744	Leucine-rich repeat (LRR) family protein
MYB21D76	Potri.004G146400	23.07067005	0.000002	AT2G15880	Leucine-rich repeat (LRR) family protein;
MYB21D77	Potri.016G140300	2.447773386	0.02539	AT5G01950	Leucine-rich repeat protein kinase family protei
MYB21D78	Potri.013G159200	4.581677779	0.000024	AT1G06840	Leucine-rich repeat protein kinase family protein
MYB21D79	Potri.015G123700	17.09344167	0.00034	AT4G08850	Leucine-rich repeat receptor-like protein kinase family protein
MYB21D80	Potri.009G010400	3.754560398	0.000006	AT2G28250	NCRK
MYB21D81	Potri.019G071200	11.39802534	0	AT2G26710	PHYB ACTIVATION TAGGED SUPPRESSOR 1
MYB21D82	Potri.017G050600	10.20758729	0.007192	AT2G02220	PHYTOSULFOKIN RECEPTOR 1
MYB21D83	Potri.010G111900	2.215600854	0.029257	AT2G01460	P-loop containing nucleoside triphosphate hydrolases superfamily protein
MYB21D84	Potri.009G134700	10.59890266	0.004676	AT2G16750	Protein kinase protein with adenine nucleotide alpha hydrolases-like domain
MYB21D85	Potri.004G076500	4.585525259	0.007192	AT1G67000	Protein kinase superfamily protein
MYB21D86	Potri.004G049200	11.27896671	0.000567	AT5G46080	Protein kinase superfamily protein
MYB21D87	Potri.001G215000	3.314970427	0.018834	AT5G22050	Protein kinase superfamily protein;
MYB21D88	Potri.011G104900	7.840143171	0.01497	AT1G71400	RECEPTOR LIKE PROTEIN 12
MYB21D89	Potri.011G105000	11.29344708	0.034579	AT1G71400	RECEPTOR LIKE PROTEIN 12
MYB21D90	Potri.T084800	14.62059379	0	AT5G60900	RECEPTOR-LIKE PROTEIN KINASE 1
MYB21D91	Potri.T084900	4.87745986	0.00793	AT5G60900	RECEPTOR-LIKE PROTEIN KINASE 1
MYB21D92	Potri.019G100800	2.596848771	0.014605	AT4G03510	RING MEMBRANE-ANCHOR 1
MYB21D93	Potri.019G053300	7.202041936	0	AT5G16490	ROP-INTERACTIVE CRIB MOTIF-CONTAINING PROTEIN 4
MYB21D94	Potri.013G055000	10.25194686	0.007342	AT5G12380	ANNEXIN 8
MYB21D95	Potri.005G141600	3.619885338	0.039733	AT1G47128	cysteine proteinase precursor-like protein/ dehydration stress-responsive gene (RD21)
MYB21D96	Potri.008G212300	95.34391756	0	AT1G24020	MLP-LIKE PROTEIN 423
MYB21D97	Potri.001G406000	4.773349589	0.000278	AT4G27220	NB-ARC domain-containing disease resistance protein
MYB21D98	Potri.015G087600	4.978458141	0.000237	AT5G61640	PEPTIDEMETHIONINE SULFOXIDE REDUCTASE 1
MYB21D99	Potri.002G079600	2.604275363	0.000548	AT3G24590	PLASTIDIC TYPE I SIGNAL PEPTIDASE 1
MYB21D100	Potri.005G111000	2.321662077	0.006737	AT5G66130	RADIATION SENSITIVE 17
MYB21D101	Potri.018G152100	13.1299726	0.017463	AT1G73190	ALPHA-TONOPLAST INTRINSIC PROTEIN
MYB21D102	Potri.011G167000	4.837521254	0.000002	AT5G23810	AMINO ACID PERMEASE 7
MYB21D103	Potri.001G469900	6.192470111	0.01273	AT5G23810	AMINO ACID PERMEASE 7
MYB21D104	Potri.004G034800	2.536649167	0.002166	AT2G34660	ATP-BINDING CASSETTE C2 TRANSPORTER
MYB21D105	Potri.009G070100	31.49340845	0	AT5G19410	ATP-BINDING CASSETTE G23 TRANSPORTER
MYB21D106	Potri.002G188900	8.789511585	0.003332	AT2G37280	ATP-BINDING CASSETTE G33 transporter
MYB21D107	Potri.015G006000	13.6080364	0.000005	AT3G53480	ATP-BINDING CASSETTE G37 TRANSPORTER
MYB21D108	Potri.017G138800	112.5584846	0	AT5G17220	GLUTATHIONE S-TRANSFERASE 26
MYB21D109	Potri.014G178800	21.99418138	0.000037	AT1G29000	Heavy metal transport/detoxification superfamily protein
MYB21D110	Potri.T132400	13.40864919	0.000422	AT2G18370	lipid transfer protein
MYB21D111	Potri.013G069400	19.18161117	0.027566	AT3G03620	MATE efflux family protein
MYB21D112	Potri.004G058900	14.97235235	0	AT1G29200	O-fucosyltransferase family protein
MYB21D113	Potri.011G068300	7.002737458	0	AT1G29200	O-fucosyltransferase family protein
MYB21D114	Potri.002G258700	3.426381992	0.014605	AT5G46050	PEPTIDE TRANSPORTER 3
MYB21D115	Potri.019G040500	6.738044703	0.011894	AT3G04440	Plasma-membrane choline transporter family protein
MYB21D116	Potri.001G158900	2.022895789	0.04032	AT5G44790	RESPONSIVE-TO-ANTAGONIST 1
MYB21D117	Potri.004G211900	2.554555004	0.03467	AT2G28315	UDP-XYLOSE TRANSPORTER1
MYB21D118	Potri.001G366200	2.178678019	0.018834	AT1G55910	ZINC TRANSPORTER 11 PRECURSOR
MYB21D119	Potri.018G108000	2.890888568	0.001801	AT5G58160	actin binding
MYB21D120	Potri.003G059400	2.074612655	0.034831	AT1G15490	alpha/beta-Hydrolases superfamily protein
MYB21D121	Potri.004G142600	3.730386206	0.024293	AT1G19190	alpha/beta-Hydrolases superfamily protein
MYB21D122	Potri.002G137200	3.486189518	0.014231	AT3G60340	alpha/beta-Hydrolases superfamily protein
MYB21D123	Potri.002G048700	11.74135495	0.004753	AT2G24600	Ankyrin repeat family protein
MYB21D124	Potri.002G048600	19.04009801	0	AT5G04700	Ankyrin repeat family protein
MYB21D125	Potri.013G083800	5.997952097	0.000058	AT3G56230	BTB/POZ domain-containing protein
MYB21D126	Potri.017G031400	3.375228091	0.000046	AT1G05910	cell division cycle protein 48-related
MYB21D127	Potri.011G101600	109.1985584	0.017012	AT3G14640	CYP72A10
MYB21D128	Potri.011G099700	8.826619457	0.040563	AT3G14680	CYP72A14
MYB21D129	Potri.011G098800	3.833329466	0.01438	AT3G14690	CYP72A15
MYB21D130	Potri.011G099200	4.416703545	0.015489	AT3G14690	CYP72A15
MYB21D131	Potri.011G117700	5.216748925	0.004282	AT3G14620	CYP72A8
MYB21D132	Potri.006G027500	8.128285068	0.017507	AT5G05070	DHHC-type zinc finger family protein
MYB21D133	Potri.010G235600	5.592417234	0.029663	AT3G52900	Family of unknown function (DUF662)
MYB21D134	Potri.007G027300	2.337656576	0.013005	AT5G49610	F-box family protein
MYB21D135	Potri.014G040500	2.451463022	0.042752	AT4G36830	HOS3-1
MYB21D136	Potri.006G205300	4.397126385	0.035511	AT2G36020	HVA22-LIKE PROTEIN J
MYB21D137	Potri.010G042900	8.30725592	0.007309	AT1G23390	Kelch repeat-containing F-box family protein
MYB21D138	Potri.007G052700	2.055161829	0.049852	AT2G23093	Major facilitator superfamily protein
MYB21D139	Potri.009G025100	4.883975625	0.019224	AT2G44260	Plant protein of unknown function (DUF946)
MYB21D140	Potri.004G114300	19.60349524	0.001924	AT5G15780	Pollen Ole e 1 allergen and extensin family protein
MYB21D141	Potri.006G015000	15.26373368	0	AT5G47530	Pollen Ole e 1 allergen and extensin family protein
MYB21D142	Potri.010G156600	16.5712899	0.000001	AT5G47530	Pollen Ole e 1 allergen and extensin family protein
MYB21D143	Potri.016G010900	15.84894605	0.002644	AT5G47530	Pollen Ole e 1 allergen and extensin family protein
MYB21D144	Potri.009G102100	8.603394544	0.000026	AT1G23710	Protein of unknown function (DUF1645)
MYB21D145	Potri.010G011700	4.459364105	0.046622	AT5G49120	Protein of unknown function (DUF581)
MYB21D146	Potri.006G089400	3.412071787	0.001075	AT2G37730	Protein of unknown function (DUF604)
MYB21D147	Potri.012G093300	16.11987889	0.000705	AT1G24440	RING/U-box superfamily protein
MYB21D148	Potri.001G371200	10.14812296	0	AT5G55970	RING/U-box superfamily protein
MYB21D149	Potri.001G251900	6.068983928	0.010642	AT5G01450	RING/U-box superfamily protein (ABERRANT POLLEN DEVELOPMENT 2)
MYB21D150	Potri.013G073500	4.353564205	0.015033	AT3G03550	RING/U-box superfamily protein;
MYB21D151	Potri.010G196900	17.16522663	0.000264	AT5G59100	Subtilisin-like serine endopeptidase family protein
MYB21D152	Potri.006G113000	2.28575694	0.049552	AT3G54190	Transducin/WD40 repeat-like superfamily protein
MYB21D153	Potri.002G048800	13.09299279	0.013624	AT1G48720	unknown protein
MYB21D154	Potri.014G122100	9.435356312	0.00016	AT4G02090	unknown protein
MYB21D155	Potri.005G044600	9.25662322	0.000175	AT4G08630	unknown protein
MYB21D156	Potri.005G076100	4.097071301	0.017691	AT5G65030	unknown protein
MYB21D157	Potri.014G122100	8.988690782	0.000332	AT4G02090	unknown protein
MYB21D158	Potri.015G135200	63.87342911	0.005035	AT5G62170	unknown protein (TRM25)
MYB21D159	Potri.011G107300	9.3642276	0.008824	NO HIT	
MYB21D160	Potri.012G142100	5.773291218	0.044201	NO HIT	
MYB21D161	Potri.013G070900	2.366698616	0.019224	NO HIT	
MYB21D162	Potri.016G139400	21.46917726	0.03467	NO HIT	
MYB21D163		9.303438326	0.010732	NO HIT	
MYB21D164	Potri.014G117200	62.18639154	0.006678	NO HIT	

Table 2. Functional classification of the 135 genes regulated by PtrMYB74.

DEG Number	Populs trichocarpa V3.0 gene model name	Fold change, as gene expression in treatment/gene expression in control	FDR value	Closest Arabidopsis homolog	Annotated name of the Arabidopsis homolog	Populus name
MYB74D1	Potri.017G031600	54.1800	0.0135	AT3G10480	ANAC050	PtrNAC125
MYB74D2	Potri.015G046800	93.9236	0.0007	AT3G18400	ANAC058	PtrNAC105
MYB74D3	Potri.018G095900	45.8771	0.0000	AT5G57620	ATMYB36	PtrMYB088
MYB74D4	Potri.004G138000	14.1247	0.0002	AT4G38620	ATMYB4	PtrMYB093
MYB74D5	Potri.007G134500	6.1595	0.0342	AT1G17950	ATMYB52	PtrMYB161
MYB74D6	Potri.015G033600	5.3795	0.0273	AT1G17950	ATMYB52	PtrMYB090
MYB74D7	Potri.019G050900	21.9084	0.0007	AT5G16770	ATMYB107	PtrMYB059
MYB74D8	Potri.005G129500	8.6055	0.0001	AT4G36870	BEL1-LIKE HOMEODOMAIN 2	PtrWBLH2
MYB74D9	Potri.004G159300	2.8006	0.0006	AT4G34610	BEL1-LIKE HOMEODOMAIN 6	PtrWBLH3
MYB74D10	Potri.017G037000	4.4089	0.0157	AT2G46410	CAPRICE R3-type MYB transcription factor	PtrMYB174
MYB74D11	Potri.003G110800	13.1050	0.0000	AT4G00150	HAIRY MERISTEM 3	PtrHAM3
MYB74D12	Potri.T138100	12.9335	0.0004	AT3G54220	SHOOT GRAVITROPISM 1	PtrSGR1
MYB74D13	Potri.011G058400	4.8490	0.0000	AT4G28500	SND2	PtrNAC123
MYB74D14	Potri.002G081800	17.8325	0.0000	AT1G44170	ALDEHYDE DEHYDROGENASE 4	
MYB74D15	Potri.011G150300	22.0102	0.0000	AT4G10500	DMR6-LIKE OXYGENASE 1	
MYB74D16	Potri.008G073800	7.3366	0.0000	AT5G05390	LACCASE 12	PtrLAC19
MYB74D17	Potri.019G121700	4.2563	0.0014	AT2G30210	LACCASE 3	PtrLAC47
MYB74D18	Potri.001G248700	58.6564	0.0000	AT2G38080	LACCASE 4	PtrLAC4
MYB74D19	Potri.009G042500	9.4640	0.0000	AT2G38080	LACCASE 4	PtrLAC21
MYB74D20	Potri.008G073700	7.0958	0.0001	AT2G40370	LACCASE 5	PtrLAC18
MYB74D21	Potri.010G183600	38.2566	0.0000	AT2G40370	LACCASE 5	PtrLAC26
MYB74D22	Potri.007G019300	6.3695	0.0000	AT5G66390	PEROXIDASE 72	PtrPERX72
MYB74D23	Potri.010G134500	7.9975	0.0002	AT1G68850	Peroxidase superfamily protein	
MYB74D24	Potri.014G049600	10.5867	0.0000	AT3G60280	UCLACYANIN 3	
MYB74D25	Potri.001G088700	3.2966	0.0467	AT5G46290	3-KETOACYL-ACYL CARRIER PROTEIN SYNTHASE I	
MYB74D26	Potri.010G177300	3.5147	0.0001	AT1G65610	GLYCOSYL HYDROLASE 9A2 (KOR2)	
MYB74D27	Potri.010G079300	17.4685	0.0000	AT2G26640	3-KETOACYL-COA SYNTHASE 11	
MYB74D28	Potri.010G079400	18.5454	0.0000	AT1G04220	3-KETOACYL-COA SYNTHASE 2	
MYB74D29	Potri.008G082700	3.7718	0.0131	AT1G79460	ARABIDOPSIS THALIANA ENT-KAURENE SYNTHASE 1	
MYB74D30	Potri.007G098600	22.4067	0.0000	AT5G64440	FATTY ACID AMIDE HYDROLASE	
MYB74D31	Potri.012G068700	50.1761	0.0000	AT1G74460	GDSL-motif esterase/acyltransferase/lipase	
MYB74D32	Potri.014G117300	6.4009	0.0021	AT1G02400	GIBBERELLIN 2-OXIDASE 6	
MYB74D33	Potri.015G060200	8.8653	0.0239	AT5G15630	COBRA-LIKE4, IRREGULAR XYLEM 6	
MYB74D34	Potri.019G121100	9.8093	0.0287	AT5G03170	FASCICLIN-LIKE ARABINOGALACTAN-PROTEIN 11, FLA11	
MYB74D35	Potri.013G151400	3.7150	0.0429	AT5G03170	FASCICLIN-LIKE ARABINOGALACTAN-PROTEIN 11, FLA11	
MYB74D36	Potri.005G141300	2.1056	0.0349	AT5G67210	IRX15-LIKE	
MYB74D37	Potri.013G151300	3.7402	0.0421	AT5G60490	FASCICLIN-LIKE ARABINOGALACTAN-PROTEIN 12, FLA12	
MYB74D38	Potri.002G223300	3.0452	0.0298	AT2G04780	FASCICLIN-LIKE ARABINOOGALACTAN 7	
MYB74D39	Potri.011G161300	6.8327	0.0147	AT1G30760	BERBERINE BRIDGE ENZYME-LIKE 13	
MYB74D40	Potri.017G138800	39.0773	0.0000	AT5G17220	GLUTATHIONE S-TRANSFERASE 26	
MYB74D41	Potri.008G201600	2.4284	0.0059	AT3G23590	MED33A	
MYB74D42	Potri.003G074700	3.0306	0.0001	AT2G35020	UDP-N-ACETYLGLUCOSAMINE-1-PHOSPHATE URIDYLYLTRANSFERASE 2	
MYB74D43	Potri.006G167200	2.1560	0.0377	AT4G30210	P450 REDUCTASE 2 (CPR2)	
MYB74D44	Potri.012G142300	4.1001	0.0002	AT5G23870	PECTIN ACETYLESTERASE 9	
MYB74D45	Potri.014G067100	8.6793	0.0002	AT2G45220	PECTIN METHYLESTERASE 17	
MYB74D46	Potri.005G199300	10.6423	0.0005	AT1G34150	Pseudouridine synthase family protein	
MYB74D47	Potri.003G074600	3.7757	0.0150	AT4G20050	QUARTET 3 (polygalacturonase)	
MYB74D48	Potri.013G118700	17.4784	0.0000	AT5G17050	UDP-GLUCOSYL TRANSFERASE 78D2	
MYB74D49	Potri.006G025300	12.9648	0.0000	AT1G67440	EMBRYO DEFECTIVE 1688	
MYB74D50	Potri.011G143700	5.6132	0.0001	AT1G56050	ENGD-2 (GTP-binding protein-related)	
MYB74D51	Potri.001G032600	3.4070	0.0000	AT4G26760	microtubule-associated protein 65-2 (MAP65-2)	
MYB74D52	Potri.008G067800	4.1711	0.0199	AT3G11220	ELONGATA 1	
MYB74D53	Potri.014G136700	3.7124	0.0281	AT2G26060	EMBRYO DEFECTIVE 1345	
MYB74D54	Potri.016G023500	4.7842	0.0000	AT1G67440	EMBRYO DEFECTIVE 1688	
MYB74D55	Potri.014G024700	3.1483	0.0001	AT5G47820	FRAGILE FIBER 1	
MYB74D56	Potri.001G233100	6.2847	0.0467	AT2G31900	MYOSIN 5	
MYB74D57	Potri.007G120200	21.0694	0.0000	AT2G32300	UCLACYANIN 1	
MYB74D58	Potri.016G108700	9.5810	0.0219	AT3G48750	CELL DIVISION CONTROL 2 (cyclin-dependent kinase)	
MYB74D59	Potri.001G274200	7.1355	0.0062	AT5G12235	CLAVATA3/ESR-RELATED 22	
MYB74D60	Potri.010G042900	6.2064	0.0487	AT1G23390	Kelch repeat-containing F-box family protein	
MYB74D61	Potri.010G121100	6.7194	0.0003	AT1G25390	BARELY ANY MERISTEM 1	
MYB74D62	Potri.010G121100	9.0085	0.0083	AT1G25390	BARELY ANY MERISTEM 1	
MYB74D63	Potri.010G121100	16.5218	0.0000	AT1G25390	BARELY ANY MERISTEM 1	
MYB74D64	Potri.003G211700	26.0176	0.0000	AT1G34300	lectin protein kinase family protein	
MYB74D65	Potri.001G302500	10.0861	0.0225	AT4G06744	Leucine-rich repeat (LRR) family protein	
MYB74D66	Potri.003G211700	6.5287	0.0028	AT1G33610	Leucine-rich repeat (LRR) family protein	
MYB74D67	Potri.013G159200	2.9872	0.0077	AT1G06840	Leucine-rich repeat protein kinase family protein	
MYB74D68	Potri.019G121000	8.8320	0.0090	AT4G08850	Leucine-rich repeat receptor-like protein kinase family protein	
MYB74D69	Potri.019G122700	6.1731	0.0145	AT4G08850	Leucine-rich repeat receptor-like protein kinase family protein	
MYB74D70	Potri.009G010400	2.7438	0.0196	AT2G28250	NCRK	
MYB74D71	Potri.014G093300	5.0466	0.0047	AT4G01190	PHOSPHATIDYLINOSITOL PHOSPHATE KINASE 10	
MYB74D72	Potri.019G071200	5.6005	0.0001	AT2G26710	PHYB ACTIVATION TAGGED SUPPRESSOR 1	
MYB74D73	Potri.017G050600	7.7719	0.0146	AT2G02220	PHYTOSULFOKIN RECEPTOR 1	

Table 2. Continued

DEG Number	Populs trichocarpa V3.0 gene model name	Fold change, as gene expression in treatment/gene expression in control	FDR value	Closest Arabidopsis homolog	Annotated name of the Arabidopsis homolog
MYB74D74	Potri.004G049200	9.2813	0.0016	AT5G46080	Protein kinase superfamily protein
MYB74D75	Potri.009G134700	16.2296	0.0000	AT2G16750	kinase with adenine nucleotide alpha hydrolases-like
MYB74D76	Potri.011G104900	9.3324	0.0090	AT1G71400	RECEPTOR LIKE PROTEIN 12
MYB74D77	Potri.011G105000	13.7319	0.0271	AT1G71400	RECEPTOR LIKE PROTEIN 12
MYB74D78	Potri.005G008600	46.6207	0.0319	AT1G74190	RECEPTOR LIKE PROTEIN 15
MYB74D79	Potri.005G009700	15.3498	0.0482	AT1G74190	RECEPTOR LIKE PROTEIN 15
MYB74D80	Potri.018G117400	30.2051	0.0006	AT1G74190	RECEPTOR LIKE PROTEIN 15
MYB74D81	Potri.T084800	12.9959	0.0000	AT5G60900	RECEPTOR-LIKE PROTEIN KINASE 1
MYB74D82	Potri.019G100800	2.1879	0.0483	AT4G03510	RING MEMBRANE-ANCHOR 1
MYB74D83	Potri.019G053300	4.4517	0.0000	AT5G16490	P-INTERACTIVE CRIB MOTIF-CONTAINING PROTE
MYB74D84	Potri.010G018000	5.4451	0.0290	AT4G27300	S-locus lectin protein kinase family protein
MYB74D85	Potri.014G093300	5.6227	0.0003	AT1G01460	Type I phosphatidylinositol-4-phosphate 5-kinase
MYB74D86	Potri.013G055000	10.4867	0.0141	AT5G12380	ANNEXIN 8
MYB74D87	Potri.007G137100	4.1957	0.0046	AT3G14460	nd NB-ARC domains-containing disease resistance p
MYB74D88	Potri.008G212300	143.9211	0.0000	AT1G24020	MLP-LIKE PROTEIN 423
MYB74D89	Potri.011G167000	4.5666	0.0000	AT5G23810	AMINO ACID PERMEASE 7
MYB74D90	Potri.001G255900	3.1583	0.0030	AT3G21090	ATP-BINDING CASSETTE G15
MYB74D91	Potri.009G070100	30.5478	0.0000	AT5G19410	ATP-BINDING CASSETTE G23 TRANSPORTER
MYB74D92	Potri.002G188900	10.7098	0.0002	AT2G37280	ATP-BINDING CASSETTE G33
MYB74D93	Potri.015G006000	20.0515	0.0000	AT3G53480	ATP-BINDING CASSETTE G37 TRANSPORTER
MYB74D94	Potri.002G072600	9.8882	0.0057	AT1G21460	ATSWEET1
MYB74D95	Potri.002G072800	10.2162	0.0045	AT1G21460	ATSWEET1
MYB74D96	Potri.016G006700	3.2556	0.0069	AT4G16380	eavy metal transport/detoxification superfamily protei
MYB74D97	Potri.006G245900	18.6393	0.0156	AT2G25680	MOLYBDATE TRANSPORTER 1
MYB74D98	Potri.008G146400	3.0502	0.0254	AT1G60030	NUCLEOBASE-ASCORBATE TRANSPORTER 7
MYB74D99	Potri.004G058900	10.7671	0.0000	AT1G29200	O-fucosyltransferase
MYB74D100	Potri.009G155800	3.4981	0.0049	AT5G06570	alpha/beta-Hydrolases superfamily protein
MYB74D101	Potri.002G048600	23.7140	0.0000	AT5G04700	Ankyrin repeat family protein
MYB74D102	Potri.006G015000	9.7352	0.0000	AT5G47530	Auxin-responsive family protein
MYB74D103	Potri.010G156600	9.1488	0.0030	AT5G47530	Auxin-responsive family protein
MYB74D104	Potri.016G010900	10.3874	0.0147	AT5G47530	Auxin-responsive family protein
MYB74D105	Potri.014G136800	3.5626	0.0033	AT1G23160	Auxin-responsive GH3 family protein
MYB74D106	Potri.014G082900	8.8301	0.0000	AT3G61320	Bestrophin-like protein
MYB74D107	Potri.013G083800	4.3121	0.0033	AT3G56230	BTB/POZ domain-containing protein
MYB74D108	Potri.011G098800	4.7180	0.0001	AT3G14690	CYP72A15
MYB74D109	Potri.011G099200	4.1990	0.0084	AT3G14690	CYP72A15
MYB74D110	Potri.012G007600	4.4436	0.0027	AT5G54130	CYP72A8
MYB74D111	Potri.006G027500	13.4038	0.0003	AT5G05070	DHHC-type zinc finger family protein
MYB74D112	Potri.006G205300	7.8621	0.0000	AT2G36020	HVA22-LIKE PROTEIN J
MYB74D113	Potri.019G108400	10.4187	0.0010	AT3G50150	Plant protein of unknown function (DUF247)
MYB74D114	Potri.019G105500	76.4354	0.0006	AT3G50150	Plant protein of unknown function (DUF247)
MYB74D115	Potri.010G111900	2.1416	0.0113	AT2G01460	taining nucleoside triphosphate hydrolases superfam
MYB74D116	Potri.004G114300	13.3552	0.0032	AT5G15780	Pollen Ole e 1 allergen and extensin family
MYB74D117	Potri.009G027500	2.6191	0.0035	AT5G59790	Protein of unknown function DUF966
MYB74D118	Potri.009G009500	2.6564	0.0239	AT5G60720	Protein of unknown function, DUF547
MYB74D119	Potri.001G396700	4.7318	0.0161	AT5G18790	Ribosomal protein L33 family protein
MYB74D120	Potri.001G371200	7.7656	0.0000	AT5G55970	RING/U-box superfamily protein
MYB74D121	Potri.012G093300	22.9765	0.0001	AT1G24440	RING/U-box superfamily protein
MYB74D122	Potri.010G220200	34.9858	0.0000	AT3G07990	SERINE CARBOXYPEPTIDASE-LIKE 27
MYB74D123	Potri.002G175400	12.2423	0.0015	AT2G46630	unknown protein
MYB74D124	Potri.003G130100	2.7173	0.0022	AT1G75060	unknown protein
MYB74D125	Potri.005G002600	7.2133	0.0041	AT3G05858	unknown protein
MYB74D126	Potri.005G044600	13.0846	0.0000	AT4G08630	unknown protein
MYB74D127	Potri.005G076100	4.1139	0.0050	AT5G65030	unknown protein
MYB74D128	Potri.011G117700	3.9670	0.0254	AT3G14620	
MYB74D129	Potri.003G152500	99.0982	0.0254		
MYB74D130	Potri.006G150800	12.0737	0.0209		
MYB74D131	Potri.016G139400	19.8147	0.0081		
MYB74D132	Potri.001G247100	3.9059	0.0067		
MYB74D133	Potri.001G247000	6.4571	0.0006		
MYB74D134	Potri.007G007000	22.7278	0.0000		
MYB74D135	Potri.017G047500	58.1856	0.0000		

Table 3. PtrMYB21 overexpression induced DEGs that are involved in cell wall formation. [a]Pathways that are involved with cell wall formation. [b] Stem differentiating xylem IDs from *Populus trichocarpa* V 3.0 gene model name. [c]The names of most homologous Arabidopsis genes with PtrMYB21 overexpression induced DEGs. The Gene IDs of the SDX-preferential expressed genes are marked as grey.

[a] cell wall biosynthesis processes	[b]Gene ID	[c]Gene name	Tissue that the gene preferential expressed in	References for the functions of the encoding proteins
Lignin polymerization	Potri.001G248700	PtrLAC04	Young shoot	(Berthet et al., 2011)
	Potri.006G096900	PtrLAC14	Stem differentiating xylem	(Berthet et al., 2011)
	Potri.006G097000	PtrLAC15	Stem differentiating xylem	(Berthet et al., 2011)
	Potri.009G042500	PtrLAC21	Stem differentiating xylem	(Berthet et al., 2011)
	Potri.016G112100	PtrLAC41	Stem differentiating xylem	(Berthet et al., 2011)
	Potri.006G097100	PtrLAC49	Stem differentiating xylem	(Berthet et al., 2011)
	Potri.008G073700	PtrLAC18	Stem differentiating xylem	(Ranocha et al., 2002)
	Potri.010G183600	PtrLAC26	Stem differentiating xylem	(Ranocha et al., 2002)
	Potri.008G073800	PtrLAC19	Stem differentiating xylem	(Ranocha et al., 2002)
Hemicellulose synthesis	Potri.016G086400	PtrIRX9	Stem differentiating xylem	(Wu et al., 2010)
	Potri.007G047500	PtrIRX14-L	Stem differentiating xylem	(Lee et al., 2010)
			Mature leaf	
Phenylalanine synthesis	Potri.011G004700	PtrADT1	Stem differentiating xylem	(Corea et al., 2012)
	Potri.008G038200	PtrPAL2		(Vanholme et al., 2012)
			Stem differentiating xylem	
Cellulose deposition	Potri.014G024700	PtrFRA1		(Zhu et al., 2015)
			Mature leaf	
Suberin biosynthesis	Potri.010G079400	PtrKCS2	Mature leaf	(Franke et al., 2009)
	Potri.015G100800	PtrHHT		(Molina et al., 2009)
			Mature leaf	
Cutin biosynthesis	Potri.009G109900	PtrLACS2		(Schnurr et al., 2004)
			Stem differentiating xylem	
Pectin formation	Potri.012G142300	PtrPec9-1	Stem differentiating xylem	(de Souza et al.,2014)
	Potri.015G145400	PtrPec9-2		(de Souza et al.,2014)

Table 4. PtrMYB74 overexpression induced DEGs that are involved in cell wall formation. [a]Pathways that are involved with cell wall formation. [b]IDs from *Populus trichocarpa* V3.0 gene model name. [c]The names of most homologous Arabidopsis genes with PtrMYB74 overexpression induced DEGs. The Gene IDs of the xylem-preferential expressed genes are marked as grey.

[a]Pathways in cell wall formation	[b]Gene ID	Gene name	[c]Tissue that the gene preferential expressed in	References for the functions of proteins
Lignin polymerization	Potri.001G248700	PtrLAC4	Young shoot	(Berthet et al., 2011)
	Potri.009G042500	PtrLAC21	Stem differentiating xylem	(Berthet et al., 2011)
	Potri.008G073700	PtrLAC18	Stem differentiating xylem	(Ranocha et al., 2002)
	Potri.010G183600	PtrLAC26	Stem differentiating xylem	(Ranocha et al., 2002)
	Potri.008G073800	PtrLAC19	Stem differentiating xylem	(Ranocha et al., 2002)
	Potri.007G019300	PtrPerx52	Stem differentiating phloem	(Herrero et al.,2013)
Monolignol metabolism	Potri.011G161300	PtrBBE-L13	Stem differentiating xylem	(Daniel et al., 2015)
Coenzyme for monolignol synthesis	Potri.006G167200	PtrCPR2	Mature Leaf	(Sundrin et al., 2014)
Cell wall modification	Potri.019G121100	PtrFLA32	Stem differentiating xylem	(Macmillan et al., 2010)
	Potri.013G151400	PtrFLA18	Stem differentiating xylem	(Macmillan et al., 2010)
	Potri.013G151300	PtrFLA17	Stem differentiating xylem	(Macmillan et al., 2010)
Hemicellulose synthesis	Potri.005G141300	PtrIRX15-L	Stem differentiating xylem	(Brown et al., 2011)
Cellulose deposition	Potri.014G024700	PtrFRA1	Stem differentiating xylem	(Zhu et al., 2015)
	Potri.015G060200	PtrIRX6	Stem differentiating xylem	(Brown et al., 2005)
Suberin biosynthesis	Potri.010G079400	PtrKCS2	Mature leaf	(Franke et al., 2009)
Pectin formation	Potri.012G142300	PtrPec9-1	Stem differentiating xylem	(de Souza et al.,2014)
	Potri.014G067100	PtrPec17	Young shoot	(Sénéchal et al., 2015)
Cell wall degradation	Potri.003G074600	PtrQRT3	Stem differentiating xylem	(Rhee et al., 2003)

Table 5. **Significant gene ontology functional classes of 161 DEGs induced by PtrMYB21 overexpression.** [a] Represent the hierarchical class of gene ontology annotation. [b]BP represents biological process; MF stand for molecular function; CC stand for cellular component represented as significant gene ontology here. [c]GO term names are listed in hierarchical order. [d]The p values of significant gene ontology are lower than 0.05.

GO term ID	Class [a]	GO term domain[b]	GO term name[c]	Number of DEGs with the GO ID	p value[d]
GO:0042546	1	BP	cell wall biogenesis	8	1.43E-03
GO:0009832	1	BP	plant-type cell wall biogenesis	6	3.83E-03
GO:0009834	1	BP	plant-type secondary cell wall biogenesis	5	4.99E-04
GO:0010345	2	BP	suberin biosynthetic process	3	1.88E-02
GO:1901361	3	BP	organic cyclic compound catabolic process	10	2.67E-05
GO:0019748	4	BP	secondary metabolic process	14	4.08E-08
GO:0009698	4	BP	phenylpropanoid metabolic process	14	1.68E-12
GO:0009808	4	BP	lignin metabolic process	9	2.53E-07
GO:0019439	5	BP	aromatic compound catabolic process	10	1.71E-05
GO:0046271	5	BP	phenylpropanoid catabolic process	9	6.95E-10
GO:0046274	5	BP	lignin catabolic process	9	6.95E-10
GO:0016679	6	MF	oxidoreductase activity, diphenols and related substances as donors	9	6.01E-08
GO:0016682	6	MF	oxidoreductase activity, diphenols and related substances as donors, oxygen as acceptor	9	1.81E-08
GO:0052716	6	MF	hydroquinone:oxygen oxidoreductase activity	9	6.95E-10
GO:0005507	7	MF	ion binding	57	4.98E-02
GO:0046914	7	MF	transition metal ion binding	27	2.34E-02
GO:0005507	7	MF	copper ion binding	11	1.79E-04
GO:0048046	8	CC	apoplast	9	3.36E-02

Table 6. **Significant gene ontology functional classes of 127 DEGs induced by PtrMYB74 overexpression.** [a] Represent the hierarchical class of gene ontology annotation. [b]BP represents biological process; MF stand for molecular function; no CC cellular component represent as significant gene ontology here. [c]GO term names are listed in hierarchical order. [d]The p values of significant gene ontology are low than 0.05.

GO term ID	class[a]	GO term domain[b]	GO term name[c]	Number of DEGs with the GO ID	P value[d]
GO:0019748	1	BP	secondary metabolic process	10	7.08E-05
GO:0009698	1	BP	phenylpropanoid metabolic process	10	5.84E-08
GO:0009808	1	BP	lignin metabolic process	7	2.36E-03
GO:0046271	2	BP	phenylpropanoid catabolic process	6	6.00E-05
GO:0046274	2	BP	lignin catabolic process	6	6.00E-05
GO:0042546	3	BP	Cell wall biogenesis	6	0.0416
GO:0016679	4	MF	oxidoreductase activity, diphenols and related substances as donors	6	9.80E-04
GO:0016682	4	MF	oxidoreductase activity, diphenols and related substances as donors, oxygen as acceptor	6	4.86E-04
GO:0052716	4	MF	hydroquinone:oxygen oxidoreductase activity	6	6.00E-05
GO:0005507	5	MF	ion binding	49	0.0163
GO:0005507	5	MF	copper ion binding	8	0.0101

Table 7. The tissue-specific transcript abundances of the cell wall biosynthetic genes regulated by PtrMYB21 and PtrMYB74. The expression values are normalized and shown here. These values are generated from GSE81077, Shi et al. 2017.

Gene ID	Gene name	Developing Xylem	Developing Phloem	Mature Leaf	Junvenile Shoot	Tissue that gene preferential expressed i
Potri.003G074600	PtrQRT3	7	1.19	0.3	0.88	***developing xylem***
Potri.005G141300	PtrIRX15-L	423.3	12.73	4.91	6.11	***developing xylem***
Potri.006G096900	PtrLAC14	64.31	3.12	1.8	3.07	***developing xylem***
Potri.006G097000	PtrLAC15	92.78	4.92	2.4	4.12	***developing xylem***
Potri.006G097100	PtrLAC49	53.52	2.88	1.41	2.71	***developing xylem***
Potri.007G047500	PtrIRX14-L	177.85	17.74	11.9	11.58	***developing xylem***
Potri.008G038200	PtrPAL2	388.74	9	64.85	74.21	***developing xylem***
Potri.008G073700	PtrLAC18	162.43	7.67	0.47	0.56	***developing xylem***
Potri.008G073800	PtrLAC19	63.66	23.65	22.32	7.66	***developing xylem***
Potri.009G042500	PtrLAC21	19.56	0.44	1.15	1.92	***developing xylem***
Potri.010G183600	PtrLAC26	38.68	0.98	0.16	0.54	***developing xylem***
Potri.011G161300	PtrBBE-L13	2.66	0.44	0.06	0.55	***developing xylem***
Potri.012G142300	PtrPec9-1	25.28	0.61	0.58	0.68	***developing xylem***
Potri.013G151300	PtrFLA17	60.29	0.18	0.12	0.22	***developing xylem***
Potri.013G151400	PtrFLA18	209.09	0.41	0.37	0.89	***developing xylem***
Potri.014G024700	PtrFRA1	80.61	6.88	23.66	23.66	***developing xylem***
Potri.015G060200	PtrIRX6	0.66	0.05	0.03	0.06	***developing xylem***
Potri.015G145400	PtrPec9-2	11.7	2.52	6.21	1.69	***developing xylem***
Potri.016G086400	PtrIRX9	238.03	10.97	1.93	1.96	***developing xylem***
Potri.016G112100	PtrLAC41	7.44	0.16	0.95	2.71	***developing xylem***
Potri.019G121100	PtrFLA32	38.08	0.07	0.06	0.18	***developing xylem***
Potri.014G067100	PtrPec17	0	0	0.03	0.22	***Mature leaf***
Potri.010G079400	PtrKCS2	0.77	0.59	158.35	30.07	***Mature leaf***
Potri.006G167200	PtrCPR2	110.27	22.98	161.27	90.68	***Mature leaf***
Potri.001G248700	PtrLAC4	0.96	0.08	0.64	1.16	***Junvenile shoot***
Potri.011G004700	PtrADT1	12.48	4.66	13.32	9.2	***Mature leaf***
Potri.015G100800	PtrHHT	0.26	0.24	73.96	3.42	***Mature leaf***
Potri.009G109900	PtrLACS2	1.85	0.5	47.76	18.54	***Mature leaf***

Table 8. The tissue-specific transcript abundances of the TF genes regulated by PtrMYB21 and PtrMYB74. The expression values are normalized and shown here. These values are generated from GSE81077, Shi et al. 2017.

Gene ID	*Gene name*	*Developing Xylem*	*Developing Phloem*	*Mature Leaf*	*Junvenile Shoot*	*Tissue that gene preferential expressed in*
Potri.017G031600	PtrNAC125	0.01	0	0	0	***Developing Xylem***
Potri.011G058400	PtrNAC123/SND2/3A1	0.01	0.91	0.93	1.05	***Mature Leaf***
Potri.006G152700	PtrNAC127/SND2/3-L1	20.85	3.23	1.57	1.27	***Developing Xylem***
Potri.019G031600	PtrNAC144	0.85	2.98	2.07	2.56	***Developing Phloem***
Potri.005G109500	PtrFD2	1.44	2.57	0.58	1.05	***Developing Phloem***
Potri.019G081500	PtrMYB168	4.35	0.24	0.64	0.27	***Developing Xylem***
Potri.018G095900	PtrMYB088	0.01	0	0	0	***Developing Xylem***
Potri.007G134500	PtrMYB161	6.15	0.37	0.07	0.07	***Developing Xylem***
Potri.015G033600	PtrMYB090	29.14	0.64	0.17	0.15	***Developing Xylem***
Potri.017G017600	PtrMYB175	0.06	0.08	0	0	***Developing Phloem***
Potri.019G050900	PtrMYB59	0.05	1.66	0.47	0.18	***Developing Phloem***
Potri.014G050000	PtrWRKY19	0.01	0.32	0.58	5.5	***Junvenile Shoot***
Potri.005G129500	PtrWBLH2	35.66	0.45	18.34	0.59	***Developing Xylem***
Potri.007G032700	PtrWBLH4	45.74	0.69	19.28	0.31	***Developing Xylem***
Potri.004G159300	PtrWBLH3	45.34	10.84	5.65	9.53	***Developing Xylem***
Potri.002G031000	PtrWBLH1	22.29	0.53	0.46	0.56	***Developing Xylem***
Potri.003G110800	PtrHAM3/PtrGRAS22	1.84	4.63	2.82	3.6	***Developing Phloem***
Potri.015G046800	PtrNAC105	0.05	0.06	0	0	***Developing Phloem***
Potri.004G138000	PtrMYB093	2.88	0.05	6.49	1.61	***Mature Leaf***
Potri.017G037000	PtrMYB174	8.07	8.47	7.66	10.25	***Junvenile Shoot***
Potri.T138100	PtrSGR1	0.05	1.66	0.47	3.8	***Developing Phloem***

Table 9. The selection of 36 cell-wall component genes as the targets in this study.

Gene ID	Pathway gene function in	FBG names
Potri.002G257900	secondary CesA	PtrCesA4
Potri.004G059600	secondary CesA	PtrCesA18
Potri.006G181900	secondary CesA	PtrCesA7
Potri.011G069600	secondary CesA	PtrCesA8
Potri.018G103900	secondary CesA	PtrCesA17
Potri.005G087500	primary CesA	PRC1-2
Potri.005G194200	primary CesA	CESA9-3
Potri.006G052600	primary CesA	IXR1-2
Potri.006G251900	primary CesA	RSW1-2
Potri.007G076500	primary CesA	PRC1-3
Potri.009G060800	primary CesA	IXR1-3
Potri.016G054900	primary CesA	IXR1-4
Potri.018G029400	primary CesA	RSW1-3
Potri.001G266400	primary CesA	IXR1-1
Potri.001G036900	monolignol	Ptr4CL3
Potri.003G188500	monolignol	Ptr4CL5
Potri.006G033300	monolignol	PtrC3H3
Potri.013G157900	monolignol	PtrC4H1
Potri.019G130700	monolignol	PtrC4H2
Potri.009G095800	monolignol	PtrCAD1
Potri.003G181400	monolignol	PtrCCR2
Potri.005G117500	monolignol	PtrCAld5H1
Potri.007G016400	monolignol	PtrCAld5H2
Potri.009G099800	monolignol	PtrCCoAOMT1
Potri.001G304800	monolignol	PtrCCoAOMT2
Potri.008G136600	monolignol	PtrCCoAOMT3
Potri.012G006400	monolignol	PtrCOMT2
Potri.003G183900	monolignol	PtrHCT1
Potri.001G042900	monolignol	PtrHCT6
Potri.006G126800	monolignol	PtrPAL1
Potri.008G038200	monolignol	PtrPAL2
Potri.016G091100	monolignol	PtrPAL3
Potri.010G224100	monolignol	PtrPAL4
Potri.010G224200	monolignol	PtrPAL5
Potri.003G059200	monolignol	PtrCSE1
Potri.001G175000	monolignol	PtrCSE2

Table 10. Protein-DNA interactions identified by ChIP assays in this study.

The annotation of TFs and targets genes were showed in Table 1 that marked as "*", and in Table 2 that marked as "**", and in Table 9 that marked as "***"

Network layers that interactions locate between	TFs (*JGI 3.0* ID)	Target genes (*JGI 3.0* ID)
lst layer to 2nd layer	PtrSND1-B1(Potri.014G104800)	PtrMYB21(Potri.009G053900)
	PtrSND1-B1(Potri.014G104800)	PtrMYB74(Potri.015G082700)
2nd layer to 3rd layer	PtrMYB21(Potri.009G053900)	PtrIRX9(Potri.016G086400)*
	PtrMYB21(Potri.009G053900)	PtrIRX14-L(Potri.007G047500)*
	PtrMYB21(Potri.009G053900)	PtrFRA1(Potri.014G024700)*
	PtrMYB21(Potri.009G053900)	PtrPAL2(Potri.008G038200)*
	PtrMYB21(Potri.009G053900)	PtrLAC21(Potri.009G042500)*
	PtrMYB21(Potri.009G053900)	PtrLAC26(Potri.010G183600)*
	PtrMYB21(Potri.009G053900)	PtrLAC41(Potri.016G112100)*
	PtrMYB21(Potri.009G053900)	PtrPec9-1(Potri.012G142300)*
	PtrMYB21(Potri.009G053900)	PtrMYB59(Potri.019G050900)*
	PtrMYB21(Potri.009G053900)	PtrMYB90(Potri.015G033600)*
	PtrMYB21(Potri.009G053900)	PtrMYB161(Potri.007G134500)*
	PtrMYB21(Potri.009G053900)	PtrMYB175(Potri.017G017600)*
	PtrMYB21(Potri.009G053900)	PtrHAM3(Potri.003G110800)*
	PtrMYB21(Potri.009G053900)	PtrWBLH1(Potri.002G031000)*
	PtrMYB21(Potri.009G053900)	PtrWBLH2(Potri.005G129500)*
	PtrMYB21(Potri.009G053900)	PtrWBLH3(Potri.004G159300)*
	PtrMYB21(Potri.009G053900)	PtrNAC123(Potri.011G058400)*
	PtrMYB21(Potri.009G053900)	PtrNAC127(Potri.006G152700)**
	PtrMYB74(Potri.013G056400)	PtrLAC19(Potri.008G073800)**
	PtrMYB74(Potri.013G056400)	PtrLAC21(Potri.009G042500)**
	PtrMYB74(Potri.013G056400)	PtrLAC26(Potri.010G183600)**
	PtrMYB74(Potri.013G056400)	PtrPec9-1(Potri.012G142300)**
	PtrMYB74(Potri.013G056400)	PtrQRT3(Potri.003G074600)**
	PtrMYB74(Potri.013G056400)	PtrFLA18(Potri.013G151400)**
	PtrMYB74(Potri.013G056400)	PtrFLA32(Potri.019G121100)**
	PtrMYB74(Potri.013G056400)	PtrMYB59(Potri.019G050900)**
	PtrMYB74(Potri.013G056400)	PtrMYB88(Potri.018G095900)**
	PtrMYB74(Potri.013G056400)	PtrMYB90(Potri.015G033600)**
	PtrMYB74(Potri.013G056400)	PtrMYB93(Potri.004G138000)**
	PtrMYB74(Potri.013G056400)	PtrMYB161(Potri.007G134500)**
	PtrMYB74(Potri.013G056400)	PtrMYB174(Potri.017G037000)**
	PtrMYB74(Potri.013G056400)	PtrNAC105(Potri.015G046800)**
	PtrMYB74(Potri.013G056400)	PtrNAC125(Potri.017G031600)**
	PtrMYB74(Potri.013G056400)	PtrNAC123(Potri.011G058400)**
	PtrMYB74(Potri.013G056400)	PtrWBLH2(Potri.005G129500)**
3rd layer to 4th layer	PtrMYB90(Potri.015G033600)	PtrCCoAOMT1(Potri.009G099800)
	PtrMYB90(Potri.015G033600)	PtrCCoAOMT2(Potri.001G304800)
	PtrMYB90(Potri.015G033600)	PtrCAld5H1(Potri.005G117500)***
	PtrMYB90(Potri.015G033600)	PtrCOMT2(Potri.012G006400)***
	PtrMYB90(Potri.015G033600)	PtrCesA17(Potri.018G103900)***
	PtrMYB90(Potri.015G033600)	PtrRSW1-2(Potri.006G251900)***
	PtrMYB90(Potri.015G033600)	PtrRSW1-3(Potri.018G029400)***
	PtrMYB161(Potri.007G134500)	PtrCAld5H1(Potri.005G117500)***
	PtrMYB161(Potri.007G134500)	PtrCAld5H2(Potri.007G016400)***
	PtrMYB161(Potri.007G134500)	PtrCCoAOMT2(Potri.001G304800)
	PtrMYB161(Potri.007G134500)	PtrCesA4(Potri.002G257900)***
	PtrMYB161(Potri.007G134500)	PtrCesA18(Potri.004G059600)***
	PtrMYB174(Potri.017G037000)	PtrCAD1(Potri.009G095800)***
	PtrWBLH1(Potri.002G031000)	PtrHCT6(Potri.001G042900)***
	PtrWBLH1(Potri.002G031000)	PtrCSE2(Potri.001G175000)***
	PtrWBLH1(Potri.002G031000)	PtrCCoAOMT2(Potri.001G304800)
	PtrWBLH2(Potri.005G129500)	PtrCAld5H1(Potri.005G117500)***
	PtrWBLH2(Potri.005G129500)	PtrHCT1(Potri.003G183900)***
	PtrNAC123(Potri.011G058400)	PtrCCoAOMT1(Potri.009G099800)
	PtrWBLH2(Potri.005G129500)	PtrC4H1(Potri.013G157900)

Table 11. The SDX cell-specific transcript abundances of the TF genes directly targeted by PtrMYB21 and PtrMYB74. The expression values are normalized and shown here. These values are from GSE81077, Shi et al. 2017.

Gene name	*Populus ID*	*Developing Xyler*	*Developing Phloem*	*Mature Leaf*
PtrHAM3	Potri.003G110800	0.494290085	0.366889281	0.217826057
PtrMYB161	Potri.007G134500	0	0	0
PtrMYB174	Potri.017G037000	19.0906694	32.47156421	6.179886011
PtrMYB175	Potri.017G017600	34.20729348	45.01208777	28.10469194
PtrMYB59	Potri.019G050900	8.600539436	15.18003677	9.795950437
PtrMYB88	Potri.018G095900	0	0	0
PtrMYB90	Potri.015G033600	0	0	0
PtrMYB93	Potri.004G138000	4.319050518	1.66620878	16.04157378
PtrNAC105	Potri.015G046800	0.015176769	0	0
PtrNAC123	Potri.011G058400	35.65979329	73.66769218	24.92889298
PtrNAC125	Potri.017G031600	0	0	0
PtrNAC127	Potri.006G152700	20.26851901	47.04109481	11.17381167
PtrWBLH1	Potri.002G031000	6.313478034	14.27598611	4.373346374
PtrWBLH2	Potri.005G129500	45.20711691	135.2608596	9.139970938
PtrWBLH3	Potri.004G159300	34.06052934	28.3401872	40.88083904

Table 12. The SDX cell-specific transcript abundances of the cell wall biosynthetic genes regulated by PtrMYB21, PtrMYB74, and their downstream TFs. The expression values are normalized and shown here. These values are from GSE81077, Shi et al. 2017.

Gene ID	Gene name	3_cell_type	Fiber cells	Vessel cells
Potri.018G103900	***PtrCesA17***	117.3708775	344.9455909	116.5447028
Potri.004G059600	***PtrCesA18***	317.6296806	1388.264435	182.8362513
Potri.002G257900	***PtrCesA4***	264.5796154	754.0145314	168.3625388
Potri.005G117500	***PtrCAld5H1***	78.98621257	200.8206453	35.03524774
Potri.007G016400	***PtrCAld5H2***	100.3368923	210.3049672	52.05156552
Potri.009G099800	***PtrCCoAOMT1***	507.6564846	883.642537	431.5994787
Potri.001G304800	***PtrCCoAOMT2***	631.4660465	1470.677116	568.2429529
Potri.006G251900	***RSW1-1***	15.23426182	19.27316019	13.73422928
Potri.018G029400	***RSW1-2***	20.53980744	25.52754395	41.62953573
Potri.003G183900	***PtrHCT1***	397.5608033	808.3664008	272.3364317
Potri.001G042900	***PtrHCT6***	27.06089248	47.77913637	37.48850634
Potri.012G006400	***PtrCOMT2***	1591.117215	3551.219324	2800.832882
Potri.013G157900	***PtrC4H1***	150.5544037	424.9688635	207.0857693
Potri.001G175000	***PtrCSE2***	22.24912342	51.71414605	23.42945797
Potri.009G095800	***PtrCAD1***	576.2340277	1131.604672	383.5221349
Potri.013G151400	***PtrFLA18***	185.5180013	1305.082287	33.5218144
Potri.019G121100	***PtrFLA32***	13.61180004	110.8650047	6.126563252
Potri.014G024700	***PtrFRA1***	9.959255747	18.95465803	15.64884766
Potri.007G047500	***PtrIRX14-L***	46.69323488	129.2385355	48.70491495
Potri.016G086400	***PtrIRX9***	56.91689758	152.3908063	51.11766995
Potri.008G073800	***PtrLAC19***	10.99240239	5.201333005	25.4741509
Potri.009G042500	***PtrLAC21***	2.705029405	0.96178545	4.270716882
Potri.010G183600	***PtrLAC26***	5.355171557	3.21596907	14.67631868
Potri.016G112100	***PtrLAC41***	0.449472908	0.679436196	1.653327989
Potri.008G038200	***PtrPAL2***	350.622511	684.3883605	161.3120673
Potri.012G142300	***PtrPec9-1***	2.455808336	10.62906595	6.095706359
Potri.003G074600	***PtrQRT3***	1.043820971	0.67913952	14.41528555

Table 13. Primers used in the study.

Usage	Gene name	Primer sequence (5'-3')	
		Forward primer	Reverse primer
RNAi fragments clone	PtrMYB21	PtrMYB21RNAiSF:TCTAGAGAAGAGATTAAAGAATCTGCAG	PtrMYB21RNAiSR: CTCGAGATACATGTTTAGGCCATGATC
	PtrMYB74	PtrMYB74RNAiSF:TCTAGAGTTCAAACATCAGCAATTAT	PtrMYB74RNAiSR: CTCGAGGAAGACATCAAAATTTGCTC
	PtrMYB21	PtrMYB21RNAiASF:ACTAGTCTTCTCTAATTTCTTAGACGTC	PtrMYB21RNAiASR:GAGCTCTATGTACAAATCCGGTACTAG
	PtrMYB74	PtrMYB74RNAiASF:ACTAGTCAAGTTTGTAGTCGTTAATA	PtrMYB74RNAiASR: GAGCTCCTTCTGTAGTTTTAAACGAG
transactivation assays in SDX protoplasts with GFP tag	PtrWBLH1	PtrWBLH1FUSF:CTAGTCTAGAATGGCTACCTATTACCCAA	PtrWBLH1FUSR: CTAGCTCGAGAACCACAAAATCATGTAAC
	PtrWBLH2	PtrWBLH2FUSF:CTAGTCTAGAATGGGAATAGCTACACCTC	PtrWBLH2FUSR: CTAGCTCGAGACAACCCCCAAAATCTCTA
	PtrWBLH3	PtrWBLH3FUSF: CTAGTCTAGAATGGCTACCTATTATACTA	PtrWBLH3FUSR:CTAGCTCGAGAGCTACGAAATCATGAAA
	PtrMYB90	PtrMYB90FUSF:CTCTAGAAATGTGTACTAGAGGCCATTGGA	PtrMYB90FUSR:TCTCGAGAGCTGAGAAAAAATCAATG
	PtrMYB161	PtrMYB161FUSF:CTAGTCTAGAATGTCTAGCAGAGGCCATT	PtrMYB161FUSR:CTAGGTCGACCAATCCACTAACTTGGTTT
	PtrMYB174	PtrMYB174FUSF:CTAGTCTAGACAACTTAATTATGGCTGACT	PtrMYB174FUSR:CTAGGTCGACCTGACTTGTAGAGTATCTTGAA
	PtrMYB175	PtrMYB175FUSF:CTAGACTAGTATGAGTACCAGAGGCCATT	PtrMYB175FUSR:CTAGCTCGAGATTAGAGTTTCCAGCAGAC
	PtrMYB21	PtrMYB21FUSF:CAGTTCTAGAATGAGGAAGCCAGAGGCCTC	PtrMYB21FUSR:AGCTCTCGAGTTGGAAATCAAGGAATGGAAAGG
	PtrMYB74	PtrMYB74FUSF:CAGTTCTAGAATGGGACGACATTCTTGTT	PtrMYB74FUSR:AGCTCTCGAGTCATATCTGGTGGAAGACA
	PtrNAC123	AGGATCCTCCTTTGTGGGATGGGAATAAGATA	ACTCGAGCTCACATCACTGCTTTCTCTGAAGC
transactivation assays in SDX protoplasts with no GFP tag	PtrWBLH1	WBLH1LRF: CACCATGGCTACCTATTACCCAAC	WBLH1LRR: AACCACAAAATCATGTAACC
	PtrWBLH2	WBLH2LRF: CACCACCAAGCTTTCAATACCACAGAA	WBLH2LRR: GCTCTTGTCAGGCACGTTTC
	PtrWBLH3	WBLH3LRF:CACCATGGCTACCTATTATACTAG	WBLH3LRR:GCTACGAAATCATGAAAT
	PtrNAC105	PtrNAC105LRF:CACCCTGCGAGCATCATCCGTACT	PtrNAC105LRR:AGGGTATGAGCTGTTTGTCCTG
	PtrNAC123	PtrNAC123LRF:CACCGCTTACTCTATATGATTTTA	PtrNAC123LRR:TTTCTCTCATCACCATTTTCTC
	PtrNAC125	PtrNAC125LRF:CACCATGGTGCCGCATGGGTTC	PtrNAC125LRR: CTAGTTCGTCCAAGACCAAAGAC
	PtrNAC127	PtrNAC127LRF:CACCAGCCATGACTACTAAGAG	PtrNAC127LRR: CTAGACCAACCCATGATGATC
	PtrHAM3	PtrHAM3LRF:CACCACTGCAAATCTTGGGC	PtrHAM3LRR:TCAGCATCTCCATGCTGAAGC
	PtrMYB59	PtrMYB59LRF:CACCTTATTTTATTTCAGGAATGAT	PtrMYB59LRR:TTACTCAATTATATCTATCCAATA
	PtrMYB88	PtrMYB88LRF:CACCATGGGTCGAGCTCCTTGTTGTG	PtrMYB88LRR:AAGCTCATACCACTCCCGAAT
	PtrMYB90	PtrMYB90LRF:CACCTCAAGTACTATAGAAATATCG	PtrMYB90:TAAACAACAAAGGTAGATGATCTTGACAT
	PtrMYB93	PtrMYB93LRF:CACCATGGGCAGATCTCCTTGCTGTGAGA	PtrMYB93LRR:TCAAGCATCCAAAGGTCTGTAAAA
	PtrMYB161	PtrMYB161LRF:CACCCCTCATCGCCATCTCTTGCT	PtrMYB161LRR:TGCATTTGTGCAGCATCTAGG
	PtrMYB174	PtrMYB174LRF:CACCATGGCTGACTTGGATCACTC	PtrMYB174LRR: CTGACTTGTAGAGTATCTTG
	PtrMYB175	PtrMYB175LRF:CACCATGAGTACCAGAGGCCATTGGA	PtrMYB175LRR:CTAATTAGAGTTTCCAGCAGACAAAA
	PtrMYB21	PtrMYB21LRF:CACCATGAGGAAGCCAGAGGCCTC	PtrMYB21LRR:TTGGAAATCAAGGAATGGAAAGG
	PtrMYB74	PtrMYB74LRF:CACCATGGGACGACATTCTTGTT	PtrMYB74LRR:TCATATCTGGTGGAAGACA
Subcellular [illegible] assays	PtrMYB21	subMYB21F:CAGTTCTAGAATGAGGAAGCCAGAGGCCTC	subMYB21R:AGCTCTCGAGTTGGAAATCAAGGAATGGAAAGG
	PtrMYB74	subMYB74F:CAGTTCTAGAATGGGACGACATTCTTGTT	subMYB74R:AGCTCTCGAGTCATATCTGGTGGAAGACA
qRT-PCR	PtrPAL1	PAL1RTF:CTTGGAAGCAATTACCAAGCTACTT	PAL1RTR:ACTTCTCCGTTGGGACCAGTG
	PtrPAL2	PAL2RTF:CCTAGAAGCCATCACCAAGTTGCTC	PAL2RTR:GTTTCTCCATTGGGTCCCACG
	PtrPAL3	PAL3RTF:CTTGGAAGCTATTACCAGGCTCCTC	PAL3RTR: ACTTCTCCGGTGGGACCAGTG
	PtrPAL4	PAL4RTF:GAGATGCTGGAAGCTATCACCAAAT	PAL4RTR:GGCTCTCCATTGGGTCCAACT
	PtrPAL5	PAL5RTF:GAGATGCTGGAAGCTATCACCAAGC	PAL5RTR:GGCTCTCCATTGGGTCCAACT
	PtrC4H1	C4H1RTF:AGTGCGCCATAGACCATATCCTC	C4H1RTR:ATTGCAGCGACGTTGATGTTCTCA
	PtrC4H2	C4H2RTF:GAAATGTGCAATTGATCATATTTTG	C4H1RTR:ATTGCAGCAACATTGATGTTCTCC
	Ptr4CL3	4CL3RTF:ACTAGCCCATCCAGAGATATCCGA	4CL3RTR:TCATCTTCGGTGGCCTGAGACTTT
	Ptr4CL5	4CL5RTF:ATTCTGTGCGTGCTGCCTATGTTC	4CL5RTR:AATTGCAGCACCAACTCTCAACCC
	PtrHCT1	HCT1RTF:ATCAGCATGTAAGGCACGCGG	HCT1RTR:TGCCAAAGTAACCAGGTGGAAGCGT
	PtrHCT6	HCT6RTF:AGATCAACATGCAAAGCACGTGA	HCT6RTR:GCCAAAGTAACCAGGAGGGAGTTG
	PtrC3H1	C3H1RTF:CTGAGGTTCAAGCTACCGCCT	C3H1RTR:ACATCTGAACATAATAAGCTTGACAT
	PtrCCoAOMT1	CCoAOMT1RTF:CAGTAATTCAGAAAGCTGGTGTTGC	CCoAOMT1RTR:GCATCCACAAAGATGAAATCAAAAC
	PtrCCoAOMT2	CCoAOMT2RTF:CCTTCCAACGCCAGGAAAGAGAGTA	CCoAOMT2RTR:GTGGCCAACTTCTTGATGCCTTCCG
	PtrCCoAOMT3	CCoAOMT3RTF:AATCCTCCAAAGCGCGGCTCTAAA	CCoAOMT3RTR:CTTCTCGTAGCTCCTTGAGCTGTT
	PtrCCR1	CCR1RTF:TGTCCTGTCACAGACGATCCAGACA	CCR1RTR:GGGTCCATGTACACAGTACCAATTGAG
	PtrCAld5H1	CAl5d5H1RTF:AATCCAATATAGGCAAGCCTGTGAACG	CAl5d5H1RTR:ATTTTTGGCCCCAAAAGCTGCTCTA
	PtrCAld5H2	CAl5d5H2RTF:AAGCCAATATAGGCAAGCCTGTGAATC	CAl5d5H2RTR:ATTTTTAGCCCCGAAAGCTGCTCTG
	PtrCOMT1	COMT1RTF:AGCACAATCGTCTCCAAGTACCCT	COMT2RTR:AACATTCTCCACACCAGGGAAAGC
	PtrCAD1	CAD1RTF:GGCAAGCTGATCTTGATGGGTGTT	CAD1RTR:TCCCGGTGATTGACTTTCTCCCAA
	PtrCSE1	CSE1RTF:GATACTGGCTGGCTGTTTCA	CSE1RTR:CATGTAGCAGCGTAAACCGT
	PtrCSE2	CSE2RTF:GGTGACATGGACAAGATTGC	CSE2RTR:AAGGCTGGTAAGCCCTTGTA
	PtCesA4	CesA4RTF:GAGTTAAGGAAGATGGAGAGGTGT	CesA4RTR:TGCACTGAGGACAGGACTGGTTGC
	PtCesA7	CesA7RTF:TCGCCTTTCTCTCAGATACGAACG	CesA7RTR:TTACCCGTAACAAGAGGGGGTTCC
	PtCesA8	CesA8RTF:GTTGGCCTCTGTCTTCTCTCTTGTC	CesA8RTR:CAATCTATAGAAATGCAGGTTTCAC
	PtCesA17	CesA17RTF:CCCCTCTAGTCACGGGCAACACAC	CesA17RTR:AAGGTGCACATTGAAGCACCATCG
	PtCesA18	CesA18RTF:GTTGGCCTCTGTCTTCTCTCTTGTT	CesA18RTR:CAATCAATGGAAATGCAGGTCTCCG
	PtrPRC1-2	PRC1-2RTF:AAGCGCCTCAAAGGTAGTCC	PRC1-2RTR:AGAGCATTGCCTCTGCAACT
	PtrPRC1-3	PRC1-3RTF:AGGTTCCAGAAGATGGTTGG	PRC1-3RTR:TTTGTCCAAGGAACACCTGA
	PtrCesA9-3	PtrCesA9-3RTF:GAATGGAGGAGTGGAGGAAA	PtrCesA9-3RTR:CTCCTTCATCCATCATAGGCA
	PtrIXR1-1	PtrIXR1-1RTF:GAACCGTTTGTTGCTTGCGA	PtrIXR1-1RTR:CACCAAGAATGGCAGGGCTA
	PtrIXR1-2	PtrIXR1-2RTF:GCTTCCAGTGAATCGTGAGA	PtrIXR1-2RTR:GTGACCAGTGGAGGTTCCTT
	PtrIXR1-3	PtrIXR1-3RTF:GCGTTGGCAGTAAGCAATAA	PtrIXR1-3RTR:CCTTCCTTGAGAGAGGTTGC
	PtrIXR1-4	PtrIXR1-4RTF:GAAAGAGCATCTTGCAACCA	PtrIXR1-4RTR:ACGAATTGCTGCATCACCTA
	PtrRSW1-2	PtrRSW1-2RTF:GGAAGCAAATGCGGGTATGG	PtrRSW1-2RTR:TCCCCACAAATCTGGCAAGT
	PtrRSW1-3	PtrRSW1-3RTF:TGCTACACCCGACAATCAAT	PtrRSW1-3RTR:AAGTCCTTTGACGGATCCAC
	PtrMYB21	PtrMYB21RTF:GCATTTTCACCCCAAGAAGA	PtrMYB21RTR:CCGCAATTTGAGACCACCTA
	PtrMYB74	PtrMYB74RTF:TTTTGGGTAACAGGTGGGCT	PtrMYB74RTR:CTTCTCCTCTTTCACCCCCAC
	Ptr18S	Ptr18SRTF:CGAAGACGATCAGATACCGTCCTA	Ptr18SRTR: TTTCTCATAAGGTGCTGGCGGAGT
transcriptional activity assays in yeast	PtrMYB21	GBKTMYB21F:CTAGCATATGATGAGGAAGCCAGAGGCCT	GBKTMYB21R:CAGTCCCGGGTCATTGGAAATCAAGGAAT
	PtrMYB74	GBKTMYB74F:CTAGCATATGATGGGACGACATTCTTGTT	GBKTMYB74R:CAGTCCCGGGTCATATCTGGTGGAAGACA

Table 13. Continued

ChIP-PCR assays for the promoters	Ptr4CL3	Ptr4CL3PF1:GTGGATGTGGAGAGGCACAA	Ptr4CL3PR1:CATTATGGCGTCCATTGCGG
	Ptr4CL3	Ptr4CL3PF2:TAACTTTTGTGTTTAGCCCTTGGC	Ptr4CL3PR2:GCCTTTCACAGACCACCGAT
	Ptr4CL3	Ptr4CL3PF3:TGGTTGCATGGGATCACTCC	Ptr4CL3PF3:TGGTTGCATGGGATCACTCC
	Ptr4CL3	Ptr4CL3PF4:ACACCGGATTCTAACAAAGA	Ptr4CL3PF4:ACACCGGATTCTAACAAAGA
	Ptr4CL5	Ptr4CL5PF1:CCACCCTCTCAACCACGTTT	Ptr4CL5PR1:GGGCTAAAGTTGCAGAGGGA
	Ptr4CL5	Ptr4CL5PF2:AACCTGAGACCACAGAGGGA	Ptr4CL5PR2:AAACGTGGTTGAGAGGGTGG
	Ptr4CL5	Ptr4CL5PF3:TCGAAACCCCTTAACAATTTGAGAT	Ptr4CL5PF3:TCGAAACCCCTTAACAATTTGAGAT
	Ptr4CL5	Ptr4CL5PF4:AGCACCGATATGTGCAATGGA	Ptr4CL5PF4:AGCACCGATATGTGCAATGGA
	PtrANAC73/SND2	PtrANAC73/SND2PF1:ACCCTAAAAGCAAAGAAGACTGC	PtrANAC73/SND2PR1:TTCCCTCTCGTCTCCCTCCAC
	PtrANAC73/SND2	PtrANAC73/SND2PF2:TCAATTAGTCATCCGTAGGCTGC	PtrANAC73/SND2PR2:TGCAGTCTTCTTTGCTTTTAGGG
	PtrANAC73/SND2	PtrANAC73/SND2PF3:TACGGTTGAAACGACCAGCA	PtrANAC73/SND2PF3:TACGGTTGAAACGACCAGCA
	PtrANAC73/SND2	PtrANAC73/SND2PF4:GTATGGGCACACACGAGAAG	PtrANAC73/SND2PF4:GTATGGGCACACACGAGAAG
	PtrBBE-L13	PtrBBE-L13PF1:CAGCAGCATCACCATCAGTAA	PtrBBE-L13PR1:TGACGTCTCAAGGTGTTCTCT
	PtrBBE-L13	PtrBBE-L13PF2:AAGAGATTTGTTGGAGTTTGCAT	PtrBBE-L13PR2:TACTGATGGTGATGCTGCTGG
	PtrBBE-L13	PtrBBE-L13PF3:GCTAGCAGTATCATCCTCACCT	PtrBBE-L13PF3:GCTAGCAGTATCATCCTCACCT
	PtrBBE-L13	PtrBBE-L13PF4:CAGTGTTCACAGTTTACCAACGAA	PtrBBE-L13PF4:CAGTGTTCACAGTTTACCAACGAA
	PtrC3H3	PtrC3H3PF1:TCTTGAGCACGTGGGACATT	PtrC3H3PR1:TTTTCTGAAGGGCCTTGGCA
	PtrC3H3	PtrC3H3PF2:TTGTGGGAGTTTGGGAGTGT	PtrC3H3PR2:AATGTCCCACGTGCTCAAGA
	PtrC3H3	PtrC3H3PF3:CCTCGAGGCCTTGACACTTT	PtrC3H3PF3:CCTCGAGGCCTTGACACTTT
	PtrC3H3	PtrC3H3PF4:ATTTATTCAACATTCTTACACACAC	PtrC3H3PF4:ATTTATTCAACATTCTTACACACAC
	PtrC4H1	PtrC4H1PF1:AGAGCAGACTGCACCCTATACT	PtrC4H1PR1:CTCCAGGAGGAGGAGATCCA
	PtrC4H1	PtrC4H1PF2:GTGACATGAGAAACTAACGTTGC	PtrC4H1PR2:GGGTGCAGTCTGCTCTT
	PtrC4H1	PtrC4H1PF3:TACACCGCAGTCCATTCACAG	PtrC4H1PF3:TACACCGCAGTCCATTCACAG
	PtrC4H1	PtrC4H1PF4:TGAGGGTGAGCGTGAAAGT	PtrC4H1PF4:TGAGGGTGAGCGTGAAAGT
	PtrC4H2	PtrC4H2PF1:AGATGAAGAGAGTCGCGCTTG	PtrC4H2PR1:TGGCAACAAAAGAACCCAACAG
	PtrC4H2	PtrC4H2PF2:GGACTATTGACGAAGTCCCGA	PtrC4H2PR2:GCGCGACTCTCTTCATCTCA
	PtrC4H2	PtrC4H2PF3:ATTTGCACCTCCGCAAAACG	PtrC4H2PF3:ATTTGCACCTCCGCAAAACG
	PtrC4H2	PtrC4H2PF4:TGCTTTTGTCGTGATGTTGTGT	PtrC4H2PF4:TGCTTTTGTCGTGATGTTGTGT
	PtrCAD1	PtrCAD1PF1:TATTGTCGCCACTCACCACC	PtrCAD1PR1:CTCTCTGTTTCAAGGCTACCCA
	PtrCAD1	PtrCAD1PF2:TTTCCACGTGAATCGATTTTT	PtrCAD1PR2:TGGCGACAATATACCCTTGG
	PtrCAD1	PtrCAD1PF3:ACCAAATACTGGAAATTGTTTTCT	PtrCAD1PF3:ACCAAATACTGGAAATTGTTTTCT
	PtrCAD1	PtrCAD1PF4:AAATTTGGTTTGGTTTCCAGG	PtrCAD1PF4:AAATTTGGTTTGGTTTCCAGG
	PtrCAld5H1	PtrCAld5H1PF1:GTTCTTAAATATTGTTCTCCATCCA	PtrCAld5H1PR1:GTAAAGTTTGCAAAGATTGGAG
	PtrCAld5H1	PtrCAld5H1PF2:GATTCAGTGAACCCTTTCGT	PtrCAld5H1PR2:TGGATGGAGAACAATATTTAAGA
	PtrCAld5H1	PtrCAld5H1PF3:AGGTGAGGCATCAAAATCTCTC	PtrCAld5H1PF3:AGGTGAGGCATCAAAATCTCTC
	PtrCAld5H1	PtrCAld5H1PF4:TCTTTCAGTGAACATGCTGCCA	PtrCAld5H1PF4:TCTTTCAGTGAACATGCTGCCA
	PtrCAld5H2	PtrCAld5H2PF1:ACCTCAACATGTGAGCTGGTT	PtrCAld5H2PR1:CTCGCAACTTTCCGATGCTG
	PtrCAld5H2	PtrCAld5H2PF2:AGTGTTACTGAAGGATTAAGTTTG	PtrCAld5H2PR2:GTTGAGGTCAAAATAACCACTACC
	PtrCAld5H2	PtrCAld5H2PF3:TTGAAGGCAAGTTTGTCTGG	PtrCAld5H2PF3:TTGAAGGCAAGTTTGTCTGG
	PtrCAld5H2	PtrCAld5H2PF4:CCACCGAGAATGTGTATGAGG	PtrCAld5H2PF4:CCACCGAGAATGTGTATGAGG
	PtrCCoAOMT1	PtrCCoAOMT1PF1:TCTTGGACGTGGAGTCCCTT	PtrCCoAOMT1PR1:CGAAAATGGTAAAGGGCGGG
	PtrCCoAOMT1	PtrCCoAOMT1PF2:TTTGTGATATCAGCGCATC	PtrCCoAOMT1PR2:TAGCCTTTGTCGGCAAAAAT
	PtrCCoAOMT1	PtrCCoAOMT1PF3:AGGTTTGCTCCCTGTCACC	PtrCCoAOMT1PF3:AGGTTTGCTCCCTGTCACC
	PtrCCoAOMT1	PtrCCoAOMT1PF4:GGTCCAGGCATTGGCATCAA	PtrCCoAOMT1PF4:GGTCCAGGCATTGGCATCAA
	PtrCCoAOMT2	PtrCCoAOMT2PF1:ACATGTAGCCATCCCCAACA	PtrCCoAOMT2PR1:CTCTTTCCTGGCGTTGGAAG
	PtrCCoAOMT2	PtrCCoAOMT2PF2:GTTTTGCTATGCCCACACGA	PtrCCoAOMT2PR2:GGGGATGGCTACATGTGCTG
	PtrCCoAOMT2	PtrCCoAOMT2PF3:CGTTTCCAAACACGATTTAATACA	PtrCCoAOMT2PF3:CGTTTCCAAACACGATTTAATACA
	PtrCCoAOMT2	PtrCCoAOMT2PF4:GGGCTACTGCATAAAGCCCAT	PtrCCoAOMT2PF4:GGGCTACTGCATAAAGCCCAT
	PtrCCoAOMT3	PtrCCoAOMT3PF1:ACGTTTGGAGGGCGTGTTAT	PtrCCoAOMT3PR1:AGCCTCGCTTTGGAGGATTC
	PtrCCoAOMT3	PtrCCoAOMT3PF2:TTGTGCTTTGTCTGGCGATG	PtrCCoAOMT3PR2:ACGCCCTCCAAACGTACTAT
	PtrCCoAOMT3	PtrCCoAOMT3PF3:TGCCGTTGTCAGTCAATCAC	PtrCCoAOMT3PF3:TGCCGTTGTCAGTCAATCAC
	PtrCCoAOMT3	PtrCCoAOMT3PF4:CAATTCTGCCAGTGTTCCGC	PtrCCoAOMT3PF4:CAATTCTGCCAGTGTTCCGC
	PtrCCR2	PtrCCR2PF1:GGTAGACGAGAAGAGAGGCCA	PtrCCR2PR1:GCCTTGGCCTGAAAGTGATG
	PtrCCR2	PtrCCR2PF2:ACAACATGCATTCTCTTTCACA	PtrCCR2PR2:CCTCTCTTCTCGTCTACCA
	PtrCCR2	PtrCCR2PF3:AGTGAAGCTCACCACTGACA	PtrCCR2PF3:AGTGAAGCTCACCACTGACA
	PtrCCR2	PtrCCR2PF4:TGTGGAAGGTTTTAGAATGTGATG	PtrCCR2PF4:TGTGGAAGGTTTTAGAATGTGATG
	PtrCesA17	PtrCesA17PF1:CTGAAAAAGGCTTGGAGAAGCA	PtrCesA17PR1:TCCAGCACTAGCTTCCATGC
	PtrCesA17	PtrCesA17PF2:TGGATTTACGCTCATTTGTTGGG	PtrCesA17PR2:AGCCTTTTTCAGTACCTCTCACA
	PtrCesA17	PtrCesA17PF3:GCAGACACGACCTGTTTTAGT	PtrCesA17PF3:GCAGACACGACCTGTTTTAGT
	PtrCesA17	PtrCesA17PF4:CTCTGTCTGGATGGAGAAGCTC	PtrCesA17PF4:CTCTGTCTGGATGGAGAAGCTC
	PtrCesA18	PtrCesA18PF1:ATGGGCTCAGCGTCGTAAAA	PtrCesA18PR1:AGGGTCTTCCTCTGCTTCCT
	PtrCesA18	PtrCesA18PF2:GGACTACTCTGTGGGTGGCT	PtrCesA18PR2:TTTACGACGCTGAGCCCATA
	PtrCesA18	PtrCesA18PF3:AAGAATTCTGAAACAAGAGCCTG	PtrCesA18PF3:AAGAATTCTGAAACAAGAGCCTG
	PtrCesA18	PtrCesA18PF4:AGGAGAACCTTTAGCTAGGA	PtrCesA18PF4:AGGAGAACCTTTAGCTAGGA
	PtrCesA4	PtrCesA4PF1:TTTTGCAGGTGATAAGTTGATT	PtrCesA4PR1:TGTAAGCAAAGCGTGCAAAT
	PtrCesA4	PtrCesA4PF2:GAAGGTGCATGATGTTTAAGCC	PtrCesA4PR2:AGATAAATCAACTTATCACCTGC
	PtrCesA4	PtrCesA4PF3:CGCTGACGAAAGCAGAACCT	PtrCesA4PF3:CGCTGACGAAAGCAGAACCT
	PtrCesA4	PtrCesA4PF4:TCAGTACACACAACCCCTGC	PtrCesA4PF4:TCAGTACACACAACCCCTGC
	PtrCesA7	PtrCesA7PF1:GAATCCATGCCCCTAGCTCTT	PtrCesA7PR1:TGTGGCATGTTAAGGGTGGT
	PtrCesA7	PtrCesA7PF2:GACATCGGAATCAACTCAACTG	PtrCesA7PR2:GCTAGGGGCATGGATTCGG
	PtrCesA7	PtrCesA7PF3:GATAGTAGGGCCTCAGCTAAT	PtrCesA7PF3:GATAGTAGGGCCTCAGCTAAT
	PtrCesA7	PtrCesA7PF4:GTAGGCTTAACCAAGCCGGG	PtrCesA7PF4:GTAGGCTTAACCAAGCCGGG
	PtrCesA8	PtrCesA8PF1:GATGCTGCCAGTTTTCGGTC	PtrCesA8PR1:ATGGCATAAAGGAGCCCCAG
	PtrCesA8	PtrCesA8PF2:ACTTCCCCCATCCCCAGAA	PtrCesA8PR2:CAAACAGTGTACTGGCGTCTCC
	PtrCesA8	PtrCesA8PF3:CTCCTGGAGAGCATGCCTTA	PtrCesA8PF3:CTCCTGGAGAGCATGCCTTA
	PtrCesA8	PtrCesA8PF4:CAGCTGCAGGTACAGGAACTC	PtrCesA8PF4:CAGCTGCAGGTACAGGAACTC
	PtrCESA9-3	PtrCESA9-3PF1:CAAGCAAAGTGGCGTCACAG	PtrCESA9-3PR1:TGAGTCTCCCTTTGGTCTCCA
	PtrCESA9-3	PtrCESA9-3PF2:CAGCACAAACCAGAGGCGTA	PtrCESA9-3PR2:CGCCACTTTGCTTGCCAAAA
	PtrCESA9-3	PtrCESA9-3PF3:CGTGACAGCTTTCCTCCTCC	PtrCESA9-3PF3:CGTGACAGCTTTCCTCCTCC
	PtrCESA9-3	PtrCESA9-3PF4:AGCAACATTTCTCTTCTTTCTCAA	PtrCESA9-3PF4:AGCAACATTTCTCTTCTTTCTCAA
	PtrCOMT2	PtrCOMT2PF1:TCGGGTGAATGTATCATTATGTGA	PtrCOMT2PR1:AGTTTCACCTGTCGAACCCA
	PtrCOMT2	PtrCOMT2PF2:TGTTGTGCTTCTTCTTTTTCTCG	PtrCOMT2PR2:TCACATAATGATACATTCACCCGA
	PtrCOMT2	PtrCOMT2PF3:CACAATCATGTTTAATAACCCTTCA	PtrCOMT2PF3:CACAATCATGTTTAATAACCCTTCA
	PtrCOMT2	PtrCOMT2PF4:CTCCTGGACTTGCAGGATGT	PtrCOMT2PF4:CTCCTGGACTTGCAGGATGT
	PtrCSE1	PtrCSE1PF1:TGCGGCACTTAAACAACGAAC	PtrCSE1PR1:GTACTCCTCCTCCGGCATGT

Table 13. Continued

ChIP-PCR assays for the promoters	PtrCSE1	PtrCSE1PF2:ACGCAAACTCTAGTTGCTATG	PtrCSE1PR2:TCGTTGTTTAAGTGCCGCAA
	PtrCSE1	PtrCSE1PF3:TCACACTCGGTCAAACTCGT	PtrCSE1PF3:TCACACTCGGTCAAACTCGT
	PtrCSE1	PtrCSE1PF4:TGTCCAAATATCCCACCAAGC	PtrCSE1PF4:TGTCCAAATATCCCACCAAGC
	PtrCSE2	PtrCSE2PF1:ACCCCCAACGAGTGAATGTTT	PtrCSE2PR1:GAAGAGCTTCCCATTTGGCG
	PtrCSE2	PtrCSE2PF2:TGTGGTGGAGGAGTTGATGG	PtrCSE2PR2:CGTTGGGGGTTGGAAGTAGG
	PtrCSE2	PtrCSE2PF3:CACAATGATTGCTTGTGTATC	PtrCSE2PF3:CACAATGATTGCTTGTGTATC
	PtrCSE2	PtrCSE2PF4:TGATAGTGATTGCGGTTCAAA	PtrCSE2PF4:TGATAGTGATTGCGGTTCAAA
	PtrFD2	PtrFD2PF1:ACTCGTAAGCTTTGATTTTTGGGT	PtrFD2PR1:TGGCGACAACATTTGGAAGAGT
	PtrFD2	PtrFD2PF2:CATCCCTGGTTTAAAAGGCCATAC	PtrFD2PR2:CACGTCTTAAGGGAAACCATAAAAA
	PtrFD2	PtrFD2PF3:TCCACTCATCTTCAGCTTTGT	PtrFD2PF3:TCCACTCATCTTCAGCTTTGT
	PtrFD2	PtrFD2PF4:ACCATTTCGCCTTAGTCCGA	PtrFD2PF4:ACCATTTCGCCTTAGTCCGA
	PtrFLA17	PtrFLA17PF1:GAAGGCTTGCCACGAACATC	PtrFLA17PR1:GCTCTGAAAGGTGGAGGGTC
	PtrFLA17	PtrFLA17PF2:CTTGACTACTGGGACCTGCC	PtrFLA17PR2:GATGTTCGTGGCAAGCCTTC
	PtrFLA17	PtrFLA17PF3:CGCAGATGCTTGCATTGAGT	PtrFLA17PF3:CGCAGATGCTTGCATTGAGT
	PtrFLA17	PtrFLA17PF4:GTCCAAATCGTGGGCTGTTG	PtrFLA17PF4:GTCCAAATCGTGGGCTGTTG
	PtrFLA18	PtrFLA18PF1:CATTTATATCCATTTTTAAGCCTCC	PtrFLA18PR1:TGTTGCTTCATCTTTAAGTTTC
	PtrFLA18	PtrFLA18PF2:CGAAAAGAACGTTCAACC	PtrFLA18PR2:TGCAACAAAGTCCTTGGAGG
	PtrFLA18	PtrFLA18PF3:GGGTCTATTCCATAACCCTAT	PtrFLA18PF3:GGGTCTATTCCATAACCCTAT
	PtrFLA18	PtrFLA18PF4:ATCTCAAGGCTCAACTCATGACA	PtrFLA18PF4:ATCTCAAGGCTCAACTCATGACA
	PtrFLA32	PtrFLA32PF1:TGCTCAAATGTTCTGCCAGTG	PtrFLA32PR1:CTGGTGACTGGGCAAAGGTA
	PtrFLA32	PtrFLA32PF2:TGGTCAGCAGGTCTGGAAGA	PtrFLA32PR2:TCACTGGCAGAACATTTGAGC
	PtrFLA32	PtrFLA32PF3:AAACCGCGGTATGGATGGTT	PtrFLA32PF3:AAACCGCGGTATGGATGGTT
	PtrFLA32	PtrFLA32PF4:CGCATTTGCTCCCCATAGGT	PtrFLA32PF4:CGCATTTGCTCCCCATAGGT
	PtrFRA1	PtrFRA1PF1:AAGTCTAAATACTGAATTTCCTGACG	PtrFRA1PR1:TACAAAGGTTATTATGTGTGTGAAA
	PtrFRA1	PtrFRA1PF2:ACGGGTCCATATGCAAAGCA	PtrFRA1PR2:TAGAGTCTACTCCGAGTCGGTTTT
	PtrFRA1	PtrFRA1PF3:CGATTTATCAAATTAATATATGAG	PtrFRA1PF3:CGATTTATCAAATTAATATATGAG
	PtrFRA1	PtrFRA1PF4:TTGTGACCCGACCCAAGAAAC	PtrFRA1PF4:TTGTGACCCGACCCAAGAAAC
	PtrHAM3/GRAS22	PtrHAM3/GRAS22PF1:GCCAAGCTGACACGAAATCT	PtrHAM3/GRAS22PR1:GAAGCCTGAGGAGTTCGGAG
	PtrHAM3/GRAS22	PtrHAM3/GRAS22PF2:GCCAAGCTGACACGAAATCT	PtrHAM3/GRAS22PR2:TGGATGCGTGCATCATAAAA
	PtrHAM3/GRAS22	PtrHAM3/GRAS22PF3:TGGACTCCAACGGGGTAAAT	PtrHAM3/GRAS22PF3:TGGACTCCAACGGGGTAAAT
	PtrHAM3/GRAS22	PtrHAM3/GRAS22PF4:TGCCCTAGATCATGAATAAGACCAC	PtrHAM3/GRAS22PF4:TGCCCTAGATCATGAATAAGACCAC
	PtrHCT1	PtrHCT1PF1:TCACCAAGTGCTACCTGCAT	PtrHCT1PR1:ACCTGTGAGCCTAGAGCAGA
	PtrHCT1	PtrHCT1PF2:TGTTTAGGACTGCGGCCAAC	PtrHCT1PR2:TGCAGGTAGCACTTGGTGAT
	PtrHCT1	PtrHCT1PF3:TCGGTTCAGCTTTGAGTCGG	PtrHCT1PF3:TCGGTTCAGCTTTGAGTCGG
	PtrHCT1	PtrHCT1PF4:GCTACGTGAGCGGAAAGACT	PtrHCT1PF4:GCTACGTGAGCGGAAAGACT
	PtrHCT6	PtrHCT6PF1:AGAGTTTCACGGGCCTTGG	PtrHCT6PR1:TCTTTCTCCGCCCTAATGCTC
	PtrHCT6	PtrHCT6PF2:TGGCATCGCTGTTGGTTGAC	PtrHCT6PR2:ACTCTTCCCAAAGACACAAGGA
	PtrHCT6	PtrHCT6PF3:TCTTTCTCCCAGCACTCAAAACA	PtrHCT6PF3:TCTTTCTCCCAGCACTCAAAACA
	PtrHCT6	PtrHCT6PF4:TGAGCCATTGTGGTCTTTCTGA	PtrHCT6PF4:TGAGCCATTGTGGTCTTTCTGA
	PtrIRX14-L	PtrIRX14-LPF1:TCGTGTAAATGAACCATGTTGT	PtrIRX14-LPR1:TTGAAGCTTGCTAAGGTGTGC
	PtrIRX14-L	PtrIRX14-LPF2:GGCCCATGTTTAGGCTTGC	PtrIRX14-LPR2:CACAACATGGTTCATTTACACG
	PtrIRX14-L	PtrIRX14-LPF3:TCCCTAGAGTTAGGCGGTGTT	PtrIRX14-LPF3:TCCCTAGAGTTAGGCGGTGTT
	PtrIRX14-L	PtrIRX14-LPF4:AAGCTATCCGATCCGCGAAG	PtrIRX14-LPF4:AAGCTATCCGATCCGCGAAG
	PtrIRX9	PtrIRX9PF1:TGTGTCACCAGCTAGGTCTT	PtrIRX9PR1:TGACCACTGAGTTTTGGGGA
	PtrIRX9	PtrIRX9PF2:ACACCGGTCACTTTCTAGTTTC	PtrIRX9PR2:GACCTAGCTGGTGACACATGA
	PtrIRX9	PtrIRX9PF3:TCACCTCACCTCACCTCTTCT	PtrIRX9PF3:TCACCTCACCTCACCTCTTCT
	PtrIRX9	PtrIRX9PF4:GCAATGAGTGTGTCTGCTTCAG	PtrIRX9PF4:GCAATGAGTGTGTCTGCTTCAG
	PtrIXR1-1	PtrIXR1-1PF1:AGGGGATGGAAGAAAGCGTG	PtrIXR1-1PR1:CCCGGTTTCACCTTCTGATTC
	PtrIXR1-1	PtrIXR1-1PF2:AGCAGCAGCTGTAGTCGAAA	PtrIXR1-1PR2:CACGCTTTCTTCCATCCCCT
	PtrIXR1-1	PtrIXR1-1PF3:CGGCCTGTCCAGTGTTTTCA	PtrIXR1-1PF3:CGGCCTGTCCAGTGTTTTCA
	PtrIXR1-1	PtrIXR1-1PF4:AGAGGGGGCAAAAATGGAAA	PtrIXR1-1PF4:AGAGGGGGCAAAAATGGAAA
	PtrIXR1-2	PtrIXR1-2PF1:CTCTTGGGCGTAGTCCGTTC	PtrIXR1-2PR1:ACTGCCCCTTCAAGCAATCA
	PtrIXR1-2	PtrIXR1-2PF2:CACATGCTACCCAAACACAA	PtrIXR1-2PR2:CGGACTACGCCCAAGAGTATAA
	PtrIXR1-2	PtrIXR1-2PF3:TGGTTATAGTAAGCTAATCCGAGC	PtrIXR1-2PF3:TGGTTATAGTAAGCTAATCCGAGC
	PtrIXR1-2	PtrIXR1-2PF4:ACAAGGTAAGCAAAAGTTTCCCAG	PtrIXR1-2PF4:ACAAGGTAAGCAAAAGTTTCCCAG
	PtrIXR1-3	PtrIXR1-3PF1:CGAACCAAGCGTGTCGTTTT	PtrIXR1-3PR1:AGCTGCTCTCTTTATCGCAGA
	PtrIXR1-3	PtrIXR1-3PF2:ACCGTCTCCCACTCATCTCC	PtrIXR1-3PR2:ACGCTTGGTTCGATCTCCTG
	PtrIXR1-3	PtrIXR1-3PF3:TGCATACCGTTCACAGACCC	PtrIXR1-3PF3:TGCATACCGTTCACAGACCC
	PtrIXR1-3	PtrIXR1-3PF4:TATCGTGGCATGGTAGGTGC	PtrIXR1-3PF4:TATCGTGGCATGGTAGGTGC
	PtrIXR1-4	PtrIXR1-4PF1:GCATTGCCGCTTTCAGTACC	PtrIXR1-4PR1:TGCTCCCGCAAAACACAAAG
	PtrIXR1-4	PtrIXR1-4PF2:CCAACCTTGCACCTCAACAAG	PtrIXR1-4PR2:GCAATGCACAACACCCTTCAT
	PtrIXR1-4	PtrIXR1-4PF3:CAATGAGGCTGACCCCTCC	PtrIXR1-4PF3:CAATGAGGCTGACCCCTCC
	PtrIXR1-4	PtrIXR1-4PF4:AGTAAATGGTCGGGTCGAGA	PtrIXR1-4PF4:AGTAAATGGTCGGGTCGAGA
	PtrLAC04	PtrLAC04PF1:TCGTGGAGCCTTTCTGCTAT	PtrLAC04PR1:TGTTGGAGCACTAAGGGGTG
	PtrLAC04	LAC04PF2:GCATTGGATGTCCAAATGGTCCTAGCAGAAAGGCTCC	PtrLAC04PR2:TAGCAGAAAGGCTCCACGAA
	PtrLAC04	PtrLAC04PF3:GGAGGCTCGCTCGGGT	PtrLAC04PF3:GGAGGCTCGCTCGGGT
	PtrLAC04	PtrLAC04PF4:TCTATCGAGTTGCCCGCTTAC	PtrLAC04PF4:TCTATCGAGTTGCCCGCTTAC
	PtrLAC14	PtrLAC14PF1:ATTGGGCTTCTTGCCCCTTT	PtrLAC14PR1:GCCAGCAAGCGTACTCCATA
	PtrLAC14	PtrLAC14PF2:CCAGATGCATGTGTTCGCTG	PtrLAC14PR2:AAAGGGGCAAGAAGCCCAAT
	PtrLAC14	PtrLAC14PF3:GTTTGAAACTTGCACAGACCCA	PtrLAC14PF3:GTTTGAAACTTGCACAGACCCA
	PtrLAC14	PtrLAC14PF4:TTTAGGATTAATGGCTTCACCAGC	PtrLAC14PF4:TTTAGGATTAATGGCTTCACCAGC
	PtrLAC15	PtrLAC15PF1:GGCCTACCAAACTTAACCCGT	PtrLAC15PR1:TGGCAATCTCTCTGTTGCTGT
	PtrLAC15	PtrLAC15PF2:CCCACAACCTCCACACCTAC	PtrLAC15PR2:TAGGACCTGGTGCTCTTCGT
	PtrLAC15	PtrLAC15PF3:GTGCAACAGTTCAAACTTGAACAAC	PtrLAC15PF3:GTGCAACAGTTCAAACTTGAACAAC
	PtrLAC15	PtrLAC15PF4:GGGTTCCTTTTGGTCTCAAT	PtrLAC15PF4:GGGTTCCTTTTGGTCTCAAT
	PtrLAC18	PtrLAC18PF1:TAACGAGTTTGACCTGCGTG	PtrLAC18PR1:TCTGTTTAAGACACCAAGCCT
	PtrLAC18	PtrLAC18PF2:GCTGGTGGAACTGCATCGT	PtrLAC18PR2:GCACGCAGGTCAAACTCG
	PtrLAC18	PtrLAC18PF3:TCGAAACACAACCCGTGATGA	PtrLAC18PF3:TCGAAACACAACCCGTGATGA
	PtrLAC18	PtrLAC18PF4:AGAAAGCAGGGTCGACCAAC	PtrLAC18PF4:AGAAAGCAGGGTCGACCAAC
	PtrLAC19	PtrLAC19PF1:ACGTCGTCCTAGCAATCACC	PtrLAC19PR1:ACCAGTTTAGGTTAAATGCCCG
	PtrLAC19	PtrLAC19PF2:TGGCCACGACTCATGTGTTT	PtrLAC19PR2:GGGTGATTGCTAGGACGACG
	PtrLAC19	PtrLAC19PF3:TATGGCCCGGGCATTTAACC	PtrLAC19PF3:TATGGCCCGGGCATTTAACC
	PtrLAC19	PtrLAC19PF4:CCACCAACAACAAGAACCACC	PtrLAC19PF4:CCACCAACAACAAGAACCACC
	PtrLAC21	PtrLAC21PF1:TCACTGTAATGACGCGAGGC	PtrLAC21PR1:TTGGTGCACAAAGCAATGCC
	PtrLAC21	PtrLAC21PF2:TAGCGGTCATGGTAGGGACT	PtrLAC21PR2:TGTTCTAATGAGCCTCGCGT
	PtrLAC21	PtrLAC21PF3:ACCTTGAAGCCTCCCGACTA	PtrLAC21PF3:ACCTTGAAGCCTCCCGACTA
	PtrLAC21	PtrLAC21PF4:CGAGTGCATTACTTGTTGAGACA	PtrLAC21PF4:CGAGTGCATTTACTTGTTGAGACA
	PtrLAC26	PtrLAC26PF1:CAACTTGTGTGCGGACCTTG	PtrLAC26PR1:GCTAGCCTGCCTTGATGTCT

Table 13. Continued

ChIP-PCR assays for the promoters	PtrLAC26	PtrLAC26PF2:ACCGGGCCGAGTTAAAAACA	PtrLAC26PR2:AAGGTCCGCACACAAGTTGA
	PtrLAC26	PtrLAC26PF3:GCGTATAATTGGGAATACAACACGA	PtrLAC26PF3:GCGTATAATTGGGAATACAACACGA
	PtrLAC26	PtrLAC26PF4:TAAGGAGGCGCCTGTGTTTT	PtrLAC26PF4:TAAGGAGGCGCCTGTGTTTT
	PtrLAC41	PtrLAC41PF1:GCCTGATGCTGAGTTGACCA	PtrLAC41PR1:CCTTTCAATCCTCTCTCTCGCT
	PtrLAC41	PtrLAC41PF2:CAGTATGGGAGACCCTGCTTG	PtrLAC41PR2:TGGTCAACTCAGCATCAGGC
	PtrLAC41	PtrLAC41PF3:CACTCTCAAACACACTTAGAAC	PtrLAC41PF3:CACTCTCAAACACACTTAGAAC
	PtrLAC41	PtrLAC41PF4:TCGGTTATCATTCATGTCAAAAAGT	PtrLAC41PF4:TCGGTTATCATTCATGTCAAAAAGT
	PtrLAC49	PtrLAC49PF1:GGCCTACCCAACTTGTAACCC	PtrLAC49PR1:TGCTGTTGGTTTCCTTCTTGC
	PtrLAC49	PtrLAC49PF2:CGATAAAGCCAAACACGTGGG	PtrLAC49PR2:TGGGTAGGCCGAACTCTCTT
	PtrLAC49	PtrLAC49PF3:TTTCCTACACTATCGTTGTGGGTT	PtrLAC49PF3:TTTCCTACACTATCGTTGTGGGTT
	PtrLAC49	PtrLAC49PF4:CAAACCTAGGCTCAAGCCACA	PtrLAC49PF4:CAAACCTAGGCTCAAGCCACA
	PtrMYB059	PtrMYB059PF1:GGCTTGTTGTCCCGTATGC	PtrMYB059PR1:AAGTGAAGCAAGGCAAACCT
	PtrMYB059	PtrMYB059PF2:CCTGTAGAGAGAGCAGCTATT	PtrMYB059PR2:GGGACAACAAGCCAAAGAACT
	PtrMYB059	PtrMYB059PF3:TGAGTTGTGAACCAATTGGAGAGA	PtrMYB059PF3:TGAGTTGTGAACCAATTGGAGAGA
	PtrMYB059	PtrMYB059PF4:AACAAGGCTCGCCGAAACTG	PtrMYB059PF4:AACAAGGCTCGCCGAAACTG
	PtrMYB088	PtrMYB088PF1:GCGACACTCGAAACAGGTTCA	PtrMYB088PR1:GTTGGGGAAGATTGGGAAAGG
	PtrMYB088	PtrMYB088PF2:AAGGCGAAATGGTGATTAGCAG	PtrMYB088PR2:TCGAGTGTCGCGATTGACTTA
	PtrMYB088	PtrMYB088PF3:AGCACGATTTATTCCGCGAT	PtrMYB088PF3:AGCACGATTTATTCCGCGAT
	PtrMYB088	PtrMYB088PF4:AGCTCGACCTTTCAATCTGATG	PtrMYB088PF4:AGCTCGACCTTTCAATCTGATG
	PtrMYB093	PtrMYB093PF1:AAGTAATGAAGGCGGGGGTA	PtrMYB093PR1:TGGGTGTGTGTGCAAATCAA
	PtrMYB093	PtrMYB093PF2:GTGTGGCCCCTTTTCGTTC	PtrMYB093PR2:AACCTAACCATACCCCCGCC
	PtrMYB093	PtrMYB093PF3:CTCGACGTATAACTTGGGTTTTGA	PtrMYB093PF3:CTCGACGTATAACTTGGGTTTTGA
	PtrMYB093	PtrMYB093PF4:ATTGAGACTCGAACACAACC	PtrMYB093PF4:ATTGAGACTCGAACACAACC
	PtrMYB161	PtrMYB161PF1:ACTTGCAAAGATGTTGAAAGGA	PtrMYB161PR1:CCTCTGCTAGACATCTGATGATGA
	PtrMYB161	PtrMYB161PF2:AAAATCAAGAAGGCCAACGC	PtrMYB161PR2:TGTTTGTGTGTTGTGTTCGT
	PtrMYB161	PtrMYB161PF3:TGACCGGGTCGGGAATTAAC	PtrMYB161PF3:TGACCGGGTCGGGAATTAAC
	PtrMYB161	PtrMYB161PF4:CGCAATTGACATGACATGAGGA	PtrMYB161PF4:CGCAATTGACATGACATGAGGA
	PtrMYB168	PtrMYB168PF1:CCAAATCCAGCCCCTGTCTG	PtrMYB168PR1:ATCTTTCTGATCGTCCTGGGT
	PtrMYB168	PtrMYB168PF2:ACTTGGAATGAAATTAAGTGAACG	PtrMYB168PR2:GTTACAGACAGGGGCTGGAT
	PtrMYB168	PtrMYB168PF3:GCATCAGCTGACACGTAATCC	PtrMYB168PF3:GCATCAGCTGACACGTAATCC
	PtrMYB168	PtrMYB168PF4:GCAACTTAATTAATTTGTTA	PtrMYB168PF4:GCAACTTAATTAATTTGTTA
	PtrMYB174	PtrMYB174PF1:GCAGAGTGACACCTAGTGGAAA	PtrMYB174PR1:TGGAAGCTGACTGAGTGTGA
	PtrMYB174	PtrMYB174PF2:CTTAGACGGTTGGTGTTGGGTA	PtrMYB174PR2:GAACTTGTTGGAGTCTACTGGG
	PtrMYB174	PtrMYB174PF3:TTCCAGAACCATGAACCCTCG	PtrMYB174PF3:TTCCAGAACCATGAACCCTCG
	PtrMYB174	PtrMYB174PF4:ACTGTTCACATGAACAGTG	PtrMYB174PF4:ACTGTTCACATGAACAGTG
	PtrMYB175	PtrMYB175PF1:GCCATGGCTAGTCAATAAGACC	PtrMYB175PR1:ATGCTCAAAGCTAGGGTTCT
	PtrMYB175	PtrMYB175PF2:CCACGTGCGCTTCTGAATTT	PtrMYB175PR2:GACTAGCCATGGCATTCTCTGA
	PtrMYB175	PtrMYB175PF3:AGTTGGGTGGGTCAACCTAT	PtrMYB175PF3:AGTTGGGTGGGTCAACCTAT
	PtrMYB175	PtrMYB175PF4:ACTCGGGTTGACTTGAGTTAC	PtrMYB175PF4:ACTCGGGTTGACTTGAGTTAC
	PtrMYB90	PtrMYB90PF1:TCACCACCCTCTCTCACACA	PtrMYB90PR1:ATCCCAAGAACCAAAAACACGA
	PtrMYB90	PtrMYB90PF2:TCTCCACATGCACCTTTCTCA	PtrMYB90PR2:GGTGGTGAGGTTGCTTGGT
	PtrMYB90	PtrMYB90PF3:CAATTAACCATTGTACACGCA	PtrMYB90PF3:CAATTAACCATTGTACACGCA
	PtrMYB90	PtrMYB90PF4:TCAGGATAACCTCATAGAAAGGA	PtrMYB90PF4:TCAGGATAACCTCATAGAAAGGA
	PtrNAC105	PtrNAC105PF1:TGCAAGAACCGACGAGTGTT	PtrNAC105PR1:AGTACGGATGATGCTCGCAG
	PtrNAC105	PtrNAC105PF2:GGAGGTTCATTACTTTCTGCCT	PtrNAC105PR2:CGTCGGTTCTTGCATCATCTC
	PtrNAC105	PtrNAC105PF3:TCACGACAATTCACGTTAGC	PtrNAC105PF3:TCACGACAATTCACGTTAGC
	PtrNAC105	PtrNAC105PF4:TCGAAGACAAACGGGGAAGT	PtrNAC105PF4:TCGAAGACAAACGGGGAAGT
	PtrNAC123	PtrNAC123PF1:ACGGCTAGCTCACTGTTGTT	PtrNAC123PR1:TGACCACTTGTTGAATCGTGT
	PtrNAC123	PtrNAC123PF2:CTTGCCTTTTGGATGGGAGTA	PtrNAC123PR2:TGAGCCAACAGGCATGAAAAC
	PtrNAC123	PtrNAC123PF3:ATGCTGAAAAGCTTGACGCC	PtrNAC123PF3:ATGCTGAAAAGCTTGACGCC
	PtrNAC123	PtrNAC123PF4:ACCTCCTCAAGTGAAAGCCA	PtrNAC123PF4:ACCTCCTCAAGTGAAAGCCA
	PtrNAC125	PtrNAC125PF1:GGCATGCTTTGTCCGTATGTA	PtrNAC125PR1:GGCCTACAATGCTGCTTCCT
	PtrNAC125	PtrNAC125PF2:ACGGGGTTACCAATGACACA	PtrNAC125PR2:CAGACTCACAAACAAAAATAATCCA
	PtrNAC125	PtrNAC125PF3:TCATCCGGTGGACTCGATAG	PtrNAC125PF3:TCATCCGGTGGACTCGATAG
	PtrNAC125	PtrNAC125PF4:CGCACATCTCAGAGGCTGTA	PtrNAC125PF4:CGCACATCTCAGAGGCTGTA
	PtrNAC127	PtrNAC127PF1:AAATCCCACGGCCACAGTTT	PtrNAC127PR1:GGCTCGTTTTCGATCACACAG
	PtrNAC127	PtrNAC127PF2:ACACGCGAAAGATTGAGTTTCC	PtrNAC127PR2:AAACTGTGGCCGTGGGATT
	PtrNAC127	PtrNAC127PF3:CTGTGTGCAGCATTCATGGG	PtrNAC127PF3:CTGTGTGCAGCATTCATGGG
	PtrNAC127	PtrNAC127PF4:ACAAAACAAGGTTCAAATCCTACT	PtrNAC127PF4:ACAAAACAAGGTTCAAATCCTACT
	PtrNAC144	PtrNAC144PF1:CGAAAGCTCCTTTTACCATTTGC	PtrNAC144PR1:TCAGCAACCTATAAGACTATGCG
	PtrNAC144	PtrNAC144PF2:TTGCTCCAACCAACCCGTTA	PtrNAC144PR2:ATCATATGCTGGTGGTGGGG
	PtrNAC144	PtrNAC144PF3:AGCTAGCACTAGGTCGGCT	PtrNAC144PF3:AGCTAGCACTAGGTCGGCT
	PtrNAC144	PtrNAC144PF4:CACTGGAAGCTTACATGATCGTT	PtrNAC144PF4:CACTGGAAGCTTACATGATCGTT
	PtrPAL1	PtrPAL1PF1:TCACCAACCACAACCTCACC	PtrPAL1PR1:TGGGTACACAAACTCTCCGA
	PtrPAL1	PtrPAL1PF2:GCTGAACATCCCACGTCAT	PtrPAL1PR2:GAAATGGGAAATTTCGTCTTGCCC
	PtrPAL1	PtrPAL1PF3:CTGGCAATCGGAGCCTAATATG	PtrPAL1PF3:CTGGCAATCGGAGCCTAATATG
	PtrPAL1	PtrPAL1PF4:TTCATTTTGTTTGGAGAGCCT	PtrPAL1PF4:TTCATTTTGTTTGGAGAGCCT
	PtrPAL2	PtrPAL2PF1:AGTGCTTATGTGCCCCCTTC	PtrPAL2PR1:GTTCAAGGGGTCATTGGGGT
	PtrPAL2	PtrPAL2PF2:TCAGACCAACGTTTAACCCAT	PtrPAL2PR2:AGTGCTTATGTGCCCCCTTC
	PtrPAL2	PtrPAL2PF3:AAGTGGGTTAACACTCTGAAAT	PtrPAL2PF3:AAGTGGGTTAACACTCTGAAAT
	PtrPAL2	PtrPAL2PF4:AATCTGAAACCCGGTTCTGG	PtrPAL2PF4:AATCTGAAACCCGGTTCTGG
	PtrPAL3	PtrPAL3PF1:TTTGCTTTACAGCCCCACGA	PtrPAL3PR1:GCCATTCTTGGTGACCGTCT
	PtrPAL3	PtrPAL3PF2:CATTGCTTTGCTTAAGTAGCCT	PtrPAL3PR2:TTAGTCTCGTGGGGCTGTAA
	PtrPAL3	PtrPAL3PF3:ATAAGTTGTGGGCGTCCGT	PtrPAL3PF3:ATAAGTTGTGGGCGTCCGT
	PtrPAL3	PtrPAL3PF4:ACAAAAACGCACAGGATTGT	PtrPAL3PF4:ACAAAAACGCACAGGATTGT
	PtrPAL4	PtrPAL4PF1:GAGCCATGACGTAGTGCTATCT	PtrPAL4PR1:TGAACCATTGCCATTGCGTG
	PtrPAL4	PtrPAL4PF2:TGGATTTACCAAGCACTCGCA	PtrPAL4PR2:AGCACTACGTCATGGCTCTA
	PtrPAL4	PtrPAL4PF3:AGAAACAGTGGTGTGCAGTG	PtrPAL4PF3:AGAAACAGTGGTGTGCAGTG
	PtrPAL4	PtrPAL4PF4:AAACTCCATTGAATCCAACAGC	PtrPAL4PF4:AAACTCCATTGAATCCAACAGC
	PtrPAL5	PtrPAL5PF1:GCCGCCATGATTCTTGGATTT	PtrPAL5PR1:TTTTCCTGTAAAGCGATGATCC
	PtrPAL5	PtrPAL5PF2:GGCCCTGGCTTTCACTTGTT	PtrPAL5PR2:CAAGAATCATGGCGGCTGGA
	PtrPAL5	PtrPAL5PF3:AACCTCACGATACTGGGAGC	PtrPAL5PF3:AACCTCACGATACTGGGAGC
	PtrPAL5	PtrPAL5PF4:TTAATTTCAACGGCACCACCG	PtrPAL5PF4:TTAATTTCAACGGCACCACCG
	PtrPec9-1	PtrPec9-1PF1:CCGTGACTTTGATCATACAGCG	PtrPec9-1PR1:GCAAGGGGAAATAGGGTGCT

Table 13. Continued

ChIP-PCR assays for the promoters	PtrPec9-1	PtrPec9-1PF2:CAATTCATACTCCACTCTCAAA	PtrPec9-1PR2:GATCAAAGTCACGGGTGAAA
	PtrPec9-1	PtrPec9-1PF3:TGGGAAATCAGGTTTCAAGAGAA	PtrPec9-1PF3:TGGGAAATCAGGTTTCAAGAGAA
	PtrPec9-1	PtrPec9-1PF4:AAAAGGTCAACCGGCATGAA	PtrPec9-1PF4:AAAAGGTCAACCGGCATGAA
	PtrPec9-2	PtrPec9-2PF1:CGTCTTCCCCACACAGACAA	PtrPec9-2PR1:GCGCTTTGTACGCTGAAAGG
	PtrPec9-2	PtrPec9-2PF2:AGCCACAACCTTGTTTCCTT	PtrPec9-2PR2:TTTGTCTGTGTGGGGAAGACG
	PtrPec9-2	PtrPec9-2PF3:GGGGGAGTGGGAACAAAGTG	PtrPec9-2PF3:GGGGGAGTGGGAACAAAGTG
	PtrPec9-2	PtrPec9-2PF4:TTACGGGCCAAACTCCAAGG	PtrPec9-2PF4:TTACGGGCCAAACTCCAAGG
	PtrPRC1-2	PtrPRC1-2PF1:TGCCAGTTTGTTCGTCTCCT	PtrPRC1-2PR1:GAGTCAACTCGTGCATCCCA
	PtrPRC1-2	PtrPRC1-2PF2:ACTGCTTCCCCTGACAATCT	PtrPRC1-2PR2:AGGAGACGAACAAACTGGCA
	PtrPRC1-2	PtrPRC1-2PF3:GGAAGTGAAGCACCTCGGTT	PtrPRC1-2PF3:GGAAGTGAAGCACCTCGGTT
	PtrPRC1-2	PtrPRC1-2PF4:AGTTGACCAAACACCTGCCA	PtrPRC1-2PF4:AGTTGACCAAACACCTGCCA
	PtrPRC1-3	PtrPRC1-3PF1:GATGGAGAGAGTGGGTGGGG	PtrPRC1-3PR1:GACCCCCGGTGTTCATTTTC
	PtrPRC1-3	PtrPRC1-3PF2:CGCAGCGTAGATCCCGTT	PtrPRC1-3PR2:TGGTGCGATGTCTCTTGCC
	PtrPRC1-3	PtrPRC1-3PF3:GCCACGGCATTTATTGTACTGG	PtrPRC1-3PF3:GCCACGGCATTTATTGTACTGG
	PtrPRC1-3	PtrPRC1-3PF4:TTGTGGTTGGTAATGTGGTGGT	PtrPRC1-3PF4:TTGTGGTTGGTAATGTGGTGGT
	PtrQRT3	PtrQRT3PF1:TGATTTGTTCCGTCCCCGTC	PtrQRT3PR1:AAGGGAGCTGGGAGAGACAT
	PtrQRT3	PtrQRT3PF2:CGGGACAAGAACGGAACAAG	PtrQRT3PR2:GACGGGGACGGAACAAATCA
	PtrQRT3	PtrQRT3PF3:ATGAGACTGGTTCCGGGTTC	PtrQRT3PF3:ATGAGACTGGTTCCGGGTTC
	PtrQRT3	PtrQRT3PF4:TTGTTTGTACCGCGCCATTG	PtrQRT3PF4:TTGTTTGTACCGCGCCATTG
	PtrRSW1-2	PtrRSW1-2PF1:AAAGTTAATCACTTCCTGCTAAG	PtrRSW1-2PR1:CCGCATTTGCTTCCATCTTT
	PtrRSW1-2	PtrRSW1-2PF2:CCGCATTTGCTTCCATCTTT	PtrRSW1-2PR2:AGCTTAGCAGGAAGTGATTAAC
	PtrRSW1-2	PtrRSW1-2PF3:AGCTTGAGCTTCTCGGCTTT	PtrRSW1-2PF3:AGCTTGAGCTTCTCGGCTTT
	PtrRSW1-2	PtrRSW1-2PF4:CGTGAAATTCATCGAGGTGTG	PtrRSW1-2PF4:CGTGAAATTCATCGAGGTGTG
	PtrRSW1-3	PtrRSW1-3PF1:AAAGGGAAGCCAAGGTGAGG	PtrRSW1-3PR1:GCATTCGCTTCCATCTTTTCCT
	PtrRSW1-3	PtrRSW1-3PF2:TGAATTGTGAATGATTAAAAGAAGA	PtrRSW1-3PR2:TTCCCTTTTATCTACTCCGGT
	PtrRSW1-3	PtrRSW1-3PF3:CTAGTGTCGCTCTCTTGACA	PtrRSW1-3PF3:CTAGTGTCGCTCTCTTGACA
	PtrRSW1-3	PtrRSW1-3PF4:TTATGAGCTGGGTAAATCAATAA	PtrRSW1-3PF4:TTATGAGCTGGGTAAATCAATAA
	PtrSGR1	PtrSGR1PF1:AGCACCATTAGCCGATCGAA	PtrSGR1PR1:TCTTCCCACCTGCTGCTTTT
	PtrSGR1	PtrSGR1PF2:GCTGCTCTGCTCTAGCCTTT	PtrSGR1PR2:GTGCTGCTGCTTGCTGAAAT
	PtrSGR1	PtrSGR1PF3:TGTGTGTGTACGTAAGATGTGA	PtrSGR1PF3:TGTGTGTGTACGTAAGATGTGA
	PtrSGR1	PtrSGR1PF4:AAGGTTGAAAGCATGTTTGTCTT	PtrSGR1PF4:AAGGTTGAAAGCATGTTTGTCTT
	PtrWBLH1	PtrWBLH1PF1:CAAGGACCGGGGTGTTTGAT	PtrWBLH1PR1:TCGAATGACGCACAAGGGAA
	PtrWBLH1	PtrWBLH1PF2:TTGCACCAATCATAAGGAGGTT	PtrWBLH1PR2:GTCCTTGTGACCATCATCAGC
	PtrWBLH1	PtrWBLH1PF3:AGGTGTTGCCGTGTTTGGTTCAGGAG	PtrWBLH1PF3:AGGTGTTGCCGTGTTTGGTTCAGGAG
	PtrWBLH1	PtrWBLH1PF4:CCCGTCTTCTTGATTTTGAGAG	PtrWBLH1PF4:CCCGTCTTCTTGATTTTGAGAG
	PtrWBLH2	PtrWBLH2PF1:GTGCTGCTAAAGAGCAACCAG	PtrWBLH2PR1:AGCACCCCCACCAACTTATT
	PtrWBLH2	PtrWBLH2PF2:ACCCCAAATTTTTCAGGGTCA	PtrWBLH2PR2:TGGTTGCTCTTTAGCAGCACT
	PtrWBLH2	PtrWBLH2PF3:TCTCTACCTCCCATGGCTGC	PtrWBLH2PF3:TCTCTACCTCCCATGGCTGC
	PtrWBLH2	PtrWBLH2PF4:GTGCTTTCTGGATTTTGGGACAT	PtrWBLH2PF4:GTGCTTTCTGGATTTTGGGACAT
	PtrWBLH3	PtrWBLH3PF1:TCTTTTCTTTTGCTTGATGGGCA	PtrWBLH3PR1:ACGCGTAGATATTGCACCCA
	PtrWBLH3	PtrWBLH3PF2:TCATTGCTGTTCCTGCTTTCA	PtrWBLH3PR2:TGATGCCCATCAAGCAAAAGAA
	PtrWBLH3	PtrWBLH3PF3:AGGATGAGAAAGACAGCCAGC	PtrWBLH3PF3:AGGATGAGAAAGACAGCCAGC
	PtrWBLH3	PtrWBLH3PF4:TCTGGGGCGAGCATTTCATT	PtrWBLH3PF4:TCTGGGGCGAGCATTTCATT
	PtrWBLH4	PtrWBLH4PF1:ACCAGTCTCTTTAATCCTCCATT	PtrWBLH4PR1:TCTTCTTTGTAGCACCCTCACA
	PtrWBLH4	PtrWBLH4PF2:CTTGAGGTTTACAAGAGGTCA	PtrWBLH4PR2:AGAGACTGGTATCCCTCTCAA
	PtrWBLH4	PtrWBLH4PF3:GAAATTATGTCACAAAAG	PtrWBLH4PF3:GAAATTATGTCACAAAAG
	PtrWBLH4	PtrWBLH4PF4:GGCTTGGAAGACTAGGTCT	PtrWBLH4PF4:GGCTTGGAAGACTAGGTCT
	PtrWRKY12	PtrWRKY12PF1:CACCGGACGAGCTTCTTCAT	PtrWRKY12PR1:CATAAGTGTCGAGCGCAAGC
	PtrWRKY12	PtrWRKY12PF2:GCTCTGCCCTATCCTCTCCT	PtrWRKY12PR2:GAAGAAGCTCGTCCGGTGAT
	PtrWRKY12	PtrWRKY12PF3:TTGATTTCAAGGCGGCTACA	PtrWRKY12PF3:TTGATTTCAAGGCGGCTACA
	PtrWRKY12	PtrWRKY12PF4:CACCTAATGTGGCAGTCATCC	PtrWRKY12PF4:CACCTAATGTGGCAGTCATCC

Table 14. PtrMYB74 regulated genes involved in brassinosteroid, gibberellin, and phosphatidylinositol metabolic processes.

term ID	GO processes	GO name	IDs
GO:0016131	BP	brassinosteroid metabolic process	POPTR_0011S10120,POPTR_0011S10150
GO:0046488	BP	phosphatidylinositol metabolic process	POPTR_0014S08900,POPTR_0014S08910
GO:0009685	BP	gibberellin metabolic process	POPTR_0008S08220

Table 15. The TF and cell wall biosynthetic genes directly regulated by AtSND1, PtrSND1-B1, AtMYB46, and PtrMYB21.

		Arabidopsis IDs	*Gene name*
AtSND1 targets	**Transcription factor**	AT5G12870	MYB46
		AT2G40470	LOB domain protein 15 (LBD15)
		AT5G64530	Xylem NAC domain 1 (XND1)
		AT1G28470	SND3
		AT5G64060	ANAC103
		AT3G21270	ADOF2
		AT2G28200	C2H2-1 (Zinc finger family protein)
		AT5G03510	C2H2-2 (Zinc finger family protein)
		AT4G35550	WOX13
		AT5G04840	bZIP protein
		AT4G28140	RAP2.4-like (AP2-domain transcription factor)
		AT1G46768	RAP2.1
		AT5G64340	SAC51
		AT2G43060	IBH1
	Cell wall biosynthetic enzyme genes	AT5G67230	IRX14-L (I14H)
		AT1G27440	IRX10
		AT1G19300	PARVUS
		AT2G32610	Cellulose synthase-like (AtCslB01)
		AT2G32620	Cellulose synthase-like (AtCslB02)
		AT2G04780	FLA7
		AT5G66390	Peroxidase 72
		AT1G71695	Peroxidase 12
		AT5G03260	LACCASE 11

		Populus trichocarpa V3.0 gene model name	**Gene name**	**IDs of Arabidopsis homologs**
PtrSND1-B1 direct targets	**Transcription factors**	Potri.008G080000	PtrSND1-L2	AT1G79580
		Potri.001G258700	PtrMYB2	AT3G08500
		Potri.009G053900	PtrMYB21	AT5G12870
		Potri.015G082700	PtrMYB74	AT1G57560
		Potri.019G118200	PtrMYB229	AT4G21440
		Potri.004G051800	PtrERF22	AT4G18450
		Potri.004G093500	Ring/FYVE/PHD	AT2G01275
		Potri.010G118700	PtrC3H21	AT1G68200
		Potri.001G154500	RING/U-box-1	AT1G68200
		Potri.016G067900	RING/U-box-2	AT2G35910
	Oxidases	Potri.010G183600	PtrLAC26	AT2G40370
		Potri.013G156500	PtrPO41	AT5G58390
		Potri.012G042800	PtrPO9	AT4G11290

Table 15. Continued

		Arabidopsis IDs	*Gene name*
AtMYB 46 targets	**Transcription factor**	AT1G79180	MYB63
		AT1G17950	MYB52
		AT1G73410	MYB54
		AT1G62990	KNAT7
		AT4G38620	MYB4
		AT2G16720	MYB7
		AT4G09460	MYB6
		AT4G34990	MYB32
		AT1G19700	Homeobox-leucine zipper family protein (BEL10)
		AT2G22850	Bzip transcription factor (bZIP6)
		AT5G53200	TRIPTYCHON(TRY)
		AT5G25890	IAA-inducible protein 28 (IAA28)
		AT4G34610	BEL1-like Homeodomain-containing protein(BLH6)
		AT1G75410	BEL1-like homeodomain 3 protein (BLH3)
		AT4G36870	BEL1-like homeobox 2 protein (BLH2)
		AT1G66810	Zinc finger family protein (AtC3H14)
		AT2G28200	Zinc finger family protein (ZAT5)
	Cell wall biosynthetic genes	AT5G67230	Family 43 glycosyltransferase (I14H) IRX14-L
		AT5G59290	UDP-xylosesynthase(UXS3)
		AT3G10340	Phenylalanine ammonia-lyase (PAL4)
		AT2G37040	PAL1
		AT3G53260	PAL2
		AT1G65060	4-Coumarate-CoA ligase (4CL3)
		AT2G23910	CCR (Cinnamoyl-CoA reductase)-like 1
		AT4G30470	CCR-like 2
		AT4G34050	CCoAOMT1
		AT3G19450	Cinnamyl-alcohol dehydrogenase (AtCAD4)
		AT5G05390	Laccase 12
		AT5G03260	Laccase 11

		Populus trichocarpa V3.0 gene model name	Gene name	IDs of Arabidopsis homologs
PtrMYB21 direct targets	**Transcription factor**	Potri.003G110800	PtrHAM3/PtrGRAS22	AT4G00150
		Potri.019G050900	PtrMYB059	AT3G02940
		Potri.015G033600	PtrMYB090	AT1G17950
		Potri.007G134500	PtrMYB161	AT1G17950
		Potri.017G017600	PtrMYB175	AT1G17950
		Potri.011G058400	PtrNAC123/SND2/3A1	AT4G28500
		Potri.006G152700	PtrNAC127/SND2/3-L1	AT4G29230
		Potri.002G031000	PtrWBLH1	AT1G75410
		Potri.005G129500	PtrWBLH2	AT4G36870
		Potri.004G159300	PtrWBLH3	AT4G34610
	cell wall biosyntheic genes	Potri.016G086400	PtrGT43C/PtrIRX9	AT2G37090
		Potri.007G047500	PtrIRX14-L	AT5G67230
		Potri.014G024700	PtrGT47C/PtrFRA	AT5G47820
		Potri.008G038200	PHE AMMONIA LYASE 1(PAL1)	AT2G37040
		Potri.008G073800	LACCASE 12	AT5G05390
		Potri.009G042500	LACCASE 4	AT2G38080
		Potri.016G112100	LACCASE 4	AT2G38080
		Potri.010G183600	LACCASE 5	AT2G40370
		Potri.008G038200	PtrPAL2	AT2G37040

Table 16. The expression of 45 genes in the four-layered PtrSND1-B1 network in tension wood. The expression of these 45 genes are from the SDX cell-specific RNA-seq in GSE81077, Shi et al. 2017.

	gene_id 3.0	Function	OW_FPKM	NW_FPKM	TW_FPKM	OW/NW	TW/NW
PtrQRT3	Potri.003G074600	Cell wall modification	0.05027	1.92289	0.06011	0.02614	0.03126
PtrPec9-1	Potri.012G142300	Cell wall modification	0.07219	3.46327	0.11235	0.02084	0.03244
PtrFLA18	Potri.013G151400	Cell wall modification	0	127.856	0.02987	0	0.00023
PtrFRA1	Potri.014G024700	Cell wall modification	7.59771	16.605	8.28454	0.45756	0.49892
PtrFLA32	Potri.019G121100	Cell wall modification	0	0.3358	0	0	0
PtrCesA4	Potri.002G257900	Cellulose	6.36883	388.798	15.2597	0.01638	0.03925
PtrCesA18	Potri.004G059600	Cellulose	4.40086	272.317	11.2857	0.01616	0.04144
PtrRSW1-2	Potri.006G251900	Cellulose	42.7911	43.707	35.6211	0.97904	0.815
PtrRSW1-3	Potri.018G029400	Cellulose	8.54738	16.5945	7.81894	0.51507	0.47118
PtrCesA17	Potri.018G103900	Cellulose	4.83277	176.136	14.4988	0.02744	0.08232
PtrIRX14-L	Potri.007G047500	Hemicellulose	6.73327	40.5534	8.0626	0.16603	0.19881
PtrIRX9	Potri.016G086400	Hemicellulose	1.76759	37.6794	3.2431	0.04691	0.08607
PtrLAC19	Potri.008G073800	LAC	1.29015	5.54398	0.46009	0.23271	0.08299
PtrLAC21	Potri.009G042500	LAC	0.19768	5.1336	0.03527	0.03851	0.00687
PtrLAC26	Potri.010G183600	LAC	0.27139	1.27237	0	0.21329	0
PtrLAC41	Potri.016G112100	LAC	0.04102	0.27607	0.18365	0.14859	0.66523
PtrHCT6	Potri.001G042900	monolignol	0.69548	31.0005	0.87748	0.02243	0.02831
PtrCSE2	Potri.001G175000	monolignol	13.6155	50.0162	13.2713	0.27222	0.26534
PtrCCoAOMT2	Potri.001G304800	monolignol	105.245	648.45	44.2977	0.1623	0.06831
PtrHCT1	Potri.003G183900	monolignol	69.3252	517.712	38.4537	0.13391	0.07428
PtrCAld5H1	Potri.005G117500	monolignol	1.49203	95.5614	3.83177	0.01561	0.0401
PtrCAld5H2	Potri.007G016400	monolignol	9.63399	389.06	20.9489	0.02476	0.05384
PtrPAL2	Potri.008G038200	monolignol	25.0434	366.64	7.42053	0.06831	0.02024
PtrCAD1	Potri.009G095800	monolignol	190.912	805.867	252.265	0.2369	0.31304
PtrCCoAOMT1	Potri.009G099800	monolignol	87.6102	519.948	54.8322	0.1685	0.10546
PtrCOMT2	Potri.012G006400	monolignol	70.682	1163.2	75.9104	0.06077	0.06526
PtrC4H1	Potri.013G157900	monolignol	38.4637	430.492	19.76	0.08935	0.0459
PtrWBLH1	Potri.002G031000	TF	0.91418	5.86817	0.82345	0.15579	0.14032
PtrHAM3	Potri.003G110800	TF	0.52425	1.29516	0.80563	0.40477	0.62203
PtrMYB93	Potri.004G138000	TF	0	12.5763	0	0	0
PtrWBLH3	Potri.004G159300	TF	85.0859	43.4209	40.8622	1.95956	0.94107
PtrWBLH2	Potri.005G129500	TF	21.6009	36.8548	19.76	0.58611	0.53616
PtrNAC127	Potri.006G152700	TF	0.59717	19.4137	1.601	0.03076	0.08247
PtrMYB161	Potri.007G134500	TF	10.4946	34.735	10.3732	0.30213	0.29864
PtrNAC123	Potri.011G058400	TF	0.86922	29.9501	1.9519	0.02902	0.06517
PtrSND1-B1	Potri.014G104800	TF	0.44858	13.0543	1.43991	0.03436	0.1103
PtrNAC105	Potri.015G046800	TF	0.02803	5.07201	0.0497	0.00553	0.0098
PtrMYB90	Potri.015G033600	TF	3.53978	26.5505	4.30014	0.13332	0.16196
PtrMYB74	Potri.015G082700	TF	0.62368	5.38374	2.20792	0.11584	0.41011
PtrMYB175	Potri.017G017600	TF	0.06883	6.98493	0	0.00985	0
PtrMYB174	Potri.017G037000	TF	38.3635	14.7645	12.0235	2.59836	0.81435
PtrMYB59	Potri.019G050900	TF	0	5.16882	0	0	0
PtrMYB21	Potri.009G053900	TF	0.41381	2.23976	0.25322	0.18476	0.11305
PtrMYB88	Potri.018G095900	TF	0	2.22754	0.09081	0	0.04077

REFERENCES

1. Nystedt Björn, Street NR, Wetterbom A, et al. The norway spruce genome sequence and conifer genome evolution. Nature. 2013;497(7451):579-584.

2. Blais A, Dynlacht BD. Constructing transcriptional regulatory networks. Genes Dev. 2005;19(13):1499-1511.

3. Bomal C, Duval I, Giguere I, et al. Opposite action of R2R3-MYBs from different subgroups on key genes of the shikimate and monolignol pathways in spruce. J Exp Bot. 2014;65(2):495-508.

4. Brady SM, Zhang L, Megraw M, et al. A stele-enriched gene regulatory network in the Arabidopsis root. Mol Syst Biol. 2011;7:459.

5. Cai B, Li C, Huang J. Systematic identification of cell-wall related genes in populus based on analysis of functional modules in co-expression network. PloS one. 2014;9(4):e95176.

6. Cassan-Wang H, Goué N, SAIDI MN, et al. Identification of novel transcription factors regulating secondary cell wall formation in Arabidopsis. Frontiers in plant science. 2013;4:189.

7. Chiang VL. From rags to riches. Nat Biotechnol. 2002;20(6):557-559.

8. Daniel B, Pavkov-Keller T, Steiner B, et al. Oxidation of monolignols by members of the berberine bridge enzyme family suggests a role in plant cell wall metabolism. J Biol Chem. 2015;290(30):18770-18781.

9. Dolzblasz A, Nardmann J, Clerici E, et al. Stem cell regulation by Arabidopsis WOX genes. Molecular plant. 2016;9(7):1028-1039.

10. Du J, Mansfield SD, Groover AT. The populus homeobox gene ARBORKNOX2 regulates cell differentiation during secondary growth. The Plant Journal. 2009;60(6):1000-1014.

11. Du J, Miura E, Robischon M, Martinez C, Groover A. The populus class III HD ZIP transcription factor POPCORONA affects cell differentiation during secondary growth of woody stems. PLoS One. 2011;6(2):e17458.

12. Duval I, Lachance D, Giguere I, et al. Large-scale screening of transcription factor-promoter interactions in spruce reveals a transcriptional network involved in vascular development. J Exp Bot. 2014;65(9):2319-2333.

13. Eriksson ME, Israelsson M, Olsson O, Moritz T. Increased gibberellin biosynthesis in transgenic trees promotes growth, biomass production and xylem fiber length. Nat Biotechnol. 2000;18(7):784-788.

14. Etchells JP, Provost CM, Mishra L, Turner SR. WOX4 and WOX14 act downstream of the PXY receptor kinase to regulate plant vascular proliferation independently of any role in vascular organisation. Development. 2013;140(10):2224-2234.

15. Evert RF. Esau's plant anatomy: Meristems, cells, and tissues of the plant body: Their structure, function, and development. John Wiley & Sons; 2006.

16. Franco-Zorrilla JM, Lopez-Vidriero I, Carrasco JL, Godoy M, Vera P, Solano R. DNA-binding specificities of plant transcription factors and their potential to define target genes. Proc Natl Acad Sci U S A. 2014;111(6):2367-2372.

17. Freshour G, Clay RP, Fuller MS, Albersheim P, Darvill AG, Hahn MG. Developmental and tissue-specific structural alterations of the cell-wall polysaccharides of Arabidopsis thaliana roots. Plant Physiol. 1996;110(4):1413-1429.

18. Gaudinier A, Zhang L, Reece-Hoyes J, et al. Enhanced Y1H assays for Arabidopsis. Nat Meth. 2011;8(12):1053-1055.

19. Gerstein MB, Kundaje A, Hariharan M, et al. Architecture of the human regulatory network derived from ENCODE data. Nature. 2012;489(7414):91-100.

20. Goicoechea M, Lacombe E, Legay S, et al. EgMYB2, a new transcriptional activator from eucalyptus xylem, regulates secondary cell wall formation and lignin biosynthesis. The Plant Journal. 2005;43(4):553-567.

21. Grant EH, Fujino T, Beers EP, Brunner AM. Characterization of NAC domain transcription factors implicated in control of vascular cell differentiation in Arabidopsis and populus. Planta. 2010;232(2):337-352.

22. Groover AT, Mansfield SD, DiFazio SP, et al. The populus homeobox gene ARBORKNOX1 reveals overlapping mechanisms regulating the shoot apical meristem and the vascular cambium. Plant Mol Biol. 2006;61(6):917-932.

23. Gujas B, Rodriguez-Villalon A. Plant phosphoglycerolipids: The gatekeepers of vascular cell differentiation. Frontiers in plant science. 2016;7.

24. Hussey SG, Mizrachi E, Spokevicius AV, Bossinger G, Berger DK, Myburg AA. SND2, a NAC transcription factor gene, regulates genes involved in secondary cell wall development in Arabidopsis fibres and increases fibre cell area in eucalyptus. BMC plant biology. 2011;11(1):173.

25. Ikeda M, Fujiwara S, Mitsuda N, Ohme-Takagi M. A triantagonistic basic helix-loop-helix system regulates cell elongation in Arabidopsis. Plant Cell. 2012;24(11):4483-4497.

26. Ito Y, Nakanomyo I, Motose H, et al. Dodeca-CLE peptides as suppressors of plant stem cell differentiation. Science. 2006;313(5788):842-845.

27. Jensen JK, Kim H, Cocuron J, Orler R, Ralph J, Wilkerson CG. The DUF579 domain containing proteins IRX15 and IRX15‐L affect xylan synthesis in Arabidopsis. The Plant Journal. 2011;66(3):387-400.

28. Joseleau J, Imai T, Kuroda K, Ruel K. Detection in situ and characterization of lignin in the G-layer of tension wood fibres of populus deltoides. Planta. 2004;219(2):338-345.

29. Karpinska B, Karlsson M, Srivastava M, et al. MYB transcription factors are differentially expressed and regulated during secondary vascular tissue development in hybrid aspen. Plant Mol Biol. 2004;56(2):255-270.

30. Kim W, Ko J, Kim J, Kim J, Bae H, Han K. MYB46 directly regulates the gene expression of secondary wall‐associated cellulose synthases in Arabidopsis. The Plant Journal. 2013;73(1):26-36.

31. Ko J, Kim H, Hwang I, Han K. Tissue‐type‐specific transcriptome analysis identifies developing xylem‐specific promoters in poplar. Plant biotechnology journal. 2012;10(5):587-596.

32. Ko J, Kim W, Han K. Ectopic expression of MYB46 identifies transcriptional regulatory genes involved in secondary wall biosynthesis in Arabidopsis. The Plant Journal. 2009;60(4):649-665.

33. Ko J, Kim W, Kim J, Ahn S, Han K. MYB46-mediated transcriptional regulation of secondary wall biosynthesis. Molecular plant. 2012;5(5):961-963.

34. Ko JH, Jeon HW, Kim WC, Kim JY, Han KH. The MYB46/MYB83-mediated transcriptional regulatory programme is a gatekeeper of secondary wall biosynthesis. Ann Bot. 2014;114(6):1099-1107.

35. Kondo Y, Ito T, Nakagami H, et al. Plant GSK3 proteins regulate xylem cell differentiation downstream of TDIF–TDR signalling. Nature communications. 2014;5.

36. Krouk G, Lingeman J, Colon AM, Coruzzi G, Shasha D. Gene regulatory networks in plants: Learning causality from time and perturbation. Genome Biol. 2013;14(6):123.

37. Kumar M, Thammannagowda S, Bulone V, et al. An update on the nomenclature for the cellulose synthase genes in populus. Trends Plant Sci. 2009;14(5):248-254.

38. Legay S, Sivadon P, Blervacq A, et al. EgMYB1, an R2R3 MYB transcription factor from eucalyptus negatively regulates secondary cell wall formation in Arabidopsis and poplar. New Phytol. 2010;188(3):774-786.

39. Li E, Bhargava A, Qiang W, et al. The class II KNOX gene KNAT7 negatively regulates secondary wall formation in Arabidopsis and is functionally conserved in populus. New Phytol. 2012;194(1):102-115.

40. Li Q, Min D, Wang JP, et al. Down-regulation of glycosyltransferase 8D genes in populus trichocarpa caused reduced mechanical strength and xylan content in wood. Tree Physiol. 2011;31(2):226-236.

41. Li W, Lin Y, Li Q, et al. A robust chromatin immunoprecipitation protocol for studying transcription factor–DNA interactions and histone modifications in wood-forming tissue. nature protocols. 2014;9(9):2180-2193.

42. Li C, Wang X, Ran L, Tian Q, Fan D, Luo K. PtoMYB92 is a transcriptional activator of the lignin biosynthetic pathway during secondary cell wall formation in populus tomentosa. Plant Cell Physiol. 2015;56(12):2436-2446.

43. Li Q, Lin YC, Sun YH, et al. Splice variant of the SND1 transcription factor is a dominant negative of SND1 members and their regulation in populus trichocarpa. Proc Natl Acad Sci U S A. 2012;109(36):14699-14704.

44. Lin Y, Li W, Chen H, et al. A simple improved-throughput xylem protoplast system for studying wood formation. nature protocols. 2014;9(9):2194-2205.

45. Lin YC, Li W, Sun YH, et al. SND1 transcription factor-directed quantitative functional hierarchical genetic regulatory network in wood formation in populus trichocarpa. Plant Cell. 2013;25(11):4324-4341.

46. Lindemose S, Jensen MK, Van de Velde J, et al. A DNA-binding-site landscape and regulatory network analysis for NAC transcription factors in Arabidopsis thaliana. Nucleic Acids Res. 2014;42(12):7681-7693.

47. Liu L, Ramsay T, Zinkgraf M, et al. A resource for characterizing genome‐wide binding and putative target genes of transcription factors expressed during secondary growth and wood formation in populus. The Plant Journal. 2015;82(5):887-898.

48. Liu L, Zinkgraf M, Petzold HE, Beers EP, Filkov V, Groover A. The populus ARBORKNOX1 homeodomain transcription factor regulates woody growth through binding to evolutionarily conserved target genes of diverse function. New Phytol. 2015;205(2):682-694.

49. Liu Y, You S, Taylor-Teeples M, et al. BEL1-LIKE HOMEODOMAIN6 and KNOTTED ARABIDOPSIS THALIANA7 interact and regulate secondary cell wall formation via repression of REVOLUTA. Plant Cell. 2014;26(12):4843-4861.

50. McCarthy RL, Zhong R, Ye ZH. MYB83 is a direct target of SND1 and acts redundantly with MYB46 in the regulation of secondary cell wall biosynthesis in Arabidopsis. Plant Cell Physiol. 2009;50(11):1950-1964.

51. Merkle SA, Dean JF. Forest tree biotechnology. Curr Opin Biotechnol. 2000;11(3):298-302.

52. Miki D, Itoh R, Shimamoto K. RNA silencing of single and multiple members in a gene family of rice. Plant Physiol. 2005;138(4):1903-1913.

53. Mitsuda N, Iwase A, Yamamoto H, et al. NAC transcription factors, NST1 and NST3, are key regulators of the formation of secondary walls in woody tissues of Arabidopsis. Plant Cell. 2007;19(1):270-280.

54. Monke G, Seifert M, Keilwagen J, et al. Toward the identification and regulation of the Arabidopsis thaliana ABI3 regulon. Nucleic Acids Res. 2012;40(17):8240-8254.

55. Nakano Y, Yamaguchi M, Endo H, Rejab NA, Ohtani M. NAC-MYB-based transcriptional regulation of secondary cell wall biosynthesis in land plants. Frontiers in plant science. 2015;6:288.

56. Noh SA, Choi Y, Cho J, Lee H. The poplar basic helix-loop-helix transcription factor BEE3–Like gene affects biomass production by enhancing proliferation of xylem cells in poplar. Biochem Biophys Res Commun. 2015;462(1):64-70.

57. Northcote D. Chemistry of the plant cell wall. Annual review of plant physiology. 1972;23(1):113-132.

58. O'Malley RC, Huang SC, Song L, et al. Cistrome and epicistrome features shape the regulatory DNA landscape. Cell. 2016;165(5):1280-1292.

59. O'Malley RC, Huang SC, Song L, et al. Cistrome and epicistrome features shape the regulatory DNA landscape. Cell. 2016;165(5):1280-1292.

60. Ohtani M, Nishikubo N, Xu B, et al. A NAC domain protein family contributing to the regulation of wood formation in poplar. The Plant Journal. 2011;67(3):499-512.

61. Ohtani M, Akiyoshi N, Takenaka Y, Sano R, Demura T. Evolution of plant conducting cells: Perspectives from key regulators of vascular cell differentiation. J Exp Bot. 2017;68(1):17-26.

62. Pastore JJ, Limpuangthip A, Yamaguchi N, et al. LATE MERISTEM IDENTITY2 acts together with LEAFY to activate APETALA1. Development. 2011;138(15):3189-3198.

63. Patzlaff A, McInnis S, Courtenay A, et al. Characterisation of a pine MYB that regulates lignification. The Plant Journal. 2003;36(6):743-754.

64. Patzlaff A, Newman LJ, Dubos C, et al. Characterisation of PtMYB1, an R2R3-MYB from pine xylem. Plant Mol Biol. 2003;53(4):597-608.

65. Pauly M, Keegstra K. Cell‐wall carbohydrates and their modification as a resource for biofuels. The Plant Journal. 2008;54(4):559-568.

66. Reimand J, Arak T, Adler P, et al. g:Profiler-a web server for functional interpretation of gene lists (2016 update). Nucleic Acids Res. 2016;44(W1):W83-9.

67. Reinhart BJ, Liu T, Newell NR, et al. Establishing a framework for the Ad/abaxial regulatory network of Arabidopsis: Ascertaining targets of class III homeodomain leucine zipper and KANADI regulation. Plant Cell. 2013;25(9):3228-3249.

68. Robinson MD, McCarthy DJ, Smyth GK. edgeR: A bioconductor package for differential expression analysis of digital gene expression data. Bioinformatics. 2010;26(1):139-140.

69. Robischon M, Du J, Miura E, Groover A. The populus class III HD ZIP, popREVOLUTA, influences cambium initiation and patterning of woody stems. Plant Physiol. 2011;155(3):1214-1225.

70. Sambrook J, Fritsch EF, Maniatis T. Molecular cloning: A laboratory manual. Cold spring harbor laboratory press; 1989.

71. Sarkanen KV, Ludwig CH. Precursors and their polymerization. In: Sarkanen KV, Ludwig CH, eds. Lignins, occurrence, formation, structure and reactions. New York: Wiley-Interscience; 1971:95-163.

72. Sato K, Ito S, Fujii T, et al. The carbohydrate-binding module (CBM)-like sequence is crucial for rice CWA1/BC1 function in proper assembly of secondary cell wall materials. Plant signaling & behavior. 2010;5(11):1433-1436.

73. Schmittgen TD, Livak KJ. Analyzing real-time PCR data by the comparative CT method. Nature protocols. 2008;3(6):1101-1108.

74. Shi R, Yang C, Lu S, Sederoff R, Chiang VL. Specific down-regulation of PAL genes by artificial microRNAs in populus trichocarpa. Planta. 2010;232(6):1281-1288.

75. Shi R, Sun YH, Li Q, Heber S, Sederoff R, Chiang VL. Towards a systems approach for lignin biosynthesis in populus trichocarpa: Transcript abundance and specificity of the monolignol biosynthetic genes. Plant Cell Physiol. 2010;51(1):144-163.

76. Song D, Shen J, Li L. Characterization of cellulose synthase complexes in populus xylem differentiation. New Phytol. 2010;187(3):777-790.

77. Song J, Lu S, Chen ZZ, Lourenco R, Chiang VL. Genetic transformation of populus trichocarpa genotype nisqually-1: A functional genomic tool for woody plants. Plant Cell Physiol. 2006;47(11):1582-1589.

78. Sorrells TR, Johnson AD. Making sense of transcription networks. Cell. 2015;161(4):714-723.

79. Sun X, Feng Z, Meng L, Zhu J, Geitmann A. Arabidopsis ASL11/LBD15 is involved in shoot apical meristem development and regulates WUS expression. Planta. 2013;237(5):1367-1378.

80. Sun Y, Fan X, Cao D, et al. Integration of brassinosteroid signal transduction with the transcription network for plant growth regulation in Arabidopsis. Developmental cell. 2010;19(5):765-777.

81. Suzuki S, Li L, Sun YH, Chiang VL. The cellulose synthase gene superfamily and biochemical functions of xylem-specific cellulose synthase-like genes in populus trichocarpa. Plant Physiol. 2006;142(3):1233-1245.

82. Taylor-Teeples M, Lin L, de Lucas M, et al. An Arabidopsis gene regulatory network for secondary cell wall synthesis. Nature. 2015;517(7536):571-575.

83. Thompson D, Regev A, Roy S. Comparative analysis of gene regulatory networks: From network reconstruction to evolution. Annu Rev Cell Dev Biol. 2015;31:399-428.

84. Tian Q, Wang X, Li C, et al. Functional characterization of the poplar R2R3-MYB transcription factor PtoMYB216 involved in the regulation of lignin biosynthesis during wood formation. PloS one. 2013;8(10):e76369.

85. Timell TE. The chemical composition of tension wood. Svensk Papp Tidn. 1969;72:173-181.

86. Trapnell C, Pachter L, Salzberg SL. TopHat: Discovering splice junctions with RNA-seq. Bioinformatics. 2009;25(9):1105-1111.

87. Tuskan GA, Difazio S, Jansson S, et al. The genome of black cottonwood, populus trichocarpa (torr. & gray). Science. 2006;313(5793):1596-1604.

88. Van Mourik H, Muiño JM, Pajoro A, Angenent GC, Kaufmann K. Characterization of in vivo DNA-binding events of plant transcription factors by ChIP-seq: Experimental protocol and computational analysis. Plant Functional Genomics: Methods and Protocols. 2015:93-121.

89. Vanholme R, Cesarino I, Rataj K, et al. Caffeoyl shikimate esterase (CSE) is an enzyme in the lignin biosynthetic pathway in Arabidopsis. Science. 2013;341(6150):1103-1106.

90. Wang H, Dixon RA. On–off switches for secondary cell wall biosynthesis. Molecular plant. 2012;5(2):297-303.

91. Wang S, Li E, Porth I, Chen J, Mansfield SD, Douglas CJ. Regulation of secondary cell wall biosynthesis by poplar R2R3 MYB transcription factor PtrMYB152 in Arabidopsis. Scientific reports. 2014;4:5054.

92. Wang H, Jiang C, Wang C, et al. Antisense expression of the fasciclin-like arabinogalactan protein FLA6 gene in populus inhibits expression of its homologous genes and alters stem biomechanics and cell wall composition in transgenic trees. J Exp Bot. 2015;66(5):1291-1302.

93. Wang JP, Naik PP, Chen HC, et al. Complete proteomic-based enzyme reaction and inhibition kinetics reveal how monolignol biosynthetic enzyme families affect metabolic flux and lignin in populus trichocarpa. Plant Cell. 2014;26(3):894-914.

94. Yamaguchi M, Nagahage ISP, Ohtani M, et al. Arabidopsis NAC domain proteins VND-INTERACTING1 and ANAC103 interact with multiple NAC domain proteins. Plant Biotechnology. 2015;32(2):119-123.

95. Yang F, Mitra P, Zhang L, et al. Engineering secondary cell wall deposition in plants. Plant biotechnology journal. 2013;11(3):325-335.

96. Yang Y, Park JW, Bebee TW, et al. Determination of a comprehensive alternative splicing regulatory network and combinatorial regulation by key factors during the epithelial-to-mesenchymal transition. Mol Cell Biol. 2016;36(11):1704-1719.

97. Ye ZH, Zhong R. Molecular control of wood formation in trees. J Exp Bot. 2015;66(14):4119-4131.

98. Yoshimoto K, Noutoshi Y, Hayashi K, Shirasu K, Takahashi T, Motose H. A chemical biology approach reveals an opposite action between thermospermine and auxin in xylem development in Arabidopsis thaliana. Plant Cell Physiol. 2012;53(4):635-645.

99. Zhong R, Lee C, McCarthy RL, Reeves CK, Jones EG, Ye Z. Transcriptional activation of secondary wall biosynthesis by rice and maize NAC and MYB transcription factors. Plant and Cell Physiology. 2011;52(10):1856-1871.

100. Zhong R, Lee C, Ye Z. Functional characterization of poplar wood-associated NAC domain transcription factors. Plant Physiol. 2010;152(2):1044-1055.

101. Zhong R, McCarthy RL, Haghighat M, Ye Z. The poplar MYB master switches bind to the SMRE site and activate the secondary wall biosynthetic program during wood formation. PLoS One. 2013;8(7):e69219.

102. Zhong R, Demura T, Ye ZH. SND1, a NAC domain transcription factor, is a key regulator of secondary wall synthesis in fibers of Arabidopsis. Plant Cell. 2006;18(11):3158-3170.

103. Zhu J, Chen H, Li H, et al. Defective in tapetal development and function 1 is essential for anther development and tapetal function for microspore maturation in Arabidopsis. The Plant Journal. 2008;55(2):266-277.

104. Zhu Y, Song D, Sun J, Wang X, Li L. PtrHB7, a class III HD-zip gene, plays a critical role in regulation of vascular cambium differentiation in populus. Molecular plant. 2013;6(4):1331-1343.

105. Zhu C, Ganguly A, Baskin TI, et al. The fragile Fiber1 kinesin contributes to cortical microtubule-mediated trafficking of cell wall components. Plant Physiol. 2015;167(3):780-792.

106. Gietz, R. D., & Woods, R. A. (2002). Transformation of yeast by lithium acetate/single-stranded carrier DNA/polyethylene glycol method. Methods in enzymology, 350, 87-96.

CHAPTER 3
ALTERNATIVE SPLICING OF VASCULAR RELATED TRANSCRIPTION FACTORS 6 CREATES A NEGATIVE REGULATOR OF WOOD ASSOCIATED NACS IN *POPULUS TRICHOCARPA*

3.1 Abstract

Secondary cell walls are the major constituent of tracheary elements and fibers in wood. Alternative splicing provides a novel mechanism for the regulation of biosynthesis of the secondary cell wall. Secondary cell wall associated NAC *SND1-A2* that generates the truncated splicing variant, serves as a dominant repressor in regulating transcriptional programing of wood formation. Here, we report three naturally occurring splicing variants of another secondary cell wall associated NAC family, PtrVND6s from stem-differentiating xylem tissue (*PtrVND6-A1^{IR}*, *PtrVND6-A2^{IR}*, and *PtrVND6-C1^{IR}*). 3'-race and RNA-seq showed that the *PtrVND6-A1^{IR}*, *PtrVND6-A2^{IR}*, and *PtrVND6-C1^{IR}* have a similar splicing pattern. The mature mRNA of PtrVND6-C1^{IR} is preferentially spliced out in xylem and translates a novel small protein. Overexpression of PtrVND6-C1^{IR} protein attenuated the expression of *PtrMYB21* that serve as a master regulator in the formation of the secondary cell wall. PtrVND6-C1^{IR} also inhibits the expression of PtrSND1 members and PtrVND6 members. PtrVND6-C1^{IR} lacks DNA binding and transactivation ability but retains dimerization capability. PtrVND6-C1^{IR} is localized exclusively in cytoplasmic foci, while PtrSND1s and PtrVND6s were found in the nucleus. PtrVND6-C1^{IR} is translocated by PtrSND1s and PtrVND6s as non-functional heterodimers, consistent with the inhibition of PtrVND6-C1^{IR} on PtrMYB21 that is activated by PtrSND1s and PtrVND6s. PtrVND6-C1^{IR} also can form non-functional heterodimers with other developing xylem-expressed NACs. The heterodimer formation can be confirmed by Bimolecular Fluorescence Complementation (BiFC). Our findings suggested that the inhibitory function of PtrVND6-C1^{IR} is not confined to the downstream genes PtrSND1s and PtrVND6s, but

acts on the downstream genes of the other members of developing xylem-expressed NAC protein family.

3.2 Introduction

Lignocellulosic biomass was used for thousands of years as the major building material, fuel and to some extent for food for humans. The major component of lignocellulosic biomass is the secondary cell walls built with cellulose and hemicellulose that are embedded with lignin to reinforce the cell wall structure. The genes involved in cellulose, hemicellulose, and lignin biosynthesis should be coordinately expressed to create the secondary cell wall. In Arabidopsis, significant progress has been made to elucidate the transcriptional regulation of secondary cell wall biosynthesis. NAC domain transcription factors act as master regulators for secondary cell wall thickening, including genes encoding SND1, NST1, VND6, and VND7 (Mitsuda et al., 2005; Zhong et al., 2006; Mitsuda et al., 2007; Ohashi-ito et al., 2010; Yamaguchi et al., 2011). To employ these NAC transcription factors for generating transgenic plants that produce more biomass, the regulation of the NAC transcription factors should be analyzed in woody plants.

Identification of secondary cell wall NAC transcription factors in poplars arose from several studies (Zhong et al., 2010; Zhong et al., 2011; Ohtani et al., 2012; Li et al., 2012). Overexpression of these secondary cell wall NAC activated enzymes involved in the secondary wall biogenesis, resulted in ectopic secondary wall thickening. Compared to the regulatory mechanisms of secondary cell wall NACs in Arabidopsis, a distinct mechanism of PtrSND1 regulation has been found in *P. trichocarpa*. *PtrSND1-A2*^{IR}, a novel splice variant generated from *PtrSND1-A2*, has been identified from *P. trichocarpa* xylem (Li et al., 2012). PtrSND1-A2^{IR} suppresses the activity of the *PtrSND1s* and *PtrMYB21*, suggesting that the splice variants serve as dominant negative regulators in secondary cell wall formation. Detailed analyses showed that

PtrSND1-A2^{IR} lacking the activation domain may form a non-functional heterodimer with *PtrSND1-A2* (Li et al., 2012) and lose its activation function.

To investigate whether other secondary cell wall NACs also generated alternative splicing variants, *Vascular-Related NAC Domain* (VNDs) transcription factors, which are the transcription switches for plant metaxylem and protoxylem vessel formation and regulate secondary cell wall growth (Kubo et al., 2005; Yamaguchi et al., 2008), were selected for further analyses. Here, three naturally occurring alternative splicing variants (*PtrVND6-A1^{IR}, PtrVND6-A2^{IR}, and PtrVND6-C1^{IR}*) of *PtrVND6s* from *P. trichocarpa* xylem tissue were identified through PCR cloning, RNA-seq, and 3' Rapid Amplification of cDNA End (3'-Race). By analyzing its transcripts and proteins of PtrVND6-C1^{IR} in *P. trichocarpa*, the PtrVND6-C1^{IR} has been shown to be preferentially expressed in stem differentiating xylem (SDX).

The alternative splicing of mRNA often produces a truncated protein rather than the full size protein with the normal function (Filichkin et al., 2010). In plants, alternative splicing of transcription factors often produces truncated proteins serving as the dominant-negative repressors in many biological processes. These dominant-negative repressors may inhibit transcription either by competing with transcriptional activators for DNA binding, or by interacting with transcriptional activators to form inactive heterodimers.

Truncated splice variants of transcription factors have been found for many processes, including starch metabolism, cold tolerance, flowering time control and secondary cell wall formation (Yuan et al., 2010; Seo et al., 2011a; Park et al., 2012; Seo et al., 2012; Li et al., 2012b; Posé et al., 2013). In differentiating xylem of *P. trichocarpa*, splicing of *PtrSND1-A2* mRNA produces a truncated isoform through intron retention (Li et al., 2012b). Full size PtrSND1-A2 can activate secondary cell wall biosynthesis genes. Ectopic expression of *PtrSND1-A2* results in xylogenesis (Ohtani et al., 2012). The

truncated isoform can suppress the expression of PtrSND1 family members and *PtrMYB21*, suggesting an inhibitory role of the truncated isoform in secondary cell wall formation. Yeast two hybrids, subcellular localization, and BiFC demonstrated that the truncated PtrSND1-A2 protein forms heterodimers with PtrSND1 members (Li et al., 2012b).

PtrVND6-C1^{IR} undergoes the same splicing process of intron retention as PtrSND1-A2^{IR}, lacking the C terminus and the last α-helix of the NAC domain (Erst et al., 2004). Thus, PtrVND6-C1^{IR} may produce a similar product and result as PtrSND1-A2^{IR} – mediated attenuation of PtrSND1s and *PtrMYB21*. To test this hypothesis, transient transcriptional perturbation in *P. trichocarpa* stem-differentiating-xylem (SDX) protoplasts, transactivation in Arabidopsis leaf protoplasts, and electrophoretic mobility shift assays (EMSAs) were conducted to show the dominant negative inhibition of PtrVND6-C1^{IR} on *PtrMYB21*. The results demonstrated the inhibition activity of PtrVND6-C1^{IR} on the expression of *PtrSND1s* and *PtrVND6s.* The underlying mechanism of the inhibition of PtrVND6-C1^{IR} is still unknown.

To elucidate the mechanism of the inhibition, the interactions between the activators of *PtrMYB21* and *PtrVND6-C1^{IR}* were analyzed. PtrVND6-C1^{IR} protein was not found in the nucleus but in cytoplasmic foci. PtrVND6s were located in the nucleus, and PtrSND1s had been reported to be in the nucleus (Li et al., 2012). PtrVND6-C1^{IR} and the activators of *PtrMYB21* have different subcellular locations. Co-localization was used to examine the interactions between PtrVND6-C1^{IR} and PtrSND1s, PtrVND6s, because PtrSND1s and PtrVND6s may form heterodimers with PtrVND6-C1^{IR} that enable them to be at the same subcellular location.

Subcellular co-localization experiments show that PtrSND1s and PtrVND6s could translocate PtrVND6-C1^{IR} from cytoplasmic foci to the nucleus, suggesting the formation of heterodimers between PtrVND6-C1^{IR} and the activators of PtrMYB21. We

employed bimolecular fluorescence complementation (BiFC) to confirm the existence of heterodimers. To analyze whether PtrVND6-C1^{IR} inhibits other developing xylem-expressed NAC transcription factors by forming heterodimers, each of the developing xylem-expressed NAC transcription factors PtrSND2/3s, PtrSND1-L1s, PtrXND1, and PtrANAC1 were co-transfected with PtrVND6-C1^{IR}. PtrVND6-C1^{IR} could be translocated into the nucleus by each member, indicating that SND2/3s, SND1-L1s, XND1, and ANAC1 also form non-functional heterodimers with PtrVND6-C1^{IR}. These findings suggest that a PtrVND6-C1^{IR} –mediated attenuation mechanism can apply to all developing xylem expressed NACs.

3.3 Results

3.3.1 Characterization of the *PtrVNDs* transcript isoforms

Several groups identified a subfamily of wood-associated NAC domain transcription factors (*PtrWNDs; PtrVNSs; PtrSND-1s/PtrSND-2/3s/PtrVNDs*) that regulate the expression of secondary cell wall biosynthetic genes in poplar (Zhong et al., 2010a; Zhong et al., 2010b; Mitusha et al., 2011; Li et al., 2012b). We focused on all six *VND6* homologs, which were named *PtrVND6-A1, PtrVND6-A2, PtrVND6-B1, PtrVND6-B2, PtrVND6-C1, and PtrVND6-C2* (Li et al., 2012). The six *PtrVND6* members have the typical NAC gene structure of three exons and two introns according to the *P. trichocarpa v3.0 database* and encode mRNAs of 1.1 to1.4 kb.

PCR products with the expected size were amplified for each of the six PtrVND6s, and three other products that have larger sizes are amplified for *PtrVND6-A1*, *-A2* and *-C1* (Figure 1A). The larger product (-1.6kb) for *PtrVND6-C1* retained the second intron from incomplete splicing of its pre-mRNA, and the products (-1.3kb) from both *PtrVND6-A1* and *PtrVND6-A2* also retained the second intron (Figure 1B). To test whether the cloned intron-retaining cDNAs that was reverse-transcribed from the mature mRNA, *PtrVND6-A2* was analyzed by 3'RACE PCR. Sequences flanking the

poly (A) tail were amplified from SDX RNAs and two products were obtained. Sequencing of these products showed that the second intron of the P*trVND6-A2* was included in the larger product, whereas the smaller product had no introns.

To verify whether the alternative splicing variants exist constitutively in SDX, RNA-seq data from the mRNAs of 36 trees were extracted, and the exon-intron structures for the mRNAs of *PtrVND-6A1, PtrVND6-A2,* and *PtrVND6-C1* were examined. These second introns were clearly included in *PtrVND6-A1, PtrVND6-A2*, and *PtrVND6-C1* mRNA (Figure 4C). Furthermore, the three larger products can be PCR-amplified from another set of nine independent *P. trichocarpa* plants collected at different times. The retained second intron is found consistently under normal growth conditions for several members of *PtrVNDs* (Figure 4C and D). These second intron-retained splice variants of transcripts were named as *PtrVND6-A1^{IR}*, *PtrVND6-A2^{IR}*, and *PtrVND6-C1^{IR}*, respectively.

3.3.2 Expression of the isoforms of *PtrVND6s*

With the identification of the three splice variants with the conserved splicing form, the expression of *PtrVND6-A1^{IR}*, *PtrVND6-A2^{IR}*, and *PtrVND6-C1^{IR}* was further analyzed (Figure 1). Real time reverse transcription followed by polymerase chain reaction (RT-PCR) and RNA-seq showed that the transcripts of *PtrVND6-C1^{IR}* were more abundant than those of *PtrVND6-A1^{IR}* and *PtrVND6-A2^{IR}* in SDX tissue (Figure 1B). Furthermore, the ratio of intron retained mRNA to intron non-retained mRNA was measured to estimate the extent of alternative splicing. The three splicing variants were detected at similar ratios in SDX. The functions of *PtrVND6s* are redundant (Ohtani et al., 2011) and the exon-intron compositions of three splicing variants are similar, suggesting that the three splice variants use a similar mechanism to regulate the downstream genes. *PtrVND6-C1^{IR}* with the highest expression level was selected for further analyses.

To identify whether in some tissues that *PtrVND6-C1*^{IR} is preferentially spliced out, qRT-PCR was conducted to analyze the expression of *PtrVND6-C1* and *PtrVND6-C1*^{IR} in xylem, phloem, young shoots, roots, and leaves (Figure 2). The transcripts of *PtrVND6-C1*^{IR} are more abundant in SDX tissue than in the phloem, young shoots, roots and leaves. Furthermore, the transcript abundance ratio of *PtrVND6-C1*^{IR} to *PtrVND6-C1* in each tissue was highest in the SDX tissue (Figure 2B). PtrVND6-C1^{IR} is likely to participate in the biological processes of SDX tissue.

3.3.3 Splice variant *VND6-C1*^{IR} encodes a truncated NAC-Domain protein

We next analyzed whether the *PtrVND6-C1* ^{IR} transcripts are translated into proteins. The full-size *PtrVND6-C1* cDNA was predicted to produce a protein of 346 amino acids (aa) with a conserved N-terminal NAC domain (166 aa) and a C-terminal activation domain (180 aa) (Figure 3). The NAC domain mainly functions in DNA-binding and protein dimerization (Erst et al., 2004). The *PtrVND6-C1* ^{IR} cDNA encodes a predicted protein of only 180 aa because of a premature termination codon (PTC) in the retained second intron. The truncated protein is composed of the protein dimerization domain, the DNA binding domain and the C-terminal amino acid sequence encoded by the retained second intron that is upstream of the PTC (Figure 3).

Based on the predicted protein sequence of *PtrVND6-C1* ^{IR} and *PtrVND6-C1*, we designed two specific antibodies for detecting these two proteins in SDX tissues. A polypeptide in the NAC domain was selected to make antibodies that can distinguish PtrVND6-C1^{IR} and PtrVND6-C1 from the other five PtrVND6s in SDX tissues (Figure 3A). This antibody was designed to hybridize with the protein sequence of PtrVND6-C1 NAC domain so that it can recognize the PtrVND6-C1 and PtrVND6-C1^{IR} as different sized bands (NAC-antibody). Another polypeptide was selected at the unique

terminus of 24 amino acids that was translated from the retained second intron. The antibody generated from the polypeptides is PtrVND6-C1^{IR}-specific (IR-antibody).

The two antibodies were firstly examined for their specificity with the seven full-size PtrVND proteins (six PtrVND6s and PtrVND6-C1^{IR}) (Figure 3B). By using the NAC-antibody, the two bands with size corresponding to the predicted molecular masses of full length PtrVND6 (43kDa) and PtrVND6-C1^{IR} (22kDa) were detected in SDX tissues. The IR-antibody was used to further distinguish PtrVND6 and PtrVND6-C1^{IR}, and the results demonstrated the presence of PtrVND6-C1^{IR} in SDX tissue (Figure 3C). The identification of PtrVND6-C1^{IR} protein in SDX tissue indicated that nonsense mediated mRNA degradation (NMD) machinery doesn't rid the PtrVND6-C1^{IR} at the transcript level. Thus, the function of PtrVND6-C1^{IR} in SDX tissue should be analyzed in the following experiments.

3.3.4 Transcriptional activities of PtrVND6s and PtrVND6-C1^{IR} towards PtrMYB21

In Arabidopsis, *AtMYB46* can be directly activated by *AtVND6* (Zhong et al., 2008). *AtMYB46* can activate many genes involved in the biosynthesis of lignin, cellulose, and hemicelluloses (Ko et al., 2009), and *P. trichocarpa PtrMYB21*, the ortholog of Arabidopsis *AtMYB46*, can also activate secondary cell wall biosynthesis related genes (Zhong et al., 2011). The transcriptional activities of PtrVND6s and PtrVND6-C1^{IR} towards the *PtrMYB21* were tested. Each of the *PtrVND6* members (*PtrVND6-A1, PtrVND6-A2, PtrVND6-B1, PtrVND6-B2, PtrVND6-C1, PtrVND6-C2, and PtrVND6-C1^{IR}*) were overexpressed in *P. trichocarpa* SDX protoplasts. The transcript abundance of *PtrMYB21* was analyzed in the transfected protoplasts. All six full-size PtrVND6s could induce a two to five-folds increase in the abundance of endogenous *PtrMYB21* transcripts in SDX protoplasts (Figure 4). In contrast, overexpression of *PtrVND6-C1^{IR}* significantly reduced the *PtrMYB21* transcript level (Figure 4B). The

results show that all full-size PtrVND6s are activators of *PtrMYB21*, while PtrVND6-C1^{IR} is an inhibitor of *PtrMYB21*.

To further investigate whether PtrVND6-C1^{IR} is either a negative regulator or a positive regulator, effector–reporter-based gene transactivation assays were performed using each of the PtrVND6s or PtrVND6-C1^{IR} as an effector and using the *PtrMYB21* promoter driven GUS as a reporter (Figure 5). Each of the PtrVND6s was found to activate the expression of *PtrMYB21*, indicated by induced GUS activities. However, GUS activities were not significantly decreased in the protoplasts transformed with PtrVND6-C1^{IR}. PtrVND6-C1^{IR} did not activate or repress the expression of *PtrMYB21*, suggesting that PtrVND6-C1^{IR} serves as a negative regulator rather than a positive regulator. It is consistent with the protein structure of PtrVND6-C1^{IR} lacking a trans-activation domain and confirms the observed PtrVND6-C1^{IR}–mediated attenuation of *PtrMYB21* expression.

3.3.5 DNA binding ability of PtrVND6s and PtrVND6-C1^{IR} on PtrMYB21 promoter

Based on the above experiments of overexpression of *PtrVND6s* and *PtrVND6-C1^{IR}* in protoplasts and the effector-reporter assays, full-size PtrVND6s serve as activators for *PtrMYB21*, while PtrVND6-C1^{IR} functions as a negative regulator. To determine whether the function of PtrVND6s and PtrVND6-C1^{IR} on *PtrMYB21* is a result of direct binding of PtrVND6s and PtrVND6-C1^{IR} to the *PtrMYB21* promoter, EMSA experiments were performed using *E. coli* expressed NAC domains of PtrVND6s and full-size PtrVND6-C1^{IR}, and using biotin-labeled *PtrMYB21* promoter probes. Retardation of DNA probe mobility and probe competition demonstrated that each of the six full-size PtrVND6s can directly bind to conserved motifs in the *PtrMYB21* promoter (Figure 6). The results suggest that PtrVND6s can directly bind to the promoter of *PtrMYB21*, linking the PtrVND6s with secondary cell wall biosynthesis genes via PtrMYB21. However, PtrVND6-C1^{IR} did not bind to the *PtrMYB21* promoter

in the same conserved motifs. It suggests the PtrVND6-C1^{IR} has no DNA binding ability, and the reason for the loss of DNA binding activities may be the loss of the β6 subdomain in the NAC domain of PtrVND6-C1^{IR}. Similarly, the PtrSND1-A2^{IR} that has no β6 subdomain also cannot bind to the promoter of PtrMYB21, suggesting that the β6 subdomain plays an important role in DNA binding (Li et al., 2012).

Transactivation and EMSA results revealed that the splice variant PtrVND6-C1^{IR} negatively regulates *PtrMYB21* gene expression through a mechanism that is independent of an activation domain and independent of direct DNA binding activity on the *PtrMYB21* promoter (Figure 6). The mechanism by which PtrVND6-C1^{IR} inhibits its downstream genes needs to be elucidated. Based on the results, PtrVND6-C1^{IR} may negatively regulate *PtrMYB21* via repressing the expression of activators of *PtrMYB21* or by interacting with the activators of *PtrMYB21*.

3.3.6 Function of PtrVND6-C1^{IR} inhibiting the expression of PtrVND6s and PtrSND1s

To test whether PtrVND6-C1^{IR} affects the expression of the six full-size PtrVND6s and four full-size PtrSND1s, expression of these *PtrVND6s and PtrSND1s* was measured in the PtrVND6-C1^{IR} overexpression SDX protoplasts. Overexpression of *PtrVND6-C1^{IR}* in *P. trichocarpa* SDX protoplasts significantly reduced transcript abundance of five PtrVND6 gene members (*PtrVND-A1, -A2, -B1, -B2, -C2*) at two to four-folds, but had no significant impact on the expression of *PtrVND6-C1* (Figure 7B). In contrast, the transcript abundance of four *PtrSND1* gene members decreased but not as significantly as the PtrVND6s (Figure 7C). PtrVND6-C1^{IR} may reduce the transcript abundance of PtrMYB21 via inhibiting the expression of the activators of *PtrMYB21*. But the mechanism of PtrVND6-C1^{IR} inhibition of *PtrVND6s* and *PtrSND1s* is still unknown. Based on the protein structure of PtrVND6-C1^{IR}, it has the intact dimerization domain but no activation domain. Therefore, PtrVND6-C1^{IR} may form non-functional heterodimers with full-size PtrSND1s and PtrVND6s, leading to

attenuation of the expression of *PtrSND1*s, *PtrVND6*s, and their downstream target genes *PtrMYB21*. Additionally, previous research (Li et al., 2012b) showed that overexpression of *PtrSND1-A2^{IR}* in *P. trichocarpa* SDX protoplasts resulted in drastically reduced transcript abundance of the endogenous *PtrSND1-A1*, *-B1*, and *-B2*. The results suggest that the inhibitory function of PtrVND6-C1^{IR} and PtrSND1-A2^{IR} could have a similar mechanism to regulate the target genes.

3.3.7 *PtrSND1s and PtrVND6s*, activators of *PtrMYB21*, translocate PtrVND6-C1^{IR} from cytoplasmic foci to the nucleus

First, we expressed fluorescent fusion proteins with PtrVND6-C1^{IR} to reveal the subcellular location of PtrVND6-C1^{IR} in *P. trichocarpa* SDX protoplasts. The plasmids of *35S-PtrVND6-C1^{IR}: sGFP* and *35S-H2A-1: mCherry* were co-transfected into protoplasts (Figure 8). H2A-1 fused to mCherry was expressed as a nuclear marker. PtrVND6-C1^{IR} was located exclusively in small foci in the cytoplasm of the protoplasts but not in the nucleus. Previous studies showed that PtrSND1-A2^{IR} was also located in cytoplasmic foci (Lin et al., 2012). To determine whether the PtrSND1-A2^{IR} and PtrVND6-C1^{IR} are co-localized, a plasmid mixure of *35S-PtrVND6-C1^{IR}: sGFP* with *35S-PtrSND1-A2^{IR}: mCherry*, and *35S-PtrVND6-C1^{IR}: mCherry* with *35S-PtrSND1-A2^{IR}: sGFP* were co-transformed into protoplasts respectively, showing that PtrVND6-C1^{IR}were co-localized in cytoplasm foci, as PtrSND1-A2^{IR} did. The subcellular location of full-sized PtrVNDs were then tested further.

We co-transfected the protoplasts with the *35S-PtrVND6s: sGFP* and *35S-H2A-1: mCherry* nuclear marker. Each of the six full-size PtrVND6s co-localized with the nuclear marker (Figure 9A). Exclusive nuclear subcellular locations of these six PtrVND6s were observed for 90–95% of the transfected protoplasts examined, whereas PtrVND6s were found in both the nucleus and cytoplasmic foci in the remaining transformed protoplasts. A similar phenomenon also has been found for the protoplasts that were transformed with *35S-PtrSND1s: sGFP,* showing a nuclear

location of these four PtrSND1s for 85–95% of the transfected protoplasts (Li et al., 2012). These results demonstrate that these full-sized PtrVNDs are primarily located in the nucleus. The subcellular locations of PtrVND6C1^{IR} and full-size NAC domain (PtrVNDs, and PtrSNDs) are different.

To investigate how PtrVND6C1^{IR} affects the expression of PtrSNDs, PtrVNDs, and their downstream gene PtrMYB21 (Figure 7), we analyzed the interaction between PtrVND6C1^{IR} with PtrSNDs and PtrVNDs. To do this, a *35S- PtrVND6C1^{IR}:mCherry* fusion gene construct was co-transfected with each of the *35S-PtrSND1:sGFP* and *35S-PtrVND6s: sGFP* constructs into *P. trichocarpa* SDX protoplasts for co-localization. In the transformed protoplasts, PtrVND6C1^{IR} was translocated from cytoplasmic foci to the nucleus, demonstrated by nuclear co-localization of PtrVND6C1^{IR} (mCherry) with each of the full size PtrSND1s and PtrVND6s (sGFP) (Figure 10 and 11). These results suggest that PtrVND6C1^{IR} can form heterodimers with each of full-size PtrSND1s and PtrVND6s in the nucleus. We further used BiFC to demonstrate the existence of heterodimers formed by PtrVND6C1^{IR} and the full-size NAC proteins (Figure 12, Figure 16). Combined with our transactivation results (Figure 7 and 8), we suggested that the heterodimers without the intact activation domain may have weak activation ability, and could be regarded as non-functional heterodimers. The formation of the non-functional heterodimers may explain the PtrVND6C1^{IR}–mediated attenuation for *PtrMYB21.*

PtrSND1 members are self-activated (Li et al., 2012). PtrVND6C1^{IR} interferes with the formation of PtrSND1 homodimers, resulting in the unprocessed self-activation for repression of these PtrSND1s in PtrVND6C1^{IR} overexpressing protoplasts (Figure 7). We analyzed whether self-activation also happen for PtrVND6s, which leads to the down-regulation of PtrVND6s in PtrVND6C1^{IR} overexpressing protoplasts (Figure 7).

3.3.8 Self-activation and cross-regulation of PtrVND6s

Transactivation assays confirmed that each of the three full-size PtrVND6B2, PtrVND6C1, and PtrVND6C2 members could activate its own promoter (self-activation), indicated by induced β-glucuronidase (GUS) activities (Figure 12A). The other full-size PtrVND6A1, PtrVND6A2, and PtrVND6B1 have no self-activation activities (Figure 12). We then tested whether these three PtrVNDs can be regulated by PtrVND6B2, PtrVND6C1, and PtrVND6C2 using transactivation assays. The results showed that PtrVND6C1 can activate the expression of *PtrVND6A2*, and *PtrVND6B1*, and PtrVND6C2 can activate the expression of *PtrVNDA1*, *PtrVND6A2*, and *PtrVND6B1*, while PtrVND6B2 showed no significant up-regulation of these PtrVNDs (Figure 12B). Therefore, we suggested that PtrVND6C1^{IR} can suppress PtrVND6B2, PtrVND6C1, and PtrVND6C2 gene expression through inhibiting the self-activation of these PtrVND6s, whereas PtrVND6C1^{IR} suppresses *PtrVNDA1*, *PtrVND6A2*, and *PtrVND6B1* gene expression through inhibiting their upstream regulators PtrVND6C1 and PtrVND6C2. This mechanism can explain the down-regulation of PtrVND6s in PtrVND6C1^{IR} overexpressing protoplasts (Figure 7).

3.3.9 Secondary cell wall-related NAC family members PtrSND-2/3s and PtrSND-1Ls translocate PtrVND6C1^{IR} from cytoplasmic foci to the nucleus

Subcellular co-localization showed that PtrSND1s and PtrVND6s can translocate PtrVND6C1^{IR} from cytoplasmic foci to the nucleus, suggesting the formation of non-functional heterodimers between PtrVND6C1^{IR} and the activators of *PtrMYB21* (Figure 14). We further focused on whether PtrVND6C1^{IR} forms non-functional heterodimers with other secondary cell wall-related NAC family members. Secondary cell wall-related NACs PtrSND-2/3s and PtrSND1-like proteins are homologs of AtSND2/3, and PtrSND1s, respectively. The interactions between these NAC members and PtrVND6C1^{IR} were analyzed in SDX protoplasts. *35S-PtrSND2/3s:sGFP*, *35S-PtrSND1-Ls: sGFP* and *35S-H2A-1:mCherry* nuclear marker

plasmids were co-transfected in SDX protoplasts. Each of the PtrSND-2/3s and PtrSND-1L were co-localized with H2A in the nucleus (Figure 14). To co-transform PtrVND6C1^{IR} with each of the PtrSND-2/3s and PtrSND-1Ls members, PtrVND6C1^{IR}: mCherry fusion gene plasmids were mixed with the plasmids of each of the *35S-PtrSND-2/3:sGFP* and *35S-PtrSND-1L:sGFP* constructs, and each plasmid mix was transfected into *P. trichocarpa* SDX protoplasts. In the presence of each of the full-size PtrSND-2/3 and PtrSND-1L members, PtrVND6C1^{IR} was translocated from the cytoplasmic foci to the nucleus (Figure 14), suggesting that PtrVND6C1^{IR} has an ability to form non-functional heterodimers with each member of PtrSND-2/3 and PtrSND-1L.

3.4 Discussion

In animals and plants, alternative splicing events regulate development, differentiation and metabolism (Tao et al., 2010; Medina et al., 2013; Yabas et al., 2016; Blaby et al., 2014; Bazin et al., 2015). In plants, a major mode of alternative splicing is the retention of introns (Ner-Gaon et al., 2004), which often results in a truncated protein due to premature termination (Seo et al., 2011a; Seo et al., 2011b; Seo et al., 2013; Kelemen et al., 2013). Such truncated proteins derived from transcription factor genes, usually act as dominant negatives to suppress the function of the cognate TFs (Li et al., 2012; Syed et al., 2012; Kelemen et al., 2013; Filichkin et al., 2015). In *P. trichocarpa*, we previously identified *PtrSND1-A2^{IR}*, expressed in the intron-retained variant of *PtrSND1-A2*, that serves as a dominant negative regulator that forms non-functional heterodimers with their targets (Li et al., 2012). Here we demonstrated that PtrVND6-C1^{IR}, another dominant negative encoded by an intron-retained variant of *PtrVND6-C1*, suppresses the function of multiple members from PtrSND1 and PtrVND6 through forming heterodimers (Figure 7). We also found other secondary cell wall related NAC family members PtrSND1-Ls and PtrSND2/3s can translocate the VND6C1 splice variant in protoplasts, suggesting that the dominant negative regulation forming

heterodimers with splice variants may be a common regulatory mechanism for several NAC family members.

3.4.1 Bioinformatic and literature based analysis of alternative splicing of PtrVNDs

The function and regulation of PtrVND6C1^{IR} can be predicted using bioinformatics. Using Pfam to predict the protein domain of PtrVND6C1^{IR}, only the NAC domain can be identified as functional (Finn et al., 2010). psROBOT was used to investigate whether the retained second intron can be recognized by microRNA, and Ubpreb (predictor of protein ubiquitination sites) was used to investigate whether the PtrVND6C1^{IR}-specific C-terminal 24 amino acid (translated from the retained second intron) could be regulated by the ubiquitin system (Radivojac et al., 2010). The transcripts and proteins of PtrVND6C1^{IR} are not targets of miRNA and ubiquitin based on these predictions.

The sequence of PtrVND6A1^{IR}, PtrVND6A2^{IR}, and PtrVND6C1^{IR} were aligned using MEGA5.2 (Tamura et al., 2012). The three transcripts share the conserved sequence “CCACAGGCAAG” before the second intron. Our previously identified splice variant PtrSND1-A2^{IR} has a similar sequence “CTACTTGCAAG” in the same place. The consensus sequences identified between exon and intron are usually recognized as the splicing site that can bind to U1-snRNP (Matlin et al., 2005). In animals, the splicing sites are usually located in front of the intron and follow a degenerate consensus sequence YAG/GURAGU (Busch et al., 2012). The consensus sequence of PtrVND6A1^{IR}, PtrVND6A2^{IR}, and PtrVND6C1^{IR} identified between exon and intron suggests that the three alternative splicing transcripts may be regulated by a similar mechanism as in animals.

The similarity of PtrSND1-A2^{IR} and PtrVND6C1^{IR} in subcellular location was also observed. Previously, the PtrSND1-A2^{IR} was shown to be co-located with the marker

of the cytoplasmic processing body (P-body) (Xu et al., 2006;, Hao et al) unpublished data). P-bodies usually play fundamental roles in general mRNA decay, nonsense-mediated mRNA decay, and microRNA silencing (Kulkami et al., 2010). The subcellular locations of PtrVND6C1^{IR} and PtrSND1-A2^{IR} in P-bodies suggests that the two splice variants may be involve with the regulation of mRNA stability (Figure 8). But the prediction of RNA binding sites in the amino acid sequences of PtrVND6C1^{IR} and PtrSND1-A2^{IR} didn't identify any RNA-binding sequences in these two splice variants.

3.4.2 Bioinformatic and literature based expression analysis identified the activators of PtrMYB21 and showed that the activators of PtrMYB21 can be co-expressed with *PtrVND6C1^{IR}*

PtrSND1 family members have been identified as the activators for *PtrMYB21* (Zhong et al., 2011; Ohtani et al., 2011; Li et al., 2012). Previous work and this research also found that full-size *PtrVND6* family members can activate the expression of *PtrMYB21* (Ohtani et al., 2011). Analysis of co-expression of these activators of *PtrMYB21* and PtrVND6C1^{IR} in developing xylem could demonstrate whether PtrVND6C1^{IR} affects the expression of these activators in the same cells.

Global gene expression analysis using microarrays and RNA-seq have greatly expanded our understanding of gene expression profiles in *P. trichocarpa* differentiating xylem (Dharmawardhana et al., 2010; Ko et al., 2012; Bao et al., 2013). With whole-transcriptome analysis of specific tissues, the stem differentiating xylem-specific transcriptome has been generated (Ko et al., 2012). Members of *PtrSND1* and *PtrVND6* families have been analyzed for expression in *P. trichocarpa* differentiating xylem. Expression of *PtrSND1s* and *PtrVND6s* increases in the stem where the transition from primary to secondary xylem occurs in *P. trichocarpa* (Dharmawardhana et al., 2010), suggesting that these activators of *PtrMYB21* are involved in wood formation. RNA-seq of 18 different trees of the single *P. trichocarpa*

genotypes collected from different places verified that these *PtrSND1s* and *PtrVND6s* are constantly expressed in developing xylem (Bao et al., 2013). Some of the *PtrSND1s* and *PtrVND6s* have been further studied using *in situ RNA hybridization* and promoter-GUS assays. In primary xylem, *PtrVND6s* are specifically expressed in vessel cells while the *PtrSND1s are* specifically expressed in fiber cells. In secondary xylem, *PtrVND6s* and *PtrSND1s* had a similar expression pattern in both vessel and fiber cells (Ohtani et al., 2011), suggesting that *PtrSND1s* and *PtrVND6s,* activators of *PtrMYB21,* function together in secondary xylem.

3.4.3 The formation of the heterodimers with PtrVND6C1^{IR} may not be confined to the secondary wall related NACs

We found PtrVND6C1^{IR} can be translocated by PtrSND1s, PtrVND6s, PtrSND2/3s, and PtrSND1-Ls, suggesting that these secondary wall related NAC proteins can form heterodimers with PtrVND6C1^{IR}. Other NACs not involving secondary wall formation may also form heterodimers with PtrVND6C1^{IR}. To test this hypothesis, we fused PtrXND1 and PtrANAC1 with GFP, and co-transformed these fused proteins with *35S-H2A-1: mCherry* and *PtrVND6C1^{IR}-cherry* in SDX protoplasts, respectively. When these fused proteins co-expressed with H2A-1: mCherry, PtrXND1 proteins were in both the nucleus and the cytosol, whereas PtrANAC1 proteins were exclusively in nucleus, with mCherry fluorescences as nucleus marker (Figure 14). By co-expressing PtrXND1-GFP with PtrVND6C1^{IR}-cherry in the protoplasts, cherry fluorescence changed from cytosol to the nucleus. Similarly, PtrVND6C1^{IR} was translocated into the nucleus by PtrANAC1. The translocations of PtrVND6C1^{IR} by the full-size NAC proteins may not be confined to secondary wall related NAC family members.

The NAC domain proteins can be classified into eight subfamilies based on their protein similarity, including NAC-a, NAC-b, NAC-c, NAC-d, NAC-e, NAC-f, NAC-g, NAC-h. A phylogenetic tree and sequence alignment of all the NAC proteins that can translocate PtrVND6C1^{IR} showed these proteins are from all eight subfamilies (Figure

15). The splice variants may exert broad inter-family regulation through the formation of heterodimers with these 72 NAC domain proteins that are expressed in *P. trichocarpa* SDX tissue (Shi et al., 2017).

3.5 Conclusion and perspectives

A naturally occurring alternative splice variant of PtrVND6C1 has been detected in stem differentiating xylem. The splice variant PtrVND6C1^{IR} has been identified as a negative regulator. This protein forms heterodimers with the normally spliced PtrVND6s and PtrSND1s, which can be self-activated or cross-regulated. We proposed that the heterodimers have no activation activity, but still bind to the promoters of their targets. Future studies should provide direct evidence for the dominant negative function of the heterodimers. Another research focus is the detection of these heterodimers in the stem differentiating xylem.

3.6 Materials and Methods

3.6.1 Plant materials

P. trichocarpa plants (genotype *Nisqually-1*) were cultured and maintained in a greenhouse as described by Song et al., (2006). Stem internodes of healthy 6- to 9-month-old plants were harvested for RNA, protein, and protoplast isolation.

3.6.2 RNA extraction, RT-PCR, PCR cloning and qRT-PCR

Total RNAs were isolated from SDX, phloem, young shoots, leaves, roots, and SDX protoplasts as described in Li et al., (2012). To synthesize cDNAs, reverse transcription was performed as described (Shi and Chiang, 2005). The full-length cDNAs of *PtrVND6A1*, *PtrVND6A2*, *PtrVND6B1*, *PtrVND6B2*, *PtrVND6C1*, *PtrVND6C2*, *PtrVND6A1^{IR}*, *PtrVND6A2^{IR}*, and *PtrVND6C1^{IR}* were amplified from SDX RNA by using primer sets (Table 1) respectively, and cloned into *pENTR/D-TOPO*

vectors (Invitrogen) for sequencing. qRT-PCR was performed as described (Li et al., 2012). It was used to detect the transcript abundances of PtrVNDs in different tissues, and of PtrMYB21 in the PtrVNDs, PtrVND6C1^{IR} and sGFP (control) transfected SDX protoplasts, using primers listed in Table 1, with three biological replicates and three technical repeats for each biological replicate.

3.6.3 RNA-Seq analysis of intron/exon sequence depth of the transcripts of *PtrVND6A1*, *PtrVND6A2*, and *PtrVND6C1* Genes

Total RNAs of SDX were isolated using the RNeasy Plant RNA Isolation kit (Qiagen). RNAseq libraries were prepared following the TruSeq RNA Sample Preparation Guide (Illumina) with modifications. Ten micrograms of total RNAs were used for mRNA purification using Sera-Mag Magnetic Oligo (dT) beads. The mRNA was fragmented and reverse transcribed into double-strand cDNA, followed by end repair and 3'end adenylation. The cDNA was ligated to adapters, where the PE adapter Oligo mix was substituted with multiplex adapters from the multiplex oligo only kit. The cDNA was electrophoresed on a 2% (wt/vol) agarose gel. The fraction of 200 ± 25 bp was excised from the gel with a GeneCatcher Disposable gel excision tip, and cDNA was purified with a QIAquick Gel Extraction Kit (Qiagen). The TruSeq protocol incorporated the following three steps to enrich the cDNA during amplification: (i) PCR Primer PE 1.0 and PE 2.0 were substituted with InPE 1.0 and 2.0 primers from the multiplex oligo only kit; (ii) 1 µL of index primer was included; and (iii) the number of PCR cycles was increased to 18. Then RNA-seq libraries were adjusted to 1 nM and pooled for a multiplex sequencing run. The pooled libraries were denatured and annealed to a lawn of oligos on a lane of a flow cell using a cBot. Once clonal clusters were produced, the sequencing primer was annealed, and the sequencing run was carried out using reversible terminator dye chemistry on a GAIIx. The RNAseq libraries were sequenced by using the Illumina GAIIx platform at the Genomic Science Laboratory, NCSU, USA. The resulting FASTAQ files from Illumina GAIIx were mapped to the genome of *P. trichocarpa* version 2.2 using Bowtie and Tophat. Multiple BAM (Binary sequence

Alignment Map) files were merged using SAM tools and the intron and exon junction of each gene was visualized using IGV (Integrative Genomics Viewer) (Tuskan et al., 2006; Langmead et al., 2009; Li et al., 2009; Thorvaldsdóttir et al., 2012; Kim et al., 2013). The intron and exon junction results that showed alternative splicing were averaged with the data of 12 libraries collected from 36 trees.

3.6.4 Western blotting

Recombinant full length protein production of PtrVND6 members in E. coli. The full length cDNAs of *PtrVND6A1*, *PtrVND6A2*, *PtrVND6B1*, *PtrVND6B2*, *PtrVND6C1*, and *PtrVND6C2* were amplified with primer sets *A1Pr-F/-FLR*, *A2Pr-F/-FLR*, *B1Pr-F/-FLR*, *B2Pr-F/-FLR*, *C1Pr-F/-FLR*, *C2Pr-F/-FLR*, and *C1Pr-F/-C1^{IR}PrFLR* (Table 1), respectively. Full length sequence of each *PtrVND6A1*, *PtrVND6A2*, *PtrVND6B1*, *PtrVND6B2*, *PtrVND6C1*, *PtrVND6C2*, and *PtrVND6C1^{IR}* were digested and cloned into *pGEXKG1* (GE Life Science) at the XbaI/XhoI sites. The expression constructs were transferred into *E. coli* BL21 (DE3) (Invitrogen). The transformed *E. coli BL21*s were subcultured in 500ml LB until the OD_{600} of the bacteria reached 0.4-0.6 and then the expression of these genes was induced with IPTG at 4mM at 16 °C for 16h.

Purification of NAC domain proteins of PtrVND6 members for western blotting. The incubated *E. coli* expressing full length proteins was collected and suspended in 20 mL of PBST buffer (1× PBS, pH 7.4, 5 mM EDTA, 1% Triton X-100, 1 mM PMSF, 0.05% β-mercaptoethanol). Cells were disrupted by using a Branson Digital Sonifier for 15 min (each pulse for 30s-10s on /20s off; 21% amplification). The cell lysates were centrifuged at 12,000 × g for 30 min at 4 °C. The supernatant was mixed with 1 mL of glutathione-S-agarose beads (Sigma) and held at 4 °C for 45 min with gentle shaking. The beads were washed eight times with PBST buffer without PMSF and were held at room temperature for 30 min in 3 mL of thrombin cleavage buffer (50 mM Tris pH 8.0, 150 mM NaCl, 2.5 mM $CaCl_2$, 0.05% β-mercaptoethanol) with 20 units of thrombin to remove GST. The protein with no GST tag was concentrated and desalted

with an Amicon Ultra centrifugal filter (Ultra-15, MWCO 10kDa used for full size PtrVND6-A1^{IR}, A2^{IR}, C1^{IR}; Ultra-4, MWCO 30kDa used for full size PtrVNDs) in 300 µl.

Antibody production and specificity test. We synthesized the several peptide sequences from VND members, including -WKATGRADKAIYSKHD from VND6A1 N-terminal NAC domain sequence, -FWKATGRDKAIYSKQ from VND6A2 N-terminal NAC domain sequence, -GFWKATGRDKSVYDKT from VND6C1 N-terminal NAC domain sequence, and -TLPPSPPQLICHTIKVKA from VND6C1^{IR} intron-translated sequence. These sequences were conjugated with keyhole limpet hemocyanin, and used to immunize rabbits for polyclonal antibody production (Antagene). The purified recombinant VND proteins (full length proteins *VND6-A1/-A2/-B1/-B2/-C1/-C2/-A1^{IR}/-A2^{IR}/-C1^{IR}*) were used in western blotting to test the specificity of these polyclonal antibodies.

SDX nuclear protein preparation. For nuclear protein extraction from *P. trichocarpa* stem differentiating xylem (SDX), three fresh and juicy SDX tissues were collected to isolate nuclei by using a CelyticTM PN Isolation kit (Sigma). The tissues were disrupted in 5 mL of 1× Nuclei Isolation Buffer (NIB; Sigma) containing 1mM DTT, 10% (wt/wt) polyvinylpolypyrrolidone, 1mM PMSF,1 mg/mL pepstatin A, 1 mg/mL leupeptin. The disrupted samples were then homogenized for 10 min in 0.5% Triton X-100 on ice. The tissue lysates were loaded onto a freshly prepared density gradient, which contained 3 mL of 60% (vol/vol) percoll in 1× NIB buffer (the second layer) and 3 mL of 2.3 M sucrose (the bottom layer). After centrifugation at 3,200 × g for 30 min, most of the nuclei are in a band between the percoll layer and the sucrose layer. The sample containing the nuclei were collected, and then washed with 8 mL of 1× NIB buffer. The washed nuclei were collected by centrifugation at 12,000 × g for 5 min. 100 µL of working extraction buffer containing 5 mM DTT were used to resuspend the nuclei. The resuspended mixtures were vortexed for 30min at 4 °C, and then centrifuged at 12,000 × g for 10 min. The supernatant containing the soluble proteins

was collected and stored for western blotting. All reagents were prepared following Li et al., (2014).

Western blotting assays for detecting PtrVND6-A1^{IR}, PtrVND6-A2^{IR}, and PtrVND6-C1^{IR} proteins in SDX nuclear protein extracts. Each antibody for the VND6C1 NAC domain and VND6C1^{IR} intron-translated sequence was used to detect PtrVND6C1 and PtrVND6-C1^{IR} in SDX nuclear protein extracts. Western blot analysis was carried out as in Chen et al. 2011.

3.6.5 EMSA (Electrophoretic Mobility Shift Assay)

Recombinant NAC domain protein production of PtrVND6 members in E. coli. The NAC domain coding regions of *PtrVND6A1*, *PtrVND6A2*, *PtrVND6B1*, *PtrVND6B2*, *PtrVND6C1*, and *PtrVND6C2* were amplified with primer sets A1Pr-F/-NACR, A2Pr-F/-NACR, B1Pr-F/-NACR, B2Pr-F/-NACR, C1Pr-F/-NACR, and C2Pr-F/-NACR (Table 1), respectively. Each NAC coding sequence of *PtrVND6A1*, *PtrVND6A2*, *PtrVND6B1*, *PtrVND6B2*, *PtrVND6C1*, and *PtrVND6C2* were digested and cloned into *pGEXKG1* (GE Life Science) at the XbaI/XhoI sites. The expression constructs were transferred into *E. coli* BL21 (DE3) (Invitrogen). The *E. coli* BL21s were subcultured in 250ml LB until the OD_{600} reached 0.5-0.8 and then protein expression (as GST fusion) was induced with 0.5 M IPTG at 28 °C for 8 h.

Purification of NAC domain proteins of PtrVND6 members for EMSA. The *E. coli* expressing NAC domain proteins was collected and treated as described for the full length VND proteins. The GST-free protein was concentrated and desalted with an Amicon Ultra centrifugal filter (Ultra-15, MWCO 10kDa) in 300 µl. The purity and concentration were measured by Bradford and Commassie Brilliant Blue assays as described in Li et al., 2012.

In vitro DNA binding assays. The motif prediction tool Multiple EM for Motif Elicitation (MEME; http://meme.sdsc.edu/meme/cgi-bin/meme.cgi) was used to

analyze the SNBE (Secondary Wall NAC Binding Elements) sequences in our the ~ 2-kb promoter of *PtrMYB021* (Zhong et al., 2010). Promoter fragments, harboring the putative SNBE motifs, were amplified by using primers 021EMSA-F/-R from *PtrMYB021* promoters, respectively (Table). The PCR products were gel-extracted following a silicon based protocol (Li et al., 2010). These fragments were biotin-labeled at the 3′ end (Biotin 3′ End DNA labeling kit; Thermo Scientific). The Lightshift® Chemiluminescent EMSA kit was used to perform the further analyses (Thermo Scientific). The biotin-labeled DNA fragments were mixed with 100 ng of each purified NAC domain protein of VND6-A1/-A2/-B1/-B2/-C1/-C2 and full length protein of VND6C1^{IR} for 20 min in the binding buffer (10 mM Tris, pH 7.5, 50 mM KCl, 1 mM DTT, 2.5% (vol/vol) glycerol, 5 mM MgCl2, 0.05% Nonidet P-40, and 100 ng/uL poly (dI-dC)) at room temperature. Unlabeled promoter fragments in 20 to 100-fold molar excess relative to the labeled probes were used in the competition assays. Protein-DNA mixtures were run on a 6% (wt/vol) native PAGE at 100 V, 4 °C for 2–3 h. The DNA was transferred to a nylon membrane (Amersham Hybond-N$^+$) at 100 V, 0.38 A, 40 min, and crosslink 60 seconds at 120mJ/cm^2 using a commercial UV-light crosslinking instrument equipped with 254nm bulbs (Cole-Parmer). The DNA on the nylon membrane was washed and detected by a chemiluminescence nucleic acid detection module (Thermo Scientific).

3.6.6 Effector-reporter based gene transactivation assays

The ~ 2-kb promoters of *PtrVND6A1, PtrVND6A2, PtrVND6B1, PtrVND6B2, PtrVND6C1*, and *PtrVND6C2* were identified based on the *Phytozome v9.1*. These promoters were amplified using primer sets MYB021prom-F/-R, A1prom-F/-R, A2prom-F/-R, B1prom-F/-R, B2prom-F/-R, C1prom-F/-R, and C2prom-F/-R (Table 1). The PCR products of VND6A1 and VND6A2 were digested using PstI and XbaI, and using SbfI and XbaI, respectively, whereas *PtrVND6-B1, PtrVND6-B2, PtrVND6-C1*, and *PtrVND6-C2* promoters were digested with PstI and BamHI. These digested

fragments were then inserted into *pUC19-35S-GUS* (Li et al., 2012), generating *pUC19-35S-PtrVND6-A1P-GUS, pUC19-35S-PtrVND6-A2P-GUS, pUC19-35S-PtrVND6-B1P-GUS, pUC19-35S-PtrVND6-B2P-GUS, pUC19-35S-PtrVND6-C1P-GUS,* and *pUC19-35S-PtrVND6-C2P-GUS*. Each of the full length cDNAs of *PtrVND6A1, PtrVND6A2, PtrVND6B1, PtrVND6B2, PtrVND6C1, PtrVND6C2,* and *PtrVND6C1 ^{IR}* was amplified by VND6A1 F/R, VND6A2 F/R, VND6B1 F/R, VND6B2 F/R, VND6C1 F/R, VND6C2 F/R, and PtrVND6C1F/ C1 ^{IR}-R (Table 1) and cloned in pENTR/D-TOPO vectors. Then these vectors were used for LR recombination to replace the *RfA* in *pUC19-35S-RfA-35S-sGFP* (Li et al., 2012). By these reactions, the effector vectors are generated as *pUC19-35S-PtrVND6A1-35S-sGFP, pUC19-35S-PtrVND6A2-35S-sGFP, pUC19-35S-PtrVND6B1-35S-sGFP, pUC19-35S-PtrVND6B2-35S-sGFP, pUC19-35S-PtrVND6C1-35S-sGFP, pUC19-35S-PtrVND6C2-35S-sGFP and pUC19-35S- PtrVND6C1 ^{IR} -35S-sGFP.* Then, the plasmid DNAs for effectors and reporters were prepared using CsCl density gradient ultracentrifugation (Sambrook et al., 1989). Each combination of effector and reporter was co-transformed into protoplasts isolated from Arabidopsis leaves as described in Yoo et al., 2007. After incubation of 12h, the transfected protoplasts were collected, frozen in liquid nitrogen, and then lysed for GUS assays.

3.6.7 Overexpression of PtrVND6A1, PtrVND6A2, PtrVND6B1, PtrVND6B2, PtrVND6C1, PtrVND6C2, and PtrVND6C1^{IR} in SDX protoplasts

Using LR reactions, PtrVNDs in *pENTR/D-TOPO* vectors were transferred to replace the RfA in *pUC19-35S-RfA-35SsGFP* described in Li et al., 2012, giving expression vectors *pUC19-35S-PtrVND6A1-35S-sGFP*, *pUC19-35S-PtrVND6A2-35S-sGFP*, *pUC19-35S-PtrVND6B1-35S-sGFP*, *pUC19-35S-PtrVND6B2-35S-sGFP*, *pUC19-35S-PtrVND6C1-35S-sGFP*, *pUC19-35S-PtrVND6C2-35S-sGFP* and *pUC19-35S-PtrVND6C1^{IR}-35S-sGFP*. Then, the plasmid DNAs of expression vectors were purified using CsCl gradients and used to transform SDX protoplasts. Each transfection reaction was carried out in a 10× volume compared to that of Chen et al. 2011 and

incubated in a 100 × 15-mm^2 Petri dish for 12 h. The protoplasts were collected by centrifugation at 300 × g for 3 min and frozen in liquid nitrogen. Total RNA of the protoplasts was isolated using an RNeasy Plant RNA Isolation kit (Qiagen), and 1 ng of total RNA was used for qRT-PCR analysis.

3.6.8 Protein subcellular localization

Constructs for full length NACs *(PtrVND6s*, *PtrSND2/3s*, *PtrSND-1Ls* as shown in Table 1) and GFP fusion proteins were prepared to examine subcellular localization of each of these NAC members. The coding regions of these full-length NACs, and *PtrVND6C1^{IR}* were amplified using primer pair sets (Table 1), respectively, with a BamHI restriction site included in the forward primers and a XhoI restriction site in the reverse primers. After being cloned into *pGEMT easy* vectors and sequenced, the coding regions were further digested to generate the fragments. These fragments then were ligated into *pUC19-35S-sGFP* (Chen et al., 2011; Li et al., 2012), giving *PUC19-SND2/3L1:sGFP, PUC19-SND2/3L2:sGFP, PUC19-SND2/3A1:sGFP, PUC19-SND2/3A2:GFP, PUC19-SND2/3B1:sGFP, PUC19-SND2/3B2:sGFP, pUC19-35S-PtrVND6A1:sGFP, pUC19-35S-PtrVND6A2:sGFP, pUC19-35S-PtrVND6B1:sGFP, pUC19-35S-PtrVND6B2:sGFP, pUC19-35S-PtrVND6C1:sGFP, pUC19-35S-PtrVND6C2:sGFP*, and *pUC19-35S- PtrVND6C1 ^{IR} :sGFP*. Additionally, we also used *pUC19-35S-PtrH2A-cherry* plasmids to mark the nucleus. *pUC19-35S-PtrSND1-A2^{IR}: mCherry, pUC19-35S-PtrSND1-A1: sGFP, pUC19-35S-PtrSND1-A2: sGFP, pUC19-35S-PtrSND1-B1: sGFP, pUC19-35S-PtrSND1-B2: sGFP, and pUC19-35SPtrSND1-A2IR:sGFP* were provided by Li et al., 2012, and *pUC19-35S-PtrVND6C1^{IR}:mCherry*, was generated by replacing H2A-1 with PtrVND6C1^{IR} in *pUC19-35S-H2A:mCherry* using BamHI/ XhoI sites. Each of the NAC-GFP fusions was cotransformed with *H2A-1: mCherry*, *PtrVND6C1^{IR}: mCherry*, *PtrSND1-A2^{IR}: mCherry*, into SDX protoplasts. The fluorescence was observed under a Zeiss LSM 710 laser scanning microscope.

The excitation wavelength and the emission wavelength are 488 nm and 492–543 nm, respectively, for GFP, and 561 nm and 582–662 nm, respectively, for mCherry.

3.6.9 BiFC

The coding region of NACs (*PtrVND6s*, *PtrSND2/3s*, *PtrSND-1Ls*) was digested out of the *pGEMT*-vectors in subcellular localization experiments using enzymes BamHI and XhoI. These BamHI/XhoI fragments were cloned into *pSCYNE(R)* vectors, resulting in *35S-CFP^{N}-NAC* vectors. Similarly, each of coding regions was cloned into *pSCYCE(R)*, resulting in *35S-CFP^{c}-NAC* vectors. Each combination of the constructed *pSCYNE(R)* and *pSCYCE(R)* together with *H2A-1:mCherry* were co-transformed into SDX protoplasts. After incubation for 12 h, SDX protoplasts were collected and examined under a Zeiss LSM 710 laser scanning microscope. For fluorescence detection, the excitation wavelength and the emission wavelength were 458 nm and 462–531 nm, respectively, for CFP, and 561 nm and 598–648 nm, respectively, for mCherry.

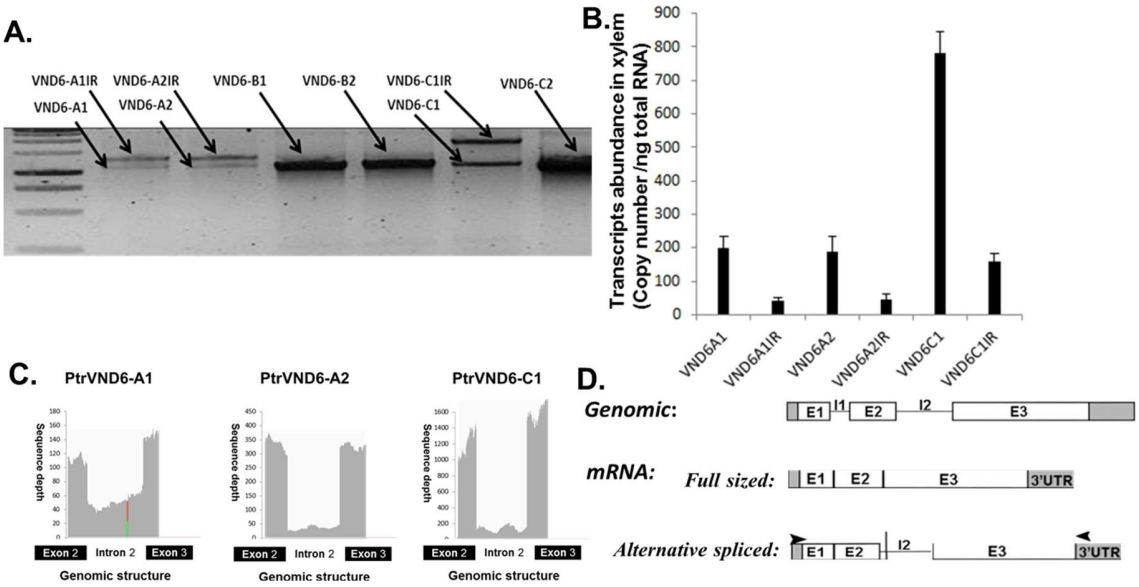

Figure 1. Discovery of alternative splicing of PtrVNDs transcripts. (A). PCR amplification of PtrVND6 members *PtrVND6A1*, *PtrVND1A2*, *PtrVND6B1*, *PtrVND6B2*, *PtrVND6C1* and *PtrVND6C2*. **(B).** The expression of splicing forms of *PtrVND6A1*, *PtrVND1A2*, *PtrVND6C1* in SDX. **(C).** RNA-seq data of *PtrVND6A1*, *PtrVND6A2*, and *PtrVND6C1*. The red line in the plot means the single nucleotide difference between RNA seq reads and genome sequence. **(D).** The diagram showing that genomic and transcript structures of PtrVND6s and the intron retained isoforms.

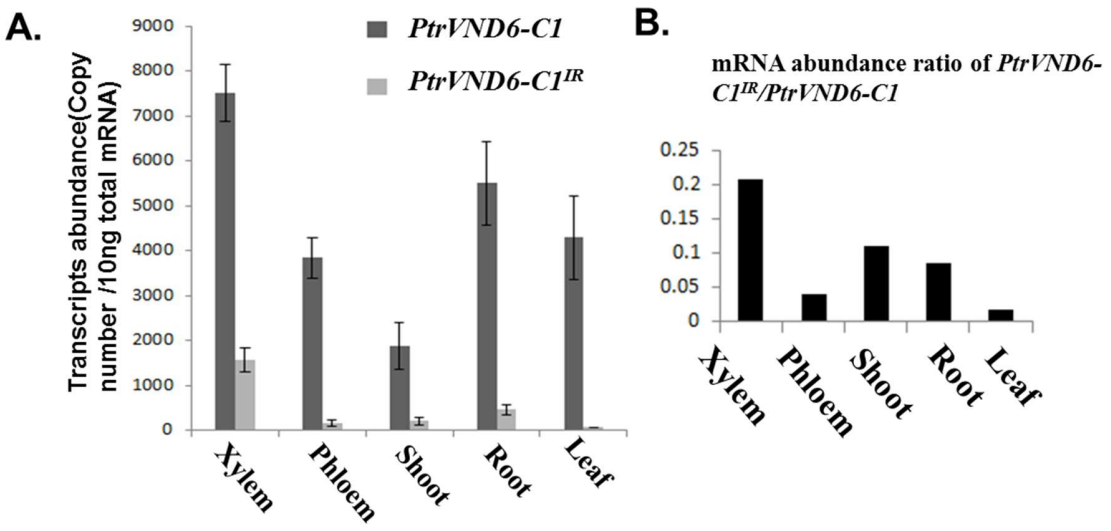

Figure 2. Expression of *PtrVND6C1* and *PtrVND6-C1^{IR}* transcripts in xylem, phloem, shoots, roots, and leaves. (A). Tissue specific expression of the *PtrVND6-C1* (non-retained form) and *PtrVND6-C1^{IR}* (retained form) in xylem, phloem, shoots, roots, and leaves. **(B).** The ratio of *PtrVND6-C1^{IR}/PtrVND6-C1* in these tissues.

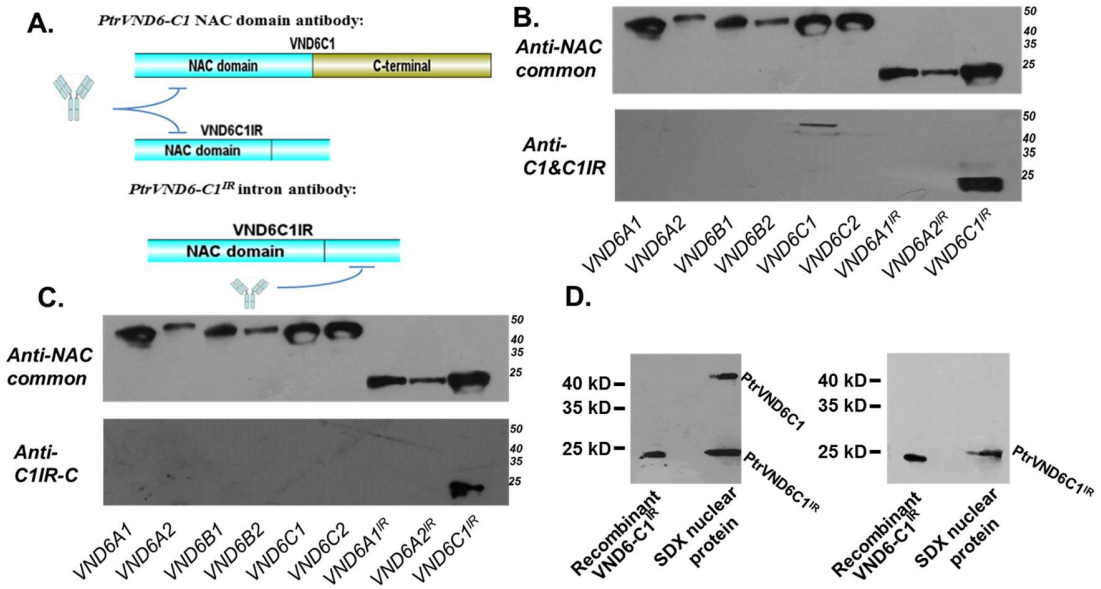

Figure 3. Western blot for antibody specificity and detecting the proteins PtrVND6C1 and PtrVND6-C1^{IR}. (A). The diagram shows the antibody that hybridizes with target proteins PtrVND6C1 and PtrVND6C1^{IR}. (**B) and (C).** Purified *E. coli* produced recombinant full length proteins from PtrVND6A1, PtrVND6A2, PtrVND6B1, PtrVND6B2, PtrVND6C1, PtrVND6C2, PtrVND6C1^{IR}, which were probed with the common NAC domain antibody, NAC antibody **(B),** and IR antibody **(C)**, respectively. **(D).** Western blot analysis of SDX total organelle proteins probed with the NAC antibody and probed with the C-terminal antibody (IR antibody).

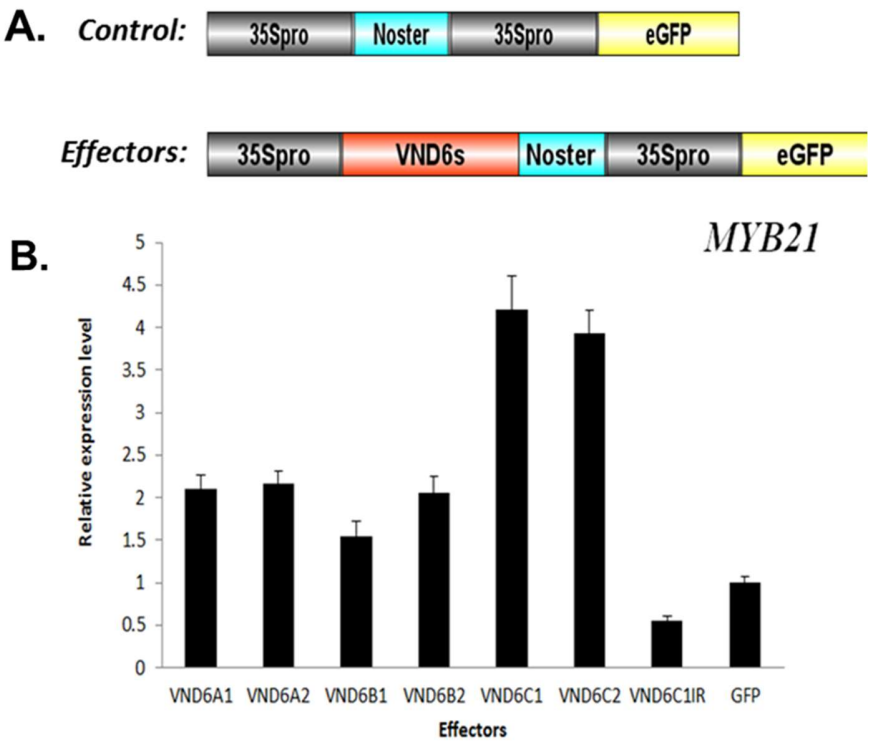

Figure 4. Relative expression level of *PtrMYB21* in protoplasts overexpressing PtrVND6s and PtrVND6-C1^{IR}. (A). Schematic diagrams of the effector plasmids that were transformed into SDX protoplast. **(B).** The relative expression level was normalized to the *PtrMYB021* transcript abundance of SDX protoplasts that expressed the modified PUC19 vector (*35s- NOS-35s-eGFP*). Error bars indicate one standard error (SE).

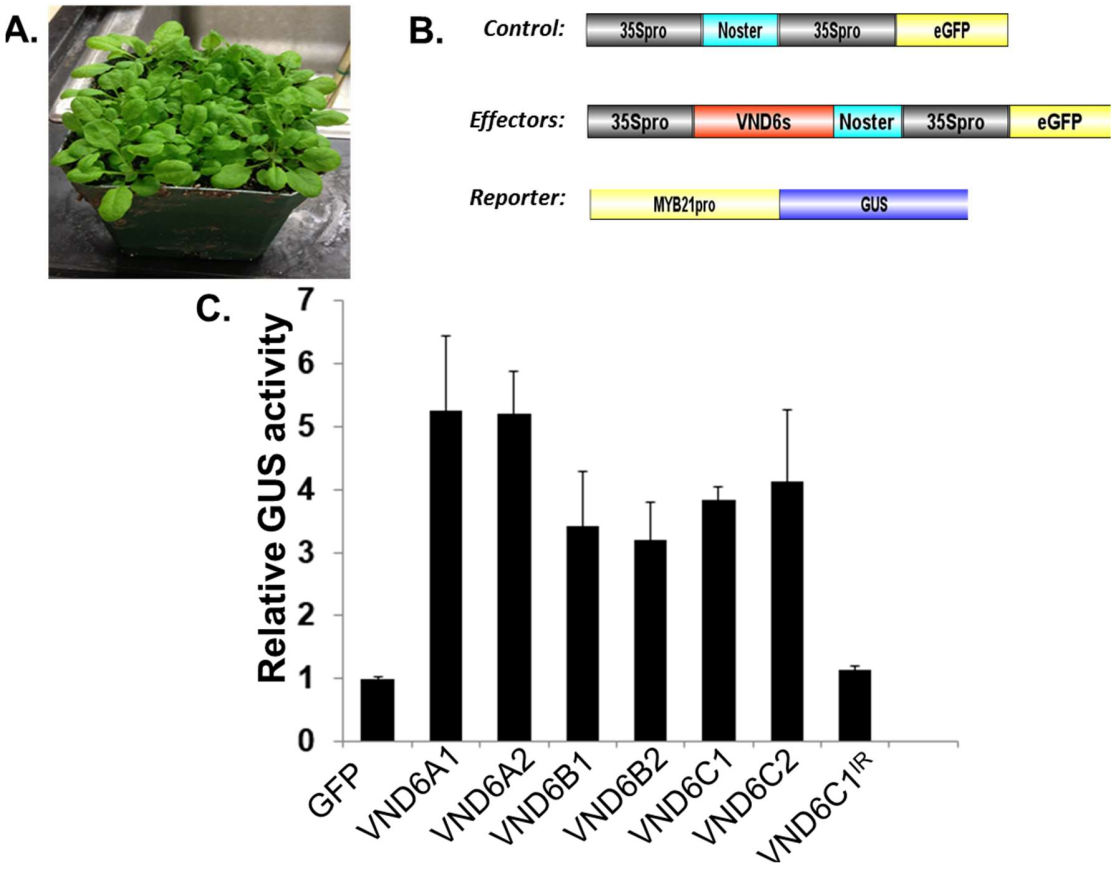

Figure 5. Effector–reporter-based gene assays for PtrVND6s activity. **(A).** The 4-week-old *Arabidopsis thaliana Col* used for extracting Arabidopsis leave protoplasts. **(B).** Schematic diagrams of the effector and reporter plasmids that were transformed into leaf protoplasts. **(C).** Effector–reporter-based gene transactivation assays in *Arabidopsis* leaf protoplasts. The activity of GUS in each sample is shown as relative value when compared to control. Error bars indicate one standard error.

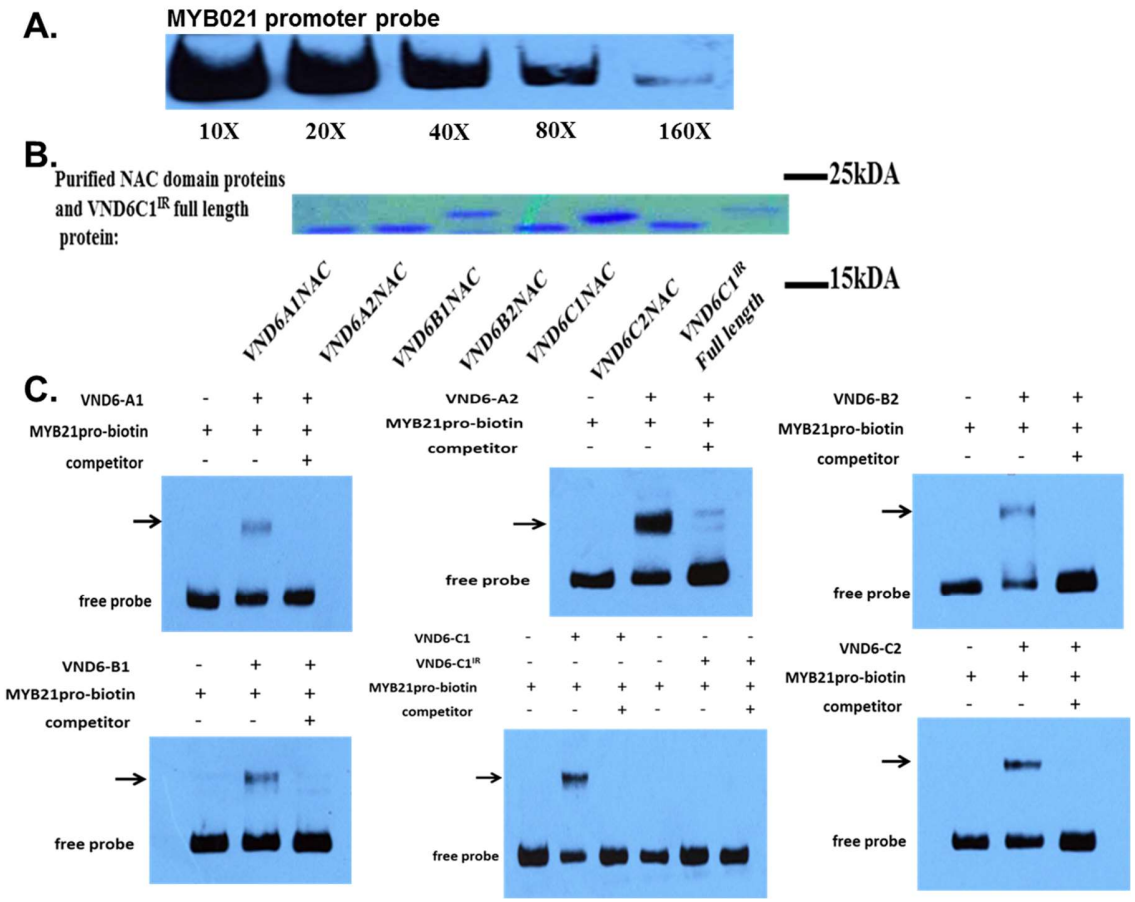

Figure 6. EMSA shows that the binding ability of PtrVND6s to *PtrMYB21* promoters. **(A).** The labeling of *PtrMYB21* promoter-biotin probe. Based on the results, the concentration was diluted to 80x and a 30s exposure time was used in the following experiments. **(B).** Commassie blue stain of PtrVND6s recombinant proteins used in the following experiments. **(C).** EMSA shows that full size PtrVND6s can bind to the promoter of *PtrMYB21*, and the PtrVND6-C1^{IR} can't. The arrow shows the shifted complex.

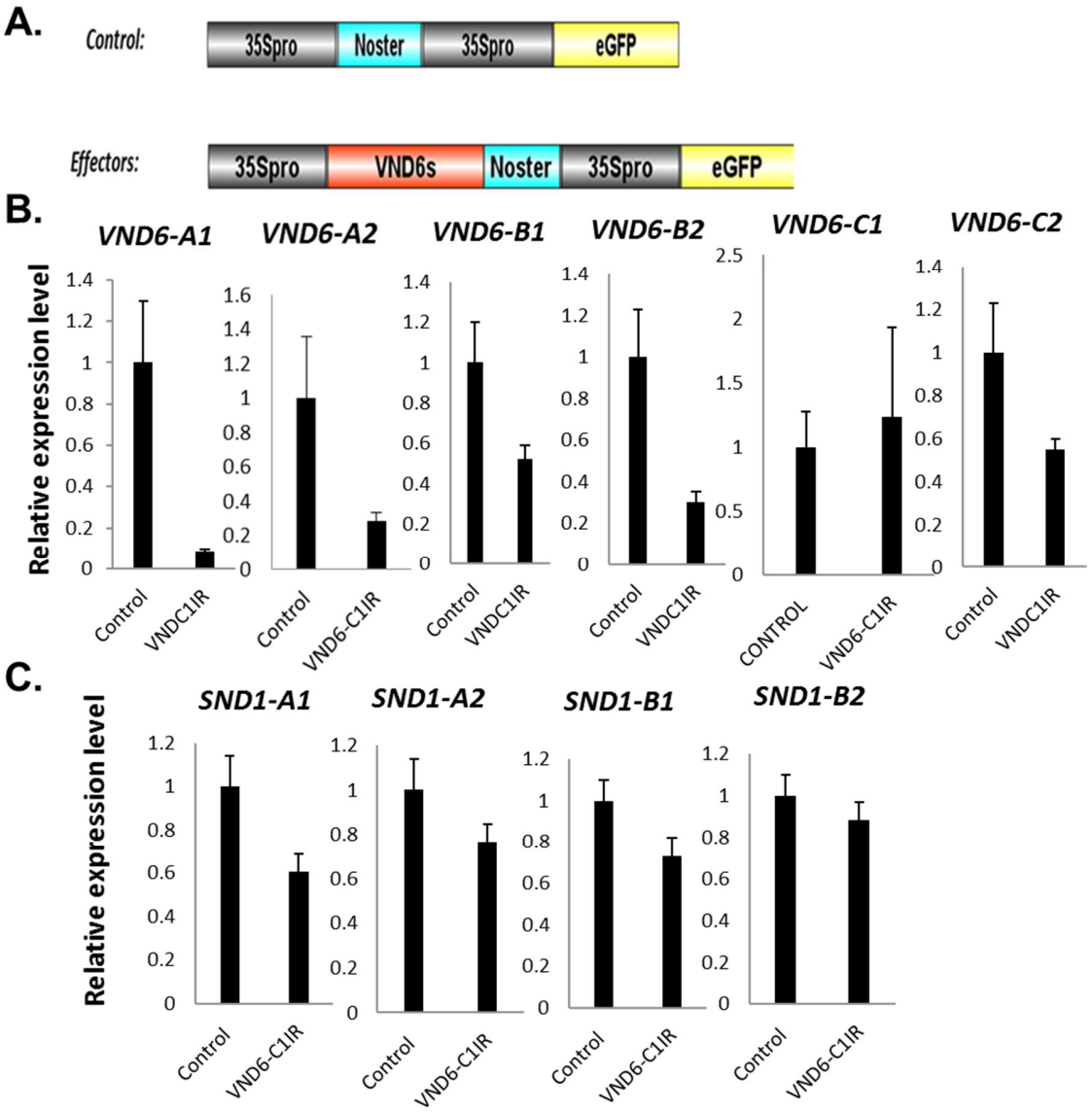

Figure 7. Relative expression levels of PtrSND1s and PtrVND6s in protoplasts overexpressing PtrVND6-C1^{IR}. (A). Schematic diagrams of the effector plasmids that were transformed into SDX protoplasts. **(B).** Relative expression levels were normalized to each transcript abundance of PtrSND1s and PtrVND6s in SDX protoplasts expressing the proteins in the modified PUC19 vectors (*35s- NACs-NOS-35s-eGFP*). Error bars indicate one SE.

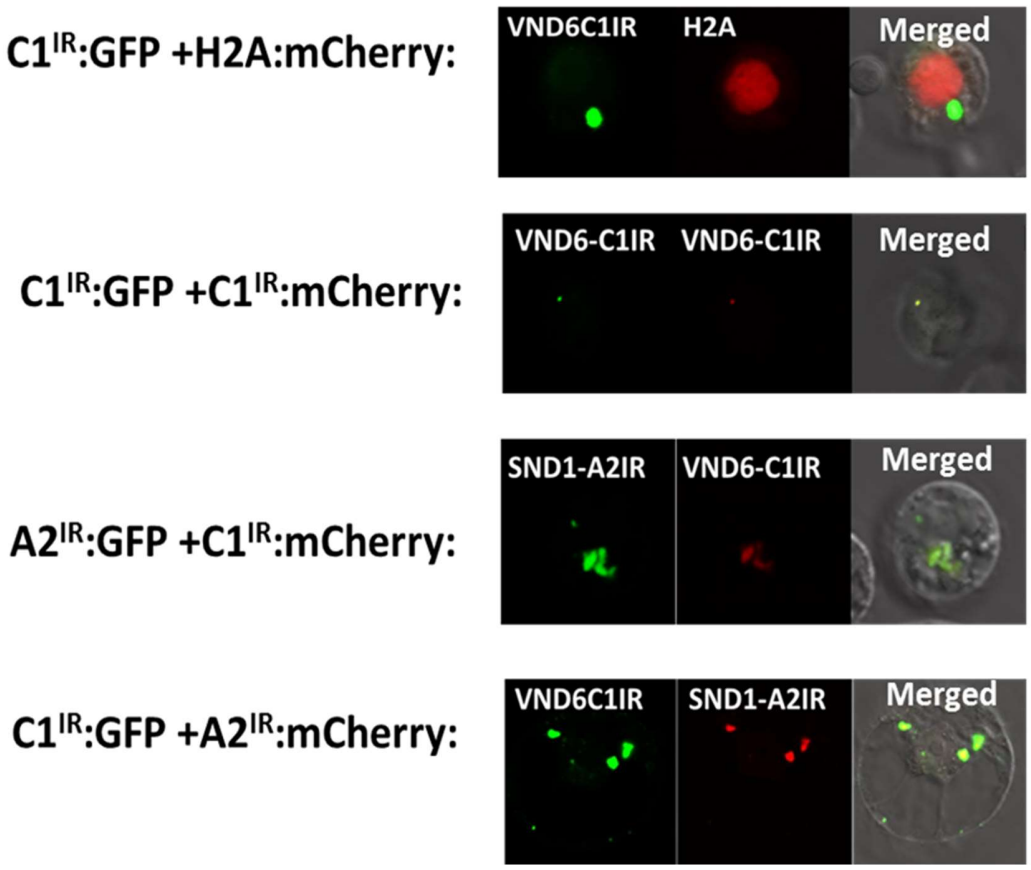

Figure 8. **Subcellular localization of PtrVND6-C1^{IR}**. Each PtrVND6-C1^{IR} was fused with sGFP and cotransferred with the nuclear marker H2A-1:mCherry, PtrVND6-C1^{IR}:mCherry into SDX protoplasts. H2A served as a nuclear marker, and PtrSND1-A2^{IR} as the cytoplasmic loci marker.

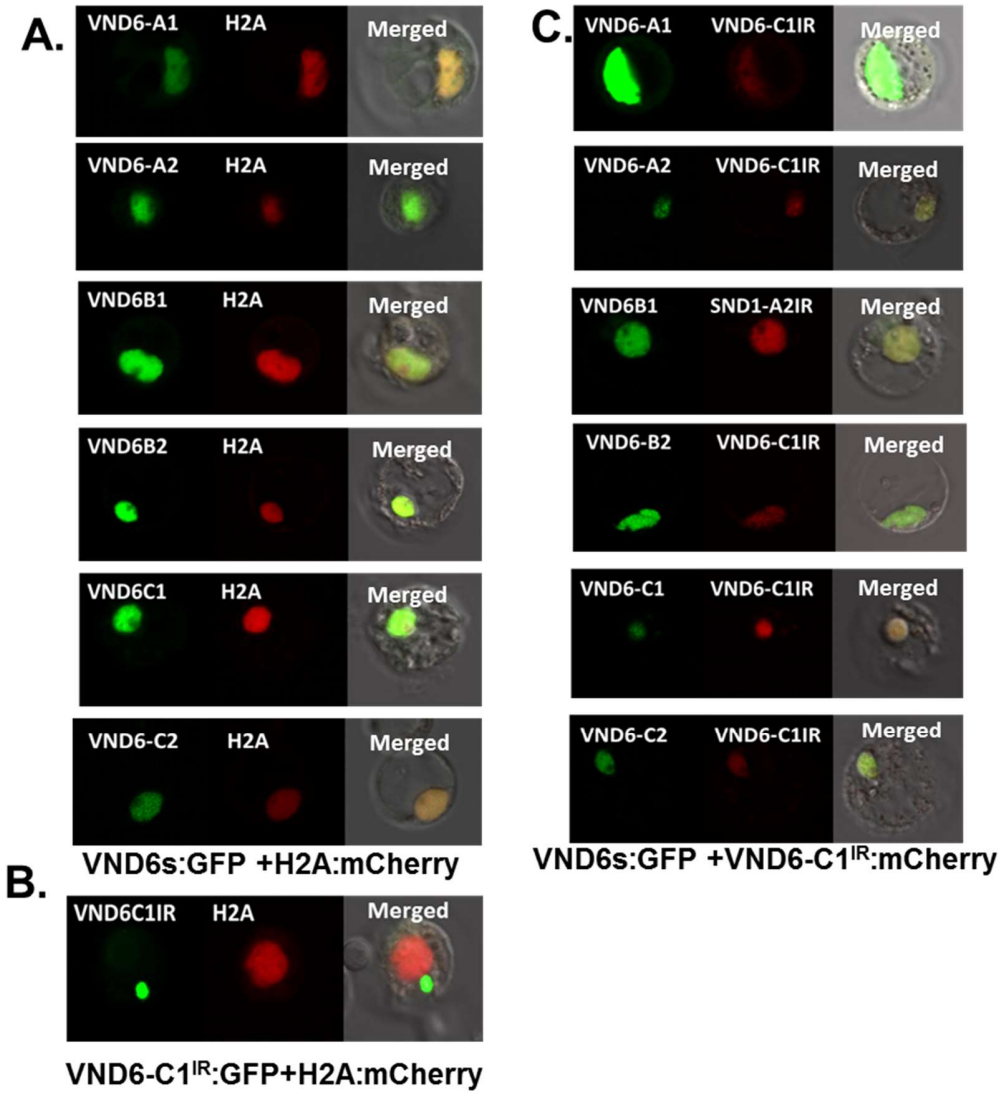

Figure 9. **Protein co-localization in SDX protoplasts demonstrate that PtrVND6-C1^{IR} is translocated from cytoplasmic foci to the nucleus by full-size PtrVND6 members. (A).** Subcellular localization of PtrVND6 fusion proteins. Each of PtrVND6A1, PtrVND6A2, PtrVND6B1, PtrVND6B2, PtrVND6C1 and PtrVND6C2 was fused to sGFP, and then co-transfected with nuclear marker H2A-cherry. **(B).** The cytoplasmic location of PtrVND6-C1^{IR} **(C).** Translocation of PtrVND6-C1^{IR} from the cytoplasmic foci into the nucleus by the full-size *PtrVND6s*.

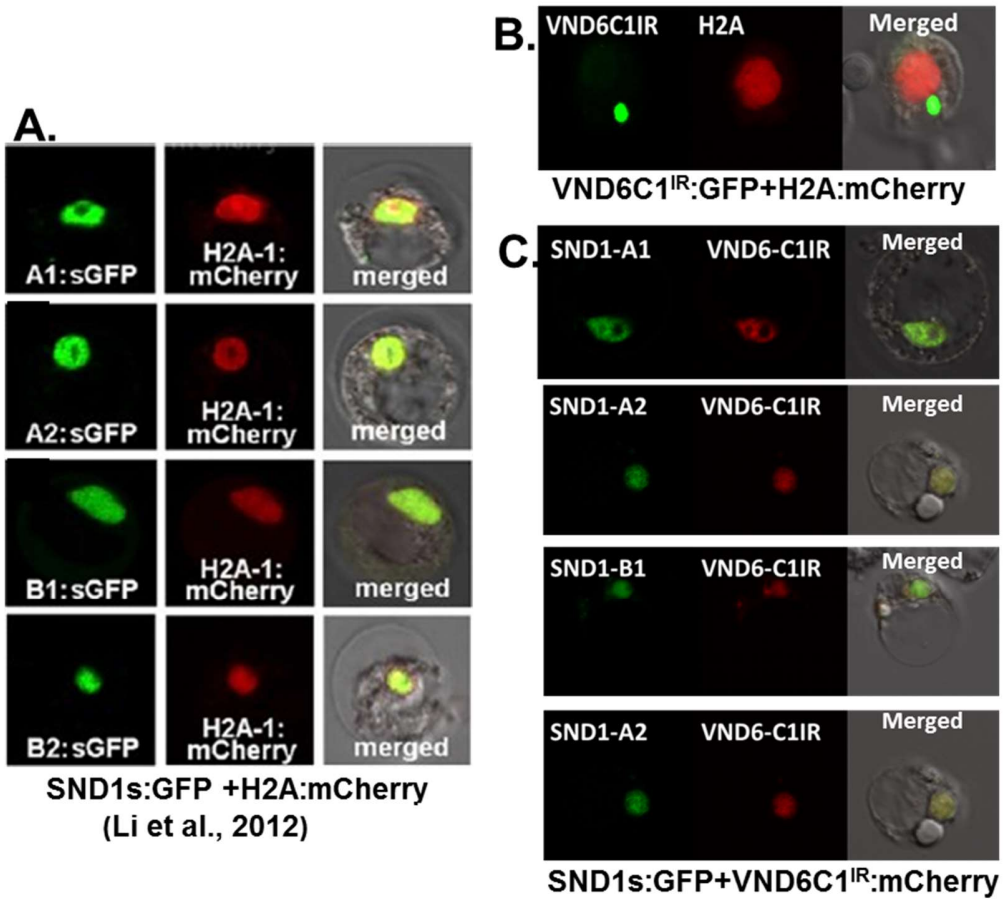

Figure 10. **Protein co-localization in SDX protoplasts demonstrate that PtrVND6-C1^{IR} is translocated from cytoplasmic foci to the nucleus by full-size PtrSND1 members. (A).** Subcellular localization of PtrSND1 fusion proteins: A1, A2, B1, B2 (Li et al., 2012). **(B).** The cytoplasmic location of PtrVND6-C1 ^{IR}. **(C).** Translocation of PtrVND6-C1 ^{IR} from the cytoplasmic foci into the nucleus by the full-size PtrSND1 members.

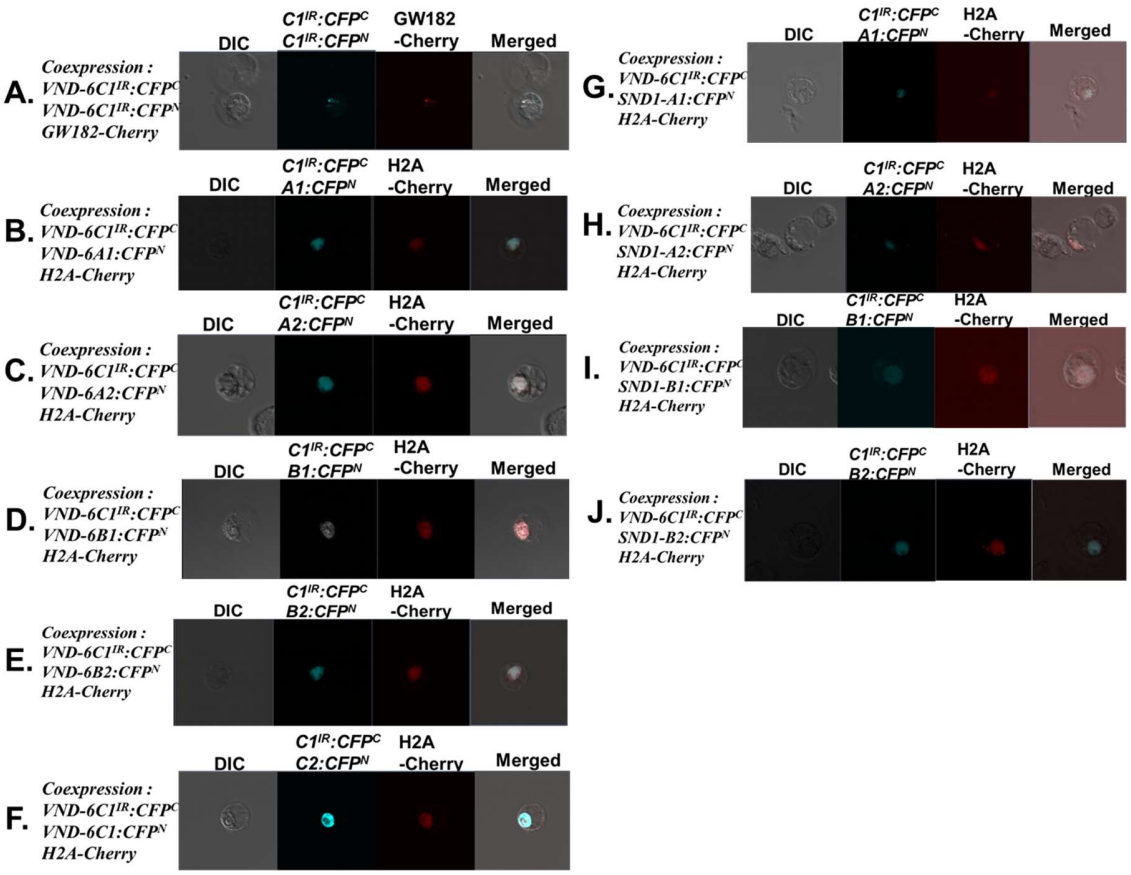

Figure 11. BiFC in *P. trichocarpa* SDX protoplasts demonstrate that VND6C1^{IR} heterodimerizes with the four full-size PtrSND1s and the six PtrVND6s

C1^{IR}:CFP^{C} cotransferred with C1^{IR}:CFP^{N} (***A***), VND6A1:CFP^{N} **(B),** VND6A2 : CFP^{N} (***C***), VND6B1:CFP^{N} (***D***), VND6B2:CFP^{N} (***E***), VND6B1: CFP^{N} (***F***), VND6B2: CFP^{N} (***G***), VND6A1:CFP^{N} (***H***), VND6A2: CFP^{N} (***I***), VND6B1: CFP^{N} (***J***), or VND6B2: CFP^{N} (***K***), into SDX protoplasts give positive BiFC signals that were colocalized with the marker H2A-1 in the nucleus, or GW182 in the cytoplasmic foci.

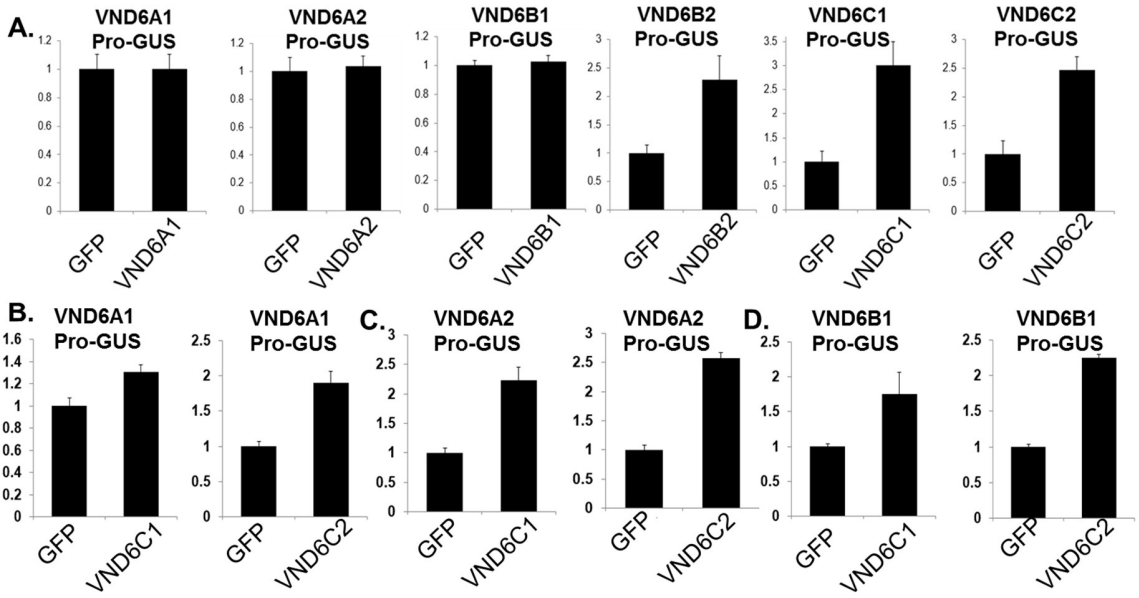

Figure 12. Effector–reporter-based gene assays for the self-activation and cross-regulation of PtrVND6s activity. **(A).** The self-activation of PtrVND6B2, PtrVND6C1, and PtrVND6C2 have been observed, and no self-activation activity of PtrVND6A1, PtrVND6A2, and PtrVND6B1 was detected. **(B).** PtrVND6B2 cannot activate PtrVND6A1, PtrVND6A2, and PtrVND6B1. **(C).** PtrVND6C1 activate PtrVND6A2, and PtrVND6B1, but not PtrVND6A1. **(D).** PtrVND6C2 activate PtrVND6A1, PtrVND6A2, and PtrVND6B1.

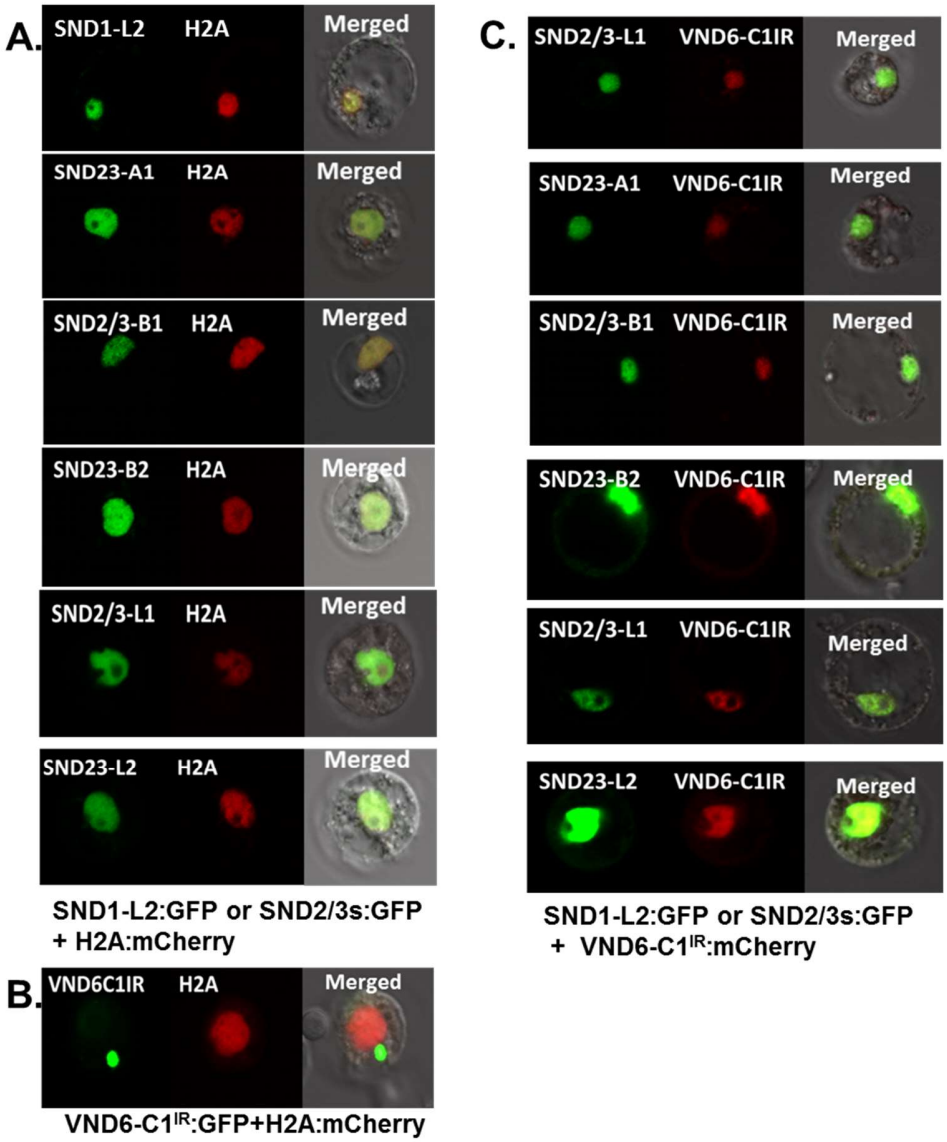

Figure 13. **Protein co-localization in SDX protoplasts demonstrate that PtrVND6-C1^{IR} is translocated from cytoplasmic foci to the nucleus by full-size PtrSND2/3 and PtrSND1-L members. (A).** Subcellular localization of PtrSND2/3s and PtrSND1-L fusion proteins: A1, A2, B1, B2, L2, 1-L1. **(B).** The cytoplasmic loci location of PtrVND6-C1^{IR}. **(C).** Translocation of PtrVND6-C1^{IR} from the cytoplasmic foci into the nucleus by the full-size PtrSND2/3s and PtrSND1-Ls.

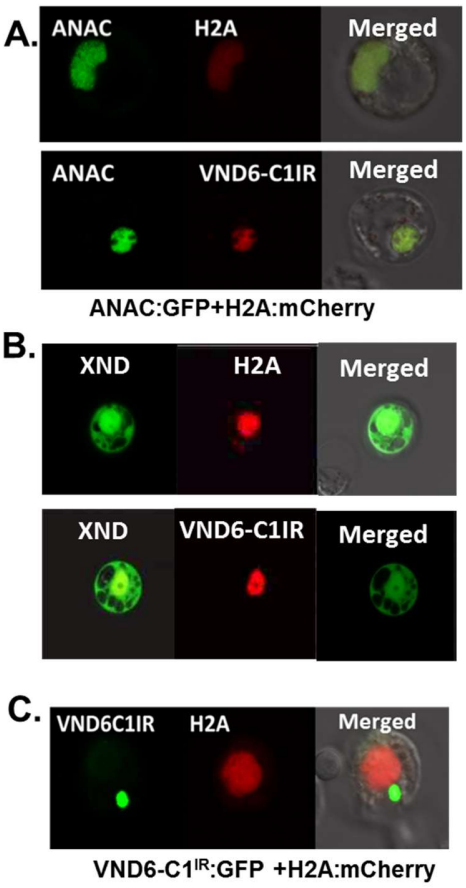

Figure 14. Protein co-localization in SDX protoplasts demonstrate that PtrVND6-C1^{IR} is translocated from cytoplasmic foci to the nucleus by ANAC1 and XND1. **(A).** Subcellular localization of ANAC1 and XND1 fusion proteins. **(B).** The cytoplasmic location of PtrVND6-C1^{IR}. **(C).** Translocation of PtrVND6-C1^{IR} from the cytoplasmic foci into the nucleus by the full-size PtrSND2/3s and PtrSND1-L.

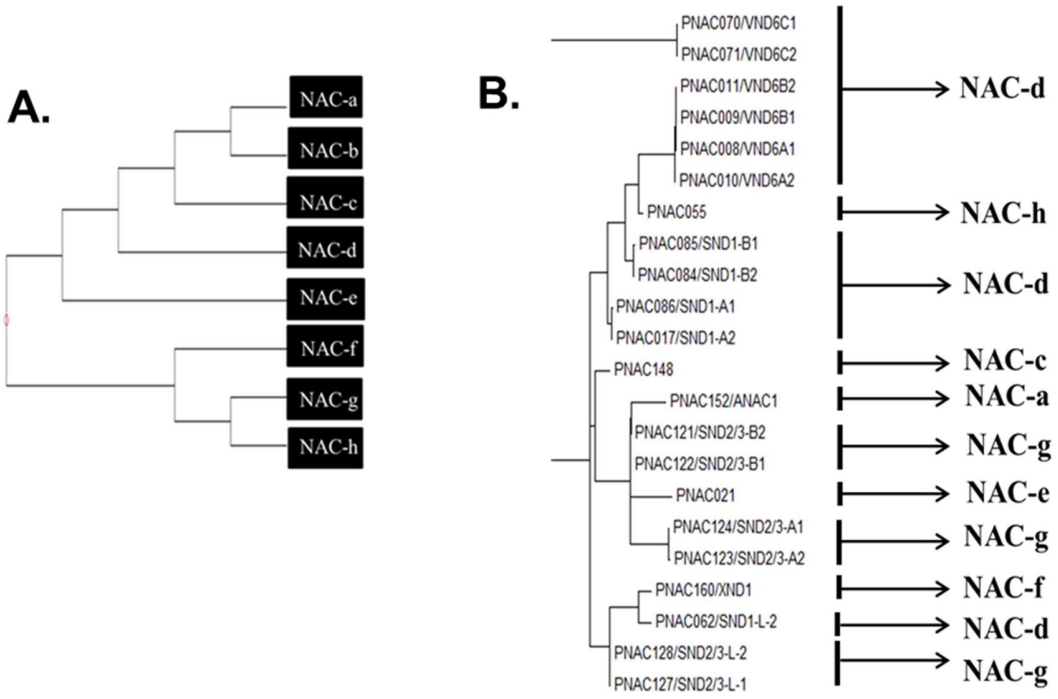

Figure 15. **Phylogenetic tree for developing xylem expressed NAC proteins. (A).** The families for *P. trichocarpa* NACs. **(B).** The phylogenetic tree and family clade for xylem expressed NAC proteins.

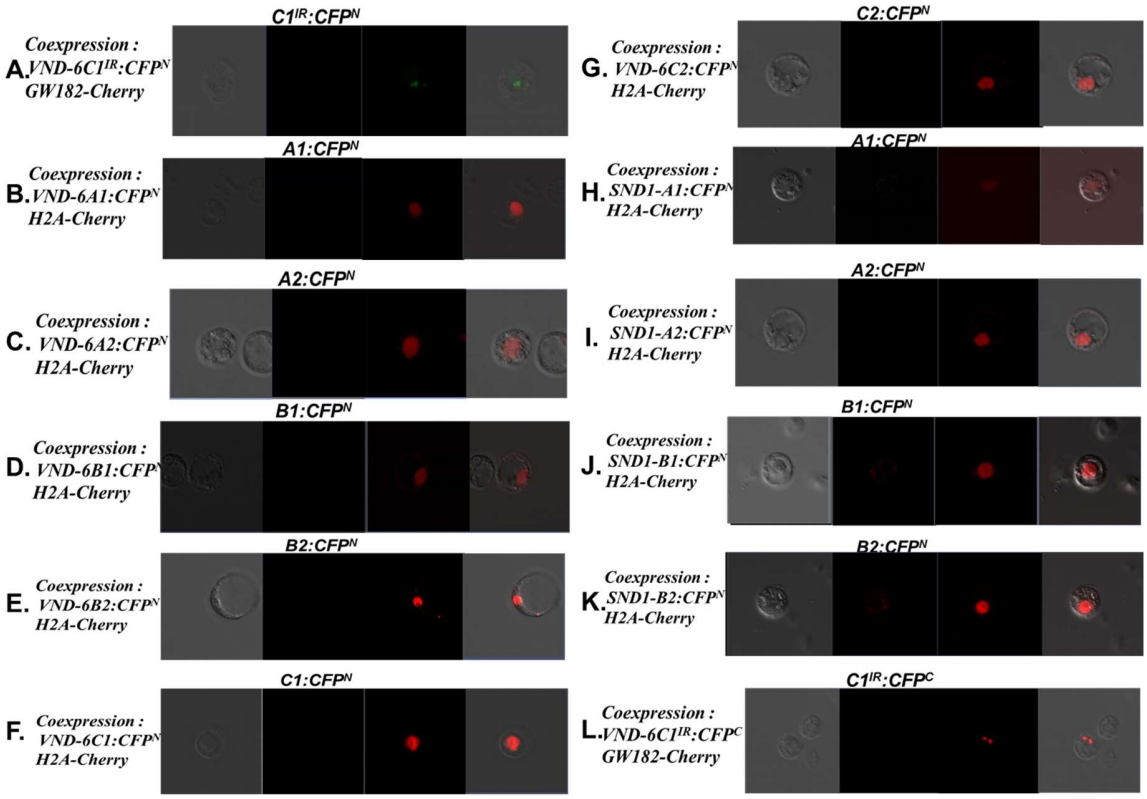

Figure 16. The controls for BiFC experiments for detecting the interactions between PtrVND6C1^{IR} and PtrVNDs, PtrSNDs. Only VND6C1^{IR}:CFP^{N}(*A*), VND6A1:CFP^{N}(*B*), VND6A2:CFP^{N} (*C*), VND6B1:CFP^{N} (*D*),VND6B2:CFP^{N} (*E*), VND6B1:CFP^{N} (*F*), VND6B2:CFP^{N} (*G*), VND6A1:CFP^{N} (*H*),VND6A2 :CFP^{N} (*I*), VND6B1:CFP^{N} (*J*),VND6B2:CFP^{N} (*K*), or C1IR:CFP^{C} (L) into SDX protoplasts individually give negative BiFC signals that were colocalized with the marker H2A-1 in the nucleus, or GW182 in the cytoplasmic foci.

Table 1. Primers used in the study.

Usages	name	primers
CDS CLONING	CDSPtrVND6-A1F	CACCTGGATTGCAGGACTCAAGGC
	CDSPtrVND6-A1R	GCCATGAATCATAGATTTTGGCTGG
	CDSPtrVND6-A2F	CACCGGAGTATGCTGAATGGATTTCAGG
	CDSPtrVND6-A2R	AACTGGATATCATCATTTCCATAGATCA
	CDSPtrVND6-B1F	CACCGCTGCATTTCAGTTCTTGGAGGAG
	CDSPtrVND6-B1R	TAAGCCTTCACTTCCACAGATCA
	CDSPtrVND6-B2F	CACCAATCTTCAGTTCTTGGAGGAGATG
	CDSPtrVND6-B2R	GCGTTCACTTCCATAGATCAATTTGG
	CDSPtrVND6-C1F	CACCTATGCAGCATCATCAACGGTTGT
	CDSPtrVND6-C1R	TCCCCAGATTCATTTCTCAAATATGC
	CDSPtrVND6-C2F	CACCGGTGGTGGTGAATTTTATGCAGC
	CDSPtrVND6-C2R	CCTCTTCAAACCCCTCTCTTCAT
	CDSPtrVND6-A1IRR	ACCCTGCACACAACCCAACC
	CDSPtrVND6-A2IRR	ACCCTACACACGACCCAACCT
	CDSPtrVND6-C1IRR	CTAGGTCAATATGTAGAGCCTGTTC
qRT-PCR	RTMYB021-F	GGACAAGGTTGCTGGAGTGATGTG
	RTMYB021-R	GGCCTCAAGTAATTAATCCAACGAAGC
	RTSND1-A1-F	TAGGCTTGATGACAGCACCCATGAA
	RTSND1-A1-R	TCTAAATACCCGGCAAACCACCCAA
	RTSND1-A2-F	TCCGGGCAACTTAACGATTGGGTA
	RTSND1-A2-R	GCATTTGGGCCGGTAGTAAAGCA
	RTSND1-B1-F	AACTGGGCAACCCTTGATCGTCTA
	RTSND1-B1-R	GTAATGGTTGGGTCAATGCAGGGT
	RTVND6A1-F	GGCCTAGACATAAACCAGACAAGCACTT
	RTVND6A1-F	GACTTGATCAACTGCTTGCTCATGATTGC
	RTVND6A2-F	CAAATAGAGCCACTGCTGCTGGG
	RTVND6A2-R	AGGTCTTCCTCATTCCGATCAAGTCT
	RTVND6B1-F	TCATGCAGCTGAGCAGATGCAT
	RTVND6B1-R	ACTGGAAGTCGACGTTGAGGCATATTC
	RTVND6B2-F	GCGAGTCCTTGACAAATTTGTTGCTTCC
	RTVND6B2-R	TGCATTAAAGGTGGCTGTACTGGAGA
	RTVND6C1-F	TCCTCAGTTAGAGAGCCCATCCCT
	RTVND6C1-R	TCTGGGTGTTGTTGTTGGACAACATTCT
	RTVND6C2-F	TGGTGATGGTGTTTCAAGCTTTGTTGAG
	RTVND6C2-R	ACTTGTTCCCGTCATCTCTACCACTTTG
	RTSND1-A2IR-F	GATTTCTTCTATGTTCGGTTCTAGGC
	RTSND1-A2IR-R	CAAACCACCCACCCTTCTTCA
	RTVND6-C1IR-F	TTCACTGTGATGTTCTCTGGAAA
	RTVND6-C1IR-R	GCCCATACCAGAAAGAGAA
	RT18S-F	CGAAGACGATCAGATACCGTCCTA
	RT18s-R	TTTCTCATAAGGTGCTGGCGGAGT

Table 1. Continued

Usages	name	primers
primers for protein expression	proteinPtrVNDA1-F	ATCTAGACATGAATACTTTTACACATGTTCCTC
	proteinPtrVNDA1-NACR	CGTCGACCTCGAGGCAAACTGATTCATGCTCAC
	proteinPtrVNDA2-F	ATCTAGACATGAATTCTTTTACACACGTTCC
	proteinPtrVNDA2-NACR	CGGATCCCTCGAGACAGACTGATTCATGCTCACTC
	proteinPtrVNDB1-F	ATCTAGACATGGTTGATATTGCTGCATTTCAGTT
	proteinPtrVNDB1-NACR	CGTCGACCTCGAGCCAACATGGTGAGTCGTAGTCA
	proteinPtrVNDB2-F	ATCTAGACATGAATACCTTCTCGCATGTC
	proteinPtrVNDB2-NACR	GCGTCGACCTCGAGCCAACATGGTGAGTCATAGTCA
	proteinPtrVNDC1-F	TCTAGACATGGAGTCAATGGAGTCG
	proteinPtrVNDC1-NACR	CGTCGACCTCGAGTTCCTCATAGAAGTAGCTTGAG
	proteinPtrVNDC2-F	TCTAGACATGATGGAGTCAATGGAGTCT
	proteinPtrVNDC2-NACR	CGTCGACCTCGAGGCTTGAGTCCCACCCTTCA
	proteinPtrVNDA1-R	ACTCGAGCTTCCATAGATCAATTTGACAACTG
	proteinPtrVNDA2-R	ACTCGAGTTTCCATAGATCAATTTGACAACT
	proteinPtrVNDB1-R	ACTCGAGCTTCCACAGATCAATTTGACAACT
	proteinPtrVNDB2-R	ACTCGAGCTTCCATAGATCAATTTGGCAACT
	proteinPtrVNDC1-R	ACTCGAGTTTCTCAAATATGCATATTCCGATA
	proteinPtrVNDC2-R	ACTCGAGTTTTTCAAATATGCATATTCCAATATC
	proteinPtrVNDC1IR-R	ACTCGAGGTATGTTGGAAGACAATGAAGA
	proteinPtrVNDA1IR-R	ACTCGAGTGCATAATCCAGTCCGATTTCTG
	proteinPtrVNDA2IR-R	ACTCGAGCACACGACCCAACCTTCTTCCTGA
EMSA Fragment clone	021EMSA-F	CACCAATTATGTGGTCCATTGA
	021EMSA-R	GGAGTTTGTTTCATAACTAAGCC
	6A1EMSA-F	TGTCCATAATTCTGCGTCACA
	6A1EMSA-R	TTGCAGTAAGGCGAACAAAA
	6A2EMSA-F	TTCCTGATCTCTCATTCGATCA
	6A2EMSA-R	ACGATCGAGTAGTTCCAAGCA
	6B1EMSA-F	CAGCTTTAATAAGATTTCTTTAAACG
	6B1EMSA-R	GGACATGGTGACATTGATG
	6B2EMSA-F	ATCATGCATGCTTTGGAATG
	6B2EMSA-R	AGGATGCATCAAGAGAAGGG
	6C1EMSA-F	GATAACCTCTCCCTATCCGTC
	6C1EMSA-R	TGGCATCAATCAGAAGAGGA
	6C2EMSA-F	GTATCTATCAAGACAAAACAAG
	6C2EMSA-R	GATAATTCTTTAATAACTAG
primer for cloning promoters	MYB021prom-F	TGCTAAGCTTCCCCACTTAATTGATGTTTGGC
	MYB021prom-R	TCGAGGATCCTAGAAAGGTGATCTATATCTC
	VND6A1prom-F	CTAGCTGCAGCTTGCTGATTTCTAGTTGGGGT
	VND6A1prom-R	CTAGTCTAGAAACAGCACACACTCTACAAG
	VND6A2prom-F	CTCCTGCAGGCCTTGGGATCCATTCCGACA
	VND6A2prom-R	CTAGTCTAGATCTGCTCAAAGACTCAACAT
	VND6B1prom-F	CTAGCTGCAGAGCCATTATACGCCCCCTTT
	VND6B1prom-R	CTAGGGATCCAATGACACAGCACGAGATTT
	VND6B2prom-F	CTAGCTGCAGTTTTTCCCTTACATTGTGCATGA
	VND6B2prom-R	CTAGGGATCCTATGTCTTGTTGACCAGAA
	VND6C1prom-F	CTAGCTGCAGTAAGCTCCCGGTTCCGATTG
	VND6C1prom-R	CTAGGGATCCTCAAGAAAGGGGTAAACGAC
	VND6C2prom-F	CTAGCTGCAGTGGCAGGTGTGTCAGAAAGT
	VND6C2prom-R	CTAGGGATCCTCGACAGAGAGGGAGAGATC
primer for effector vector construction	VND6-A1CDSF	CACCTGGATTGCAGGACTCAAGGC
	VND6-A1CDSR	GCCATGAATCATAGATTTTGGCTGG
	VND6-A2CDSF	CACCGGAGTATGCTGAATGGATTTCAGG
	VND6-A2CDSR	AACTGGATATCATCATTTCCATAGATCA
	VND6-B1CDSF	CACCGCTGCATTTCAGTTCTTGGAGGAG
	VND6-B1CDSR	TAAGCCTTCACTTCCACAGATCA
	VND6-B2CDSF	CACCAATCTTCAGTTCTTGGAGGAGATG
	VND6-B2CDSR	GCGTTCACTTCCATAGATCAATTTGG
	VND6-C1CDSF	CACCTATGCAGCATCATCAACGGTTGT
	VND6-C1CDSR	TCCCCAGATTCATTTCTCAAATATGC
	VND6-C2CDSF	CACCGGTGGTGGTGAATTTTATGCAGC
	VND6-C2CDSR	CCTCTTCAAACCCCTCTCTTCAT
	VND6-C1IRCDSR	CTAGGTCAATATGTAGAGCCTGTTC

Table 1. Continued

Usages	name	primers
subcellular location	subSND1-L-1F	AGGATCCGATTTAAGGGAGAATGATGGCAGG
	subSND1-L-1R	ACTCGAGCTTGGAACGTCGCAACTCTACTTC
	subSND1-L-2F	AGGATCCTCGATACTAGATTTAGGGAGAATGAT
	subSND1-L-2R	ACTCGAGCTGCAACTCTACTTGGAAAATCTCAG
	subSND2/3-A1F	AGGATCCTCCTTTGTGGGATGGGAATAAGATA
	subSND2/3-A1R	ACTCGAGCTCACATCACTGCTTTCTCTGAAGC
	subSND2/3-A2F	AGGATCCAAAAACGTGTATCCAGAGACAAGTT
	subSND2/3-A2R	ACTCGAGCCCAAATGCTCTTTCTCTCATAGGATC
	subSND2/3-B1F	AGGATCCTGTGGGCATAAGAGGAAACCTAAG
	subSND2/3-B1R	ACTCGAGCTTCAAGGGATAAGAGAAGATCCATC
	subSND2/3-B2F	AGGATCCGGGCATAAGAGGAAACCAAAGGA
	subSND2/3-B2R	ACTCGAGCTTCAGGGGATAAAAGAAGATCCATC
	subSND2/3-L-1F	AGGATCCGCTGTGTGATCGAAAACGAGCC
	subSND2/3-L-1R	ACTCGAGCCTCTGGTCCTACCCATGATGATC
	subSND2/3-L-2F	AGGATCCGCTTGGGAGAAAGAAGATACTTGTAC
	subSND2/3-L-2R	ACTCGAGCCCTTCGGTTCTACCCATGATGATC
	sub VND6-A1F	AGGATCCATGAATTCTTTTACACACGTTCCTC
	subVND6-A1R	ACTCGAGCTTCCATAGATCAATTTGACAACTG
	subVND6-A2F	AGGATCCATGAATACTTTTACACATGTTCCTC
	subVND6-A2R	ACTCGAGTTTCCATAGATCAATTTGACAACT
	subVND6-B1F	AGGATCCATGGTTGATATTGCTGCATTTCAGTT
	subVND6-B1R	ACTCGAGCTTCCACAGATCAATTTGACAACT
	subVND6-B2F	AGGATCCATGAATACCTTCTCGCATGTC
	subVND6-B2R	ACTCGAGCTTCCATAGATCAATTTGGCAACT
	subVND6-C1F	AGGATCCATGATGGAGTCAATGGAGTCGTGTGT
	subVND6-C1R	ACTCGAGTTTCTCAAATATGCATATTCCGATA
	subVND6-C2R	ATCTAGAATGGAGTCAATGGAGTCTTGTG
	subVND6-C2R	ACTCGAGTTTTTCAAATATGCATATTCCAATATC
	subSND1-A1F	AGCTGGATCCATGCCTGAAGATATGGTGAATCT
	subSND1-A1R	TCTCGAGTACCGACAAGTGGCATAATGG
	subSND1-A2F	AGCTGGATCCATGCCTGAGGATATGATGAATCT
	subSND1-A2R	TCTCGAGTACCGATAAGTGGCATAATGGG
	subSND1-B1F	TGGATCCATGACAGAAAACATGAGTATATCTGT
	subSND1-B1R	TCTCGAGTGCACCTGTGTTTGACAACTG
	subVND6-C1IRR	ACTCGAGGTATGTTGGAAGACAATGAAGA
	subANAC1-F	CGGATCCATGGCTGCCAATCTTC
	subANAC1-R	GCTCGAGATAATGATTCCATAAGTTGGGC
	subXND1-F	CGGATCCATGGCTGCCAATCTTC
	subXND1-R	GCTCGAGATTTGGCAAGCTTATTTCATCA

REFERENCES

1. Anders N, Dupree P. Glycosyltransferases of the GT43 family. *Annual Plant Reviews: Plant Polysaccharides, Biosynthesis and Bioengineering, Volume 41*. 2010:251-263.

2. Aspeborg H, Schrader J, Coutinho PM, et al. Carbohydrate-active enzymes involved in the secondary cell wall biogenesis in hybrid aspen. *Plant Physiol*. 2005;137(3):983-997.

3. Bhargava, A., Mansfield, S.D., Hall, H.C., Douglas, C.J. and Ellis, B.E. (2010) MYB75 functions in regulation of secondary cell wall formation in the Arabidopsis inflorescence stem. Plant Physiol. 154, 1428–1438.

4. Bhargava A, Mansfield SD, Hall HC, Douglas CJ, Ellis BE. MYB75 functions in regulation of secondary cell wall formation in the Arabidopsis inflorescence stem. *Plant Physiol*. 2010;154(3):1428-1438.

5. Bomal C, Bedon F, Caron S, et al. Involvement of pinus taeda MYB1 and MYB8 in phenylpropanoid metabolism and secondary cell wall biogenesis: A comparative in planta analysis. *J Exp Bot*. 2008;59(14):3925-3939.

6. Brown DM, Goubet F, Wong VW, et al. Comparison of five xylan synthesis mutants reveals new insight into the mechanisms of xylan synthesis. *The Plant Journal*. 2007;52(6):1154-1168.

7. Brown DM, Zeef LA, Ellis J, Goodacre R, Turner SR. Identification of novel genes in Arabidopsis involved in secondary cell wall formation using expression profiling and reverse genetics. *The Plant Cell*. 2005;17(8):2281-2295.

8. Busch A, Hertel KJ. Evolution of SR protein and hnRNP splicing regulatory factors. *Wiley Interdisciplinary Reviews: RNA*. 2012;3(1):1-12.

9. Campbell M, Haas B, Hamilton J, Mount S, Buell CR. Comprehensive analysis of alternative splicing in rice and comparative analyses with Arabidopsis. *BMC Genomics*. 2006;7(1):327.

10. Cassan-Wang H, Goué N, Saidi MN, et al. Identification of novel transcription factors regulating secondary cell wall formation in Arabidopsis. *Frontiers in plant science*. 2013;4.

11. Chapman EJ, Estelle M. Mechanism of auxin-regulated gene expression in plants. *Annu Rev Genet*. 2009; 43:265-285.

12. Chen H, Li Q, Shuford CM, et al. Membrane protein complexes catalyze both 4- and 3-hydroxylation of cinnamic acid derivatives in monolignol biosynthesis. *Proceedings of the National Academy of Sciences*. 2011;108(52):21253-21258.

13. Craven-Bartle B, Pascual M, Cánovas FM, Ávila C. A MYB transcription factor regulates genes of the phenylalanine pathway in maritime pine. *The Plant Journal*. 2013;74(5):755-766.

14. Das PK, Shin DH, Choi S, Yoo S, Choi G, Park Y. Cytokinins enhance sugar-induced anthocyanin biosynthesis in Arabidopsis. *Mol Cells*. 2012;34(1):93-101.

15. Delmer DP. Cellulose biosynthesis: Exciting times for a difficult field of study. *Annual review of plant biology*. 1999;50(1):245-276.

16. Demura T, Fukuda H. Transcriptional regulation in wood formation. *Trends Plant Sci*. 2007;12(2):64-70.

17. Demura T, Tashiro G, Horiguchi G, et al. Visualization by comprehensive microarray analysis of gene expression programs during transdifferentiation of mesophyll cells into xylem cells. *Proceedings of the National Academy of Sciences*. 2002;99(24):15794-15799.

18. Demura T, Ye Z. Regulation of plant biomass production. *Curr Opin Plant Biol*. 2010;13(3):298-303.

19. Dhugga KS, Barreiro R, Whitten B, et al. Guar seed ß-mannan synthase is a member of the cellulose synthase super gene family. *Science*. 2004;303(5656):363-366.

20. Dong MA, Farré EM, Thomashow MF. Circadian clock-associated 1 and late elongated hypocotyl regulate expression of the C-repeat binding factor (CBF) pathway in Arabidopsis. *Proceedings of the National Academy of Sciences*. 2011;108(17):7241-7246.

21. Du J, Mansfield SD, Groover AT. The populus homeobox gene ARBORKNOX2 regulates cell differentiation during secondary growth. *The Plant Journal*. 2009;60(6):1000-1014.

22. Du J, Miura E, Robischon M, Martinez C, Groover A. The populus class III HD ZIP transcription factor POPCORONA affects cell differentiation during secondary growth of woody stems. *PLoS One*. 2011;6(2): e17458.

23. Ernst HA, Olsen AN, Skriver K, Larsen S, Leggio LL. Structure of the conserved domain of ANAC, a member of the NAC family of transcription factors. *EMBO Rep*. 2004;5(3):297-303.

24. Finn RD, Mistry J, Tate J, et al. The pfam protein families database. *Nucleic Acids Res*. 2010;38: D211-D222.

25. Goicoechea M, Lacombe E, Legay S, et al. EgMYB2, a new transcriptional activator from eucalyptus xylem, regulates secondary cell wall formation and lignin biosynthesis. *The Plant Journal*. 2005;43(4):553-567.

26. Hofmann NR. Alternative splicing links the circadian clock to cold tolerance. *The Plant Cell Online*. 2012;24(6):2238-2238.

27. Hu R, Qi G, Kong Y, Kong D, Gao Q, Zhou G. Comprehensive analysis of NAC domain transcription factor gene family in *Populus trichocarpa*. *BMC plant biology*. 2010;10(1):145.

28. Hussey SG, Mizrachi E, Spokevicius AV, Bossinger G, Berger DK, MYBurg AA. SND2, a NAC transcription factor gene, regulates genes involved in secondary cell wall development in Arabidopsis fibres and increases fibre cell area in eucalyptus. *BMC plant biology*. 2011;11(1):173.

29. Jansson S, Douglas CJ. Populus: A model system for plant biology. *Annu.Rev.Plant Biol.* 2007;58:435-458.

30. Jones L, Ennos AR, Turner SR. Cloning and characterization of irregular xylem4 (irx4): A severely lignin-deficient mutant of Arabidopsis. *The Plant Journal*. 2001;26(2):205-216.

31. Joshi CP, Mansfield SD. The cellulose paradox—simple molecule, complex biosynthesis. *Curr Opin Plant Biol*. 2007;10(3):220-226.

32. Kalluri UC, Joshi CP. Differential expression patterns of two cellulose synthase genes are associated with primary and secondary cell wall development in aspen trees. *Planta*. 2004;220(1):47-55.

33. Kalsotra A, Cooper TA. Functional consequences of developmentally regulated alternative splicing. *Nature Reviews Genetics*. 2011;12(10):715-729.

34. Karpinska B, Karlsson M, Srivastava M, et al. MYB transcription factors are differentially expressed and regulated during secondary vascular tissue development in hybrid aspen. *Plant Mol Biol*. 2004;56(2):255-270.

35. Kim D, Pertea G, Trapnell C, Pimentel H, Kelley R, Salzberg SL. TopHat2: Accurate alignment of transcriptomes in the presence of insertions, deletions and gene fusions. *Genome Biol*. 2013;14(4): R36.

36. Kim W, Kim J, Ko J, Kim J, Han K. Transcription factor MYB46 is an obligate component of the transcriptional regulatory complex for functional expression of secondary wall-associated cellulose synthases in Arabidopsis thaliana. *J Plant Physiol*. 2013.

37. Kim W, Ko J, Kim J, Kim J, Bae H, Han K. MYB46 directly regulates the gene expression of secondary wall-associated cellulose synthases in Arabidopsis. *The Plant Journal*. 2013;73(1):26-36.

38. Ko J, Kim H, Hwang I, Han K. Tissue-type-specific transcriptome analysis identifies developing xylem-specific promoters in poplar. *Plant biotechnology journal*. 2012;10(5):587-596.

39. Ko J, Kim W, Han K. Ectopic expression of MYB46 identifies transcriptional regulatory genes involved in secondary wall biosynthesis in Arabidopsis. *The Plant Journal*. 2009;60(4):649-665.

40. Kubo M, Udagawa M, Nishikubo N, et al. Transcription switches for protoxylem and metaxylem vessel formation. *Genes Dev*. 2005;19(16):1855-1860.

41. Kulkarni M, Ozgur S, Stoecklin G. On track with P-bodies. *Biochem Soc Trans*. 2010;38(1):242.

42. Langmead B, Trapnell C, Pop M, Salzberg SL. Ultrafast and memory-efficient alignment of short DNA sequences to the human genome. *Genome Biol*. 2009;10(3): R25.

43. Lee C, Teng Q, Zhong R, Ye Z. Molecular dissection of xylan biosynthesis during wood formation in poplar. *Molecular plant*. 2011;4(4):730-747.

44. Lee HW, Kim NY, Lee DJ, Kim J. LBD18/ASL20 regulates lateral root formation in combination with LBD16/ASL18 downstream of ARF7 and ARF19 in Arabidopsis. *Plant Physiol*. 2009;151(3):1377-1389.

45. Legay S, Lacombe E, Goicoechea M, et al. Molecular characterization of< i> EgMYB1, a putative transcriptional repressor of the lignin biosynthetic pathway. *Plant Science*. 2007;173(5):542-549.

46. Lewis DR, Ramirez MV, Miller ND, et al. Auxin and ethylene induce flavonol accumulation through distinct transcriptional networks. *Plant Physiol*. 2011;156(1):144-164.

47. Li E, Bhargava A, Qiang W, et al. The class II KNOX gene KNAT7 negatively regulates secondary wall formation in Arabidopsis and is functionally conserved in populus. *New Phytol*. 2012;194(1):102-115.

48. Li E, Wang S, Liu Y, Chen J, Douglas CJ. OVATE FAMILY PROTEIN4 (OFP4) interaction with KNAT7 regulates secondary cell wall formation in Arabidopsis thaliana. *The Plant Journal*. 2011;67(2):328-341.

49. Li H, Handsaker B, Wysoker A, et al. The sequence alignment/map format and SAMtools. *Bioinformatics*. 2009;25(16):2078-2079.

50. Li J, Li L, Sheen J. Protocol: A rapid and economical procedure for purification of plasmid or plant DNA with diverse applications in plant biology. *Plant Methods*. 2010;6(1):1.

51. Liepman AH, Nairn CJ, Willats WG, Sørensen I, Roberts AW, Keegstra K. Functional genomic analysis supports conservation of function among cellulose synthase-like A gene family members and suggests diverse roles of mannans in plants. *Plant Physiol*. 2007;143(4):1881-1893.

52. Mangeon A, Lin W, Springer PS. Functional divergence in the Arabidopsis LOB-domain gene family. *Plant signaling & behavior*. 2012;7(12):1544-1547.

53. Maquat LE. Nonsense-mediated mRNA decay in mammals. *J Cell Sci*. 2005;118(9):1773-1776.

54. Matlin AJ, Clark F, Smith CW. Understanding alternative splicing: Towards a cellular code. *Nature Reviews Molecular Cell Biology*. 2005;6(5):386-398.

55. McCarthy RL, Zhong R, Fowler S, et al. The poplar MYB transcription factors, PtrMYB3 and PtrMYB20, are involved in the regulation of secondary wall biosynthesis. *Plant and cell physiology*. 2010;51(6):1084-1090.

56. Mendell JT, Sharifi NA, Meyers JL, Martinez-Murillo F, Dietz HC. Nonsense surveillance regulates expression of diverse classes of mammalian transcripts and mutes genomic noise. *Nat Genet*. 2004;36(10):1073-1078.

57. Miller S, Dykes D, Polesky H. A simple salting out procedure for extracting DNA from human nucleated cells. *Nucleic Acids Res*. 1988;16(3):1215.

58. Mitsuda N, Iwase A, Yamamoto H, et al. NAC transcription factors, NST1 and NST3, are key regulators of the formation of secondary walls in woody tissues of Arabidopsis. *The Plant Cell Online*. 2007;19(1):270-280.

59. Mitsuda N, Seki M, Shinozaki K, Ohme-Takagi M. The NAC transcription factors NST1 and NST2 of Arabidopsis regulate secondary wall thickenings and are required for anther dehiscence. *The Plant Cell Online*. 2005;17(11):2993-3006.

60. Nakano Y, Nishikubo N, Goué N, et al. MYB transcription factors orchestrating the developmental program of xylem vessels in Arabidopsis roots. *Plant biotechnology*. 2010;27(3):267-272.

61. Nelson BK, Cai X, Nebenführ A. A multicolored set of in vivo organelle markers for co-localization studies in Arabidopsis and other plants. *The Plant Journal*. 2007;51(6):1126-1136.

62. Nilsen TW, Graveley BR. Expansion of the eukaryotic proteome by alternative splicing. *Nature*. 2010;463(7280):457-463.

63. Oda Y, Hasezawa S. Cytoskeletal organization during xylem cell differentiation. *J Plant Res*. 2006;119(3):167-177.

64. Öhman D, Demedts B, Kumar M, et al. MYB103 is required for FERULATE-5-HYDROXYLASE expression and syringyl lignin biosynthesis in Arabidopsis stems. *The Plant Journal*. 2013;73(1):63-76.

65. Paredez AR, Somerville CR, Ehrhardt DW. Visualization of cellulose synthase demonstrates functional association with microtubules. *Science*. 2006;312(5779):1491-1495.

66. Patzlaff A, McInnis S, Courtenay A, et al. Characterisation of a pine MYB that regulates lignification. *The Plant Journal*. 2003;36(6):743-754.

67. Patzlaff A, Newman LJ, Dubos C, et al. Characterisation of PtMYB1, an R2R3-MYB from pine xylem. *Plant Mol Biol*. 2003;53(4):597-608.

68. Peña MJ, Zhong R, Zhou G, et al. Arabidopsis irregular xylem8 and irregular xylem9: Implications for the complexity of glucuronoxylan biosynthesis. *The Plant Cell Online*. 2007;19(2):549-563.

69. Peng Z, Han C, Yuan L, Zhang K, Huang H, Ren C. Brassinosteroid enhances Jasmonate-Induced anthocyanin accumulation in Arabidopsis seedlings. *Journal of Integrative Plant Biology*. 2011;53(8):632-640.

70. Radivojac P, Vacic V, Haynes C, et al. Identification, analysis, and prediction of protein ubiquitination sites. *Proteins: Structure, Function, and Bioinformatics*. 2010;78(2):365-380.

71. Robischon M, Du J, Miura E, Groover A. The populus class III HD ZIP, popREVOLUTA, influences cambium initiation and patterning of woody stems. *Plant Physiol*. 2011;155(3):1214-1225.

72. Roman C, Cohn L, Calame K. A dominant negative form of transcription activator mTFE3 created by differential splicing. *Science*. 1991;254(5028):94-97.

73. Rozen S, Skaletsky H. Primer3 on the WWW for general users and for biologist programmers. In: *Bioinformatics methods and protocols.* Springer; 1999:365-386.

74. Sambrook J, Fritsch E, Maniatis T. Molecular cloning: A laboratory reference manual. . 1989.

75. Sasaki K, Nakamura Y, Maki K, et al. Functional analysis of a dominant-negative ΔETS TEL/ETV6 isoform. *Biochem Biophys Res Commun*. 2004;317(4):1128-1137.

76. Seo PJ, Hong S, Kim S, Park C. Competitive inhibition of transcription factors by small interfering peptides. *Trends Plant Sci*. 2011;16(10):541-549.

77. Seo PJ, Park M, Lim M, et al. A self-regulatory circuit of CIRCADIAN CLOCK-ASSOCIATED1 underlies the circadian clock regulation of temperature responses in Arabidopsis. *The Plant Cell Online*. 2012;24(6):2427-2442.

78. Seo PJ, Park M, Park C. Alternative splicing of transcription factors in plant responses to low temperature stress: Mechanisms and functions. *Planta*. 2013:1-10.

79. Somerville C. Cellulose synthesis in higher plants. *Annu Rev Cell Dev Biol*. 2006;22:53-78.

80. Song D, Shen J, Li L. Characterization of cellulose synthase complexes in populus xylem differentiation. *New Phytol*. 2010;187(3):777-790.

81. Soyano T, Thitamadee S, Machida Y, Chua N. Asymmetric leaves2-like19/lateral organ boundaries domain30 and Asl20/Lbd18 regulate tracheary element differentiation in Arabidopsis. *The Plant Cell Online*. 2008;20(12):3359-3373.

82. Sunkar R, Zhu J. Novel and stress-regulated microRNAs and other small RNAs from Arabidopsis. *The Plant Cell Online*. 2004;16(8):2001-2019.

83. Tanaka K, Murata K, Yamazaki M, Onosato K, Miyao A, Hirochika H. Three distinct rice cellulose synthase catalytic subunit genes required for cellulose synthesis in the secondary wall. *Plant Physiol*. 2003;133(1):73-83.

84. Taylor NG, Gardiner JC, Whiteman R, Turner SR. Cellulose synthesis in the Arabidopsis secondary cell wall. *Cellulose*. 2004;11(3-4):329-338.

85. Tenea GN, Spantzel J, Lee L, et al. Overexpression of several Arabidopsis histone genes increases agrobacterium-mediated transformation and transgene expression in plants. *The Plant Cell Online*. 2009;21(10):3350-3367.

86. Thorvaldsdóttir H, Robinson JT, Mesirov JP. Integrative genomics viewer (IGV): High-performance genomics data visualization and exploration. *Briefings in bioinformatics*. 2013;14(2):178-192.

87. Timell TE. Recent progress in the chemistry of wood hemicelluloses. *Wood Sci Technol*. 1967;1(1):45-70.

88. Turner SR, Somerville CR. Collapsed xylem phenotype of Arabidopsis identifies mutants deficient in cellulose deposition in the secondary cell wall. *The Plant Cell Online*. 1997;9(5):689-701.

89. Wang H, Avci U, Nakashima J, Hahn MG, Chen F, Dixon RA. Mutation of WRKY transcription factors initiates pith secondary wall formation and increases stem biomass in dicotyledonous plants. *Proceedings of the National Academy of Sciences*. 2010;107(51):22338-22343.

90. Wang H, Dixon RA. On–off switches for secondary cell wall biosynthesis. *Molecular plant*. 2012;5(2):297-303.

91. Wang H, Zhao Q, Chen F, Wang M, Dixon RA. NAC domain function and transcriptional control of a secondary cell wall master switch. *The Plant Journal*. 2011;68(6):1104-1114.

92. Wang X, Li X, Li Y. A modified coomassie brilliant blue staining method at nanogram sensitivity compatible with proteomic analysis. *Biotechnol Lett*. 2007;29(10):1599-1603.

93. Wu H, Ma Y, Chen T, Wang M, Wang X. PsRobot: A web-based plant small RNA meta-analysis toolbox. *Nucleic Acids Res*. 2012;40(W1):W22-W28.

94. Xu J, Yang J, Niu Q, Chua N. Arabidopsis DCP2, DCP1, and VARICOSE form a decapping complex required for postembryonic development. *The Plant Cell Online*. 2006;18(12):3386-3398.

95. Yamaguchi M, Goué N, Igarashi H, et al. VASCULAR-RELATED NAC-DOMAIN6 and VASCULAR-RELATED NAC-DOMAIN7 effectively induce transdifferentiation into xylem vessel elements under control of an induction system. *Plant Physiol*. 2010;153(3):906-914.

96. Yamaguchi M, Kubo M, Fukuda H, Demura T. VASCULAR-RELATED NAC-DOMAIN7 is involved in the differentiation of all types of xylem vessels in Arabidopsis roots and shoots. *The Plant Journal*. 2008;55(4):652-664.

97. Yamaguchi M, Ohtani M, Mitsuda N, et al. VND-INTERACTING2, a NAC domain transcription factor, negatively regulates xylem vessel formation in Arabidopsis. *The Plant Cell Online*. 2010;22(4):1249-1263.

98. Yan L, Xu C, Kang Y, et al. The heterologous expression in Arabidopsis thaliana of sorghum transcription factor SbbHLH1 downregulates lignin synthesis. *J Exp Bot*. 2013.

99. Yang C, Xu Z, Song J, Conner K, Barrena GV, Wilson ZA. Arabidopsis MYB26/MALE STERILE35 regulates secondary thickening in the endothecium and is essential for anther dehiscence. *The Plant Cell Online*. 2007;19(2):534-548.

100. Yang S, Seo PJ, Yoon H, Park C. The Arabidopsis NAC transcription factor VNI2 integrates abscisic acid signals into leaf senescence via the COR/RD genes. *The Plant Cell Online*. 2011;23(6):2155-2168.

101. Yoo S, Cho Y, Sheen J. Arabidopsis mesophyll protoplasts: A versatile cell system for transient gene expression analysis. *Nature protocols*. 2007;2(7):1565-1572.

102. Yordanov YS, Regan S, Busov V. Members of the *LATERAL ORGAN BOUNDARIES DOMAIN* transcription factor family are involved in the regulation of secondary growth in *Populus*. *The Plant Cell Online*. 2010;22(11):3662-3677.

103. Yuan Y, Wu J, Sun R, et al. A naturally occurring splicing site mutation in the *brassica rapa* FLC1 gene is associated with variation in flowering time. *J Exp Bot*. 2009;60(4):1299-1308.

104. Zhang P, Dreher K, Karthikeyan A, et al. Creation of a genome-wide metabolic pathway database for *Populus trichocarpa* using a new approach for reconstruction and curation of metabolic pathways for plants. *Plant Physiol*. 2010;153(4):1479-1491.

105. Zhao C, Craig JC, Petzold HE, Dickerman AW, Beers EP. The xylem and phloem transcriptomes from secondary tissues of the Arabidopsis root-hypocotyl. *Plant Physiol*. 2005;138(2):803-818.

106. Zhong R, Burk DH, Morrison WH, Ye Z. A kinesin-like protein is essential for oriented deposition of cellulose microfibrils and cell wall strength. *The Plant Cell Online*. 2002;14(12):3101-3117.

107. Zhong R, Demura T, Ye Z. SND1, a NAC domain transcription factor, is a key regulator of secondary wall synthesis in fibers of Arabidopsis. *The Plant Cell Online*. 2006;18(11):3158-3170.

108. Zhong R, Lee C, Ye Z. Evolutionary conservation of the transcriptional network regulating secondary cell wall biosynthesis. *Trends Plant Sci*. 2010;15(11):625-632.

109. Zhong R, Lee C, Ye Z. Functional characterization of poplar wood-associated NAC domain transcription factors. *Plant Physiol*. 2010;152(2):1044-1055.

110. Zhong R, Lee C, Zhou J, McCarthy RL, Ye Z. A battery of transcription factors involved in the regulation of secondary cell wall biosynthesis in Arabidopsis. *The Plant Cell Online*. 2008;20(10):2763-2782.

111. Zhong R, McCarthy RL, Haghighat M, Ye Z. The poplar MYB master switches bind to the SMRE site and activate the secondary wall biosynthetic program during wood formation. *PLOS ONE*. 2013;8(7): e69219.

112. Zhong R, McCarthy RL, Lee C, Ye Z. Dissection of the transcriptional program regulating secondary wall biosynthesis during wood formation in poplar. *Plant Physiol*. 2011;157(3):1452-1468.

113. Zhong R, Ye Z. MYB46 and MYB83 bind to the SMRE sites and directly activate a suite of transcription factors and secondary wall biosynthetic genes. *Plant and Cell Physiology*. 2012;53(2):368-380.

114. Zhong R, Ye Z. Regulation of cell wall biosynthesis. *Curr Opin Plant Biol*. 2007;10(6):564-572.

115. Zhou J, Qiu J, Ye Z. Alteration in secondary wall deposition by overexpression of the fragile Fiber1 Kinesin-Like protein in Arabidopsis. *Journal of Integrative Plant Biology*. 2007;49(8):1235-1243.

116. Zhu Y, Song D, Sun J, Wang X, Li L. PtrHB7, a class III HD-zip gene, plays a critical role in regulation of vascular cambium differentiation in populus. *Molecular plant*. 2013.